A remote sensing assessment of irrigation land use land cover change in the Sokoto Rima River Basin, Nigeria

By

Abdulmajid Aminu

Student No.: ABDAMI004

A dissertation submitted in partial fulfilment of the requirement for the award of Master of Science degree in the Department of Environmental and Geographical Science

University of Cape Town

Supervised by:

Associate Professor Frank Eckardt; Department of Environmental and Geographical Science, and

Dr Patroba Odera; Division of Geomatics

June 2019

Declaration

I certify that the work in this thesis is based on the research work carried out by me, and that it has not been presented previously for another degree at any institution.

Abdulmajid Aminu	Signed by candidate	June 2019
Student Name	**Signature**	**Date**

Acknowledgement

I express my gratitude to Almighty Allah for granting me the ability to carry out this research in spite of all odds.

My sincere appreciation goes to my supervisors, Associate professor Frank Eckardt, Dr. Patroba Odera, and my mentor Dr. Yahaya Z. Ibrahim, for their immense and relentless effort towards enhancing my learning process, encouragement, useful suggestions and criticisms throughout this research.

My sincere gratitude goes to Mastercard Foundation and the entire program staff at the University of Cape Town, for their support and the scholarship offered to me throughout my research at the University. I look forward to using my knowledge as a contribution to Africa through its local unit, to its regional precinct, and to the continent at large as earlier promised.

My appreciation also goes to my family members for their support and words of encouragement. My friends Bishar Mohamed, Dr. Ibrahim Abdulganiyyu, Lucia Mokubedi, Julie Ogutu, Dr. Shakiruddeen Lawal, and Jabir Lawal for being there always. Also my appreciation goes to the staff of National Bureau of Statistics data shop in Abuja, and staff of Sokoto Rima River Basin Development Authority, for their support and provision of necessary data used in this research.

Table of Content

Table of Figures

List of Appendices

List of Tables

List of Abbreviations

API: Application program Interface.

AVHRR: Advanced Very High Resolution Radiometer.

ETM: Enhanced Thematic Mapper.

GEE: Google Earth Engine.

GSWE: Global Surface Water Explorer

IPCC: Intergovernmental Panel on Climate Change.

LU/ LC: Land Use / Land Cover.

MODIS: Moderate Resolution Imaging Spectrometer.

MSS: Multi Spectral Scanner.

NASA: National Aeronautics and Space Administration.

NDVI: Normalized Difference Vegetation Index.

NOAA: National Oceanic and Atmospheric Administration.

OLI/ TIR: Operation Land Imager/ Thermal Infrared Sensor.

SPEI: Standardized Precipitation and Evapotranspiration Index

SRRBDA: Sokoto Rima River Basin Development Authority.

SRRB: Sokoto Rima River Basin.

TM: Thematic mapper

USGS: United State Geological Survey.

WMO: World meteorological Organization.

Abstract

This study examines the expansion and utilisation of Fadama irrigation in the Sokoto Rima River Basin using the ground yield and remote sensing data. Decadal land use land cover (LU/LC) change detection was conducted using remotely sensed data from Landsat 4,5,7 ETM for 1988, 1998 and Landsat 8 OLI for 2018 using a digital classification and a cloud-based classification provided by Google Earth Engine (GEE) API, with an overall accuracy of 97% in 1988, 92% in 1998 and 90% in 2018. Additionally, the Normalised Difference Vegetation Index (NDVI) derived from MODIS, GEE NDVI, and the Landsat was used to assess the crop yield patterns of the irrigation farming at the Fadama sites in conjunction with the limited ground yield data from 2000-2005, and was found to be a positive change over the years. The result generated from the classification was juxtaposed with observable field characteristics of the LU/LC identified. The decadal trend between 1988 to 1998 saw an increase of 114% in dam surface water and 166% of the natural vegetation, while the non-vegetated areas and the Fadama areas decreased in size by -100% and -65% respectively. Between 1998 and 2018, the reverse of the previous pattern was observed, with water and vegetated areas decreasing in their surface area in hectares by -80% and -23% respectively. Non-vegetated areas increased by 3% while Fadama areas increased in size by 112%, indicating that the Fadama areas were under-utilised by -65% of the total hectarage in the past, and in recent years a 47% increase was recorded between the two periods. In addition, the Standardised Precipitation and Evapotranspiration Index (SPEI) data from 1950 was used to analyze the meteorological and hydrological drought pattern at four locations within the basin and was found to be a moderate drought. The SPEI data was then correlated with the Global Surface Water Explorer data to observe the surface water dynamics and to show the drought extent around Bakolori, Goronyo, Jibia, Wurno and Zobe dams. The result showed that the dams are shrinking in size due to risen temperature and consequent evaporation caused by moderate drought and water use for irrigation. Lastly, this research uncovers the utilization of the Fadama in recent years by 47%, but with mismanagement of the resources in the Sokoto Rima River floodplain because not all the irrigation fields are put into cultivation, with 39,907 ha put into use from the planned irrigation of 105,472 ha in the entire basin. Therefore, this research recommends a proper intervention of the government to promote and enhance sustainable management of the Fadama lands, water, and the vegetation resource. This should be done in consideration of the deteriorating climate to close yield gaps, with much emphasis on engaging the local farmers by monitoring yearly ground yield data and ensuring all incentives are distributed effectively to brace an active and sustainable management of the entire basin and its vast resource.

1 CHAPTER ONE

1.1 General background

The word "*Fadama*" means, seasonally inundated land in Hausa, the major language in northern Nigeria. Usually, the low-lying plains are underlaid by shallow aquifers bordering major river systems that act as a source of water during the dry season. *Fadamas* also support diverse permanent or transitory wildlife including carnivores, herbivores, and the migratory birds (World Bank, 2010) **Figure 1-1.**

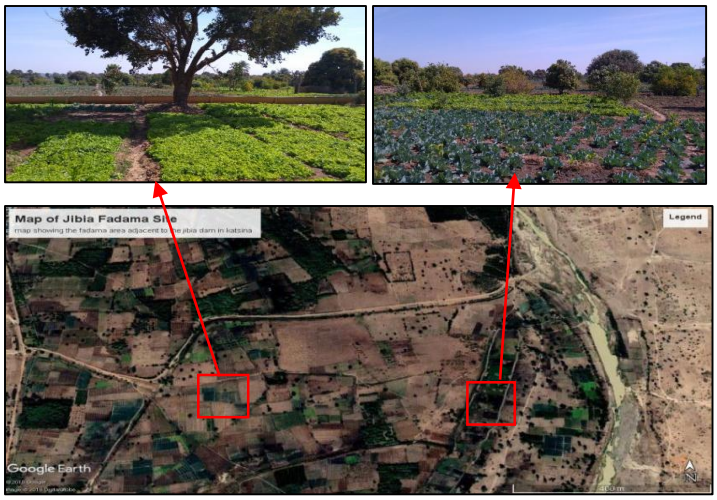

(a) Map of Jibia *Fadama* site showing the *Fadama* areas adjacent to the jibia dam in Katsina 13.086^0 N and 7.243^0 E, with ground pictures depicting Fadama crops (Lettuce and carbbage).

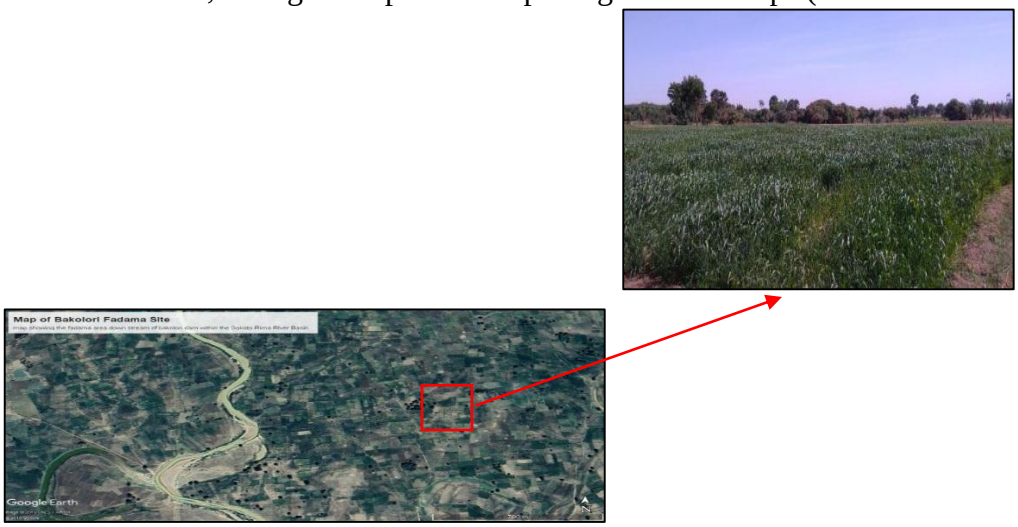

(b) Map of Bakolori *Fadama* site showing the *Fadama* areas downstream of bakolori dam within the Sokoto Rima River Basin at 12.778^0 N and 5.849^0 E, depicting one among the grown crops.

Figure 1-1 (a-b): Map showing some *Fadama* sites in the basin at Jibia and Bakolori area during the dry season farming (Google Earth 2019).

Nigeria is endowed with underground and surface water, abundant pasture and a favourable agro-ecological conditions within the country's low-lying plains. There are over 3,000,000ha of fertile soil with residual moisture in the dry season which are extensively used by smallholders for crop and livestock production (Dan-Azumi, 2010). Due to the high moisture retention capability of the floodplains, they are widely used for recession farming. Thus, *Fadamas* are of profound importance to the survival and economic development of smallholder farmers, especially in the savannah regions of Nigeria as well as a vital safety net for the rural poor, which constitutes a primary alternative source of food supply, especially during the dry season. It also serves as a support for food security within the local units and regional precinct.

The *Fadama* or wetlands have been used for dry season farming in the country, and it has significantly contributed to food crop production (Ishaya *et al.*, 2008) with over 333,494.5 metric tons of rice production from some part of the Sokoto Rima River basin as observed from the ground yield data. Over the years, many of the farmers in the study area cultivate small areas in the *Fadama* during the dry season using water directly obtained from rivers and streams, which are manually or using electrical/mechanically powered generators to pump water into the irrigation lands (Ishaya *et al.*, 2008).

However, *Fadama* lands are under pressure from the natural and human-made factors. These includes drought, rapid population growth, land degradation, expansion of cultivation on fragile forest cover, loss of soil fertility on arable lands, soil erosion, and insufficiency in food production (FAO & IITA, 1999; Ewuim *et al.*, 1998). Other pressures experienced by smallholders in *Fadama* areas are conflicts from competing land usage, the intensification of agricultural land by farmers, nomadic pastoralists, fishermen and other *Fadama* users (Ardo, 2004).

Realising optimal crop yield at a minimum cost is one of the goals of agricultural system. Because early detection and management of problems in connection with crop yield indicators can brace to increase yield and subsequent profit. Though aerial images

have been widely used for crop yield predictions before they are harvested as well (Gopala *et al.*1999). These images can provide very high spatial and cloud free information of the crop's spectral attributes and characteristics, while vegetation analysis and detection of changes in vegetation pattern is essential for natural resource monitoring and management, such as crop vigour analysis (Thiam *et al.*, 1999).

Healthy crops absorb energy in the visible wavelength spectrum and reflect near infrared energy. The stronger the contrast of absorption, the better the scattering of the red and near-infrared bands that can be combined into numerous quantitative indices of vegetation conditions. These quantitative mathematical combinations are referred to as vegetation indices(VI). Since the late 1980s, numerous studies like Funk & Budde, (2009), have been conducted on crop growth analysis using Normalised Difference Vegetation Index (NDVI) to support precision agriculture. Presently, site-specific crop management (SSCM) and essential component of precision agriculture are being researched to increase production, which comprise five main processes that involves spatial referencing, crop and climate monitoring, decision support systems, attribute mapping, and differential action.

Remote Sensing techniques produces a source of information for surveying, identifying, classifying, mapping, monitoring, and planning of natural resources, disasters mitigation, as well as preparedness and management. Also, multiband, multi-date and multi-stage satellite imaging have been widely used for water resource studies, monitoring, and management of agricultural lands (Pramanik *et al.*,1992). This research entails a remote sensing assessment of irrigated land use land cover change in the Sokoto Rima River Basin. GIS is used for delineating land use/cover change through time.

1.1.1 Statement of the problem

The population of Nigeria is estimated at 200 million in 2019, with a national growth rate estimated at 3 % per year (Annual Abstract, 2017). With these estimated

population of 200 million, Nigeria is the most populous country in the African continent. Still Nigeria is amongst the countries that are now unable to provide their food requirement from rain-fed agricultural output. Even though agricultural practice still remains an important sector of the Nigerian economy, and hire two-thirds of the total labour force, the production obstacles have largely stifled the accomplishment of the entire sector (FAO, 2010). Over the last 20 years, value-added per capita in agricultural system has increased by less than 1% yearly. It has been quatified that Nigeria has lost 10 billion US Dollars in annual exportation opportunity from palm oil, cotton, and groundnut alone due to a continuous reduction in the production of these commodities (FAO, 2010). The production of food crop has not kept pace with the thriving growth in population which is a problem, this has resulted in an increase in food importation and a reduction in national food self-sufficiency (Dan-Azumi, 2010). The major factors hindering production include dependance on rain fed agricultural practice hampered by weather extremes, smallholder land tenure, and smaller production level due to poor planting material, weaker agricultural extension system, insufficient fertilizer application, and among others (Dikko, 2011).

Nigeria is a leading consumer of rice in the continent, also one of the largest rice producers in Africa, and simultaneously one among the largest rice importers globally. In the year 2008, Nigeria yielded approximately two million metric tons of milled rice and imported three million metric tons, including the estimated eight hundred thousand metric tons that is believed to come into the country illegally on an annual basis (Eniolorunda, 2017).

Therefore, the adoption of *Fadama* cropping system which is a small-scale farmer based private irrigation farming system for crop production, to augment food production during the dry season considered in this reasearch, is indeed essential as an alternative to bracing food security in the country. Although some still regard it as a less productive form of farming, albeit the world bank and the government are trying

everything possible to make a facelift to it; so as to bolster its utilisation through *Fadama III projects* (World bank, 2010).

Rapid population growth and increased pressure on land use/ cover, unplanned urban sprawl processes, land degradation, lack of modified seedlings to farmers, lack of seed capital, inaccessible proximity to market and infrastructural development are shrinking the size of arable *Fadama* areas. As Such, for any meaningful development to take place in any given area, there is a need for adequate information on the past and present land use change and pattern. Sufficient records on land uses have not been adequate over time in the basin; this may be due to the enormous nature and cost of conducting ground surveys, while the nature of data generated is substantial; which is impossible to be appropriately kept by manual or existing obsolete methods of filing information on papers. Hence, the use of GIS and remote sensing to capture data and process it for safekeeping, management and regular updating, serves as a reliable substitute, as it is also found to be the most efficient and cost-effective method of data gathering, data processing over large areas and long time series analysis.

1.1.2 Justification

With the current review on sustainable development largely centred on understanding land use and land cover change as opine by Shao *et al.,* (2005). The changes that are occurring on land use and land cover needs to be characterised first. Where information is readily available on the characteristics of LU/LC, chances of taking appropriate measures towards achieving a sustainable and efficient development becomes brighter.

Research conducted established that climate change has a negative impact on soil, vegetation and water resources of the basin (Ezemonye & Emeribe, 2015), but with no much information on the impact it has on crop yield pattern. The Sokoto Rima River Basin has suffered acute climate change impact, with low annual rainfall, late

arrival and early cessation of the wet season, moderate drought and extended dry season with rising temperature. These resulted in a constricted rainfall pattern and consequent abnormal flood occurrence, conversely affecting the land use/ cover pattern of the basin and associated surface water dynamics.

As such, this research will further fill the gap and add to the existing literature by observing the change that have occured using GIS and remote sensing technique. While considering climate and surface water dynamics to appraise how land use/cover changes have an impact on estimated crop yield with the aid of time series data from remotely sensed images, for an informed decision making.

1.2 Aim and objectives

This research is to assess long term *Fadama* irrigation land use land cover change in the Sokoto Rima River Basin, using remote sensing. The following objectives will achieve this aim.

1.2.1 Objectives

1. To analyze the extent of *Fadama* utilization for crop production using ground yield data.

2. To analyze the trend/extent of *Fadama* utilization for crop production using remote sensing technique.

3. To analyze the impact of climate change on surface water and land use/cover change in the Sokoto Rima River Basin.

1.3 Study area

1.3.1 Sokoto Rima River Basin (SRRB)

Sokoto Rima river is in the North-West region of Nigeria and serves as a tributary of the river Niger. The river source is near Funtua in the south of Katsina

State; it flows north-west through Gusau in Zamfara State. Further downstream, the stream connects to Sokoto state and connects with the Rima river proper, then turning south and flowing through Birnin Kebbi in Kebbi State. Finally merges with river Niger (Akané & Jürgen, 2005).

Sokoto-Rima River Basin (SRRB) has over 15million people and one among the eight (8) basins demarcated in Nigeria. It is located in the North-Western region of Nigeria between latitudes 10° N and 14° N and longitudes 3° E and 8°E, (**Figures 1-2 and 1-3**).

It covers a land area of 131,600 km^2 and shares its borders with the Niger Republic up north, covers Sokoto, Kebbi, Zamfara and part of Katsina State. It also bordered Niger State to the South-east and then the Benin Republic to the west. The whole basin can be delineated as Sudan and Sahel Savannah, and also extends beyond the border to the Niger Republic and the northern part of Benin Republic. The basin has six major rivers, namely: river Bunsuru, Gagere, Rima, Sokoto, Zamfara and river Ka. The topography consists of a vast seasonal floodplain next to the river channels, i.e. (*Fadama* lands) that are rich in alluvial soils and suitable for cultivation of a variety of crops. There are also isolated hills (inselberg) and hill ranges scattered all over the area (Ekpoh & Ekpenyong, 2011).

1.3.2 The Fadama plains of the basin

The plains around the rivers are widely cultivated, and the rivers are used as a source of water for irrigation, domestic water supply and navigation. The Bakolori, Goronyo, Wurno, Jibia, and Zobe Dams are having a significant impact on downstream flood plain cultivation.

1.3.3 Hydrology of the river basin

The Sokoto river drains the entire basin into the river Niger (see **Figures 1-2** and **1-3).** The Sokoto river main tributaries are the Rima river in Zamfara and river Ka. They come from about 600 to 900 meters high of Dunia and Mashika high land, this borders the part of the basin easterly, then flows downward or slightly sluggish down a gentle slope relative to the Northwest. The Rima river make a nexus in the north around Sokoto town after which it makes a southward turn, emptying the Zamfara and Ka rivers before flowing into the river Niger properly. The river system is drained into the whole basin at the source areas in the east where it is connected by Konni river and the Sokoto river system which is only seasonal.

However, through the western parts of the basin, the river becomes perennial as it begins to receive substantial groundwater contribution to its flow year in year out. The annual discharge of the Sokoto valley varied across the basin, and reliable data are limited.

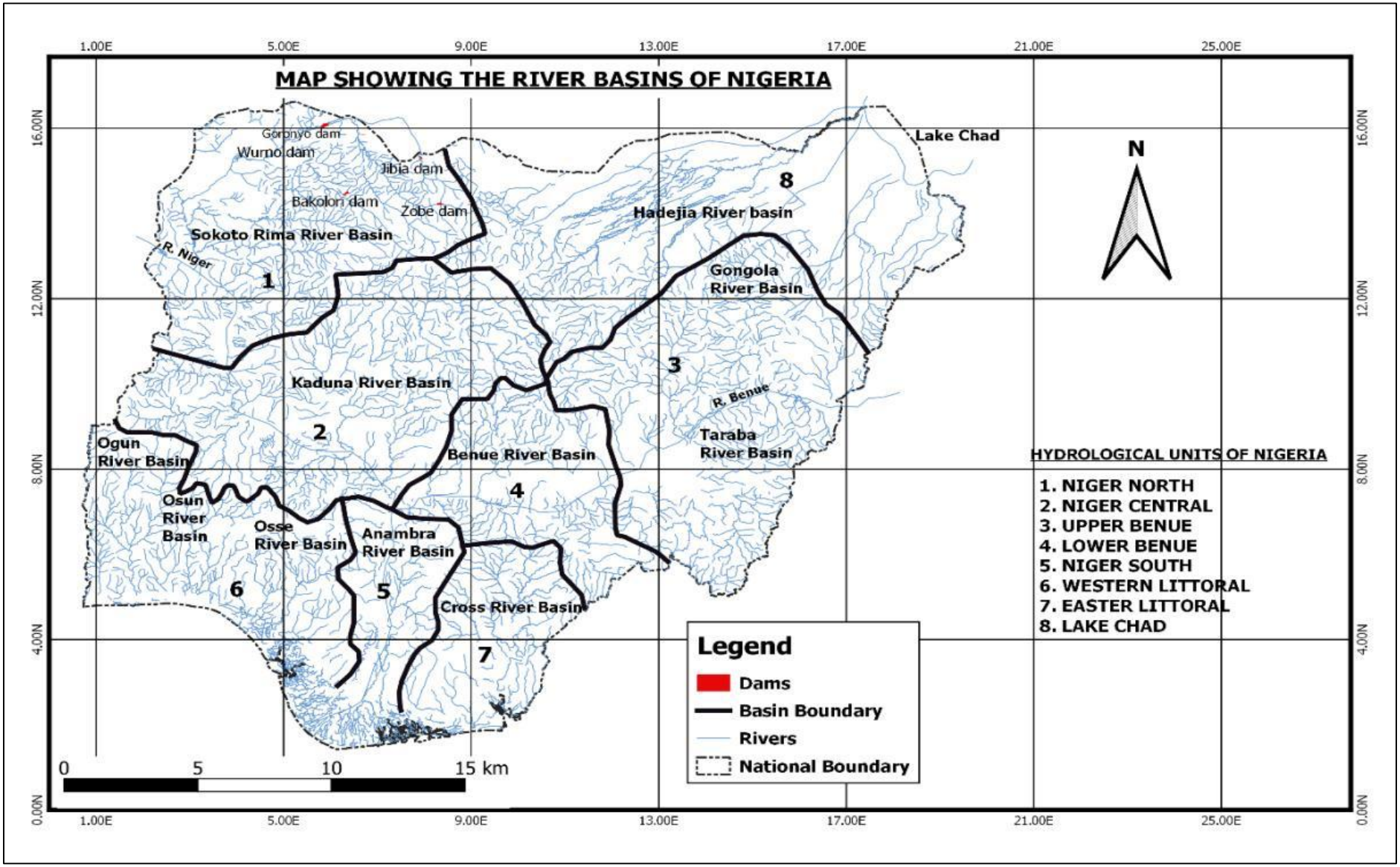

Figure 1-2: Map showing the entire 8 river basins in Nigeria, with major dams and hydrological boundaries.

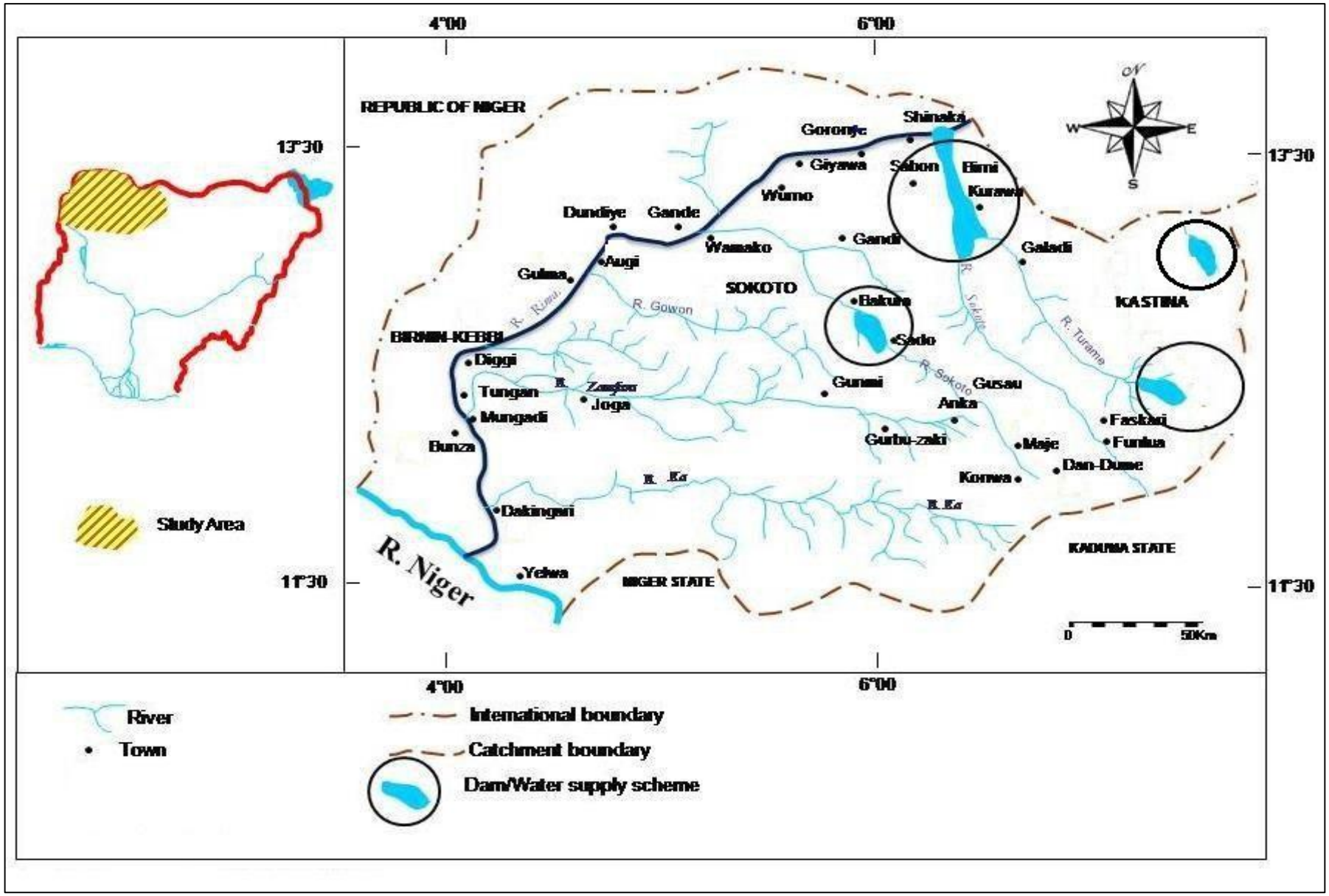

Figure 1-3: Map showing the Sokoto Rima River Basin (SRRB) as the study area.

1.3.4 Climate characteristics of the river basin

The climate of the Basin is largely characterized by two dominant air masses affecting the sub-region like the whole of West Africa. These are the warm, tropical-maritime (mT) air mass (which originates from the Atlantic Ocean), and the dusty dry tropical-continental (cT) air mass (which arises from the Sahara region). The influence of the air masses on the West African region is determined by the convergence of the two air masses at the Inter-Tropical Convergence Zone (ITCZ), this is a zone representing the surface boundary between the two air masses. The interplay of these two air masses give rise to two distinct seasons within the region (Abdullahi, 2011). The wet season is characterised by a tropical maritime air mass, while the dry season is a by-product of the tropical continental air mass.

The intensity and influence of the wet season attenuate from the West African coast towards the north (Ekpoh & Ekpenyong, 2011), whereas, precipitation in the whole sub-region of West African countries depends on thunderstorm, which occurs along a disturbance line refers to *'squall line'*. The annual rainfall for Sokoto ranges between 300 mm and 800 mm, and the average rainfall per-annum for over 35 years is about 470 mm (Annual Abstract of Statistics, 2017). Higher rainfalls are experienced between May and September, while the dry months are October to April. Squall Lines are prevalent in June and September (Ekpoh & Ekpenyong, 2011).

The Sokoto basin is within the hottest part of Nigeria, (**Figure 1-4** and **Figure 1-5**). The zone is located above latitude 10^{o}N, and is within the Sahel region of Africa, and as well an area that is most affected by moderate droughts. Temperature is usually low during the coldest month of January and December with average daily minimum of 16^{o}C, and higher in the hottest month in April to June, with an average maximum of 38^{o}C. Throughout the year, the average maximum temperature is 36 ^{o}C and average daily minimum of 21 ^{o}C. The mean annual temperature is 35 ^{o}C, although dry season temperature of the region often exceeds 40 ^{o}C in some locations (Ekpoh & Ekpenyong, 2011)

Comparatively to the temperature, evaporation is high and ranges between 80 mm in July to about 210 mm in April and May. Monthly average evaporation ranges from 140 mm representing 30% of monthly average precipitation within the catchment (**Figure 1-7** and **Figure 1-6)**, while the hottest months from April to May are the period of high evaporation (Abdullahi, 2011). The relative humidity is low in most of the year and only increases during the raining seasons in June-September.

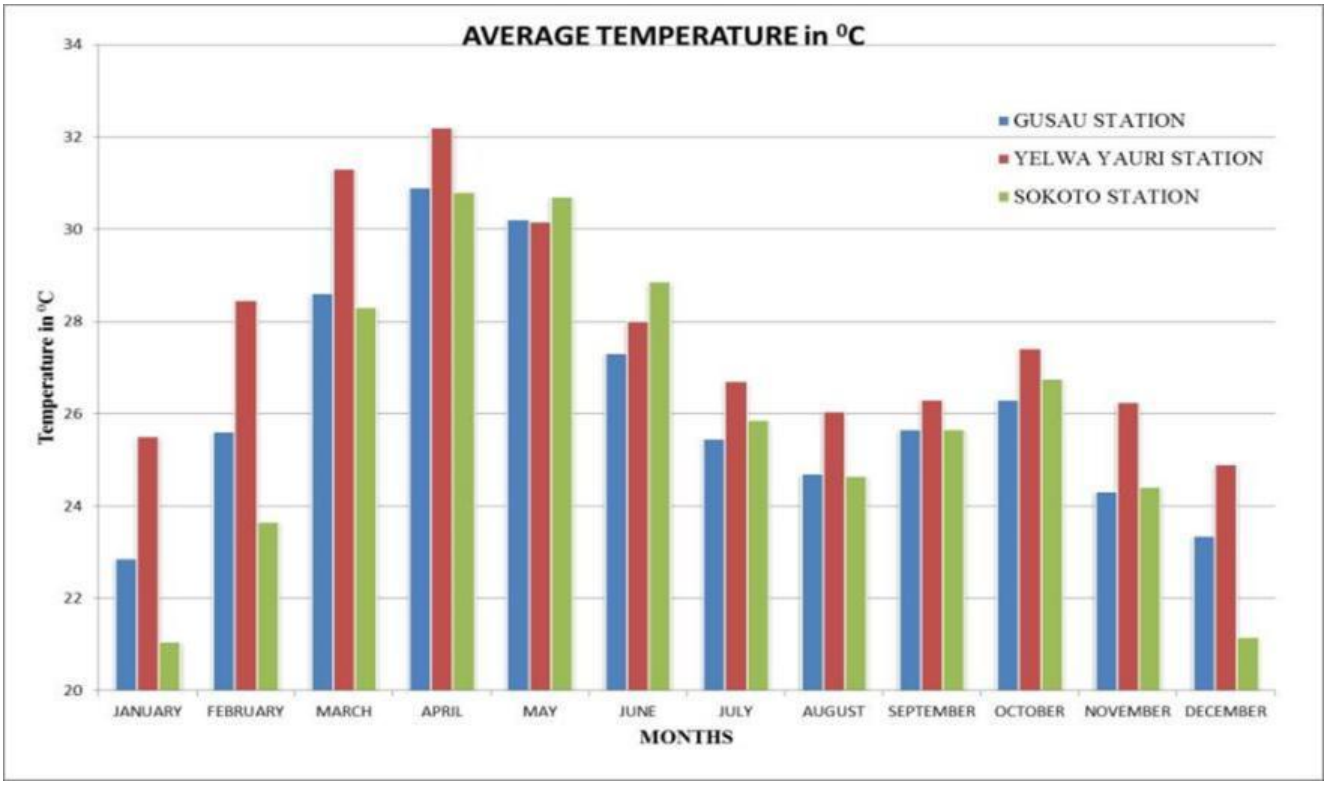

Figure 1-4: Mean temperature of some data stations within the basin. showing the mean monthly temperature in degree celcius. At the Gusau station, the average temp. is 26.3 ^{0}C for the whole months, with maximum temperature of 31 ^{0}C in April and the minimum temperature is 23 ^{0}C in the month of December. At Yelwa station, the average temperature is 28 ^{0}C, with a minimum temperature of 25 ^{0}C in the month of January/December, and a maximum temperature of 32 ^{0}C in April as shown above. At the Sokoto station; the average temp. value is 26 ^{0}C while the min. temp. is 21 ^{0}C in January and December, and the maximum temperature is 31 ^{0}C in the month of April (source: Annual Abstract of Statistics, 2017).

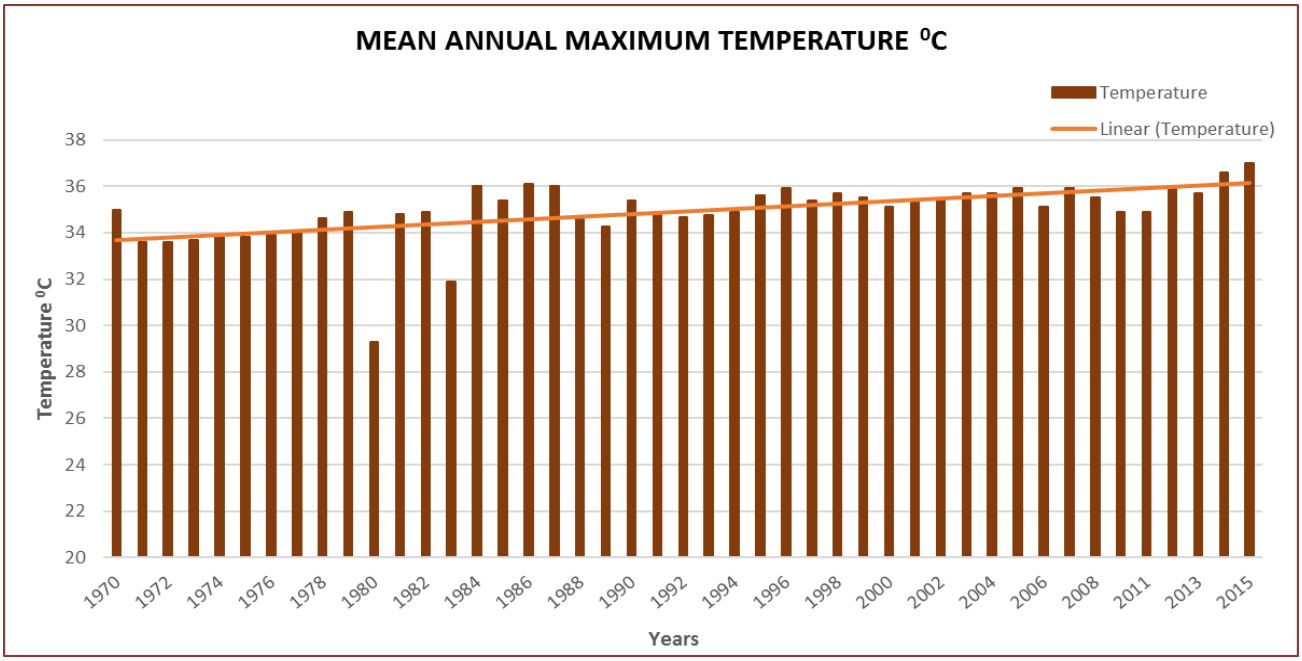

Figure 1-5: Annual mean temperature of the basin. The graph is showing the annual mean of temperature in the basin with an average temperature value of 35 ^{0}C through the years. The minimum temperature is 29 ^{0}C in the 1980 and the maximum value of temperature was recorded as 37 ^{0}C in 2015. From the observed data from 1970 to 2015 using the trend line, the temperature is increasing over time (source: Annual Abstract of Statistics 2017).

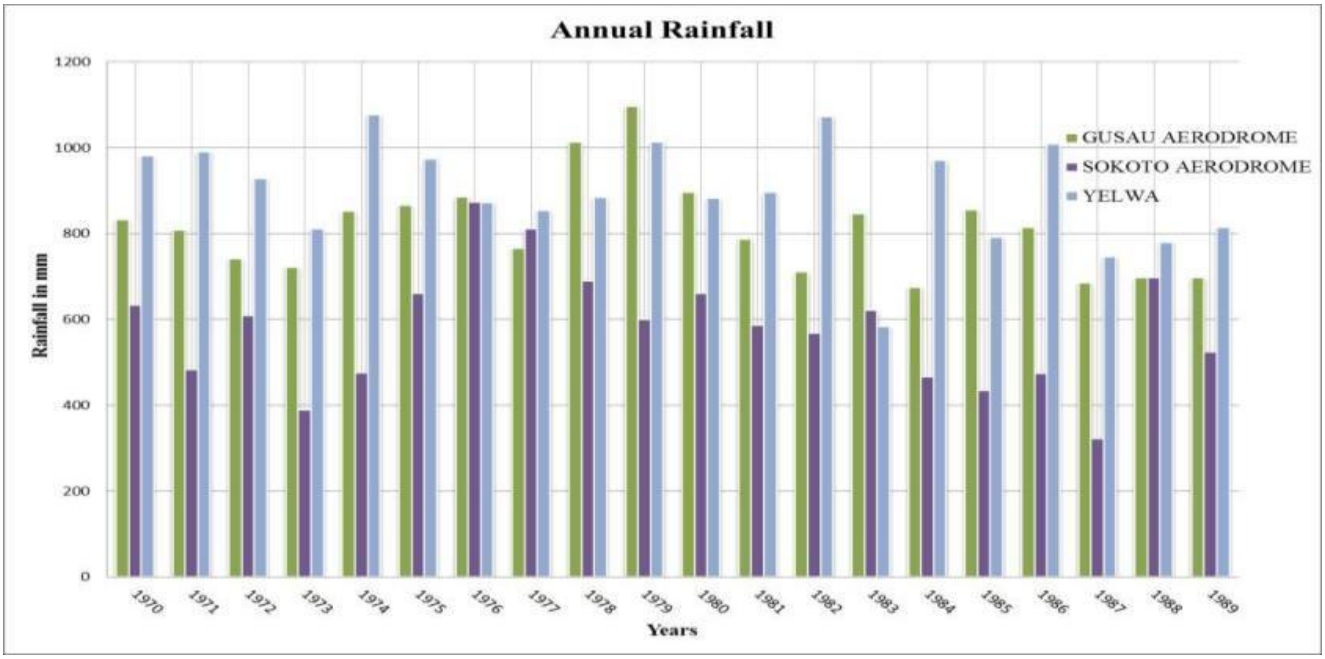

Figure 1-6: Annual rainfall of some data stations in the basin. Gusau station recorded a maximum annual rainfall of 1,100 mm in 1979, while the minimum is 681 mm in 1984. At the Sokoto Station; the maximum and minimum value is 875 mm and 355 mm in 1976 and 1987 respectively. While at the Yelwa station; the values were 1,065 mm as the maximum in 1974, and 590 mm in 1983 (source: Annual Abstract of Statistics 2017).

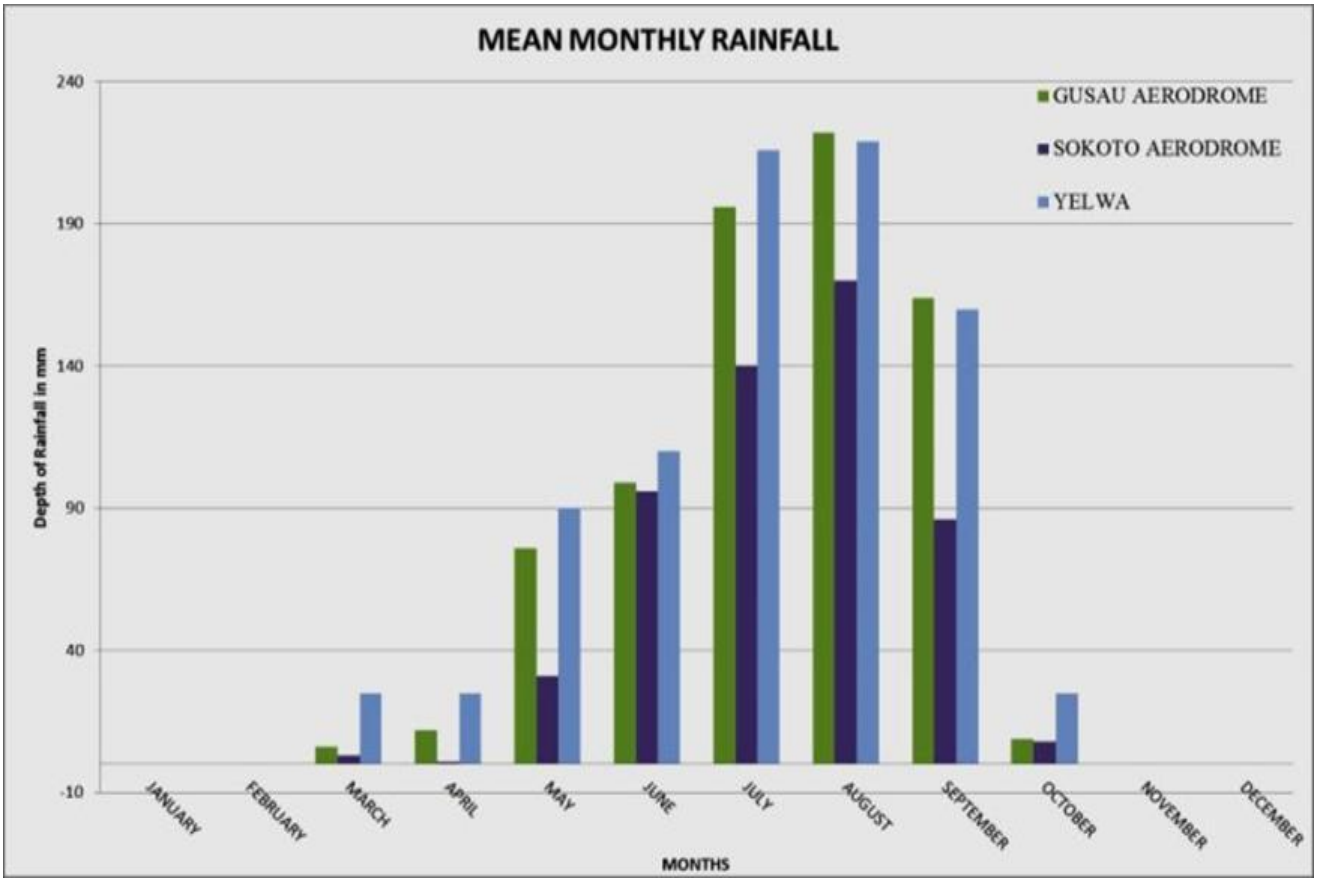

Figure 1-7: Mean monthly rainfall of some data stations within the basin. The graph shows the monthly rainfall in millimeters at Gusau, Sokoto and Yelwa station while all months with no rainfall appears empty. At the Gusau station, the average rainfall was 65 mm, with the max. value of 222 mm in August. At the Sokoto station; the average is 45 mm, while the maximum value is 170 mm in August. Lastly, at the Yelwa station, the average precipitation is 73 mm, while the maximum value was 219 mm in August (source: Annual Abstract of Statistics, 2017).

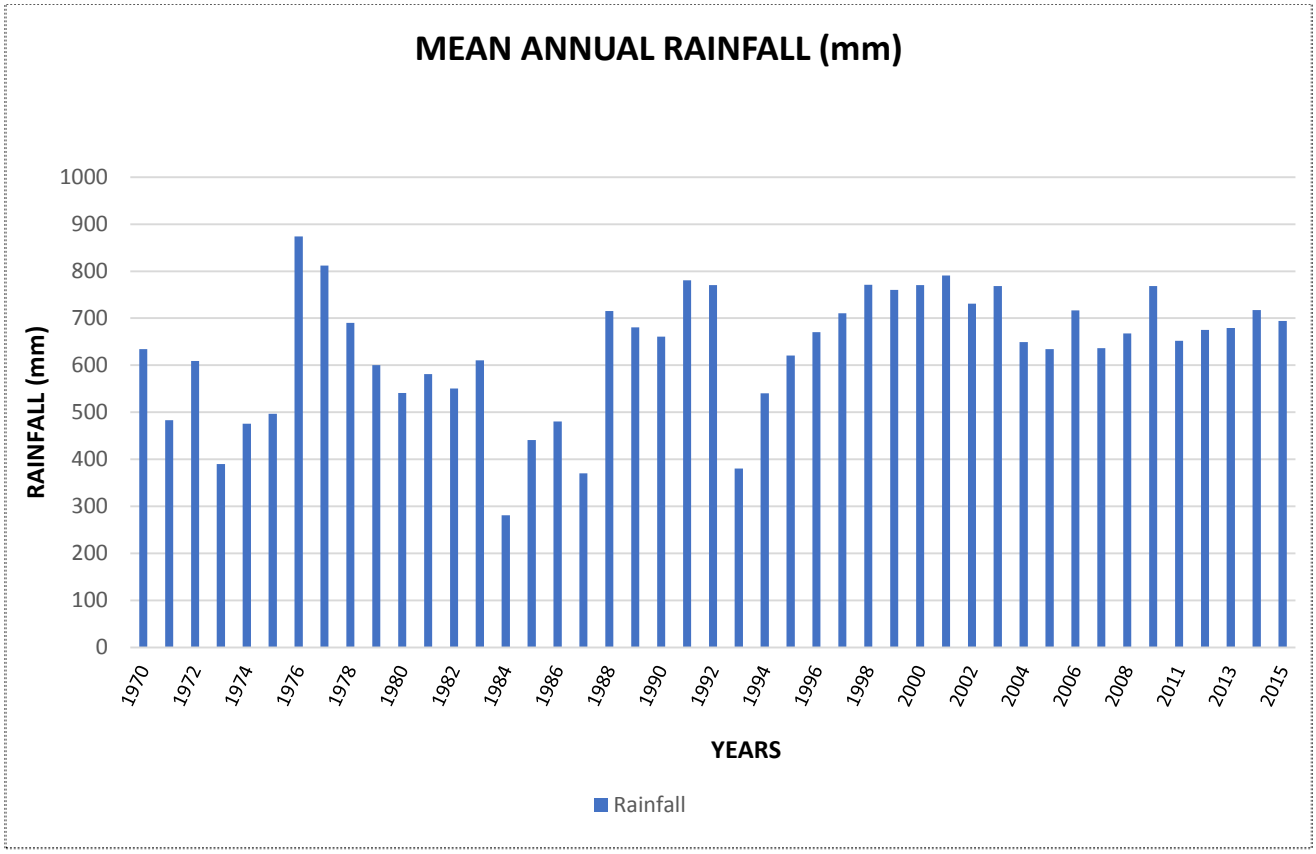

Figure 1-8: Mean annual rainfall of the basin. the chart above displays the mean annual precipitation pattern from 1970-2015, with the minimum and maximum mean annual rainfall of 281 mm and 874 mm in 1984 and 1976 respectively. From 1994 to 2008, the rainfall increased from 540 mm to 791 mm in 2001, and reduced in 2005 with 635 mm. From this point, the ranfall pattern maintains a slight improvement but with lesser rain in 2015 recorded as 695 mm (source: Annual Abstract of Statistics, 2017).

1.3.5 General land use/cover of the basin

The land use/cover of the basin are grouped into seven categories: forested land, grassland, and agricultural land. Agricultural land is further divided into three categories: (i) *Fadama* (ii) Tudu i.e. land which lies above the floodplain, mostly dependent on rainfall for its moisture, and (iii) land formed by modern method of irrigation, for instance the Talata-Mafara irrigation scheme. Other categories of the land use also include wet land, bare land, water area and urban land. (refer to **Table 1-1** for more details).

Table 1-1: **Land use and land cover of Sokoto-Rima River Basin**

Category	Area in Km^2	Percentage
Forest land/wood land	2,755	2
Agricultural land	69,520	5
Grass land	46,615	35
Wet land	970	1
Urban land	10	0.01
Water area	1,400	1
Bare land	10,330	8
Grand Total	**131,600**	**100**

Source: (Abdullahi, 2011)

1.3.6 Major dams within the Sokoto Rima River Basin (SRRB)

The major dams in the SRRB are the Bakolori and Goronyo dams (**Figure 1-9** below), whereas the Jibia and Zobe dams are lower in capacity and less utilized when compared to the former. Wurno dam is the smallest in the basin but with significant *Fadama* irrigation **Table 1-2**.

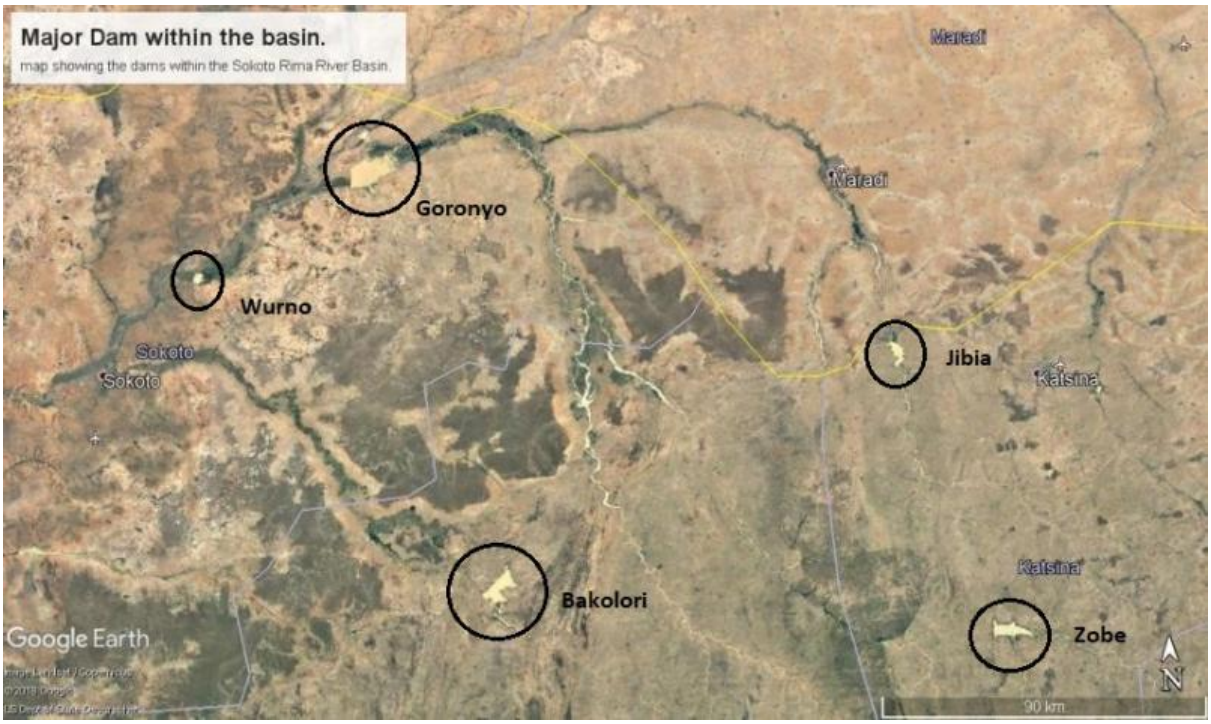

Figure 1-9: Satellite image showing the location of five dams within the basin (source: Google Earth; 2019).

Table 1-2: Operational and physical parameters of the major dams in the basin

Name of the dam	Bakolori	Jibia	Goronyo	Wurno	Zobe
Type	Earth	Earth	Concrete	Earth	Earth
Construction Date	1978	1989	1984	1965	1983
Catchment Area ($km^{2)}$	21,445	400	4,857	4.37	1000
Storage Capacity (Million m^3)	942	142	450	19.5	179
Active Capacity (Million m^3)	933	121	403	-	177
Dead Capacity (Million m^3)	9	21	47	-	-
Full water Level (m)	288.0	-	334	-	-
Lower water Level (m)	280	-	320	-	-
Planned irrigation (ha)	69 000	3,472	23,000	2,000	8,000
Operated irrigation (ha)	17 000	3,450	16,000	1,457	<2,000
Reservoir Area (ha)	200	17	80	1.5	31
Mean Annual Flow (km)	656	-	757	-	-
Height (m)	20	23.5	48	-	19
Length (m)	5,285	3,366	5,500	-	2,750
Max. Hydraulic outflow (m^3/s)	1,697	2,100	3,750	-	2,083

(Source: SRRBDA,1992)

1.3.6.1 Bakalori dam

The Bakolori (**Figure 1-10)** dam is located in Zamfara State earlier under Sokoto state, It has a coordinate of 12.512^0 N and 6.183^0 E and was completed in 1978, whereas the reservoir got filled by 1981. It is a significant reservoir to the Sokoto river as well as a tributary to the Rima river, which in return feeds the Niger river. Water from the dam serves enormous importance as it supplies the Bakolori Irrigation Project in Talata Mafara. The dam has a capacity of 450 million cubic meters, with a reservoir covering 8,000 hectares extending 19 km (12 miles) upstream (en.wikipedia.org/Bakolori_Dam). Other operational parameters of the dam are shown in **Table 1-2**.

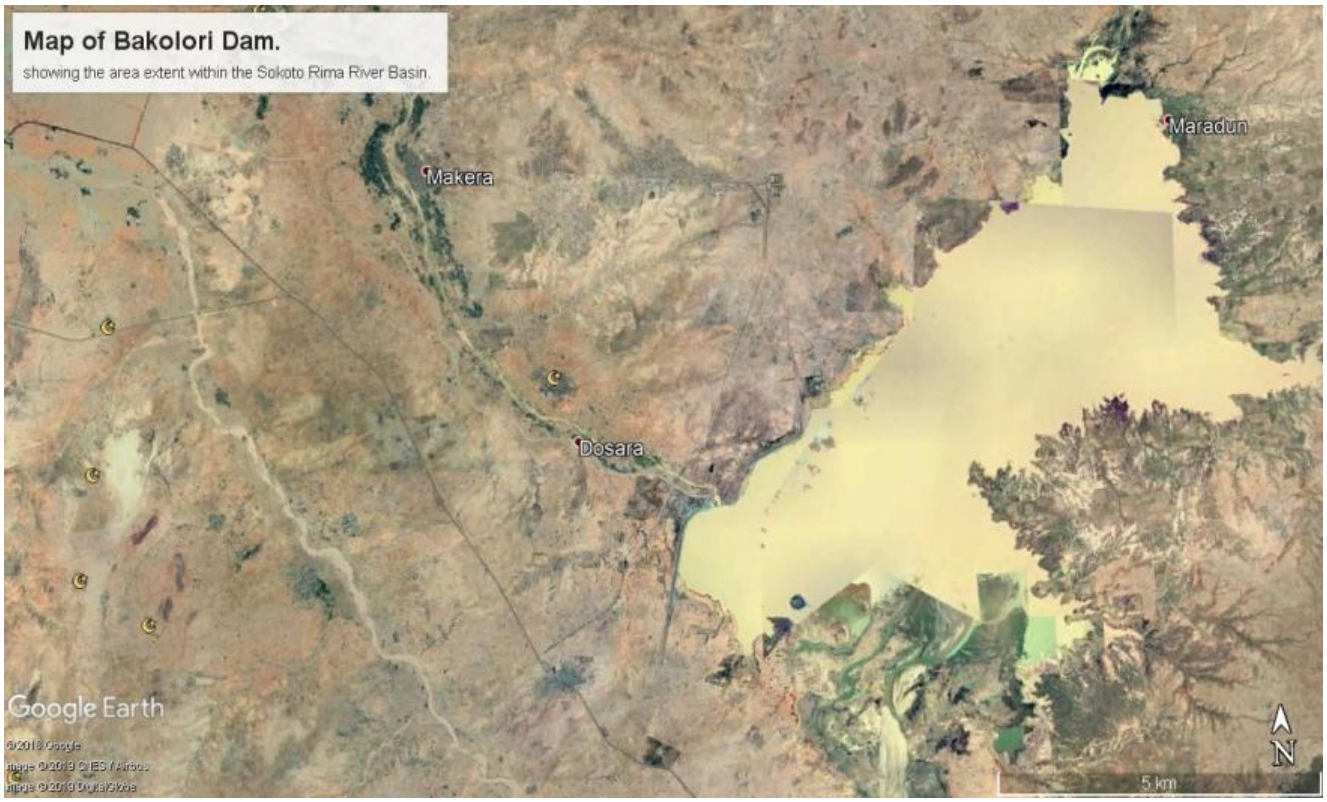

Figure 1-10: Satellite image of the Bakolori dam extent during the dry season between November and March (Source: Google Earth, 2018).

A notable development within the Sokoto valley in north-western Nigeria instigated the construction of the Bakolori dam, and of course the 69,000 ha irrigation scheme connected to it (Adams, 1983, 1985)

Based on the availability of water resource within the country and its potentials to boost agricultural production in the country. The Federal Government established the River Basin Development Authority (RBDA). The scheme is entirely necessary because of the varying raining season in most part of the northern states. This led to the commissioning of the project in 1975.

The Bakolori dam project: Food and Agricultural Organisation (FAO) and United Nations Development Programme (UNDP), identified the project in the Sokoto Valley in 1969 during a soil and water resource survey. The feasibility of this project was actualized by the Impresit Bakolori (Nigeria) Ltd. and its Italian associate, Nuovo Castoro. The contract was at inception worth 174 million Naira in 1974 and afterwards 500 million Naira in 1982, i.e. 400 million U.S. dollars (SRRBDA, 1992).

The dam construction contract was signed in June 1975 with Impresit Bakolori (Nig.) Ltd. and work commenced that very year. A supplementary agreement for the erection of land levelling, gates and gearing, diesel power station, sprinkler system, etc. was later signed in June 1977 to finish the remaining part of the project. The total cost of the project indicated in the two-construction agreement amounted to about N154 million based on the mid-1974 price level.

The Bakolori dam and the supply canal was completed and commissioned in December 1978 on behalf of the Head of State, by the Chief of Staff Supreme Council Headquarters, late Major-General Shehu Musa Yar'adua. The project was formulated to supply irrigation water to 11,200 km area through gravity, and 12,000 ha area by sprinkler system of the irrigation. More so, the power capacity of 12,000 KVA of electricity was among the ambition of this project, but from my field observation, this is indeed elusive. The construction of 200 km road network to assist farmers by providing them with needed inputs was as well part of the project (SRRBDA, 1992).

The major target of the project was the irrigation water supply to the estimated population in the adjacent project sites of about forty to fifty thousand farmsteads. The majority of the settlers in Sokoto valley are peasant farmers. They mostly engage in both rainfed and

traditional irrigation farming in the dry season i.e. *Fadama* farming. As such, this account for the production of vegetables and spices cultivated in the area, which includes among onion, garlic, tomatoes et cetera.

In General, the expectations of the Government from the project was very high. It was expected to counter food importation with focus on importation substitutes. For instance, rice, sugar and wheat accounted for much of the food import bills in Nigeria as at that time. Hence, this has remain herculean till date. In contrast to this position, (Ken, 1985) opined that the issue of an irrigation scheme in most of the northern states of Nigeria emanates from the political necessity of redistributing some of the benefits of the oil revenue boom towards economically less-developed northern states of Nigeria.

1.3.6.2 Goronyo dam

The Goronyo dam (**Figure 1-11**) impounds Rima river east of Goronyo in Goronyo local government area of Sokoto State. It was completed in 1984 and commissioned in 1992. The dam is a sand-fill structure with a height of 21 m and a total length of 13 kilometres. It has the storage capacity of 976 million cubic meters (MCM). The dam controls flood and more so, releasing water in the dry season for the planned Zauro polder project downstream in Kebbi State (en.wikipedia.org/Goronyo_Dam), refer to **Table 1-5** for more details.

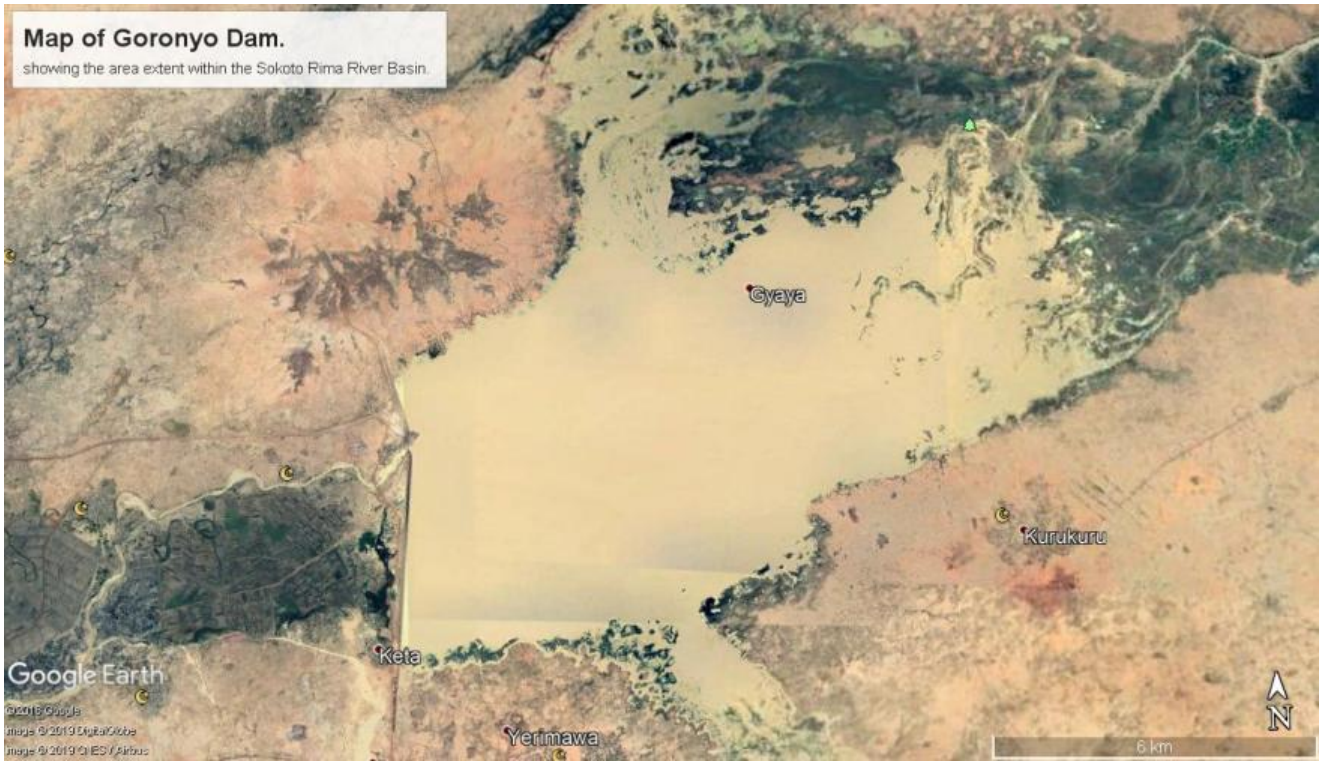

Figure 1-11: Aerial view of the Goronyo dam extent during the dry season between November and March (Source: Google Earth, 2018).

The farmers downstream of the floodplains obviously requires large amount of water to be released during the dry season. Though during the raining season; the channel flow inundate rice field which requires a large amount of water. Hence, with a decrease in water flow later in the dry season, the farmers then practised flood recession agriculture, i.e. *Fadama* farming (Adams, 1993). However, the dam operators are not cautious about this need,

sometimes releasing insufficient water. The dam significantly reduces its peak flows and the extent of flooding downstream during the dry season (Adams, 1993, 2000). It also retards the total amount of water available for farming, since a large amount of water in a hot and arid area like this one is lost to evaporation (Mohammed, 2002).

In the downstream areas of 19,000 hectares of the floodplain land, the dam once caused a loss of 7,000 hectares of rice production and as well 5,000 hectares of dry season crops (Adams, 2000). This loss further increased low value millet and sorghum production, while 12,000 people were forced to move due to flooding (Adams, 2001). The loss of agricultural output was valued to be at 7 million USD annually due to phenological contrast within the catchment (De Schutter, 2003).

Irrigation area and the reservoir**:** The littoral areas within the reservoir are small; as such, it deters the size of spawning and breeding areas of most fish species. The water is turbid, retaining suspended soil particles that block the penetration of light and disturbs the growth of submerged aquatic plants on which fish absolutely depends on for food. Conversely, this reduces the capacity of the reservoir for fish production (FAO, 2010).

However, within the irrigational areas, the higher water table in combination to higher evaporation rate do cause salinisation of the water sometimes, which in a real sense, has ruined almost half of the irrigable land and also higher level of water borne diseases (Mohammed, 2002). An attempt to introduce new varieties of cowpea to be inter-cropped with sorghum, millet and groundnuts were having little success due to the low yield of this traditional crop and the high cost of the irrigation systems (Orode, 1984). During 2003, the sprinkler system installed was not in operation and only 7,500 hectares were farmed, of which most is rice using gravity-inclined irrigation (Kebbeh *et al.,* 2003). Most of the land is left wasted inducing many of the residents moving away to the urban cities that are depicting a change in land use/ cover through space and time. As such, the dam also resulted in a 53% decrease in the usable cropped area due to specific environmental externalities (UN, 2010).

Consequently, the 1988 classic report authors on *Wise use of wetlands* published by UNESCO draw a precision that… "an independent economic appraisal of the scheme at Goronyo and Bakolori would have been less favouring than the calculation upon which it was granted approval'' (Mohammed, 2002).

1.3.6.3 Jibia dam

Jibiya dam (**Figure 1-12)** is located in Jibiya local government area of Katsina State northwest Nigeria with coordinates 13.072^0 N and 7.252^0 E. The dam construction started in 1987 and completed in 1989, purposely built to support irrigation water supply (Sembenelli, 2011). The dam is sand-filled with a geomembrane or impervious lining, having a height of 24 m and a total length of 3,366 m. The capacity of the dam is 142 million cubic meters, with an exception in the rainy season, the Gada river which is a tributary to the dam is transient and only flows for four months every year, with a catchment area around Jibiya of approximately more than 400 km^2. Due to the characteristics of the soil type being sandy, a flexible impervious lining was constructed so as to adapt to the settling or deformation of the dam embankment.

Figure 1-12: Map showing an aerial extent of Jibia dam during the dry season and the adjacent *Fadama* site between November and March (source: Google Earth 2018).

Hence, an assessment of the dam in 2004 was rated as in good condition, though it was noted that no instrument readings were made since 1994 due to lack of training and technical know-how of the operators (Enplan Group, 2004). As at 2007, the dam was left and not being used for irrigational farming due to lack of fuel to run the pumps, which in reality, has caused a less utilisation of the dam resource readily available to be harnessed (Independent, 2007). The Gada River flows from Nigeria into the Niger Republic northward, and then back into Nigeria as a tributary to Goronyo dam via the Rima river. In the past, it used to be dry for eight months of the year, though, is now having a regulated flow throughout the year, which has improved the water supply into the Niger Republic.

1.3.6.4 Wurno dam

Wurno dam (**Figure 1-13**) is located within 13.287^0 N and 5.478^0 E at Wurno Local Government Area of Sokoto state in Nigeria. The dam is quite small if compared with other dams within the basin. Recently, the dam covers an estimated area of about 1.74 sqkm or 174.44 ha. The dam has a storage capacity of about 19,501,200 m^3 mostly being supplied from Goronyo dam upstream. The reservoir is linked to two main canals at lugu village and Tutudawa main canal that passes through the Tutudawa village, with a main drain and secondary canals (Dikko *et al.,* 2011).

At inception, the preliminary investigation by the British colonial administrators in 1955/56 led to the idea of looking into the possibility of harnessing, protecting and controlling water for irrigation scheme around the floodplain of Rima. As such, after this reconnaissance survey's recommendation, led to the rice cultivation scheme at Wurno (Ijir, 1994). This was achieved by the construction of a bund to protect an area of about 2000 ha. The strategy employed was to provide a backup plan for all farmers already engaged in the wet season rice farming in the *Fadama* areas which is constantly flooded by the Rima river. This was intended to later extend the bund so that the reservoir can be used for dry season cultivation on a limited area with a gross irrigable area of about 1,457 ha (3600 acres).

Figure 1-13: Map showing an aerial extent of Wurno dam and the adjacent *Fadama* sites during the dry season between November and March (source: Google Earth 2019).

The design of the dam commenced properly in 1957, while the construction of the main bund of the Wurno irrigation scheme and its field channels started in 1958 (Ijir, 1994). Conversely, due to the slow progress of work and the frequent breaching of the bund in the wet season led to the thought of abandoning the project in 1960. However, the expert invited advised on the situation and recommended the completion of the project. Following the recommendation, a contract was awarded by the end of 1963 for the completion of the scheme, with the intention of completing the project in 1964 but was later completed in 1965.

The initially carved out area was equipped with canals and drainage network of about 600 ha, and the sole responsibility of operation, maintenance and expansion was then handed over to the Northern Region Ministry of Agriculture, later to the native authority in Sokoto, and now to the Sokoto Rima River Basin Development Authority.

1.3.6.5 Zobe dam

Zobe dam (**Figure 1-14**)is located in Dustin-ma local government area of Katsina state in north-western Nigeria, with a coordinate of 12.388^0 N and 7.475^0 E. The dam is an earth-filled dam characterised with a height of 19 m and a total length of 2,750 m (International database and gallery structure). More so, the dam has a storage capacity of 179 Mca (Meter water column) with an active capacity of 177 million m^3 as well as irrigation potential of 8,000 hectares of land (UNEP, 2005). Though the barrier was initiated in 1972 and was completed in 1983, which as at 2010 was comparatively not being used for water supply to Katsina city, nor the local irrigation or for power generation as initially built for that purpose.

Figure 1-14: Map of Zobe dam showing the aerial extent of the dam during the dry season with *Fadama* site close to the dam between November and March(source: Google Earth 2018).

Among the environmental impact of the dam was that; heavy rain once caused the Zobe dam to overflow in September 1999, which resulted in massive crop loss (FAO & IITA, 1999). The flooded areas were inundated which caused the washing away of the planted millet,

groundnuts, guinea corn and beans. Consequently, the farmers who were inadequately deprived of their compensation at inception when the dam site was acquired, were destitute the more with the rainy season nearing its end and their crops completely destroyed (Irin, 1999). In short, this has further shaped the land use and land cover pattern of the catchment area as I observed during my field survey of the entire area.

On the other hand, in 2003 the water of the dam was seeming to be completely muddy and stagnant, as evaporation and leakages around the dam were gradually emptying the dam. Nonetheless, the authorities taking charge of the dam were then subdued to sink relief wells to augment the reservoir's water content. Due to this, the Sokoto-Rima River Basin Development Authority did not clear the land nor release water for irrigation farming. As such, the villagers could not use the water for their crops, and the new lake was almost empty of fish. In Aug. 2003, a director of Katsina State Water Board said that; lack of dedication and direction were the main problems that led to the non-completion of the Zobe dam for water supply. He also added that Zobe dam is one of the largest bodies of water in Nigeria commissioned since 1982, and with colossal irrigation potential but still lying wasted (Lawal, 2003). In December 2005, farmers were demanding the release of water from the dam, though nothing tangible has been staged to solve the problem due to poor policy implementation.

Domestic water supply capacity: The domestic water supply capacity was intended to deliver 65,000 cubic metres of potable water to Katsina metropolis on a daily basis. Which in January 2003, the water treatment plant which is 2.5 km from the reservoir was left half completed and as well abandoned. Booster stations and water tanks in numerous stages of completion along the route to the city was as well left. The only pipe that had been underlaid of 111 km required was the 2.1 km stretching from the reservoir to the treatment plant (Salisu, 2003). The water supply project needed thirteen billion naira to be completed, and President *Olusegun Obasanjo* approved the funding, which in the next month he paid a visit to the dam. Thus, when I checked the budget appropriation for each year from the National Assembly Budget and Research Office

(NABRO), funds are allocated, but from my field survey in Jan. 2018, nothing good is to be reckoned with.

1.3.7 Demography of the population within the catchment states

Nigeria's population growth depicts a very rapid growth rate to be more specific with the urban areas. In 1991, the total population in the states of Katsina, Kebbi, Sokoto, and Zamfara was having a total sum of 10,291,799 people, consisting of the Urban and rural population at the same time. While on the other hand, the total population as shown in the 2006 census of those states is 16,039,674 people, as cited in **Table 1-3**. The entire states within the basin have an average of inter-census growth rate of 3% and the average population density of 130 per square kilometer in the year 2006 (Annual Abstract of Statistics, 2012).

Table 1-3: Population census of the states within the River Basin.

States	1991Census Total Population	2006 Census Total Population			Land Size (/Km^2)	Inter Census Growth Rate (%)	Population Density (Km^2)
		Male	Female	Both Sexes			
Katsina	3,753,133	2,948,279	2,853,305	5,801,584	24,971	3	232
Kebbi	2,068,490	1,631,629	1,624,912	3,256,541	37,727	3	86
Sokoto	2,397,000	1,863,713	1,838,963	3,702,676	33,776	3	110
Zamfara	2,073,176	1,641,623	1,637,250	3,278,873	35,170	3	93

Sources: Annual Abstract of statistics 2012.

1.4 Ground-based Fadama yield data

1.4.1 Irrigation in Nigeria

The modern method of irrigation commonly used in Nigeria at different scales include:

(1) **The Sprinkler Irrigation:** here water is usually supplied to the field by overhead irrigation supply through an oscillating sprinkler head, or through continuous perforated holes in a pipe.

(2) **The Tubewells:** the tubewells supply irrigated areas with water from the well. These are usually an investment made on a broader holding. As such, this method is only gainful if surplus labour is available and if the pump is available.

(3) **Underground irrigation:** This irrigation type supplies water by surface irrigation, where 20 to 30 percent is usually lost through evaporation. Consequently, such lose is removed by an underground systems where the water is positioned directly in the root area of the plant using a perforated plastic tube through which the water is pumped under high pressure.

(4) **The Trickle or drip irrigation:** This is a method of irrigation that requires higher value crops where water is not readily available. The system conveys the water in a plastic piping through the main laterals, the sub-laterals and in due course through a tube and to each plant in the field. Hence, it sprays a continuous drip of water when the need for irrigation arise.

The development of agricultural strategies tailored by most of the national governments and the international organizations during the 50s and 60s were more of additional land resources for irrigation development.

There are significant component of the plan put forth by the UN in 1974 at the world food conference in Rome. This emphasize the role of agricultural development in the developing nations as paramount. Without any dynamics in the growth of agriculture, sustainable economic growth will remain unlikely, and the population growth rate will be rapid and very high. Therefore, the government must acknowledge that the industrial

policies may fail if they decide to neglect agricultural development even at a smaller scale level. It is only when agricultural development foster the desired increase in economic well being and sufficient demand as an essential factor for the elimination of the food problem, that is when industrial development will be highly achieved.

As outlined by (Norman, 1996), the benefits of development in irrigation are; thus:

(1) It Increases the range of choices in crop production and livestock rearing, thus providing feasible decision-making.
(2) Reduces the risk of crop failure and the range of crop yield fluctuation, hence reducing the number of uncertainties.
(3) It increases the capacity of the land input concerning other irrigation factors;
(4) It increases the size of farm businesses.
(5) It supports the shifting of the factor-product curves towards a higher input and greater crop production.

Additionally, it is evident that socio-economic profits are essential features of any irrigation project. Generally, to any agriculturist, irrigation promotes optimum yield per hectare. Nonetheless, socio-economic considerations can as well be an advocate of irrigation farming. Because, with the irrigation, it is expected that there will be much sufficient food available in the irrigated areas and more areas of cultivated land with large output are the expected advantages one can derive from irrigation farming.

Dry season farming within the *Fadama* areas has the dyadic advantage of crop rotation and diversification. Such that if a particular crop fails or gets ruined, another plant will augment the food security and economic returns. Because dry season crops allow the farmer to supplement his household financial security and investment, while on one hand, gets the money to buy food in case of crop failure. Consequently, this will boost the economic fortunes of farmers and alleviate their shortages in the event of adverse conditions or any disaster.

More so, another argument with regards to the irrigation project implementation as derived from above. It was said that if all the afore-stated criteria become the fortune

of many farmers, they will be more likely having the capability to improve their production or more individuals are likely to influence and end up as contact innovators. It is with no doubt to be an operation at higher socio-economic status.

Conversely, irrigation may also give the government the mandate to exercise greater supremacy over farmer's cropping decisions through the use of extension services, and this will make it easier for the government to regulate agricultural taxation.

Indigenous *Fadama* irrigation farming system has a long history in the Northern part of Nigeria. World Bank impact evaluation report on Nigeria revealed that dry season *Fadama* land has existed for a very long time between twenty and fifty years in this region. The simplest indigenous irrigation method is the bucket-lift system or the 'shadoof' **Figure 1-15c**. According to history from rural community leaders, the shadoof was brought from Sudan over a century ago by the trans-Saharan traders. While such a device is low cost, it also depends mostly on farmers' labour for construction and operations, their irrigation potential is limited to only small plots. Water lifting by such devices is hard and laborious, however, the area which can be irrigated is limited to about 0.1ha per shadoof (World Bank, 1995).

From the history of shadoof use in the northern part of Nigeria, it can be confirmed as not new, the practice is confined to a smaller proportion of farmers two or three decades ago. The World Bank, 2010 reported that in the part of Sokoto state for instance, several community leaders states that only about five to ten percent of the rural households were cultivating their own *Fadama* lands during the dry season twenty or more years ago. Although, most of the villages sampled had some in use as at that time. Now, almost all the farmers are involved in recent years, this indicates a progressive change that has occurred over the past years (Eniolorunda, 2017).

Shadoof usage is one of the different irrigation methods used in the dry season farming in the northern part of Nigeria. However, each method depends on the economic capacity of the farmer's involvement and the level of crop production. Whichever way, it is an established norm that the dry season *Fadama* farming is a

coping mechanism to extend the farming period so as to boost agricultural production and productivity after the wet season.

The concept of *Fadama* Irrigation emanate from one of the World Bank assisted programmes with the invention of the (NFDP) National *Fadama* Development Programmes in the early 90s, (Mohammed, 2002). The *Fadama* concept is an age-old traditional practice in Hausa land of most northern Nigeria, where the seasonally flooded *Fadama* land at the valley bottom, allows the cultivation of a variety of crops under small scale irrigation farming system. Irrigation farming in modern agriculture, depend on damming substantial streams to store and control the flow of water that will allow delivery of the desired amount whenever the need arises. Examples of modern irrigation used are surface irrigation, border or drip irrigation; corrugation and sprinkler irrigation just as cited earlier (Cox & Akin, 1979). In another perspective, modern irrigation types are further dichotomized into two:

(1) Large-scale, i.e. (gravity flow irrigation) through which dams or water carrying channels and structures are constructed to transport water into the field. This is very common in the dry region of northern Nigeria.

(2) Pump irrigation; here the water is pumped either from the groundwater storage or surface water sources to the field.

(a): Parabolic canal coveying water to the field. Jibia dam *Fadama* site.

(b): Water being pumped from the reservoir to the field at Ruwasanyi *Fadama* site

(c): A local shadoof or bucket lift used for water delivery in the irrigation areas.

(d): Sprinkler irrigation at Bakura irrigation project site.

Figure 1-15 (a-d): Showing how water is transferred to the field for *Fadama* irrigation (field visit Jan. 2018).

In an attempt to define *Fadama* irrigation as a good technology in the agrarian revolution in Nigeria, it will be wise to clearly state the right technology that will systematically apply collective human rationality to problem-solving through the basic assertion of control over nature and all kind of human activities. In this context, agricultural technology can be perceived as the application of the specific technique for the development and promotion of agricultural system (Umar, 1994).

Furthermore, the apt technology carved out for the peasant farmers should encompass the set of gadgets or objectives that will unlock new resource, increase productivity and at the latter, brings new capacities to produce goods and services in the farms.

With regards to the choice for an appropriate technology as suggested by Mohammed, (2002), Erhabho & Nwagbo, (1985), should base on the socio-cultural consideration of the farmers with specific attention to the simple nature of the technology. Such that the majority of farmers can put that into use at a reasonable cost and capital returns, while the technology should minimize the cost and maximize the profit at the verge.

Also, national sovereignty consideration should be a choice of which technology should be seen for national economic consciousness. Additionally, the World Bank, (1989) recommended that for a project to be right and viable, it should be formed and structured so that it is sustainable under prevailing socio-economic conditions, and it should be viewed as an added advantage to those intended to benefit from it and as a plus for efficient use of national resources.

It has also been observed that the major infrastructural facilities are only one among the social, technical, and economic criteria which determine the success of any irrigation project in Nigeria. The farmer's participation and their acceptance to use the new technology depend on their involvement in the design, selection, and construction of the irrigation project.

Therefore, the most disturbing problem in the development of any irrigation does not directly relate to storage and delivery of water alone, but rather the success of the

irrigation programme in the long-term, and also covers water resources management, control of salinization as a matter of concern and as well water-logging.

One way to formulate appropriate and adaptable technology to farmers is by analyzing the biophysical and socio-economic constraints of farmers production. This needs both an ecological and an economic approach. Hence, this formalizes the body of complex relationship characterized in traditional farming systems in general.

In making a comparison to alternative water lift technologies in the irrigation system, many variables must be considered adequately. The rationale in making a choice depends on the resource and the environmental situation of each farmer. Factors like water supply, i.e. (source), labour supply, farm sizes, marketing and among others must be checked upon (Erhabo & Nwagbo, 1985; Jamusz, 1990). In order to plan productive land and water development programmes in the system, it is vital for the institution of concern to have clear and accurate information about the present uses of these resources for a well informed and explicit explanation of the whole system.

1.4.2 The existing irrigation scheme and types within the river basin

Irrigation has been defined in the literature as the application of water on the soil to augment moisture essential for plant growth (Mohammed, 2002). It is also to provides cover against droughts, cooling the land and atmosphere.

Irrigation would not be necessary if the distribution of rainfall were ideal for the cultivation of plants (Baba, 1993). In Nigeria, the variations or difference between the north and south are quite significant in terms of agro-climate conditions and several agricultural practices across the country due to the disparity. The concept of development in agriculture is within the context of numerous developmental paradigms assumed by eminent scholars in the field of agriculture, sociology, communication, and economics. Both in policy and practice, these postulations shows that many countries in the developing world are experiencing changes within the agricultural sector. For

example, the Problem Solver Model has significant implication for agricultural development efforts in Nigeria.

Fadama irrigation farming in Nigeria, is by far the most significant water-use sector with over 1,732 million cubic meters of water storage in the Sokoto Rima River basin, it is affected by the change in water availability that is disturbed by climate change in general. Climate change impacts bring about an increase in evaporation and moisture deficits to most water bodies **Figure 4-8**. This deficit produces a change in the need to increase the amount of water that is needed for irrigational farming. Higher temperature and a more pronounced variability in rainfall tend to increase the water demand per unit of the irrigated area, unless if the total rainfall rises so as to sufficiently augment the demand (Gerten *et al.*, 2011).

The climatic conditions of SRRB enhances the need for irrigational farming, specifically for the cultivation of cereal and vegetable dominant farming system. (Ekpoh & Ekpenyong, 2011).

Furthermore, as shown in **Table 1-4** below, the small-scale irrigation projects within the basin that are found at Bakura, Gagere, and Kware comprise a total area of 950 km^2. The farmers in those places usually grow rice, tomato, watermelon et cetera, with carrying capacity of 5 m^3/sec to 20 m^3/sec of water through the different capacity of the supply canals and also the spillway (Abdullahi, 2011).

Table 1-4: Small scale existing irrigation

Project	River	Water Source Works	Irrigation area (km^2)
Gagere	Gagare	Weir	100
Bakura	Lake Natu	Pump	50
Kware	Rima	Pump	800

(Source: Abdullahi, 2011)

The medium scale irrigation projects found in Rima valley, Bakalori, Zauro and Wurno covers a total area of 44,000 km^2 as shown in **Table 1-5** within the basin. The Bakolori project was formed to supply water to 15,000 km^2 area by gravity inclined canals and 8,000 km^2 area by sprinklers. The system is supplied by a 15 km long concrete lined supply canal which is crossed by 35 culverts in numerous points, and as well foot and vehicular bridges within the catchments. It has a carrying capacity of 30 m^3/sec and at the end of the supply canal, a spillway is positioned and automatically syphon the water to curb overloading.

Table 1-5: Existing medium scale irrigation

Project	**River**	**Water source**	**Irrigation area (Km^2)**
Bakolori	Sokoto	Dam	23000
Zauro Folder	Rima	Dam/Boreholes	13000
Middle Rima Valley	Rima	Dam	6500
Wurno	Rima	Dam	1500

(sources: Abdullahi, 2011)

1.4.3 Understanding the driving factors of intensification through an in-depth yield gap

The enormous potential for improving agricultural production through intensified farm practice is frequently mentioned in several kinds of literature (Mueller *et al.*, 2012). The yield gap shows the differences between yield potential and average farmers' yields over a specific spatial and temporal scale (Lobell *et al.*, 2009). Yield potential is defined and measured in numerous ways; often, it is referred as the attainable yield, i.e. the yield that can be realised at a location under the optimal management of the whole process. Which at the global level, the analysis of yield gap is either based on comparing or weighing crop growth models with a contrast on actual yields as reported in statistics. Or it may be based on empirical techniques that compare the highest realized yield with the actual yield that is reported in the same database, so as not to be bias due to the use of multiple and inconsistent data sources (Neumann *et al.*, 2010).

However, there are many cogent reasons for the deviation from the actual and as well the attainable yield between actual and potential cropping cycle intensity, that is; the time of fallow periods and the number of crops cultivated per annum (Neumann *et al.,* 2010, Verburg *et al.,* 2000). Though one reason may be diminishing returns on inputs, which reduces the economic profit capacity of increasing contributions (Duflo *et al.,* 2008). While an increase in the price of agricultural produce will likely increase the use of inputs for more profit.

As such, there are several other reasons for non-optimal management of most croplands. These include land manager's openness to credits which are of limited access, limited opportunities for agricultural inputs and knowledge, and high risk of losses on crop failure base on climate change variability. In certain cases, sub-optimal inputs are associated with land governance and tenure, e.g. because of insecure property rights. While on the other hand, tenure does not always assure higher investments (Place, 2009). In several cases, the yield gap is different for rain fed and irrigated or *Fadama* agriculture (Lobell *et al.,* 2009).

Irrigation is hence, a norm for intensification in many areas, but not completely defined to drylands. We should bear in mind that irrigation often requires central investments in infrastructure (Neumann *et al.,* 2011), and of course, water availability for irrigation is shrinking in some areas due to the menace of climate change (Gerten *et al.,* 2011) see **Figure 4-8a**.

Closing the yield gap clearly comes at the cost of social and environmental externalities like pollution of surface and groundwater by agrochemicals as the loss of employment due to mechanization is also a factor (Pretty *et al.,* 2011). The ecological costs of closing the yield gap can be reduced by directing all efforts to increase yields in regions with the lower yield, but it requires global efforts on technology transfer from richer to poorer countries. Which such a strategy will indeed enhance the soil fertility in the region in relation to using fertilizer inputs efficiently (Tilman *et al.,* 2011)

The underlying purposes for the yield gap and the implication of intensified agriculture, have been analyzed in many case studies (Keys & McConnell, 2005). But further research is needed to synchronize the understanding involved in most of the constraints closing the yield gap at a local scale to the global level of assessments. This will assist to point at the regions where different solutions like technical, infrastructural or socio-economic factors may relief the constraints of intensified production with low social and environmental externalities.

Pretty *et al.*, (2005) reports a meta-analysis of a case study of sustainable intensification option identified in 286 projects worldwide. The result showed that, despite high variation in success, there is a possibility to increase agricultural practice without increasing more of the environmental externalities. The meta-analysis precisely outlined measures for more efficient water use in both the dryland and the irrigated farmland, improvements in the accumulation of organic matter in soils and pest, weed, and disease control, which emphasizes the in-field biodiversity as means that yielded both positive impacts on yield and as well an improved supply of ecosystem services. Hence, sustainable intensification that will not compromise is indeed an option, but it requires full consideration of the socio-economic and environmental drivers underlying the contemporary of non-optimal yields.

1.5 Remote sensing data

1.5.1 Fadama utilisation from remote sensing change detection analysis

Changes in land use/cover are of critical concern for the environmental change research community globally, because identifying change on land use/cover will help decision makers to provide solutions efficiently. Land use change is influenced and determined by the loss of biodiversity, climate change, and the sustainability of human interactions with the environment such as food cultivation, water use, and most importantly human health. Land use/ cover changes encompass not only the changes in land cover but also the characteristics in which the land is used and the intent describing that usage (Turner *et al.*, 1995).

Therefore, Land change science has a characteristic of place-based studies, with much concern on local causes of land use/cover changes and amending national and global indices as boundary conditions (Lambin & Geist, 2006). Several independent streams of research have recently come together to identify the growing concern of the relevant drivers of land use/cover changes; with interconnections between socio-ecological system that is geographically separated, and as well the indirect consequence of land use changes as it arise across the international boundaries and in the context of differing policies at national regimes. Hence, the purpose of this review is to trace the multiple write up of the literature and propose paths to synergise them where possible as in the case of this research (Lambin & Geist, 2006).

From local processes to highly globalised land use/cover changes, the cause and agent of land cover changes are being studied over the years (Rudel *et al.*, 2009). Ranging from the 1960s to 1980s, small-holder farmers sometimes get encouraged by state programs of agricultural modernisation, which are sometimes seen as the main actors of tropical land cover change.

However, internationally, some pushing forces are recognised, as deforestation and other land change phenomena were examined as domestic processes shaping the whole scenario by connecting socio-economic survey data on land change with GIS and remote sensing data on land use decisions (Fox *et al.,* 2003, Rindfuss *et al.*, 2004). Therefore, Verburg *et al.,* (2002) state that explicit spatial land use models account for a closer determinant of land use changes.

As such, change detection in the Sokoto Rima River Basin is the process that identifies the difference in the state of the basin and its phenomenon, by observing that phenomenon at different times (Singh, 1989). Change detection is an essential task in monitoring and managing natural resources and as well urban development, because it shows a quantitative analysis of the spatial distribution of all population under consideration.

A list of three aspects of change detection which are important when monitoring natural resources were observed by Macleod & Congalton, (1998):

i. Detecting any changes that have occurred

ii. Measuring the extent of the change

iii. Assessing the spatial pattern of all the changes observed

1.5.2 Satellite remote sensing and Normalised Difference Vegetation Index (NDVI) as a source and tool for land change observation

Remote sensing is characterised as a source of thematic mapping like those portraying land cover which show a map like representation of the Earth's surface that is highly consistent and spatially elaborate, and as well readily available at an array of temporal and spatial scales. Environmental researchers often use remotely sensed imagery, by superimposing them on other geographic information or demographic information to provide a more refined and detailed picture of the earth's landscape (Carlson, 2003).

Spectral vegetation indices usually composed of the red and near-infrared reflectance radiance (Tucker, 1979), which sometimes include additional channels. Remote sensing measurements; are most effective and are widely used (Cracknell, 2001) for useful result, and they are usually analysed with the photosynthetically active biomass in plants, chlorophyll presence, and of course energy absorption capacity (Myneni *et al.*, 1995).

The Normalized Difference Vegetation Index (NDVI); has become the most used analysis derived from NOAA AVHRR data (Cracknell, 2001), which is mostly associated by the use of NDVI datasets gotten through the maximum value composites (Holben, 1986). The AVHRR NDVI data have been extensively used since 1981 in the study of numerous global land processes or activities (Townshend, 1994, D'Souza *et al.*, 1996; Cracknell, 1997; Defries & Belward, 2000). Though this was never anticipated by those that design the AVHRR instrument which had no idea what a vegetation index was at inception.

Long-term satellite images are essential to help us understand land cover dynamics, and they are especially useful to detect vegetation change (Gong, 2012). Other studies on vegetation change detection focus on using two or more dates of Landsat archives at an interval of five(5) or ten(10) years (Griffiths *et al.,* 2014).

Researchers have applied Remote Sensing and Geographic Information System (GIS) to peruse the landuse and landcover change detection around artificial lakes in some part of the world. As seen with Mattikalli, (1995), he applied remote sensing and GIS to assess the landuse change of the River Glen catchments area in England from 1931 to 1989 satellite data. His work showed that much of the grassland changed to arable land in the study area. Okhimanhe, (1993) combines Spot HRV imagery of 1986 and aerial photographs of 1974 to examine the environmental impact assessment of Bunimburum and Tiga dam in Kano state of Nigeria. The work uncovers that the construction of Tiga dam depleted the vegetation that could have assisted in curbing desert encroachment.

Adeniyi & Omojola (1999) used aerial photographs, Spot XS/Panchromatic Image Transparency, Landsat MSS and Topographical maps to study landuse /landcover changes in Sokoto and Goronyo dams Nigeria, between 1962 and 1986. Their work showed that settlement covers some part of the area before and after the construction of the dam. Ikusemoran, (2001) used Landsat multispectral land use and vegetation cover maps of 1978, 1995 and as well as 1965 aerial photographs to study the land use /landcover change of Kainji lakes in Niger state. The study depicts that the reservoir of the Kainji lake was expanding with an increasing agricultural activity around the lake.

1.6 Climate and surface water data

1.6.1 Climate change impact

An unprecedented warming of the global climate has been observed in the past 1000 years (IPCC, 2001). This phenomenon is inevitably disturbing the characteristics of most local and the entire weather of the globe. IPCC, (2007) [a,b] Fourth Assessment Report (AR4), defines climate change as the change in the state of climate that can be identified using statistical datasets, which depicts a change in the mean variability of its properties, and persists for an extended period usually a decade or long (**Figure 1-16 and Figure** 1-17).

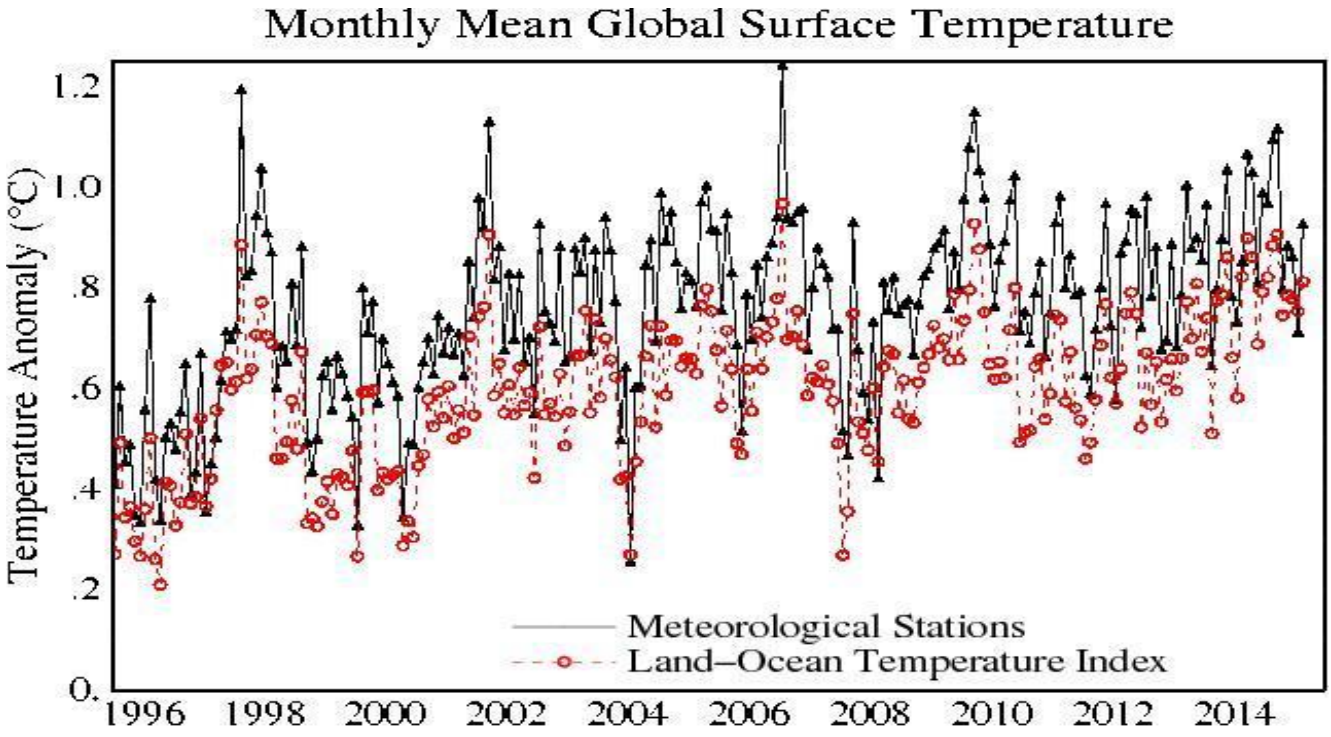

Figure 1-16: Variation of the earth temperature for the last 20 years. Depicting that the atmospheric heating is not evenly distributed at the surface as we should expect, and the historical records advices that the land surface temperature will increase more rapidly than its global average (Source: NASA http://www.giss.nasa.gov/)

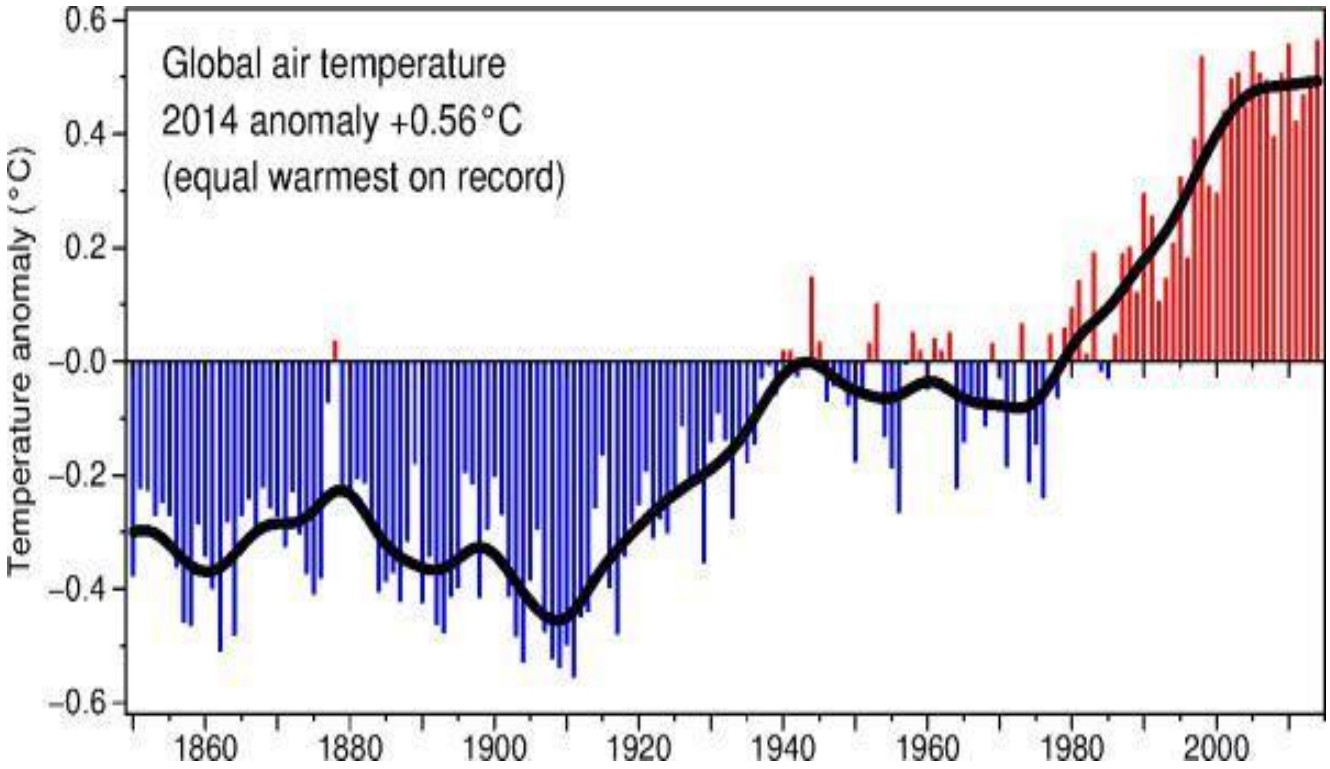

Figure 1-17: Variation of the earth temperature for the past 140 years. From the linear trend of the global surface temperature starting from 1906 to 2010, the earth is obviously warming up to about 0.56°C, i.e. for the past 50 years, the earth's surface shows a quiker warming trend. (Source: Trenberth *et.al.*, 2007)

Among the most significant changes, are observable trends concerning the rising of temperature over land and sea as shown in (**Figure 1-16 and Figure** 1-17), receding glaciers and rising sea level. As such, the evidence of climate change in Nigeria as reviewed by Odjugo (2005; 2009), is the increase in precipitation amount around the coastal areas since the 1970s. While on one hand, there is a decline in rainfall duration and a rising temperature in the interior hinterland of the semi-arid region of Nigeria in the North; like the Sokoto Rima River Basin. From **Figure 1-18** as shown below, the annual mean of temperature and rainfall around the basin can also be tailored towards understanding that the climate is changing, with rising temperature and cessation of rainfall duration in the SRRB.

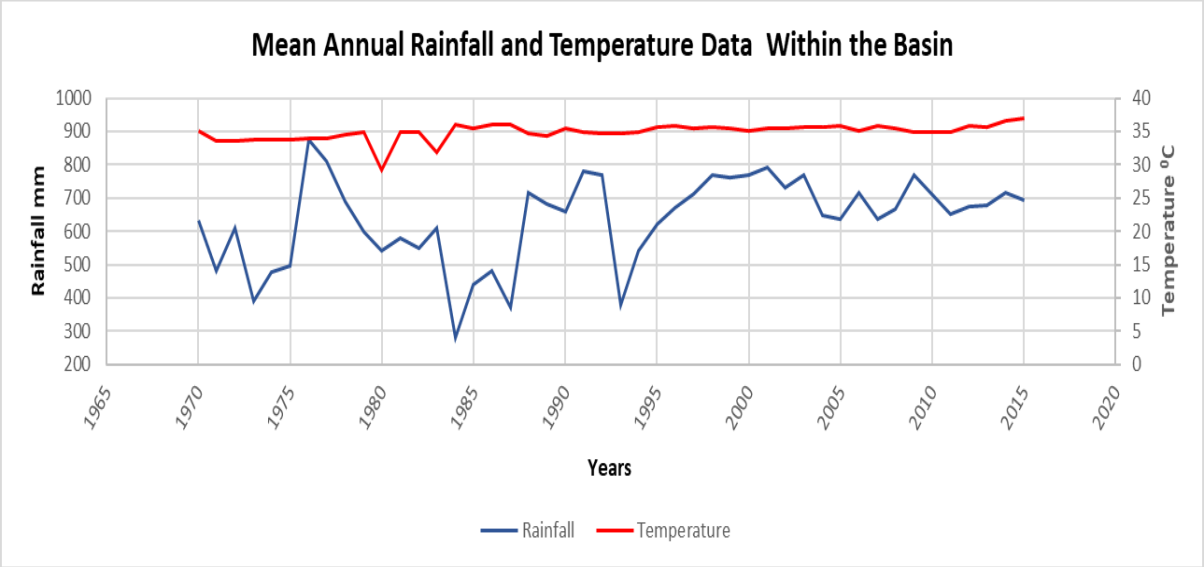

Figure 1-18: Graph of annual rainfall data against the temperature data over the past 45 years within the Sokoto Rima River Basin. The chart shows that from 1970 to 2015, there is a great rainfall variability from 874 mm in 1976 to 694 mm in 2015. Whereas the temperature ranges from 34 ^{0}C in 1976 to 37 ^{0}C in 2015. As such, this has great influence on surface water dynamics and landcover because, with varying rainfall pattern in the basin and a corresponding increase in temperature, there will be an increase in evapotranspiration, which will in turn affect the dam levels, vegetation cover and cropping pattern as well.

As observed by (Odjugo, 2010), the increasing amount of rainfall in the coastal cities and other areas around heavy water bodies, is partly responsible for the recurring floods devastating the towns of Warri, Lagos, Port Harcourt, Calabar and Benue around the Benue Trough. While the increasing temperature and decreasing precipitation rate in the semi-arid region of Northern Nigeria in Sokoto, Katsina, Kano, Yobe and Maiduguri around the chad basin, have resulted in the rapid evapotranspiration, recurring moderate drought and desertification (Odjugo & Ikhuoria, 2003). Hence, the continuous loss of forest cover and biodiversity in Nigeria, is however, linked to the global warming and climate change within recent years (NEST, 2003; Ayuba *et al*., 2007).

The Sahara is expanding to all directions trying to engulf the Sahelian region of Africa to be precise with the verge of the northern Nigeria (Yaqub, 2007). Odjugo and Ikhuoria, (2003) also observed that around 12^0 N of Nigeria's northern region, the place is under severe threat of desert encroachment because, sand dunes are now apparent features of desertification in states like Katsina, Sokoto, Yobe, and Borno. Thence, the transported sand dunes have covered a vast expanse of arable lands in the

far north, thus; gradually reducing viable arable lands and crops' production **Figure 1-19.**

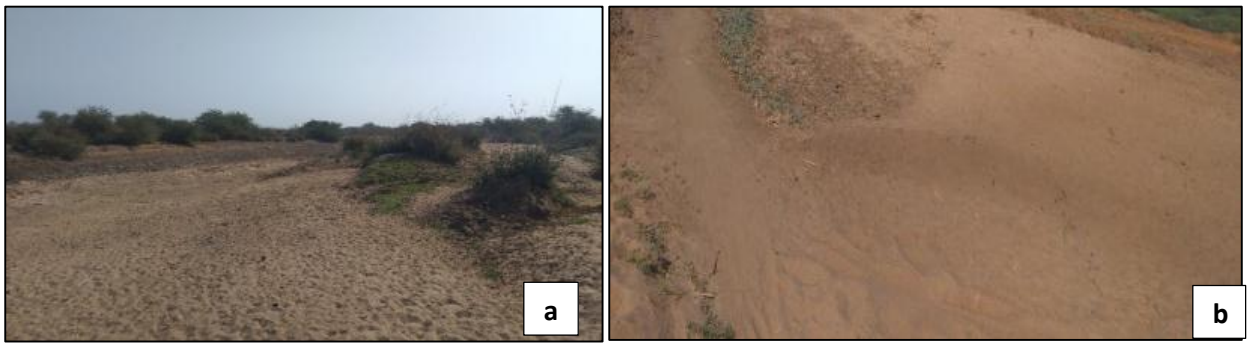

Figure 1-19 (a-b): Evidence of desert sand and dry spell in the rivers around Goronyo area Lat. 13.451^0 N Long. 5.711^0 E, within the Sokoto Rima River Basin.

1.6.2 Effect of climate change within the basin

The Sokoto-Rima river basin lies within the Sudano-Sahelian belt, and it is generally considered as an agricultural region, predominantly over 70 percent of the population engaged in subsistence farming (Emeribe *et al.*, 2017). The main crops produced in the study area are millet, guinea corn, potatoes, rice, maize, beans, wheat, cassava, groundnut, cotton, sugar cane, and tobacco (Ita, 1993).

Thus, the changes in climatic variables or a prolonged climatic variability in rainfall, have adversely affected farming operations in this basin see **figure 1-20** below. Similarly, Adelana *et al.,* (2003) also uncovered that less frequent and short period of precipitation within recent years (usually less than 60 raining days) in most of the basin have deterred the development of agriculture, restricting crop production to only one planting season per year.

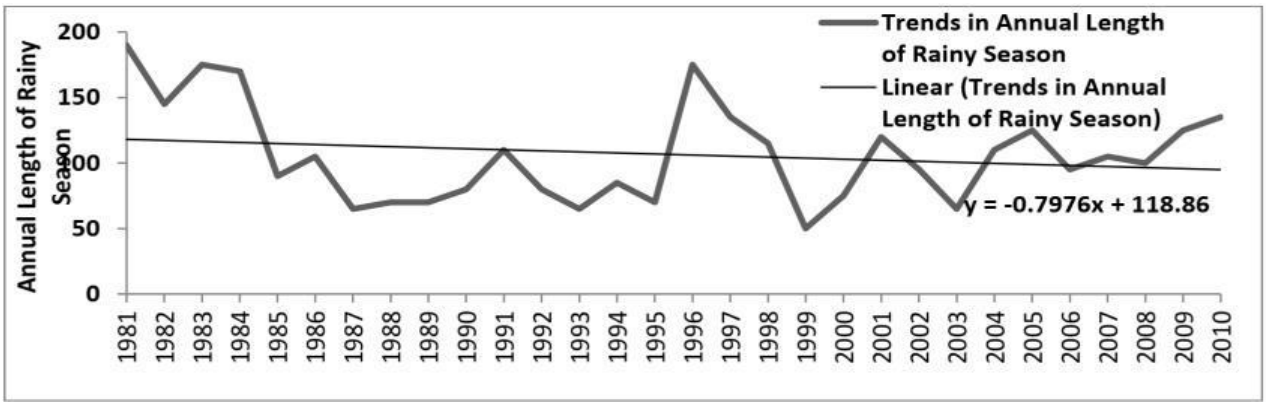

Figure 1-20: Trend in length of the raining season at Goronyo from 1981-2010. (source: Ikpe & Sawa, 2016).

From the linear trend of the line equation for the length of the wet season**,** y = -0.7976x +119, this is depicting that it is significant and there is a negative trend with the length of raining season decreasing in Goronyo. The peak length of the wet season within the thirty years of observation in 1981 was recorded to be 190 days out of the 365 days of the year. While the shortest duration of the raining season was recorded in 1999 with 50 days only. Nonetheless, the mean length of the wet season was calculated to be 107 days. As such, with this observation, it can be deduced that the effect of climate change on rainfall within the basin is indeed clear and will disturb crop production and further exacerbate a decline in the yield of crop which is a threat to food security. Though with possible adaptation strategies, the issue can be managed as shown in section 1.6.5 below.

1.6.3 Impact of climate change on surface water and landcover change

Climate is defined as the average weather condition of a place. Or it can be further defined as the statistical description of the mean and variability of relevant factors over a long period of time, ranging from months to many or thousands of years. As defined by the (WMO) World Meteorological Organization, the classical period for averaging these variables 30 years, as it will give you a more defined and precise picture of how the climatic condition of that place tends to look like.

The most observable climate drivers in terms of water availability are usually temperature, precipitation, and evaporative demand; (normally determined by the net radiation from the ground surface, to atmospheric humidity, wind speed, and temperature).

The observed global warming through the past decades is attributed to changes in components of the hydrological or water cycle. At the same time, certain phenomenum of the hydrological systems like; altering the precipitation patterns, intensity and extremes of the weather; widespread snow and ice melting; increasing atmospheric water vapour; increased evaporation; and likewise changes in soil

moisture and surface runoff are some factors experienced (Abdullahi, 2011). See **Figure 4-5a-f.**

1.6.4 Climate variability impact on crop yield

Climate variability and the impact it has on the human population in most sub-saharan African countries is quite a global concern. The Sudan and Sahelian regions that are mostly characterised as an agrarian region in Nigeria is most likely affected by the unprecedented patterns in the climatic condition of the region. This is because, farming activities in this region of Nigeria is predominantly of rural type, with over 80% of the farmers practising rain-fed agriculture at subsistence level (Ekpoh, 2010). The smallholder farmers cultivate their land on a subsistence scale rather than commercial purposes. This is absolutely depicting that the aim of crop production is not to improve profit, but just for domestic sustenance to meet their nutritional needs and the surplus for income generation mostly during the dry season when foodstuff is a bit costly in the local market across the country.

Climate is a paramount determinant of agricultural activities, to be specific with the developing nations like Nigeria; where agricultural practices are basically dependent on natural phenology of the environment. As such, climate change is influencing crop yield to a greater extent in developing countries juxtapose to crop production. Because valid characters in climate change that influences an increase in temperature, changes in precipitation pattern and climatic extremes like droughts and flooding will eventually affect crop yields. As such, an increase in temperature will reduce yields and quality of crops, as it will exacerbate the vulnerability in the supply of food. Also, changes in precipitation pattern for example high rainfall concentration in a particular month; has a devastating effect on crop production (Mendelsohn, 2008; McCarl *et al.,* 2001) just as cited in the Zobe dam incident which caused a great loss to most farmers as aforementioned.

The challenges infringed by climate change on agriculture generally ranges from profound seasonality in rainfall pattern. Which in essence, confines the cultivation pattern to a short period of three (3) to five (5) months, this is due to severe recurrent moderate drought that is absolutely disrupting the usual pattern of seasonal hydrological characteristics of water availability see (**Figure 4-2** (a, b) to **Figure 4-5** (a, b)**)**, and at the verge, leads to alterations of seasonal rainfall distribution pattern (Adefolalu, 1986; Aondover & Ming-Ko, 1998; Anyadike, 1993; Anyanwole, 2007). These climatic constraints attributed to crop cultivation in the region distribute a timing of farm operations that are essential for obtaining optimum yield difficult. Due to this problem, there have been recurrent crop failures and declining yields that led to low farm income and as well associated problems of food shortage or food insecurity, malnutrition and the general impoverishment of local farmers (Mortimore, 1989; Ekpoh, 1999; Mortimore & Adams, 2001).

Numerous studies have perused the impacts of rainfall variability on crops yield solely to examine the impacts on some specific crops using statistical modelling. Among these are the works by Tim, (2000), Adejuwon & Odekunle (2006), Adejuwon (2004), and Onafeso *et al.*, (2015). However, Tim, (2000) examined that; from 1961 to 1990, the Northeast arid zone of Nigeria has experienced a decrease in annual rainfall. These have led to a decline in the production of millet, and the variability of rainfall pattern in the region is seen to bring about differences in the types of plants cultivated and as well the yield of the crops (Adejuwon & Odekunle, 2006).

More so, the high spatial and temporal variability of rainfall pattern depicted by the dry spells, flooding and continuous moderate droughts, may be seen closely as the most relevant factor disturbing agricultural productivity in sub-saharan Africa. This is often seen as the main reason for crop failure and food insecurity or food shortages (Sivakumar, 1988; Sultan *et al.*, 2005; Onafeso *et al.*, 2015).

1.6.5 Crop yield variability and climate change adaptation.

Several studies have shown that the yield of crops will likely decrease by 10% by 2050 (Akumaga *et al.* 2018) due to climate change and the chronic history of underperformance in agricultural production, and as well the rising population growth in West Africa. And to keep pace with this, a five-fold increase in the production of food needs to be achieved (Thornton *et al.* 2011).

In spite this projection, potential adaptation and mitigation strategies have braced the presage of this phenological constraint. For example, using Cropsyt simulation model (Tingem & Rivington, 2009), the effect of changing crop cultivars of sorghum, maize and sowing date was investigated in Cameroun. Their results showed that by changing the sowing date, a yield gain of 8% on maize and 12% for sorghum was realized, which compensate the expected yield lost due to climate change (Akumaga et al. 2018). While impressive, other farm management strategies could significantly alleviate the effect of climate change (IFPRI, 2009). For example, in spite the increase in temperature and the unprecedented rainfall variability in the semi-arid region of West Africa since the 1960, farmers have managed to double yields of several crops grown using cultivars in the region.

Akumaga *et al.* 2018, investigated climate change mitigation and adaptation on yield of crops within the Niger basin of West Africa using AquaCrop developed by FAO. It first quantify crop yield response in the basin, then examined the effect of various adaptation strategies in mollifying climate change impact on crop yield. AquaCrop simulates yield of crops based on water consumption, and has proved to be effective in modelling crop yields in various parts of Africa. Using experimental field data at the Institute for Agricultural Research, Zaria in Nigeria. The authors arrived at the agreement that simulated and observed yields is consistent with those reported in other places, and suggests that the model can be used as a tool in the modelling and study of maize productivity in the region (Akumaga *et al.* 2018).

AquaCrop calibration and evaluation of maize, sorghum and millet was used for each site using historical climate data and the same cultivar, time of planting, plant

density, soil characteristics, and soil fertility levels obtained from the observed samples. Then they further assessed the model fidelity between the simulated historical yield and the measured yield using an index of agreement which measures the level to which the simulated values matched the observed values. Thirdly, with the achieved simulation of the historical yield, the calibrated model was then used without further adjustment to predict future crop yield. Finally, the work of Akumaga *et al.* 2018, showed that in all cases, soil fertility is assumed to be poor so that crop yield is a function of ambient soil fertility status only. The index values show that AquaCrop simulated for maize and sorghum yield can be considered good to very good in all the ecological zone.

1.6.6 Management strategies and climate change adaptation.

As opined by Akumaga *et al.* 2018, the possible adaptation strategies investigated in mollifying the effect of climate change on agricultural production within the Niger basin include:

1. Adjusting sowing date: changes in planting date from early planting to mid planting date and late planting date have proved to be effective in the mitigation of climate change. Climate change may result to an increase or decrease in the length of growing season relative to historical period. As such, with the afore-stated changes in sowing dates, the yield of crops will differ as you practice any of the mitigation strategies with late planting date yielding less agricultural produce in the sahel zone due short duration of rainfall.
2. Increased soil fertility: increasing soil nutrient in the event of adverse climatic condition will ameliorate the expected climate change induced yield loss. This is because, using AquaCrop model by Akumaga *et al.*, 2018, four level of soil fertility was used to assess the process. The four levels include poor, moderate, near optimal and optimal soil fertility corresponding to nitrogen content of 0 kg/ha, 60 kg/ha, 90 kg/ha and 120 kg/ha respectively. The fertility level was tested for each location based on the ratio generated from soil fertility stress determined by crop biomass production. The ratio was calculated as the total

dry above the ground biomass at the end of the planting window in a field with soil fertility stress, divided by the dry above the ground biomass at the end of the growing period of the field without soil fertility stress. Therefore, it appears that the increase in soil fertility serves as a compensation for the decrease, ameliorating the impact of phenological constraint.

3. Change in cultivar: To investigate how effective this process is, two cultivars were used to determine the yield and response of each crop variety to climate change, i.e. long duration and the medium duration cultivars. Thus, the resulted simulation integrates both the first and the second adaptation strategies. Hence, the result shows a good level agreement between the simulated and actual yield of maize at Markurdi in Benue state and sorghum at Zaria in Kaduna state.

Overall, the selection of planting date in relation to an increased soil fertility and the type of cultivar to be used in the field will indeed enhance crop yield, and serve as a good strategy in the mitigation and adaption of climate change across the ecological zones in West Africa.

Summarily, from the reviewed literature, the Sokoto Rima River Basin has a vast resource that requires much attention with regards to *Fadama* farming system. In spite all the research conducted in the basin, it is evident that more research is required to further fill the identified gaps in terms of understanding climate change and its presage within the contemporaries, issues associated with the land use and land cover change, crop yield pattern and how the water resource can be efficiently managed in the basin. This will actively brace food security and as well boost the entire agricultural system in Nigeria, which is major target of the government in recent years.

1.7 Outline of the thesis

This thesis is sub-divided into four data and analyses chapters. The first chapter deals with the irrigation farming system within the Sokoto Rima River Basin and the *Fadama* crop yield. This will give the research an insight on what the *Fadama* irrigation is and how does the crop yield pattern vary across the basin using the ground-based yield data.

In chapter three, it delineates the remote sensing of the *Fadama* areas using the land use and land cover change classification from 1988, through 1998, and to 2018 using Landsat and Google Earth Engine classification methods to assess the change. Nonetheless, the Normalised Difference Vegetation Index (NDVI) is also examined in this chapter to determine the level of green cover vegetation, and the extent of the *Fadama* farming. With much emphasis on how the vegetation index influences the estimated crop yield, using the Pekko NDVI and the Google Earth Engine NDVI time series data from MODIS and the GEE Landsat archives respectively.

In chapter four, the climate and the surface water data from the standardised precipitation and evapotranspiration index (SPEI), was used to observe the extent of meteorological and hydrological drought within the basin and how does this recurring moderate drought affect the surface water dynamics using the global surface water explorer data. While in chapter five, the synergy of the aforestated chapters was done to correlate the various data observed within the basin, and what kind of relationship exists between them in terms how they affect the *Fadama* farming system in the Sokoto Rima River Basin (SRRB). And on one hand, further recommendations were made to enhance future research.

CHAPTER TWO

2 Irrigation and Fadama crop yield

2.1 Introduction

A reliable estimation of crop yield in tons of grain harvested per hectare from the farmland is essential for informed decision making, crop monitoring, and cultivation enhancement. The yield estimates or measurements that show individual fields and what type of crop they contain within an agricultural landscape are useful for understanding how most crop productivity responds to various abiotic, edaphic, environmental, and management factors (Lobell, 2013).

Nigerian agriculture is characterised by regional crop diversity as you move across the ecological zones from the far north down south. Analysis of this sector, particularly the data related to the dry season farming is attributed with less documented data particularly in the Sokoto Rima River Basin (SRRB). However, most of the statistics available are for rain-fed agriculture, with little or no data for the irrigation farming. Hence, this provides a broad overview of development in agriculture upon which we can make a broad generalization about its role in the economic development and structural changes in Nigeria.

Usually, the Annual Abstract of Statistics or the Statistical year Book at the state level, shows updated information on the Nigerian agricultural data but not really constant and sufficient. This publication by the National Bureau of Statistics as Annual Abstract of Statistics is significant as it affords stakeholders such as academics, government agencies, and researchers with relevant information. In addition to the produced data by National Bureau of Statistics (NBS), the publication is also a valid source of statistical information, because it contains data obtained from the public sector, government ministries, and the private sector.

Hence, with the limited data on yield due to the cost of ground survey, to be precise with Nigeria where the government is not willing to fund an intermittent survey to collect ground data on yield. Researchers in the field of remote sensing have

long been interested in measuring crop yields from space, with a focus typically on estimating production at the regional or a river basin scale rather than for individual crop fields (Becker-Reshef *et al.*, 2010). This work is dated back to at least the late 1970s when the primary goal was to anticipate harvests in countries of strategic interest (Macdonald & Hall, 1980).

2.1.1 The dry-season (Fadama) crops

The outstanding feature of *Fadama* cropping is the potentials for cultivation after the end of the raining season using residual soil moisture. This cultivation is referred to as *aikin rani* in Hausa (dry season farming), and the small plots in which it is carried out is called *lambu i.e* garden (Adams, 1986).

In some parts of the floodplain, shallow wells are used to supplement soil moisture. In the study area at Shinaka, Taloka and many other places, shallow excavation in the river bed and temporary boreholes are used to augment the water moisture within the *Fadama* areas from my field visit in Jan. 2018. Sometimes, simple bucket lift or shadoof devices are used in conjunction with the wells. While in other locations; well-structured canals are used to convey water to the field from the dam via the pumping stations (see **Figure 2-1, Figure** 2-2**, Figure** 2-3).

Figure 2-1: Temporary borehole used for irrigation using the pumping machine at Shinaka *Fadama* site.

Figure 2-2: Water being siphoned from the parabolic canal to the farmland at Jibia *Fadama* Site.

Figure 2-3: Water pumping station at Jibia dam, from this point water is further pushed to reach the canals around the *Fadama* field.

A wide variety of *Fadama* crops are grown in the Sokoto floodplain See **Figure 2-4** below. The most cultivated crops include garlic, rice, wheat, sorghum, sweet potatoes, maize, and millet. Some other crops grown, include onion, sugar-cane, tobacco, a variety of cucurbit and spinach-like vegetables, cabbage etc.

(a) Lettuce at Jibia *Fadama* site

(b) Cabbage at Jibia *Fadama* site

(c) Cassava plant at Jibia *Fadama* site

(d) Garlic plant at Goronyo *Fadama* site

(e) Harvested Onion at shinaka *Fadama* site

(f) Wheat plant at Jibia *Fadama* site

Figure 2-4(a-f): Pictures showing various crops within the *Fadama* site of the river basin (source: Field Survey Jan. 2018).

Within the *Fadama*, crops are selected based on ecological requirement and the amount of flooding in each plot. Two basic combinations of crops could be identified in the Sokoto floodplain: the wet crop strategy and the dry crop strategy. Floods are unpredictable in extent, duration and timing because this in turn have effect on the *Fadama* farming immediately after the wet season, and determine the type of crop to be planted. Therefore, there is an element of risk in the choice of cropping pattern based on the flood recession around areas next to river channels (Wharton, 1971; Faulkingham, 1977). Hence, where the risk of cropping pattern is great, the risk aversion strategy could be identified. However, extension of the growing season in the *Fadama* could cause conflict with other dry-season activities, for example, *cin rani* (dry season labour circulation), and also, labour shortages, sickness or simply the remoteness of fields could bring similar problems, and in such circumstance other cropping pattern or the low labour strategy could be recognised (Mohammed, 2002).

2.2 Method

The estimated yield data was acquired from the 2010 Sokoto State statistical year book in the data shop repository of the National Bureau of Statistics in Abuja, Nigeria. This comprises of six selected crops from 2000-2005 identified in the statistical book which ranges from rice, millet, sorghum, maize, potatoes, and onion. Other crops include sugarcane, garlic, vegetables et cetera. But to be specific in this research, the five-former stated *Fadama* crops were considered for crop yield estimation within the basin in metric tonnes, using statistical analysis with a fitted regression line to show the trend.

Due to limited data on yield with regards to *Fadama* farming, the research was limited to certain locations within the basin which include Binji, Gada, Goronyo, Gwadabawa, Illela, Isa, Kware, Raba, Sabon Birni, Silame, Sokoto North, Sokoto South, Wamako, and Wurno Local Govt. Areas of Sokoto State **Figure 3-1**.

2.3 Results

A significant estimate of crop yield harvested per hectare can be useful for functional purposes within a range of spatial extent. The measurement that can show specific fields within an agricultural cropping system is precisely helpful for us to understand how crop produce responds to numerous environmental and management factors (Lobell, 2013).

As such, this research also tries to look at the estimated ground yield data using a trend analysis with fitted regression for each crop, to assess how this can be juxtaposed with the change in Land use and Land cover of Sokoto Rima River Basin, so that it can be integrated with the remotely sensed data. Hence, **Figure 2-5** below, contains the yield data in a continuous time series from 2000 to 2005.

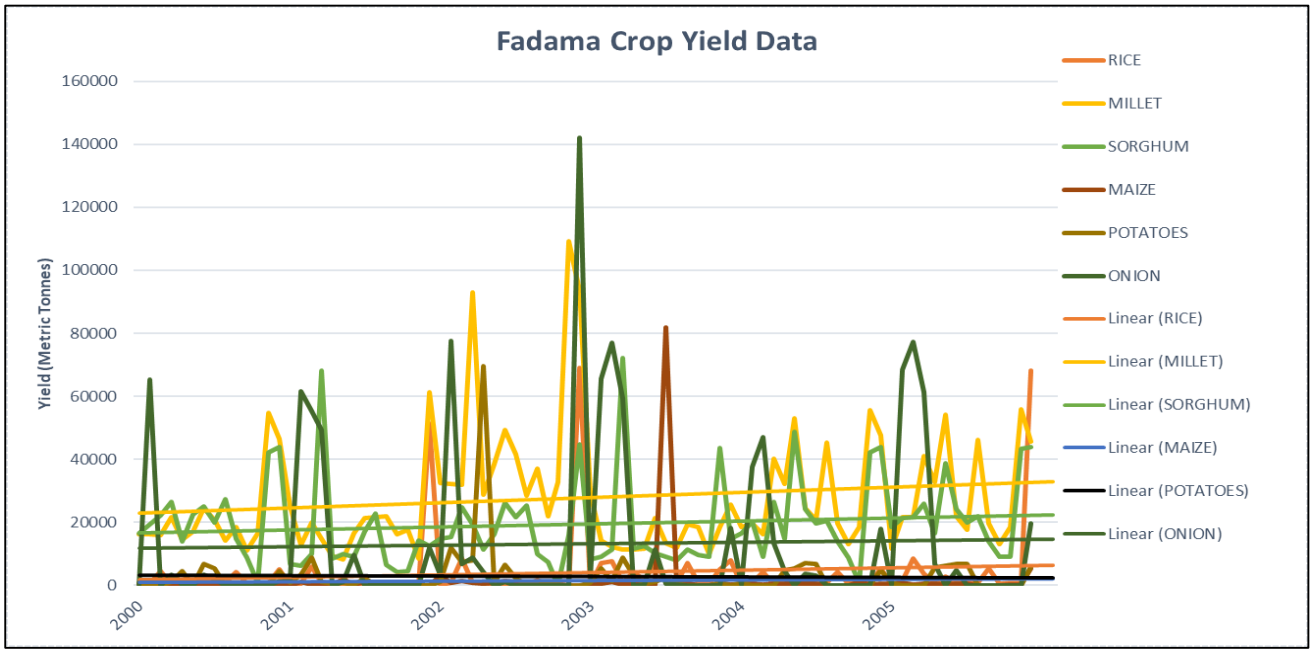

Figure 2-5: Estimated *Fadama* crop yield time series with a fitted trend line from 2000-2005. Using some part of the basin in this order at Binji, Gada, Goronyo, Gwadabawa, Illela, Isa, Kware, Raba, Sabon Birni, Silame, Sokoto North, Sokoto South, Wamako, and Wurno for each year from 2000-2005. Showing the yield estimate of rice, millet, sorghum, maize, potatoes, and onion in metric tonnes.

From the time series of the estimated yield in some part of the Sokoto Rima River Basin **Figure 2-5**, rice production seems to be the least crop produced. Although from my field visit and the interaction I had with the farmers; this can be

validated on the fact that the cost of farm input or labour required for rice farming is enormous. As such, pumping water into the field since rice requires a large amount of water will be a huge effort if profit is to be maximized. However, during the raining season, the farmers do cultivate rice because the areas adjacent to the channels and river banks get inundated which is of advantage for them to utilize the natural flooding of the *Fadama* areas for their farming activities of most crops that require a large amount of water.

In the year 2000, the highest peak observed with rice production is in Wurno *Fadama* site with about 5,077 metric tonnes. In the year 2001 at the same location; the rice production increased to 51,215 metric tonnes, while in the year 2002, 2003, 2004, and 2005, the highest rice produced is 69,142 metric tonnes, 7,995 metric tonnes, 5,472 metric tonnes, and 68,142 metric tonnes at Wurno *Fadama* site respectively.

For millet production, the highest harvest of the estimated yield was 54,634 metric tonnes at Wammako in the year 2000, while in 2001 is 61,422 metric tonnes at Wurno. In the year 2002, it is 109,268 metric tonnes at Wammako, in 2003 is 29,215 metric tonnes at Binji, whilst in the year 2004 & 2005 is 55,634 metric tonnes and 55,735 metric tonnes at Wammako respectively.

Sorghum production is also one among the crops being planted, in the year 2000; the highest harvested yield was 43,859 metric tonnes at Wurno, 69,216 metric tonnes at Gwadabawa in 2001 and 44,622 metric tonnes at Wurno in 2002, 72,271 metric tonnes at Gwadabawa in the year 2003, 48,778 metric tonnes at Isa in the year 2004, then 43,979 metric tonnes at Wurno in 2005.

In this part of the basin, maize cultivation doesn't seem to be of utmost priority to the farmers, most of the maize produced is for domestic consumption from the values obtained using the estimated yield. In the year 2000; 570 metric tonnes was recorded at Wammako as the highest yield. While in 2001; 2,031 metric tonnes was obtained at Isa, in 2002; 1,422 metric tonnes was seen at Goronyo. In the year 2003,

2004, 2005, the highest estimated yield for maize was 820 metric tonnes at Wammako, 1,007 metric tonnes at Sokoto South, and 5,412 metric tonnes at Wurno.

Sweet potatoes is also one among the *Fadama* crops in this part of the basin. In the year 2000; 6,741 metric tonnes was observed to be the highest yield at Kware. While in 2001; the estimated yield was 8,859 metric tonnes at Goronyo *Fadama* sites. In the year 2002; 69,671 metric tonnes was obtained at Illela. In 2003, 8,771 metric tonnes was recorded at Gwadabawa. While at Kware in the year 2004, the yield was 6,941 metric tonnes been the maximum among other locations. Lastly, in the year 2005; the estimated yield for potatoes was observed to be 6,825 metric tonnes at Rabah.

Onion being the last chosen crop to assess the estimated crop yield in this research, it was observed that in the year 2000, 2001 and 2002; 65,280 metric tonnes, 61,621 metric tonnes and 77,441 metric tonnes were all obtained in Gada *Fadama* areas respectively. However, from the year 2003, 2004, and 2005; the record shows that 77,122 metric tonnes, 47,120 metric tonnes, and 77,315 metric tonnes were obtained from Goronyo *Fadama* area.

2.4 Discussion

It was identified that the flooded plain is perennially or continuously cultivated with rice in the raining season because of the high amount of water available in the flooded plains that do not require human effort. While onions, garlic, sweet potatoes, etc, are cultivated in the dry season; but this requires intensive inputs of labour because water must be supplied to the field anthropogenically. Moreso, the peripheral deposit of soils in the floodplain are enriched with alluvial and manure inputs from local animal dungs kept by the villagers or from the direct droppings by the grazing animals on the uncultivated *Fadama* areas, most specifically in the dry season.

The crop yield data obtained was for specific locations within the basin i.e. Binji, Gada, Goronyo, Gwadabawa, Illela, Isa, Kware, Raba, Sabon-Birni, Silame,

Sokoto North, Sokoto South, Wamako, and Wurno, with yearly tonnage estimate from 2000 to 2005. The crops identified are rice, millet, sorghum, maize, potatoes and onion. As observed in **Figure 2-5**, the fitted regression trend line shows that the estimated yield increases over time. In the course of field visit and the observed remotely sensed images over three decades as shown in chapter three of this thesis, the yield increase was attributable to increase in hectarage under cultivation see **Table 3-1**, increased intensification influence by the government policy in recent years, and renewed soil fertility since it is a floodable plain riched in alluvial deposit.

However, farm size is estimated to be around 1 ha or even less for individual *Fadama* land; as the irrigation farming is mainly subsistence agriculture. The land is usually under the customary right of occupancy (CRO) status and can be interchanged from one party to another by sale or lease of the CRO. In general, farmers do own the CROs to most of the land they are cultivating. While in some locations before the establishment of some of the dams in the basin, the farmlands are fragmented into several plots, which can affect the yield of crops, though this is influenced by the growing population pressure that in turn, threaten crop productivity as farmlands are over-cultivated. In antecedent, the flooded plain is cultivated during the flood recession timing. But with the establishment of the Goronyo project in 1984 and the other dam projects, farming is now carried out all through the year and at larger scale.

Therefore, using the available data obtained from the statistical yearbook of the Sokoto state from 2000-2005, it was observed that the selected crops are specifically cultivated in certain locations within the basin and not evenly distributed. Generally, as the year progresses, it appears that the estimated yield tends to increase through the years, with millet, sorghum, and onion been cultivated in commercial quantities.

CHAPTER THREE

3 Remote sensing of Fadama irrigation

3.1 Introduction

Anthropogenic or man-made activities have gradually transformed the natural landscapes. As such, understanding and monitoring the land cover dynamics is vital to recognise the influence of man on the structure and function of the ecosystem (Dronova *et al.,* 2015). Annual changes in green vegetation cover are a vital source of information to the studies on crop yield pattern and estimation, and as well crop stress (Huang *et al.,* 2017).

Due to limited ground data with regards to crop yield, experts in the field of remote sensing have long been interested to measure crop yield from space, with a focus typically on estimating production at the regional or river basin scales rather than for individual crop field (Becker-Reshef *et al.,* 2010). This work is dated back to at least the late 1970s, when the major goal was to examine harvests in countries of strategic interest (Macdonald & Hall, 1980). Subsequent research that was focused on the field-scale, has shown numerous examples where half or more of the yield difference across a landscape could be captured by satellite-based estimates (Lobell *et al.,* 2005).

Yet, despite these numerous examples, field-level yield mapping from remote sensing has not yet become extensive, because of a combination of factors including (i) The expertise associated with obtaining, rectifying, and processing the imagery was often prolix before now. But more technologies are evolving to ease the process; and (ii) There is a lack of proven accuracy sometimes, partly because "ground-truth" estimates are much harder to obtain at the field scales due to limited field survey, because the government does not publish routine survey-based estimates with respect to *Fadama* irrigation particularly in Nigeria.

Recently, the widespread availability of imageries and modified platforms for processing data have reduced the cost of obtaining and pre-processing imagery. For

example, georeferenced and atmospherically corrected Landsat dataset is now freely accesible, and can be mosaiced, masked for clouds, and composited within Google Earth Engine (GEE) Platform (Google Earth Engine Team, 2015) or using manual GIS techniques.

Taking full advantage of the datasets for crop yield mapping requires more scalable approach to convert images into estimated yields. Most existing methods often rely on calibrated relationship between vegetation indices (VIs) and yields that are specific to individual location and year, often with new ground-measurements needed for each of the new setting (Baez-Gonzalez *et al.,* 2002).

Hence, the production of remote sensing datasets or images by various types of sensor flown aboard on different platforms at varying height above the earth's surface, and at different time of the day and that of the year does not bring about a simple classification system in general.

Thence, It is believed that not all classification could be used with all types of imagery and at all scales. To date, the most successfull general purpose classification scheme compatible with remote sensing data has been developed by Anderson *et al.*, (1976) which is also referred to as the United State Geological Survey (USGS) classification scheme. Other classification schemes are basically a modification of the above classification scheme.

Maximum likelihood algorithm is used to provide a consistent classifier for multi-date classification. These shows an increased classification accuracy, especially after the application of post-classification procedures. A combination of classification with other techniques such as classification with the NDVI, or classification with PCA (Principal Component Analysis) and CVA (Change Vector Analysis), have been immensely used in some of the studies to increase the classification accuracy as well as to avoid the leak training sample sets for image classification. For instance, Li and Yeh, (1998) combined interactive supervised maximum likelihood classification with combined PCA to prevent over-estimation in the amount of change. (Abd El-Kawy, 2011) also used map interpretation to improve classification accuracy and to

recognise areas with effective use of water for irrigations and areas of privately reclaimed land.

As such, within the field of GIS and remote sensing. The use of spectral vegetation indices and normalised difference vegetation indices derived from AVHRR satellite data, followed the launch of NOAA-6 in June 1979 and NOAA-7 in July 1981 or Landsat data (Cracknell, 2001). Have greatly contributed to geospatial observation of the earth's surface with comparative ease in the whole process, with the greater advantage of examining a very large area.

Several vegetation change detection processes have emerged through the analysis of Landsat archives or the integration of MODIS (Moderate Resolution Imaging Spectroradiometer) time-series with the spectral information derived from Landsat datasets (Huang *et al.,* 2017). The MODIS data has frequent coverage with 250 m resolution, and the Landsat data has a resolution of 30 m. Therefore, the 8-day interval between MODIS data composites is superior for monitoring phenology changes in vegetation (Schmidt *et al.,* 2015).

The accuracy of forest disturbance or the *Fadama* vegetation change detection depends on the scale and the extent of the distribution pattern which can be related to the quality of MODIS data (Sulla-Menashe *et al.,* 2010). However, it is not possible to acquire MODIS data over the past (30) thirty years given that its data is short which is only available from 2000. In contrast, Landsat based time series datasets are a substitute for vegetation change monitoring because they have a high spatiotemporal resolution if all of the 16-day revisit Landsat images are available, especially within the Google Earth Engine Landsat archives. But also have its limitation due to Landsat 7 sensor error of scan line correction error from 2003 onward which can as well be substituted with MODIS data because it is available from 2000 as earlier stated.

Most recently, high-performing computer systems are becoming abundant (Cossu *et al.,* 2010; Nemani *et al.,* 2011) and the large-scale cloud computing platforms are universally available for use. At the same time, petabyte-scale archives

of remotely sensed data have become freely available from the U.S. Government agencies that include NASA, the USGS, and NOAA (Loveland & Dwyer, 2012).

In December 2010, Google invented a technology called (GEE) Google Earth Engine (U.S. Geological Survey, 2010). This geospatial platform composed of more than (40) forty years of satellite images available online for scientists and researchers to analyse real-time changes that are occurring on the Earth's surface (Housman *et al.,* 2015). Google Earth Engine has numerous servers around the globe and has enabled the science community to analyse millions of images using a parallel processing (Dong *et al.*, 2016).

Google Earth Engine as a cloud-based computing platform, provides access to high-performing computing resources, that processes substantial geospatial datasets without having to pass through the IT stress. GEE gives online access to the archived of Landsat data; these include the Landsat 4, Landsat 5 TM that ranges from 1985 to 2011, Landsat 7 ETM+ from 1999 to 2014, and the Landsat 8 OLI/TIRS from the year 2013 to 2018 (Google Earth Engine Team, 2015). Google Earth Engine is as well structured to assist researchers to easily share their results to other researchers and policy makers, NGOs, and the general public. Once an algorithm is developed within the Earth Engine API, users can produce a systematic data products or place an interactive application backed by GEE's resources, without needing to be a web programmer, application developer, or HTML expert.

3.1.1 GEE platform overview

Google Earth Engine (GEE) consists of multi-petabyte analysis of a ready data catalogue co-located with a high-performance and parallel computation service. It is accessed and controlled via the accessible Internet API (Application Programming Interface), and it is associated with a web-based interactive development environment (IDE) that enhance rapid prototyping and the visualisation of remotely sensed results (Gorelick *et al.*, 2017).

The data catalogue contains a vast repository of publicly available geospatial datasets, including the observations from a variety of satellite and aerial imaging systems in both the optical and non-optical wave-lengths, environmental variables, climate and weather forecasts, hindcasts, land cover, topographical and socio-economical datasets (Gorelick *et al.*, 2017). All of these datasets are pre-processed and ready-to-use. Users can access and analyse datasets from the public catalogue and as well their private datasets using a library of operators that are provided by the Earth Engine API. These operators are shown in a parallel processing system that automatically subdivides and distributes computations by providing high throughput analysis. As such, users access the GEE API either through a thin client library or through a web-based interactive development environment built on top of the client library.

Hitherto, prior experience with GIS, remote sensing and scripting languages make it easier to get started in GEE (Gorelick *et al.*, 2017). However, they are not strictly required, because the user's guide is oriented towards most of the domain novices. The GEE accounts come with a quota for uploading most personal data and saving the intermediate products, and all inputs or results can be downloaded for offline use in other geospatial software. Users can request for additional datasets that are new to the public catalogue, or they can upload their private data through the REST interface using either the browser-based or a command-line tool and share with other users or groups as they desired.

Related images, such as most of the images produced by a particular sensor, are grouped and shown as an “Image Collection”. Image Collections provide fast ways of filtering and sorting the images that make it much easier for users to explore through millions of individual satellite images and select the data that meets their specifications of spatial, temporal or any other criteria they need. However, satellite images inserted into Google Earth Engine are pre-processed to facilitate fast and efficient access. First, the images are cut into several *tiles* in the image's original projection and resolution, then stored in a useful and replicated tile database of the Earth Engine.

Additionally, in order to enhance quick visualisation during the algorithm process, a pyramid of reduced resolution tile is created for each image and stored in the tile database. Each level of the pyramid is produced by down-sampling the previous level using a factor of two until the entire image fits into a single tile. When down-sampling, continuous-valued band are averaged, while the discrete-valued bands like the classification labels are sampled using min. max. mode or a fixed sampling. When a portion of the data from an image is needed for computation at a reduced resolution, only the most relevant tile from the appropriate pyramid level needs to be retrieved from the tile database. This power of two downscaling enables the data ready at a variety of scales without bringing significant overhead in the storage and this aligns with the common usage patterns in the web-based mapping (Gorelick *et al.*, 2017).

GEE also inter-operates with Google Fusion Tables (Gonzalez *et al.,* 2010). This is a web-based database that supports tables of geometric data that include points, lines, and polygons with their attributes.

In the Earth Engine, users write programs using the client libraries which are currently available for Python and Java Script languages **Figure A3;** this allows the user to delineate processing graphs using a known procedural programming paradigm (Zurqani, 2018). The client libraries provide a proxy object for images, collections, and other data types such as strings, numbers, geometries, and lists. The user scripts used, manipulate these proxy objects which record a chain of operations and assemble them into a directed acyclic graph (DAG) that expresses the complete computations. The DAG is then sent to the Earth Engine service for evaluation.

3.1.1.1 Data processing in Google Earth Engine API

GEE cloud based platform allows its users to upload and download global satellite imageries, as well as enable them to perform complex calculations at the same time (Sidhu *et al.,* 2018). The platform comprises of two main components that work in sync with each other; this is the Google Earth Engine (GEE) Explorer for

viewing datasets and the Google Earth Engine (GEE) Playground. Any outputs dataset produced within GEE can be exported to other geospatial environments like the (R, ArcGIS, QuantumGIS) for further analysis (Sidhu *et al.*, 2018).

3.1.1.2 Ease of functionality

Producing a global, continental or a country scale analysis using geospatial tools would take the user a significant amount of time and computing resource (Sidhu *et al.*, 2018). In contrast, having the cloud computing capabilities of GEE, users can search the image they need in the GEE, and the Imagery retains it's in situ spatial reference and metadata without much stress.

As such, this comes with ease of function and operation, and an interface that produce fast result.

3.1.1.3 GEE processing capability

The parallel processing capabilities of the GEE infrastructure makes it useful to run spatial reductions over image collections (Gorelick *et al.*, 2017). The tile-by-tile processing ability of the earth engine applies a spatial e.g. Median() reducer to each of the tiles. First, each scene is sub-divided into several tiles, with each tile being sent to the numerous Google servers to be processed. These servers work in parallel and independent of one another. The result is the "reduced image" which tends to be the outcome of the reconstruction of the tiles. This applies a temporal reducer by filtering through a collection to get a specific time of the year, although, one has no much control of the image to be produced from the Image Collections which proves to be slightly challenging.

3.2 Method

Long-term satellite images are vital to understand land cover dynamics and are useful for detecting changes in vegetation cover (Gong, 2012). It provides a unique chance to monitor progressive annual land cover changes at high spatial and temporal resolutions.

Previous studies on vegetation change detection concentrated on using multi-dates of Landsat images at intervals of five or ten years (Griffiths *et al.,* 2014; Kim *et al.,* 2014; Masek *et al.,* 2008; Teferi *et al.,* 2013) as in the case of this research. Since the USGS made the entire Landsat archives freely available for public use in 2008, numerous studies on continuous long-term land use change monitoring are under review by multiple researchers (Loveland & Dwyer, 2012). As such, the methods used are as follows:

3.2.1 Landsat data source

Dry season imagery data between November to March of 1988, 1998, and that of 2018 (**Figure A1**) of the Landsat archives were downloaded via the United States Geological Survey. The GeoTIFF images were cloud free, and in level 1 tier 1, i.e. the images are georeferenced and are of higher resolution which does not require any further geographical coordinate to proceed with the analysis. Other reference maps were obtained to get the shapefile of the study area after being georeferenced. Moreso, ground truthing point was noted to enhance the landcover classification and accuracy assessment.

The 2008 Landsat 7 images were as well downloaded for analysis. but, due to the satellite malfunction from the year 2003 onward, the images have scan line correction failure and will not provide usefull land use land cover change detection results if used. Conversely, the missing gaps can be interpolated in some locations, but specific to this study, the interpolation cannot be done because the lines are consistent in all the images. Hence, they were only used to produce the NDVI data in GEE.

3.2.2 Material and software used

In this study, the materials used are: high speed core i7 Dell computer, ArcGIS 10.5 software, Erdas Imagine (64, 32bit), 2TB storage hard drive, cloud based Earth Observation tools (EO); thus: Google Earth Engine (GEE) API & GEE Code Editor,

Google Earth Explorer, Landviewer EOS data analytics, Google Earth and the Earth Engine Time Lapse.

3.2.3 Image processing

For this study, the algorithm computed to produce aposteriori results are as follows:

3.2.3.1 Layer stacking and mosaicking

The spectral response and characteristics of Landsat images are entirely different in all the bands and across all Landsat types (Imager, 2014). Depending on the kind of analysis a researcher wishes to perform, the band selection plays a vital role when computing any algorithm in remote sensing.

Therefore, the selected six (6) bands (i.e. B1, B2, B3, B4, B5, B7 in landsat 5 and 7 respectively and B2, B3, B4, B5, B6, B7 in landsat 8) from the Landsat images were layer stacked and mosaicked all in Erdas Imagine. After this stage, the mosaicked image was then saved in the Imagine format (.img) and then imported into the ArcGIS 10.5 environment to extract the study area using the shapefile generated earlier. After this, the layer was then re-projected to *Albers* so as to avoid further distortion because the image cut across two zones i.e. UTM zone 31N and 32 N.

3.2.3.2 Radiometric corrections

Radiometric normalisation is a required process for change detection and multi-temporal remote sensing image classification. Though it is not always compulsory when the image to be classified and the training data are on the same relative scale (Chen & Rao, 2008). However, the images downloaded were all cloud-free, but a simple haze adjustment by dark object subtraction was done in each different subset scene.

For each band, the lowest value that is extracted from the histogram value of the entire scene was used as a DN haze value (Eastman, 2009). This procedure works on the assumption that most haze effect is uniform across the whole scene (Eniolorunda *et al.,* 2017).

3.2.3.3 Nesting and scaling

The entire basin was considered for the Landcover classification and change detection at inception; this comprises an area extent or catchment of Katsina, Zamfara, Sokoto and Kebbi. But due to limited data on crop yield specific to *Fadama* farming, and expansive extent of the area, some of the computation were not possible in the ArcGIS Environment . Hence, a nested scale of a part within the basin was done, which includes; Binji, Gada, Goronyo, Gwadabawa, Illela, Isa, Kware, Rabah, Sabon-birni, Silame, Sokoto North, Sokoto South, Wamakko, and Wurno **Figure 3-1** below**,** and all of these areas are within the jurisdiction of Sokoto state. On the other hand, the estimated yield data specific to that area was used to assess the magnitude of the yield in the year 2000-2005 as seen in **Figure 2-5**.

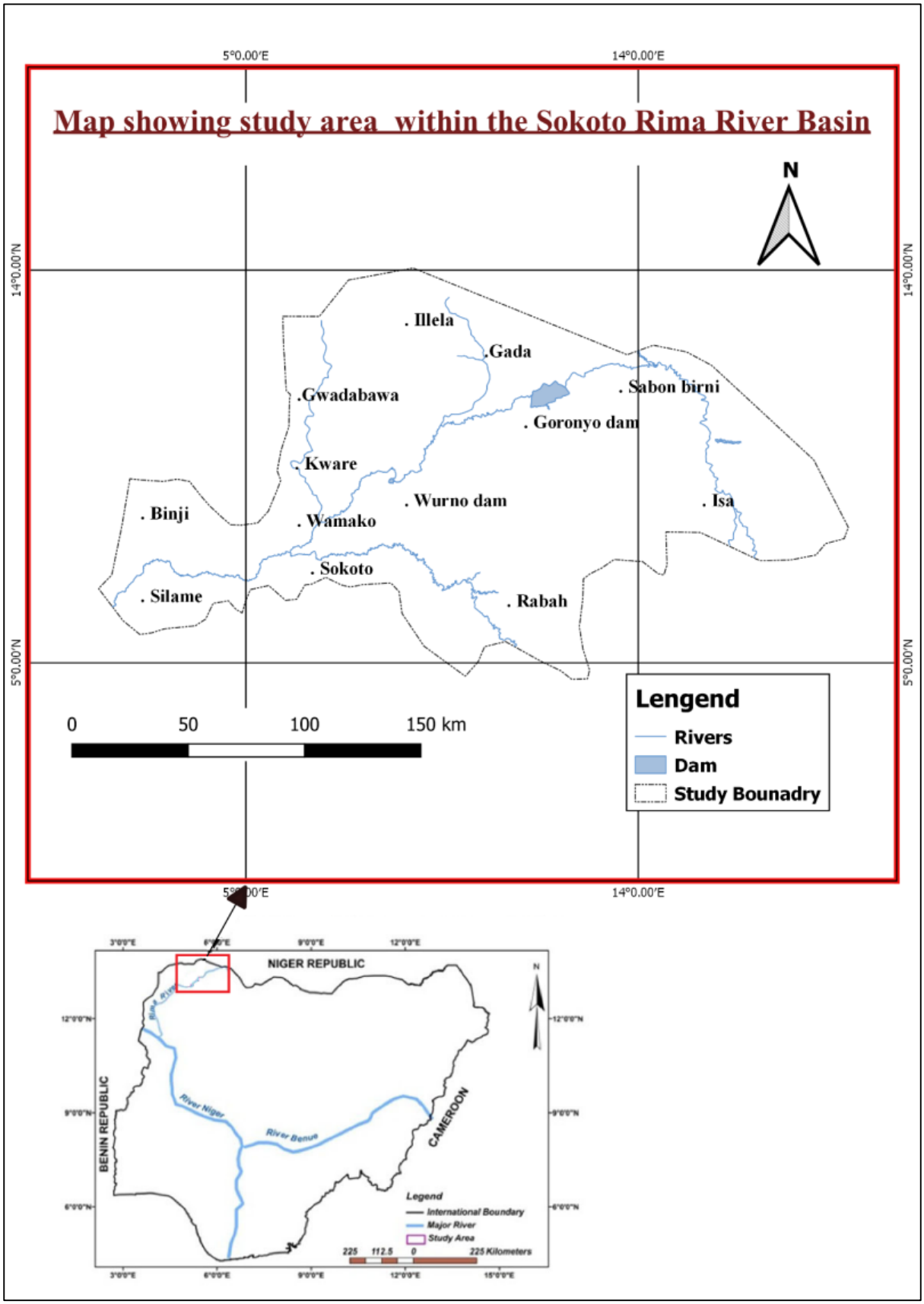

Figure 3-1: Map of the nested and scaled area (Binji, Gada, Goronyo, Gwadabawa, Illela, Isa, Kware, Rabah, Sabon-birni, Silame, Sokoto North, Sokoto South, Wamakko, and Wurno) within the Sokoto Rima River Basin showing the study boundary and the major dams.

3.2.4 Landsat classification and NDVI

A supervised classification using maximum likelihood (Abdullah & Lalit, 2013) was used to identify training sites on the Landsat images using false colour band combination of 5, 4, 3 and 6, 4, 3 on Landsat 4, 5, 7 and Landsat 8 respectively. This assisted the research to identify pixels with high vegetation. Hence, with the band combination as afore-stated, the study was able to set a distinction between the natural vegetation, grassland areas, and areas with dense tree population. While on the other hand, other land uses and land cover were as well delineated.

In this study, the change detection analysis or classification was set into five classes using maximum likelihood; namely: Built-up areas, *Fadama* areas, natural vegetation, water and bare soil. Although, due to spectral confusion of some of the pixel within the bare soil being classified as built-up areas in ArcGIS and Erdas, a reclassification was done to make a facelift to the classification. After critical observation, the reason was that most of the materials used in building the structures were mostly mined from the red lateritic soil in the study area. That is why some of the pixels are wrongly classified. To further enhance the classification, the classes were then reduced to four (4) by combining the spectrally confused pixels. The Landcover classes were then further ramified into Natural vegetation, *Fadama* areas, Water and Non-vegetated areas.

3.2.4.1 Landsat NDVI

The Landsat Normalized Difference Vegetation Index was carried out within the ArcGIS 10.5 environment using the image analysis tab and the nearest neighbor. The NDVI was set to scientific output, and the appropriate band combination was selected for Landsat 4, 5, and 7 as band 3 being the Red band and band 4 being the Near Infrared (NIR) band respectively, although before this was done, the integer was scaled up by 100 to come up with a range between -100 to +100 to further make a natural break that set a distinction between the natural and *Fadama* vegetation. For Landsat 8, the band combination was band 4 as the Red band, and band 5 as the Near Infrared (NIR) band. Finally, the NDVI was then generated, from the symbology tab

using the classified, with 15 natural break classes generated, and the *Fadama* vegetation was then differentiated from other vegetation using the Value field. See **Figure 3-5, Figure 3-6, Figure 3-7.**

3.2.5 Cloud based classification using Google Earth Engine (GEE) and NDVI

The GEE classification was done using a cloud based parallel computing that uses the java scripting in the code editor interface and the GEE playground.

A wide variety of classification algorithm was used to map out the changes in land cover and land use from remotely sensed data (Lam, 2008; Butt *et al.*, 2015). Supervised machine learning classifiers such as Classification and Regression Trees (CART) and Random Forest (RF), are widely used to classify remotely sensed data (Wingate *et al.*, 2016).

The change detection analysis used in this study requires image pre-processing and normalization. Therefore, the change detection technique was applied and evaluated by creating code in the GEE code editor interface using a supervised classifier algorithm and Landsat time series subsequently for each chosen year, see (**Figure A3**). High-resolution satellite imagery available in GEE see (**Figure A2**), was used as a reference layer for training and validating the classifications. Comparisons were made between the classified images for each study year to find locations where the land cover and the *Fadama* farming changed.

In this research, using the GEE Landsat archives, a calibrated top-of-atmosphere (TOA) reflectance data from Landsat 4, 5, 7 and 8 was used (**Figure A2**). These images were orthorectified and calibrated to top-of-atmosphere reflectance, and the imagery with the least cloud cover was filtered as the primary input data into the GEE API, (**Figure A3 line 2-3**)

From (**Figure A3**), the GEE search was used to obtain the *Image Collection* ID of the USGS Landsat 4, 5, TM and Landsat 7, 8 Collection 1 Tier 1 TOA (top-of-atmosphere) reflectance of the three epochs respectively. The image ID was then used to filter the Landsat data from the *Image Collection* repository of the Google Earth Engine.

After filtering the Landsat data, a variable was created to get the image from the *Image Collection* using the image ID i.e. ('LANDSAT/LC08/C01/T1_TOA'). Then it was commanded to filter by region of interest (roi) from the point geometry import created, filtering the image by the date range, sorting it by the least cloud cover and then the first in the collection. To know when the image was taken, a variable was created which appears in the console, with specific band combination when added to the GEE playground.

Secondly, the geometry import was then configured into four classes, imported as a *Feature Collection*, and the property was set to be "landcover" and numbered from 0-3 for non_vegetated class, water class, *Fadama* class and natural_vegetation class respectively.

Next, the created point geometry imports of the *Feature Collections* were then merged. To print the *Feature Colletion,* a command was created to inspect the training sites by overlaying the points. Furthermore, to train the classifier which is (optional); a variable was produced using the class property and the input properties of the bands.

Finally, to classify the image using the training points on the selected training sites, and to display the classification on the GEE playground. The classification variable was scripted using the initial band combination and the colour palettes (**Figure A3**).

It is noteworthy that when classifying the image, the band combination used in the training sites must be noted. On the other hand, when selecting the colour palette, the min. & max. numbers must be the same as the numbers created when inserting the properties of the *Feature Collection*. The colour code used are; light grey for non_vegetated areas, blue for water, bright green for *Fadama*, and dark green for natural vegetation.

3.2.5.1 Google Earth Engine (GEE) NDVI time series

The GEE NDVI time series is also a cloud computation within the Google Earth Engine API. The machine calculates the time series from the values obtained using the Landsat archives in the GEE *Image Collection* repository after creating an area of interest (i.e. polygon geometry imports) by masking.

For this research using GEE to compute for NDVI time series, five *Fadama* areas adjacent to the dams were masked and used **Figure 5-6**. The first step was to filter the image from the *Image Collections*. To calculate the NDVI from the inserted image in the GEE playground, the bands variable was created, and the NDVI formula was used to compute for the vegetation index within the image (**Figure A4 a & b**).

It should be noted that when combining the bands for NDVI calculation, the type of Landsat used should as well be considered because the bands are not the same, to be precise with Landsat 8 if compared with the other Landsat types.

To further display and to add the map layer of the NDVI into the GEE playground, the colour palette variables were created, and the NDVI function was added so that the NDVI time series can be computed for the selected *Fadama* areas. To test the *addNDVI* that was created, the variable for the NDVI was created using the *addNDVI*. Then the variable for the Landsat image (*l8)* that was imported is generated to align it with the *addNDVI*.

Finally, to produce the NDVI chart and the time series as shown in (**Figure A4 a & b**). The chart variable was created using the *Image Collection*, specifying the area or region of interest and giving it a title. And at the latter, the chart was printed in the console to have a graphic display of the time series, See (**Figure A4 a & b**).

To show the data of the NDVI time series from the Google Earth Engine, the data was downloaded in a CSV format, and a continuous time series for the whole data was plotted in excel **Figure 3-15**.

3.2.6 The Pekko NDVI time series

The Pekko MODIS NDVI Time Series is a web-based tool from the Global Agriculture Monitoring (GLAM) project; this tool is used to derive MODIS NDVI images and to sketch graph data for any year. Getting the annual graph of NDVI time series enables a researcher to pinpoint the peak and nadir of greenness within that specific area, and also to compare the annual NDVI trend with the long-term average (NDVI Anomalies).

First, the region of interest was selected by clicking the globe, from the drop-down box under the polygon option, the parameters were selected, and the graph was then updated after choosing the date or time of interest, as well as the point of interest within the five selected *Fadama* areas adjacent to the dams. A point data was first derived; then expanded to 1.5 km resolution to obtain data for Jibia and Zobe dam *Fadama* sites respectively, while a 2 km resolution was used for Bakolori, Wurno and Goronyo *Fadama* sites respectively because of the *Fadama* site here is quite more extensive. Hence, a series of dates were computed at the same time to have a continuous time series after the graph data was downloaded for further smoothing analysis.

Specific to this study, five *Fadama* areas adjacent to the major dams were perused, but to further nest and scale the observation area, not all the *Fadama* areas were computed. The obtained Pekko NDVI data range from the year 2000-2019, to get a continuous time series using the NDVI datasets acquired, all the data through the years were juxtaposed and a yearly time series was generated (**Figure 3-20**).

3.3 Results

3.3.1 Landsat classification

The Land use Land cover change detection in the Sokoto Rima River Basin was carried out using the maximum likelihood (Abdullah & Lalit 2013; Eniolorunda *et al.,* 2017) within the ArcGIS 10.5 and Erdas Imagine Environment **(Figure 3-2)**. A total of 288 ground truthing points (**Figure A5**) were used for the accuracy assessment, with an overall accuracy of 97% in 1988, 92% in 1998, and 90% in 2018.

Several land uses were identified, though at inception, five classes were noted and classified. But, due to spectral confusion of the pixels, the classes were then reduced to four by combining the spectrally confused pixels so as to enhance the classification accuracy. Among the land use and land cover observed in the course of the field reconnaissance, and as opined by Eniolorunda *et al.,* (2017). The floodplain is where irrigation supports the farmers with all-year-round farming activities; land tillage, crop planting, irrigation farming, crop harvesting, agricultural lands, grazing, tree felling for domestic firewood, urban expansion, and among others were identified.

As such, the diversity in land cover gives a more complex change detection if all the land use land cover is to be considered. Thus, given the advantage of the moderate resolution of the Landsat data, the classification was carried out using level III of Anderson *et al.*, (1976). The classification was aggregated base on the similarity of land use land cover as suggested by Anderson *et al.,* (1976). The classes assessed by this study are the natural vegetation, *fadama* areas, built-up areas, water and bare soil. Therefore, the aggregation of the five classes yielded four classes which are: water, natural vegetation, *fadama* areas and non-vegetated areas **(Figure 3-2)**.

For an elaborate expression of the whole process, the water class comprises of the dams, streams flows, weir, and turbid waters. While natural vegetation; encompasses the dense tree populations, scrubs, shrubs, riparian vegetation, fallow lands, grasslands and the montane vegetation. Nonetheless, the *Fadama* areas cover all the riparian or floodable areas with shallow aquifers cultivated for irrigation.

Furthermore, the non-vegetated areas comprised of the built-up areas, the lateritic rocks, red soil, white soil deposit, bare lands, and rocky surfaces. Although the built-up area was at first envisaged as a threat to *Fadama* farming, but to a certain degree, it has no such effect on the *Fadama* areas in spite a significant expansion within the urban fringe of the study area. However, proximal areas to the urban fringe were observed to be absorbed for human settlement and other commercial purposes. But this contributes a meagre portion if compared to the uncultivated vast land resource within the basin.

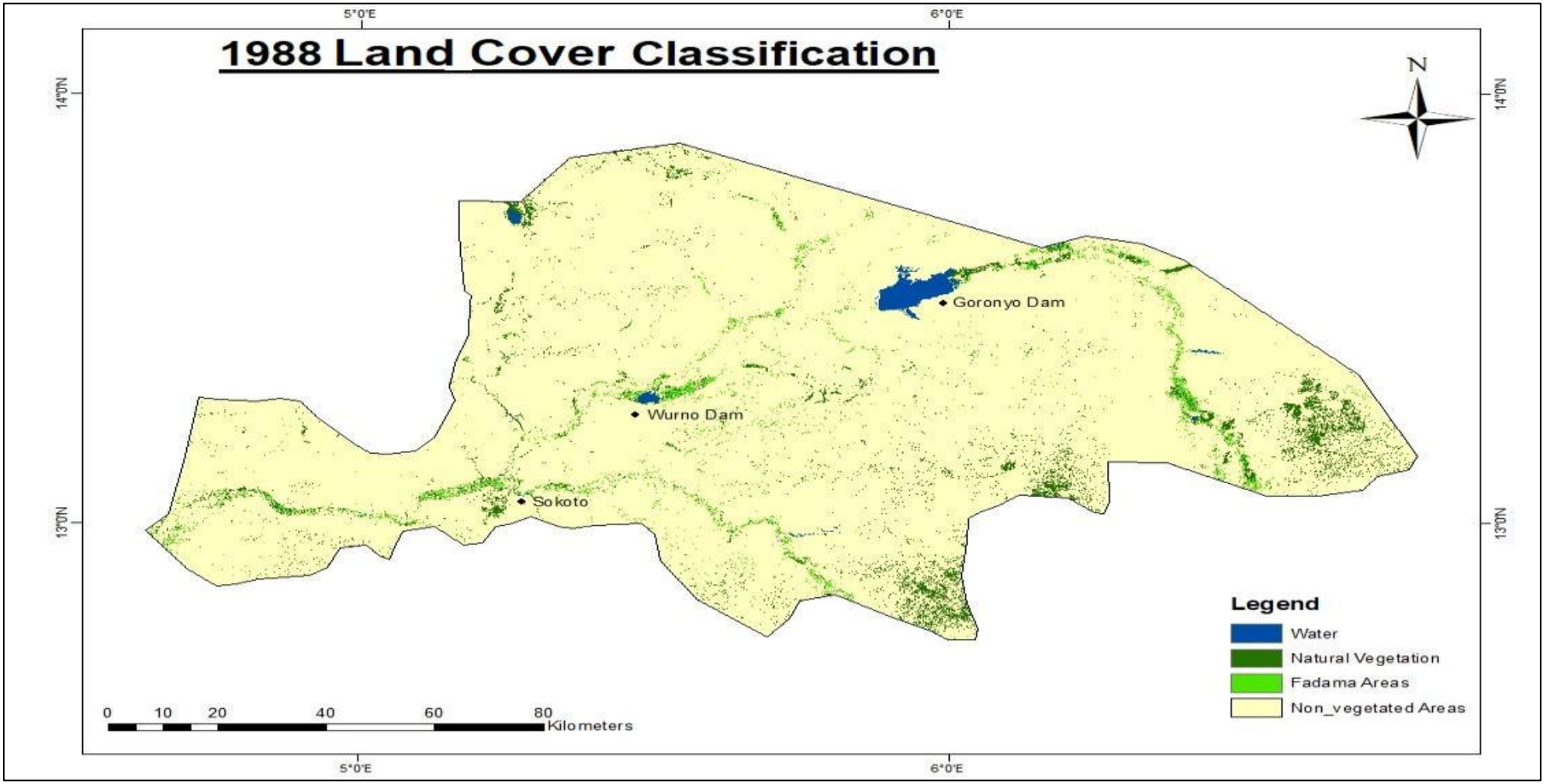

Figure 3-2: Classification map of 1988. Showing the four classes of the land use land cover classes within the Sokoto Rima River Basin around Goroyo and Wurno dam from November 1987 to March 1988 when the dry season *Fadama* farming starts. Which when related to **Figure 1-8** and **Table 3-1**, the dam size can be harmonised with the rainfall data.

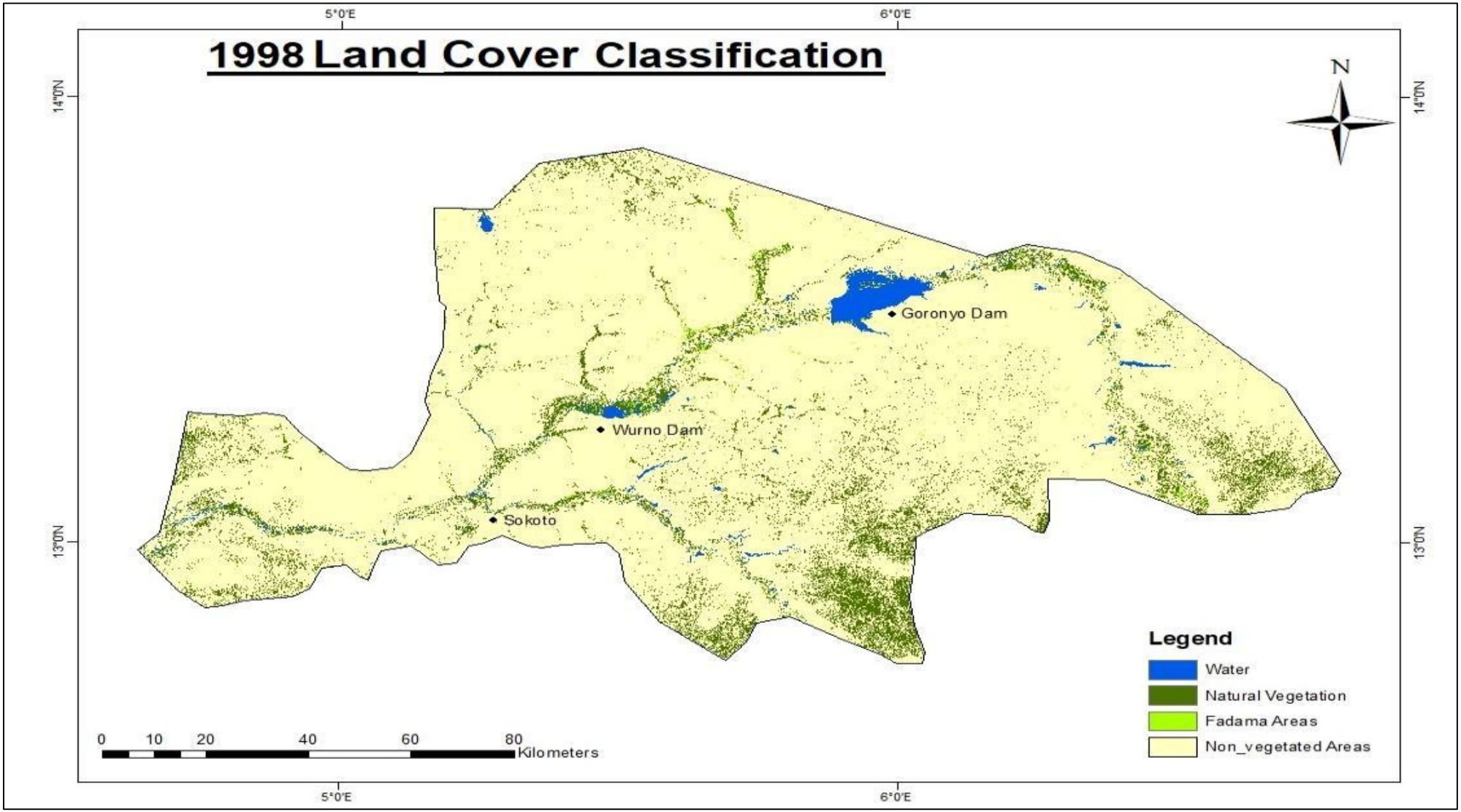

Figure 3-3: Classification map of 1998. Showing the four classes of the land use land cover classes within the Sokoto Rima River Basin around the Goroyo and Wurno dam from November 1997 to March 1998 when the dry season *Fadama* farming starts. Which when related to **Figure 1-8** and **Table 3-1**, the dam size can be harmonised with the rainfall data.

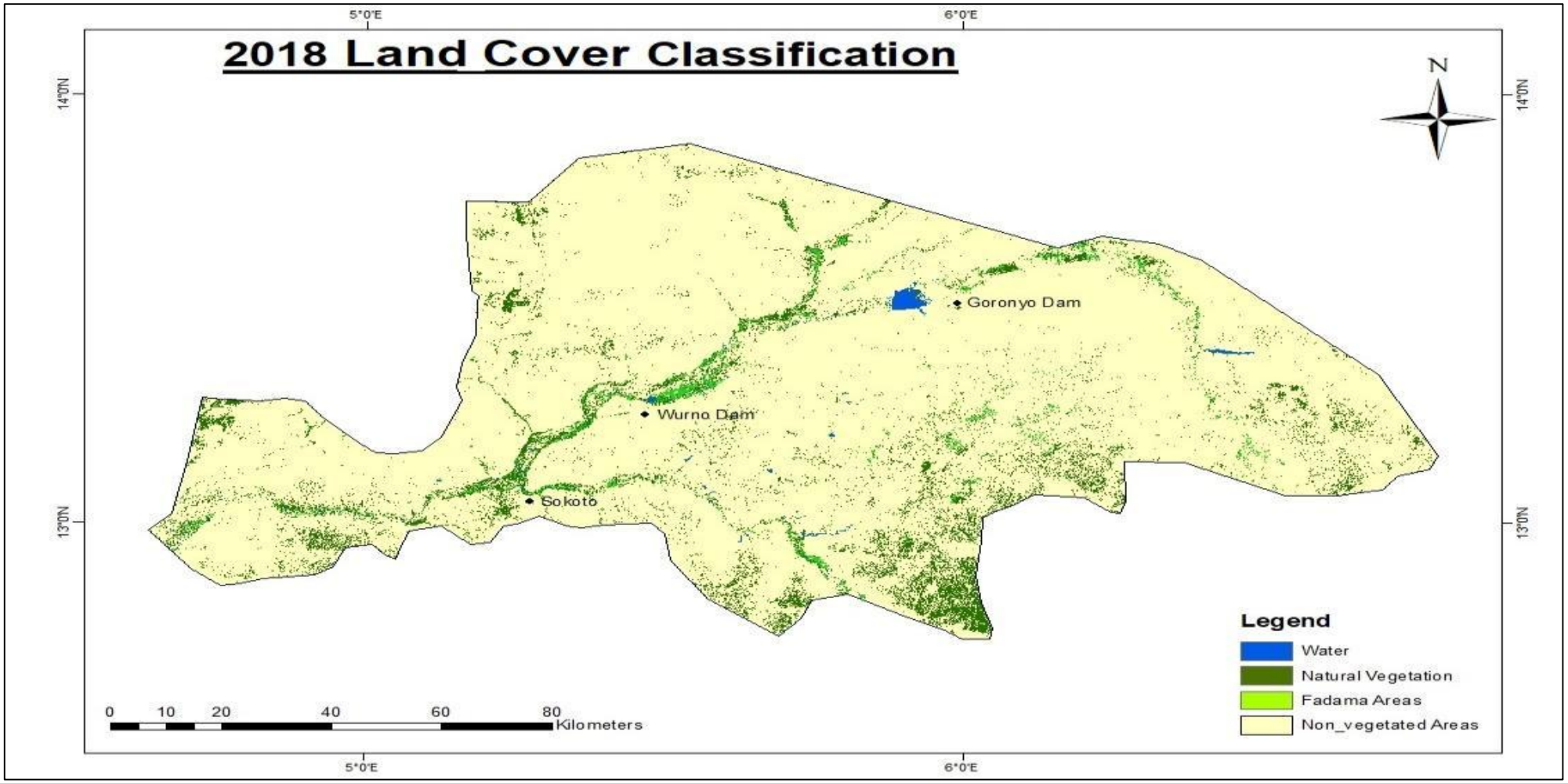

Figure 3-4: Classification map of 2018. Showing the four classes of the land use land cover classes within the Sokoto Rima River Basin around the Goroyo and Wurno dam from November 1997 to March 1998 when the dry season *Fadama* farming starts. Which when related to **Table 3-1** and **Figure 4-4** (a, b), the dam size can be harmonised with the recurring moderate drought that is occurring around the basin which also have effect on vegetation cover compared to the previous epochs.

In *epoch 1* of the 1988 classification **Figure 3-2,** land area covered by water within the classified extent is 12,343 ha which is (1%), natural vegetation covers 49,926 ha that is (3%), *Fadama* areas covers 27,632 ha (i.e. 2%), while the non-vegetated areas covered 1,474,613 ha which is (94%). These depict that areas that are left with no vegetation are more in preponderance than the total area covered by the natural and *Fadama* vegetation.

In *epoch 2* of the 1998 classification **Figure 3-3,** the area covered by water is 26,468 ha (2%); it depicts that there is more water available in 1998 than in 1988 see **Figure 1-8** on rainfall data. Natural vegetation covers 133,019 ha (9%); this shows that there is more vegetation cover than in 1988 which may be influenced by the amount of rainfall experienced. More so, the *Fadama* area covers a total area of 9,753 ha (1%); it is evident that in 1998 there is a decline in the number of cultivated *Fadama* lands if compared with 1988. Perhaps the amount of water has influenced flooding rate and may hamper crop cultivation if more *Fadama* areas are inundated. While on the other hand, rainfed agriculture most have thrived due to the amount of rainfall experienced, and making the farmers feel reluctant to cultivate crops during the dry season.. At the latter of this epoch, the non-vegetated area covers a total area of 1,394,235 ha (89%).

Hence, there is a decline in the number of hectares with no vegetation. Therefore, this is influenced by the amount of moisture in 1998 which favours more vegetation growth, and may be the amount of deforestation was as well restricted. While as observed, more trees were planted as shelter belts to counter the wind as windbreakers during the harmattan season that is mostly characterised by turbulence wind across the basin.

Percentage change between 1988 and 1998

The percentage change was computed between the two epochs to derive a decadal sense of direction on how the land use land cover has changed. Consequently, the percentage change was calculated by getting the difference between the recent and previous year, then the change was divided by the previous year times 100%.

Thus, from **Figure 3-2** and **Figure 3-3,** the percentage change between 1988 and 1998 was 114% with water; which depicts an increase. 166% with the natural vegetation which is also a positive change within the period of that ten years. However, the *Fadama* areas decrease by -65%, while the non-vegetated areas also reduced by -100%. Therefore, the change depicts that water and natural vegetation increases within the interval, while the *Fadama* and non-vegetated areas decreased by some percentages between the years.

In *epoch 3* of the 2018 classification **Figure 3-4**, the water was observed to cover 5,216 ha (0.3%), the natural vegetation covers 102,382 ha which stand to be (7%). The *Fadama* areas, on the other hand, covers 20,713 ha, i.e. (1%), while the non-vegetated areas covered a total area of 1,435,167 ha (92%).

From the computed values, we can decipher that the water was drastically reduced in the total area covered; this is heavenly influenced by the issue of climate change and high amount of evaporation (Annual Abstract of Statistics, 2017). The amount of vegetation is affected by the amount of moisture as seen in 1998. Because, as the amount of water increases; the amount of vegetation will proportionately increase as well. Hence, in 2018 the reverse of 1998 was obviously observed with a sharp decline.

Also, in this third epoch, the number of areas cultivated as *Fadamas* increased if compared with 1998. From the field visit, it can be validated that more people are willing to grow more crops because the government is doing everything possible to revamp the farming system within the basin and across Nigeria. While on the other hand, more market sphere was created for the farmers so as to incentivise and encourage people to go back to land rather than depending on oil revenue as a major source of income to the economy and to boost food security. The non-vegetated area in the 2018 classification increased in

contrast with 1998, this was influenced by the fact that more areas are covered by the increase in urbanization, vegetation decrease and more tree felling were in preponderance. To further checkmate this, tree felling must be curbed and planting more trees will suppress the desert encroachment into the basin as observed from the field visit.

Percentage change between 1998 and 2018

The percentage change within the two dates **Figure 3-3** and **Figure 3-4** was examined to be a decrease with water bodies as stated earlier, the change was rated at -80 %, and natural vegetation was seen to be -23%. Converse to the previous year, in 2018, the *Fadama* farming increased by 112% while the non-vegetated area also increased by 3%. Therefore, this illustrates that there is an increase in the urban expansion which serves as a compensation for the areas covered by vegetation in 1998, while certain areas covered by natural vegetation were interchanged by *Fadama* farming, which in essence, it is an indication of improvement to the whole *Fadama* farming within the recent years, see the table below for more clarification.

For an explicit explanation of the land use and land cover change detection analysis of the basin, **Table 3-1** below gives a more vantage point of the change based on the classification during the dry season between November to March.

Table 3-1: Total area of the landcover classification in hectares which if related to Figure 1-8 and , the changes can be validated with water, and vegetation cover as a product of climate variability.

Landcover	**Area 1988**(ha)	**Area 1998**(ha)	**Area 2018**(ha)	**% in 1988**	**% in 1998**	**% in 2018**	**△ 1988/1998**	**△ 1998/2018**	**% △1988/1998**	**%△1998/2018**
Water	12,343	26,468	5,216	1	1.7	0.3	14,125	-21,252	114 ⇧	-80 ⇩
Natural Vegetation	49,926	133,019	102,382	3	9	7	83,094	-30,638	166 ⇧	-23 ⇩
Fadama Areas	27,632	9,753	20,713	2	1	1	-17,879	10,960	-65 ⇩	112 ⇧
Non_vegetated Areas	1,474,613	1,394,235	1,435,167	94	89	92	-147,4524	40,932	-100 ⇩	3 ⇧
Total	**1,564,514**	**1,563,475**	**1,563,477**	**100**	**100**	**100**				

Change pattern: ⇩ *Decrease* ⇧ *Increase* △ *Change:*

3.3.2 Landsat image NDVI: The Normalized Difference Vegetation Index was carried out in ArcGIS 10.5 environment using the Landsat data as shown below **Figure 3-5, Figure 3-6, Figure 3-7.**

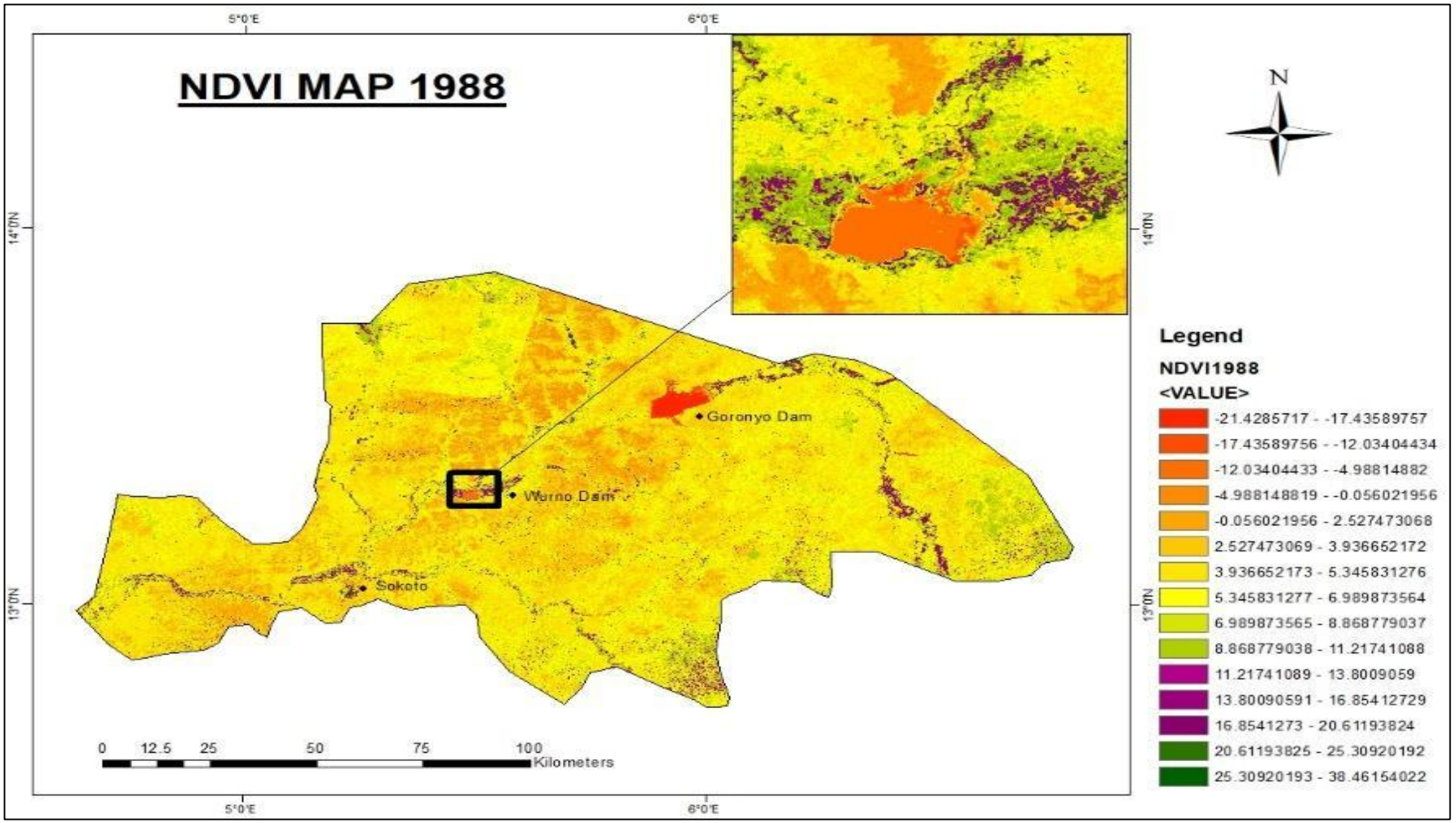

Figure 3-5: Normalised Difference Vegetation Index map 1988. Showing the values of the vegetation indices with purple colour as *Fadamas* between November to March of the *Fadama* farming season.

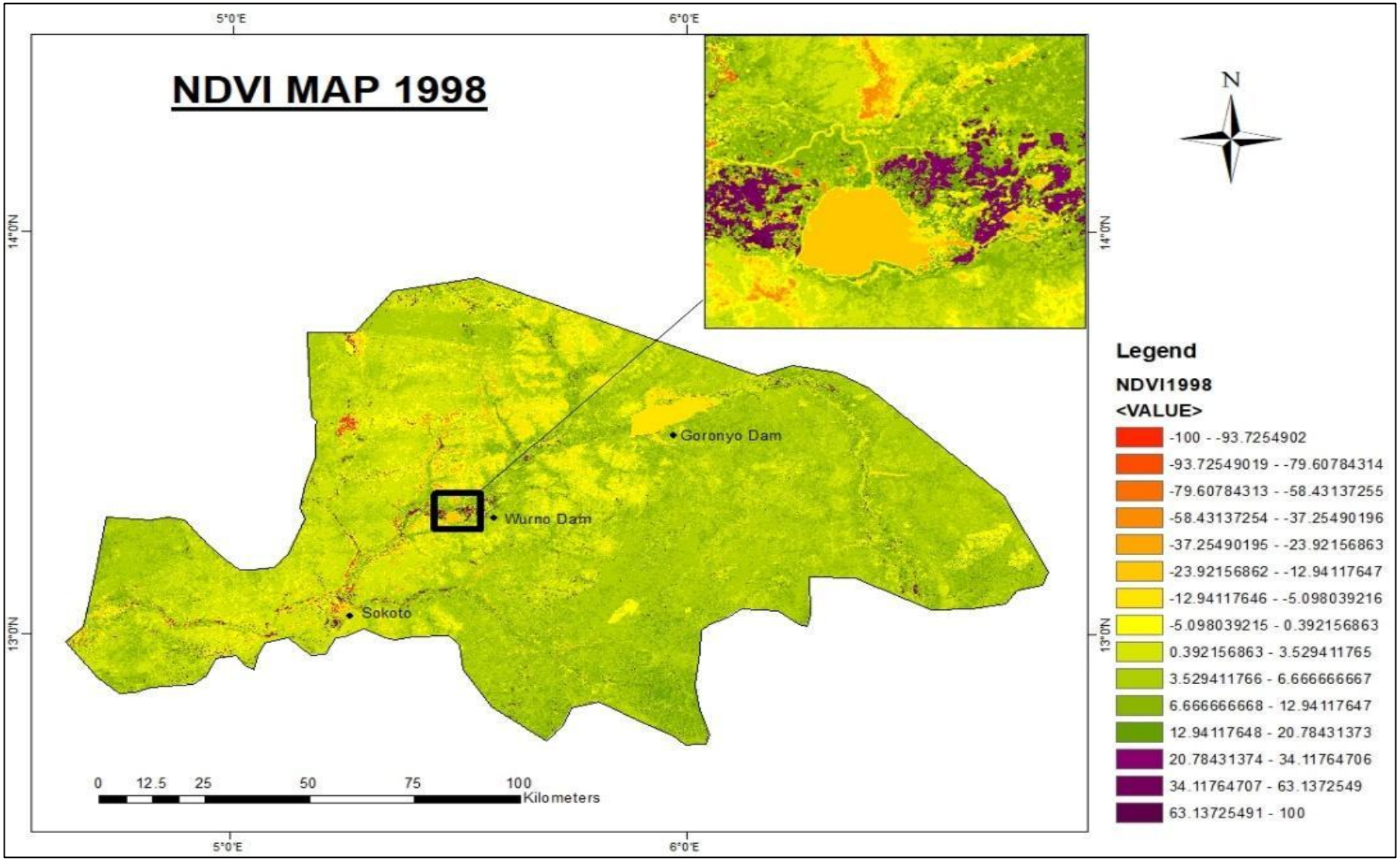

Figure 3-6: Normalised Difference Vegetation Index map 1998 . Showing the values of the vegetation indices with purple colour as *Fadamas* between November to March of the *Fadama* farming season.

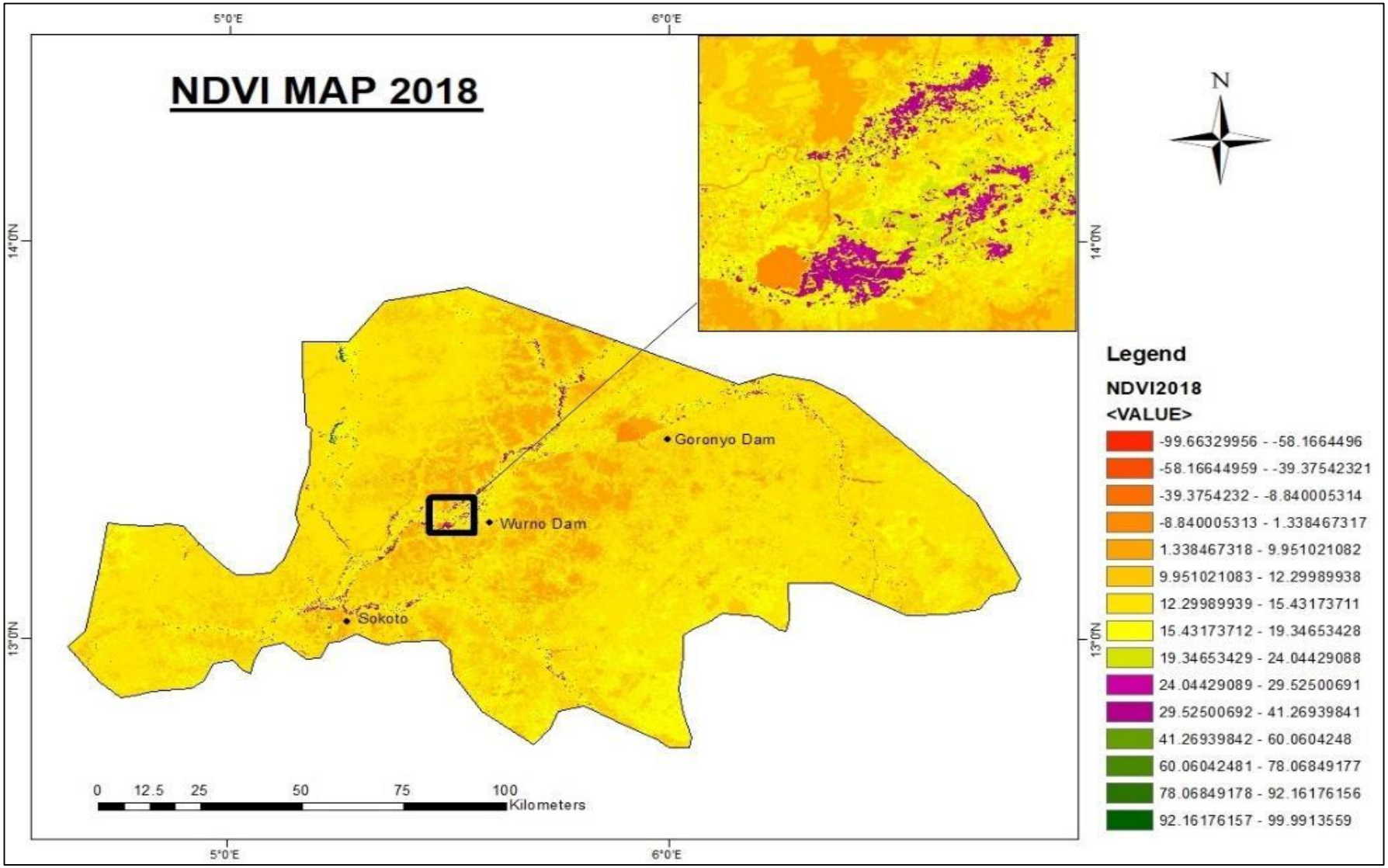

Figure 3-7: Normalised Difference Vegetation Index map 2018. Showing the values of the vegetation indices with purple colour as *Fadamas* between November to March of the *Fadama* farming season

From **Figure 3-5** above, the vegetation index in 1988 ranges from -21.4 to 38.5. The areas with negative values depict no amount of vegetation. Areas with the purple colour palette were identified as the *Fadama* vegetation, which in this case, ranges between 14 to 21. As the choropleth gets greener, it shows a higher amount of natural vegetation which comprises of dense tree populations and other natural vegetation.

The Normalised Difference Vegetation Index in the 1998 map as shown in **Figure 3-6** showed the values that range from -100 to 100, all areas that fall between -5 to -100 have no vegetation, this comprises of bare soil, rocky surface and water bodies. All areas that range between 20.78 to 100 in this map depict *Fadama* vegetation, while areas that fall below 21 to 0.4 have sparse vegetation, this mostly encompass the natural vegetation that is more of grasslands and tree vegetation.

In **Figure 3-7,** the NDVI value ranges from -99.9 to 99.9. Hence, the *Fadama* vegetation ranges from 24 to 41. If this is to be compared with previous **Figure 3-5** and **Figure** 3-6 using the extent indicator in the map. It will be noted that in 2018 there is more *Fadama* vegetation adjacent to the Wurno dam, this can then be validated that as observed in the field visit, within the recent time more *Fadama* cultivation is taking place even when the dam size is reducing drastically.

As such, this gives a clear indication that the higher the spread of NDVI value within the identified *Fadama* areas, the higher the *Fadama* farming going on in that area, and this will influence the yield pattern as well.

3.3.3 Cloud based classification using Google Earth Engine (GEE)

The GEE classification was carried out without any data download, see **Figure 3-8, Figure 3-9, & Figure 3-10.** The classification is considerably accurate with no much spectral confusion. All the imageries are automatically gotten from the Landsat archives using the script in the code editor to display the images in the GEE playground. Although, when dealing with a very large area, there is all likelihood that you can fall into error due to many training sites. To avoid error, I ensured that the script is written well and in line with the command and the variables created in the code editor respectively.

For this study, the classification was done for 1988, 1998 and 2018 during the dry season when *Fadama* farming starts during the month of November to March of the preceding year, although some of the images are + or – one year from the stated epochs. The GEE API allows for data export should in case further analysis needs to be done. But for this study, an assessment of the classification has been done using ArcGIS and Erdas Imagine Environment as shown above. Hence, it will be a duplication if further analysis is carried out on the classified GEE images. Because the result generated are all the same but only shows a different mode of approach into the classification method.

The images below (**Figure 3-8, Figure** 3-9**, Figure** 3-10) depict the classifications done in the Google Earth Engine.

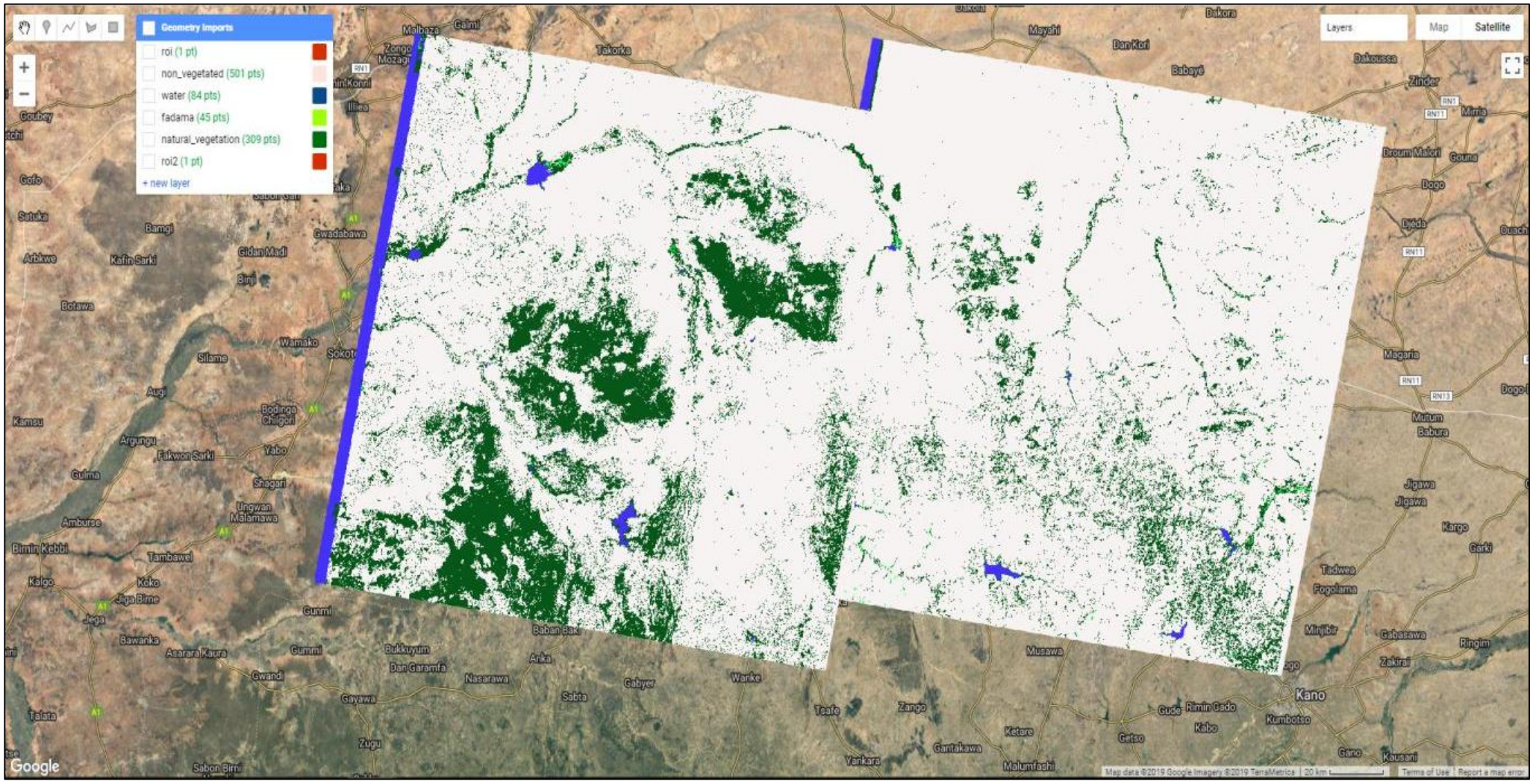

Figure 3-8: 1988 GEE land use/ cover classification of Sokoto Rima River Basin. Showing the image tile that covers the study area and the geometry import (Classes) used for the classification between November to March of the *Fadama* farming season, while the **roi** point geometry was used to get the image from the image collection.

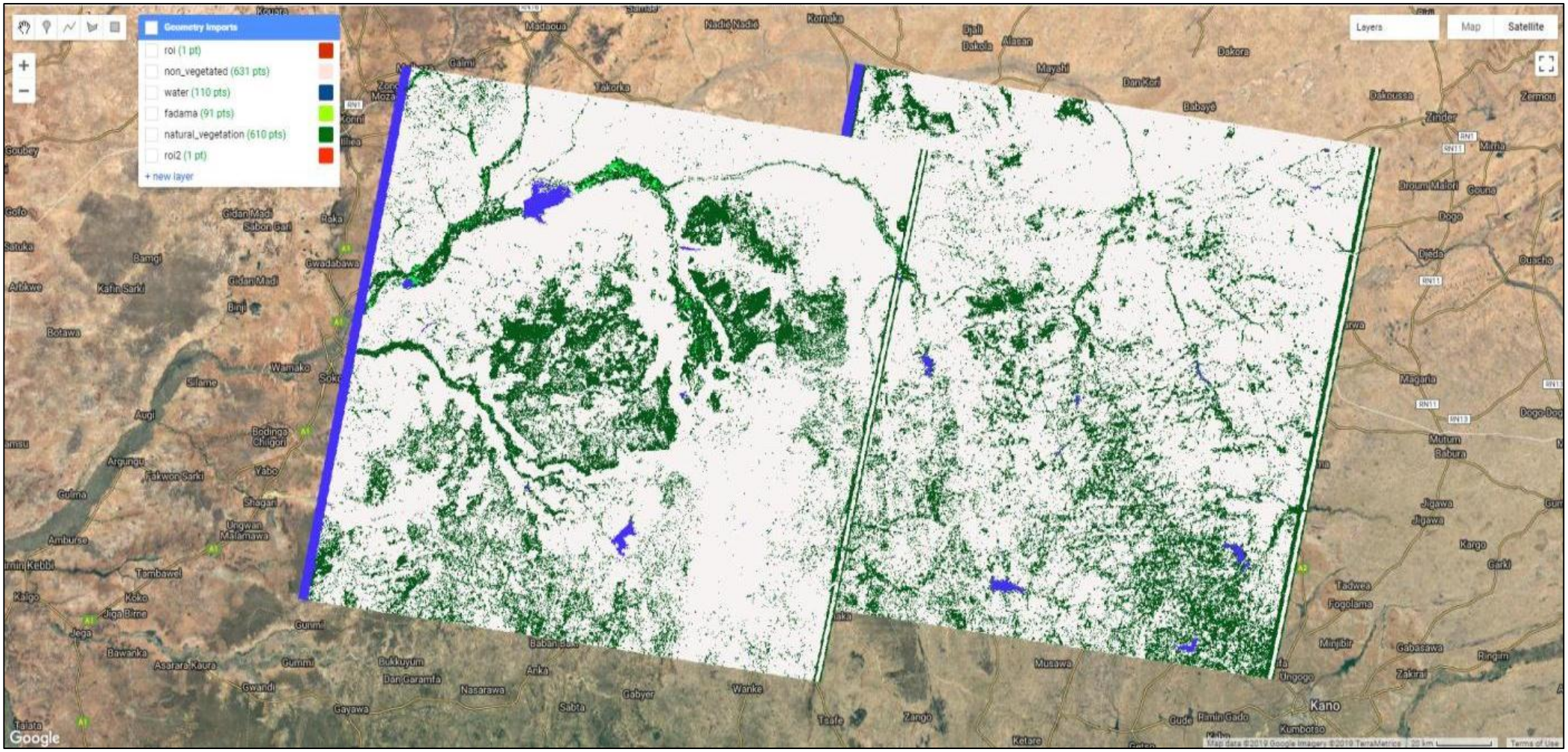

Figure 3-9: 1998 GEE land use/ cover classification of Sokoto Rima River Basin. Showing the image tile that covers the study area and the geometry import (Classes) used for the classification between November to March of the *Fadama* farming season, while the **roi** point geometry was used to get the image from the image collection.

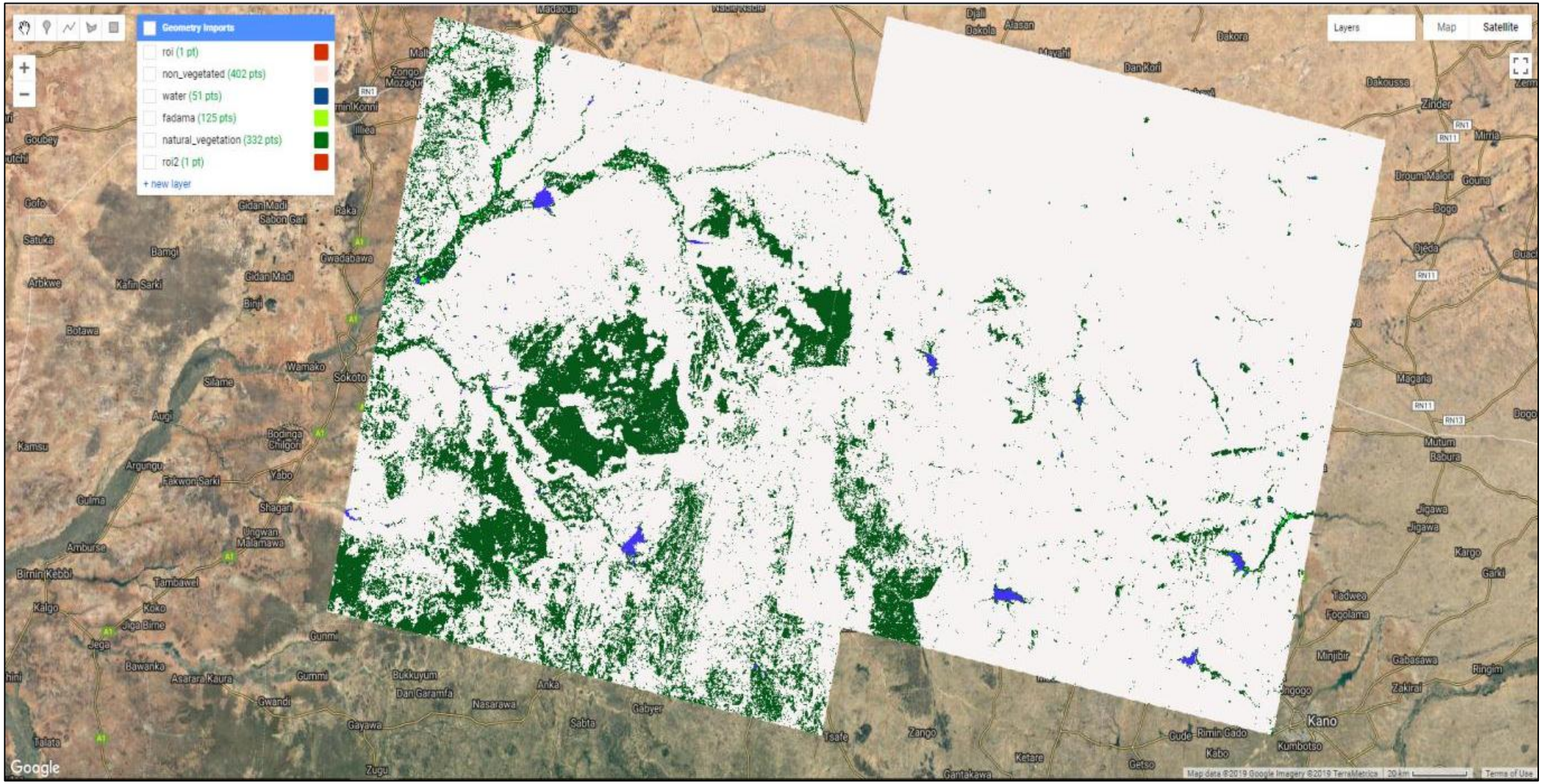

Figure 3-10: 2018 GEE land use/ cover classification of Sokoto Rima River Basin. Showing the image tile that covers the study area and the geometry import (Classes) used for the classification between November to March of the *Fadama* farming season, while the **roi** point geometry was used to get the image from the image collection.

3.3.4 Google Earth Engine (GEE) NDVI time series data

The Normalized Difference Vegetation Index data from the Google Earth Engine was carried out within the GEE API using the code in (**Figure A4a and b**), while the Landsat data was displayed in the GEE playground; see (**Figure 3-11 and Figure 3-14**). All buffered areas **(Figure 5-6**) of the respective *Fadama* sites and data acquired, were printed in the console to have a view on the time series through time from Landsat 4, 5, 7 and 8 respectively, see (**Fig. A4a-b**). To efficiently refine the data, values from 1984-2018 using the Landsat archives were taken from the holistic data to have a continuous time series and good assessment of the trend, by downloading the data in a CSV format from the Earth Engine. Although due to sensor error of the Landsat 7, it will be observed that the data have gaps in them from 2003 when the Landsat 7 satellite developed a fault.

Therefore, a continuous time series of the NDVI and the relative locations where the data was obtained at Jibia, Bakolori, Goronyo, Wurno and Zobe *Fadama* sites were shown in **(Figure 3-11 and Figure 3-14).** While on the other hand, the collected data were further analysed in excel and are shown in (**Figure 3-15 to Figure 3-19**). As such, these values can be assigned to monitor or assess yield and can be used to delineate or estimate the crop yield of *Fadama* farming using the NDVI pattern.

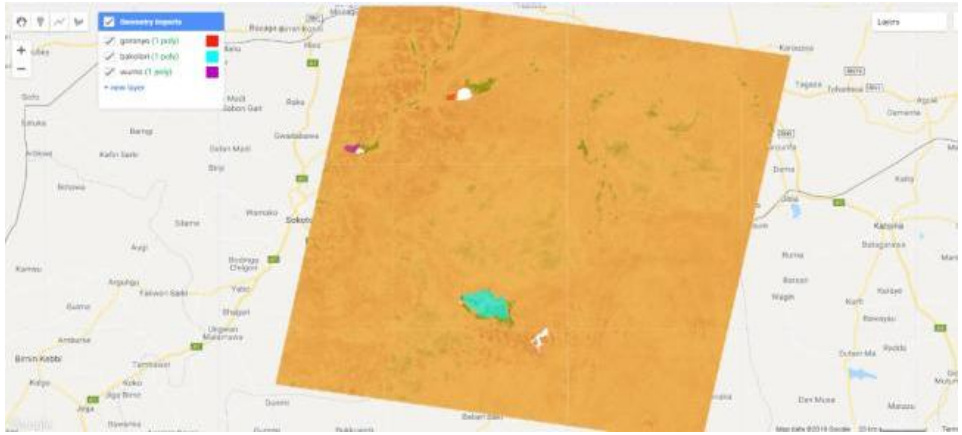

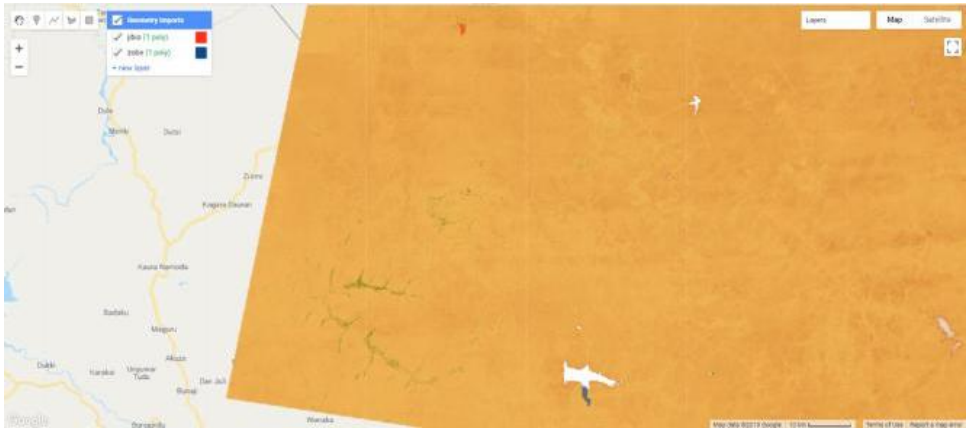

(a) Bakolori, Goronyo and Wurno *Fadama* sites **(b)** Jibia and Zobe *Fadama* Site

Figure 3-11 (a-b):1988 GEE NDVI Image showing five *Fadama* site where values are obtained by masking the areas specifically that are *Fadama*s adjacent to the dam from Landsat 4 ETM, at 30m resolution during the dry season from Nov. to Mar. of the preceding year when *Fadama* farming is taking place.

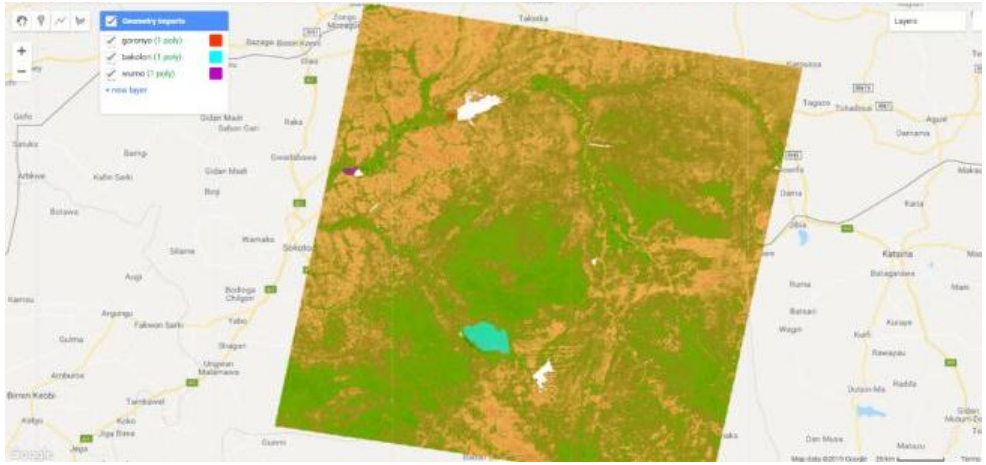

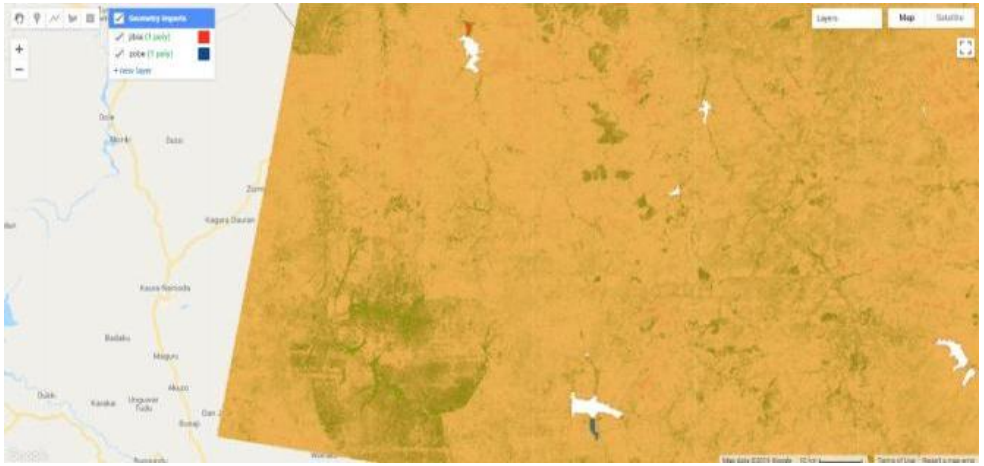

(a) Bakolori, Goronyo and Wurno *Fadama* sites **(b)** Jibia and Zobe *Fadama* Site

Figure 3-12 (a-b):1998 GEE NDVI Image showing five *Fadama* site where values are obtained by masking the areas specifically that are *Fadamas* adjacent to the dam from Landsat 5 ETM, at 30m resolution during the dry season from Nov. to Mar. of the preceding year when *Fadama* farming is taking place.

.

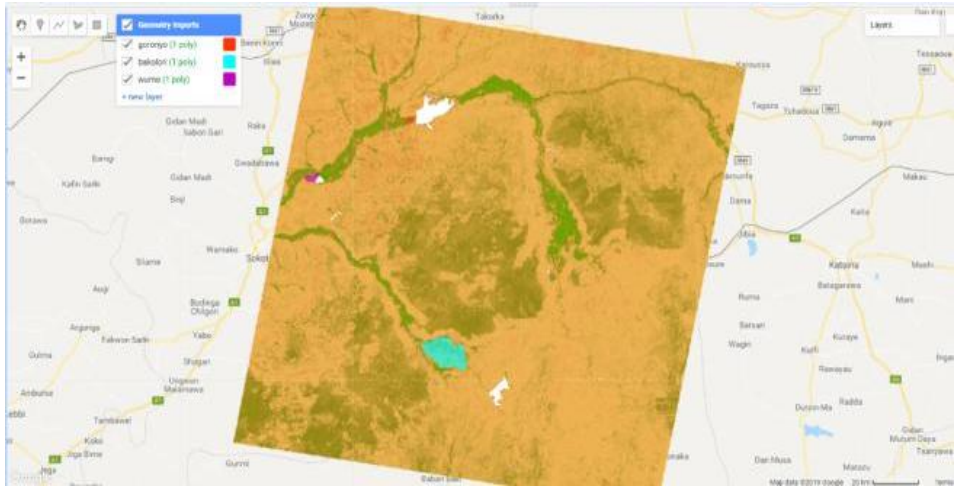

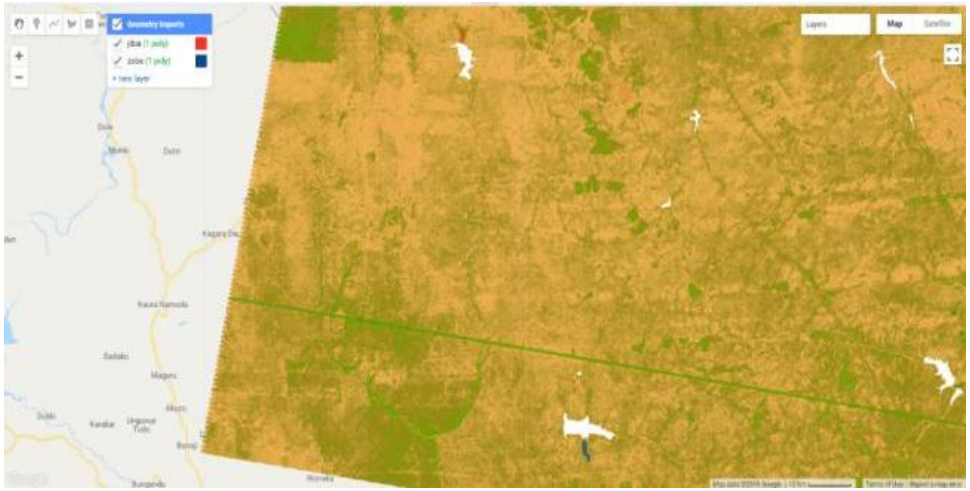

(a) Bakolori, Goronyo and Wurno *Fadama* sites **(b)** Jibia and Zobe *Fadama* Site

Figure -3-13 (a-b): 2000 GEE NDVI Image showing five *fadama* site where values are obtained by masking the areas specifically that are *Fadama*s adjacent to the dam from Landsat 7 ETM, at 30m resolution during the dry season from Nov. to Mar. of the preceding year when *Fadama* farming is taking place.

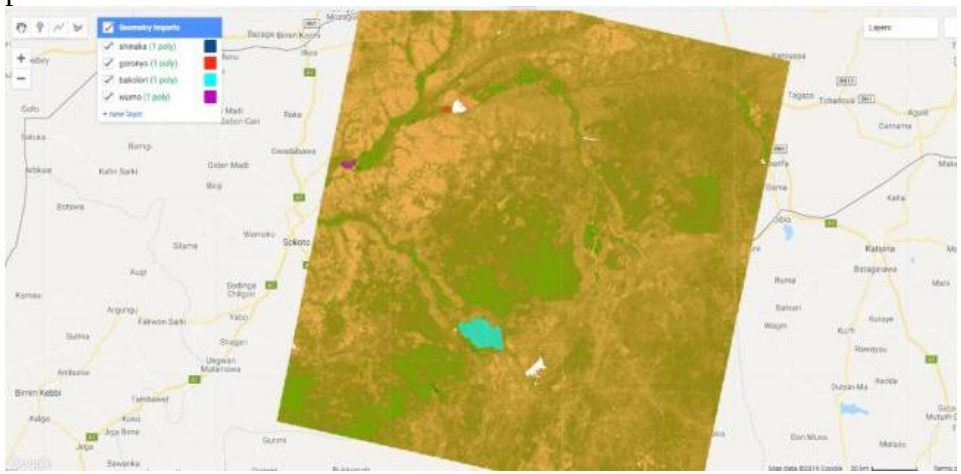

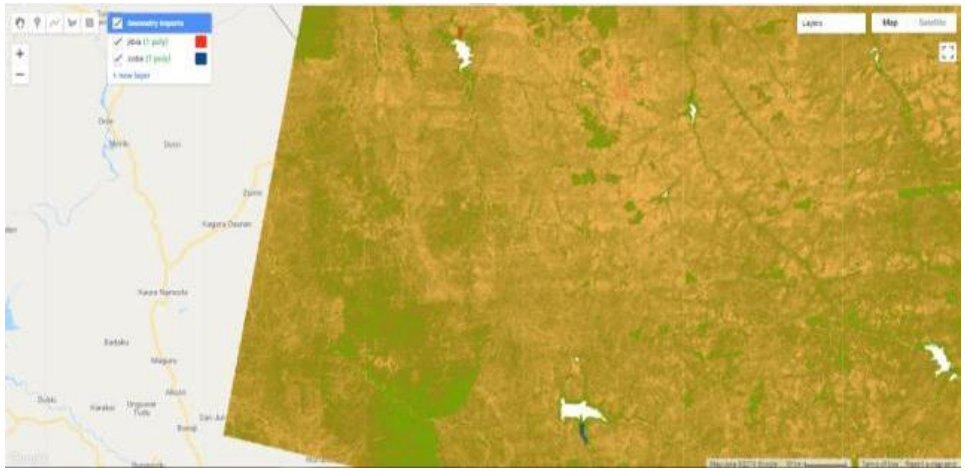

(a) Bakolori, Goronyo and Wurno *Fadama* sites **(b)** Jibia and Zobe *Fadama* Site

Figure 3-14 (a-b): 2018 GEE NDVI Image showing five Fadama site where values are obtained by masking the areas specifically that are *Fadama*s adjacent to the dam from Landsat 8 OLI, at 30m resolution during the dry season from Nov. to Mar. of the preceding year when *Fadama* farming is taking place.

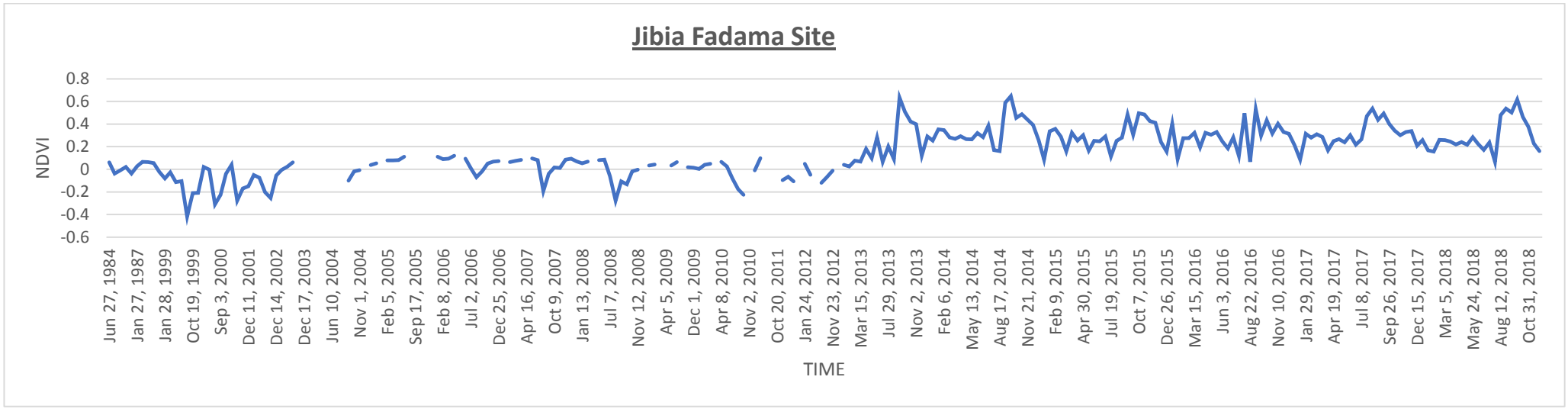

Figure 3-15: NDVI time series for Jibia *Fadama* Area from (1984-2018) showing the vegetation values obtained from the Landsat data in GEE at 30m resolution.

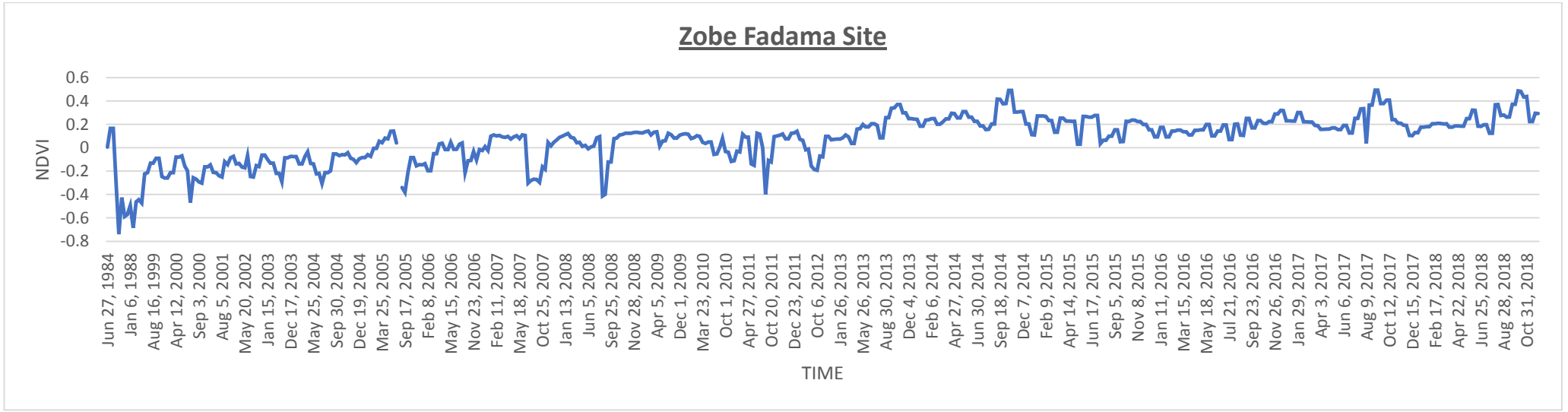

Figure 3-16: NDVI time series for Zobe *Fadama* Area from (1984-2018) showing the vegetation values obtained from the Landsat data in GEE at 30m resolution.

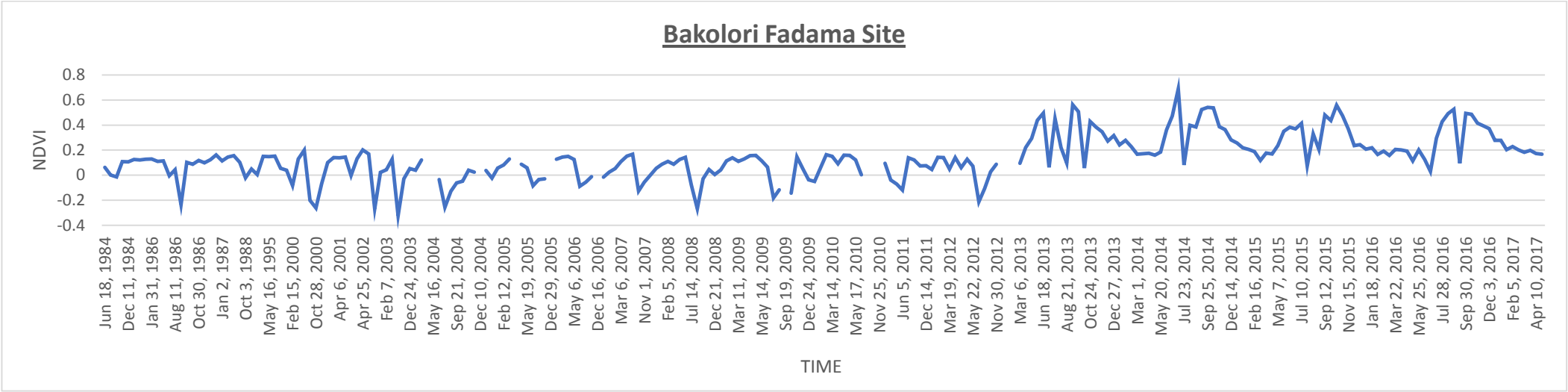

Figure 3-17: NDVI time series for Bakolori *Fadama* Area from (1984-2018) showing the vegetation values obtained from the Landsat data in GEE at 30m resolution.

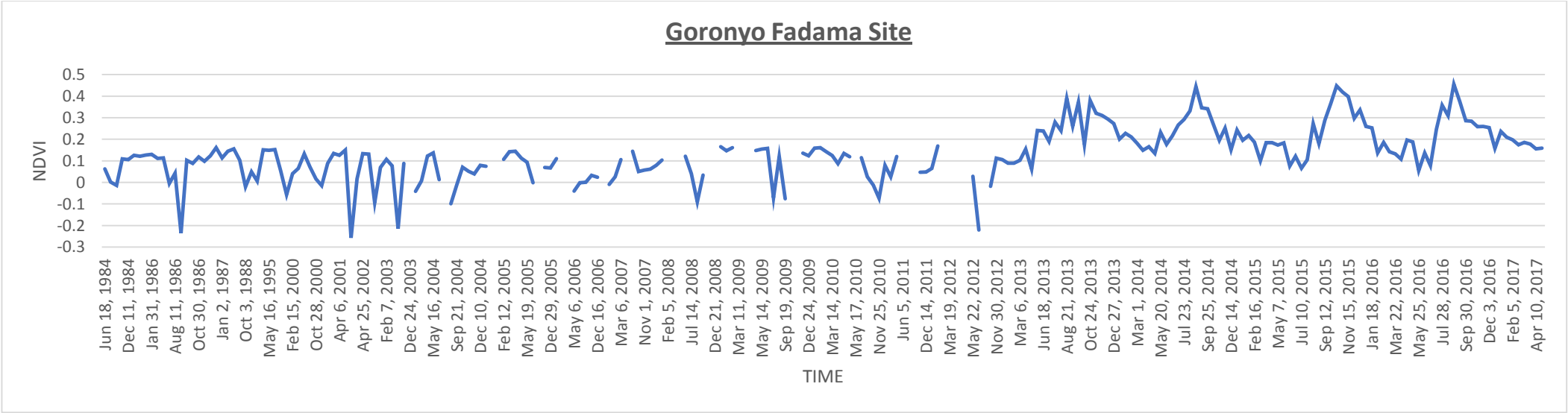

Figure 3-18: NDVI time series for Goronyo *Fadama* Area from (1984-2018) showing the vegetation values obtained from the Landsat data in GEE at 30m resolution, which if this correlated with the yield data, the peak and nadir of the data can be ascertained with how the NDVI values also fluctuate due harvest.

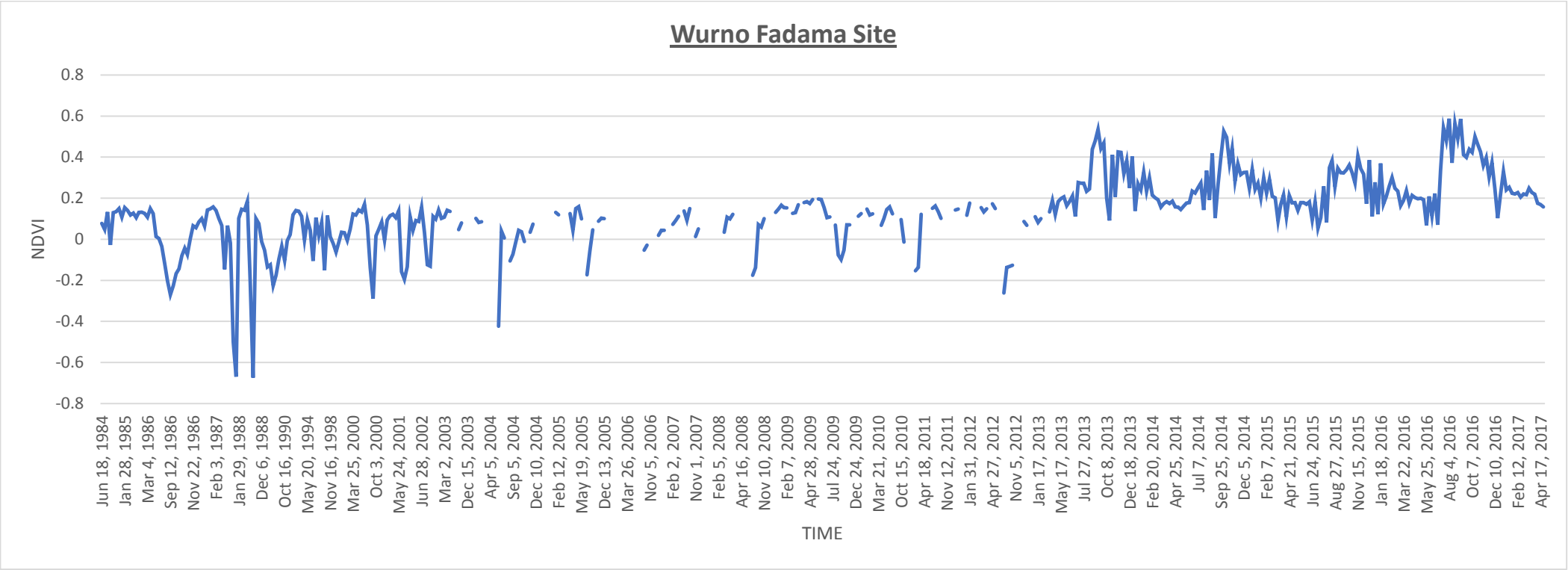

Figure 3-19: NDVI time series for Wurno *Fadama* Area from (1984-2018) showing the vegetation values obtained from the Landsat data in GEE at 30m resolution. Which if this is correlated with the yield data, the peak and nadir of the data can be ascertained with how the NDVI values also fluctuate due pos harvest period which can render the land bare before other plants are replanted.

Unlike the Pekko data that only have NDVI data available from 2000 onward, the Landsat data using the Earth Engine can be obtained as far back as 40 years (Google Earth Engine Team, 2015).

From **Figure 3-15** at the Jibia *Fadama* site; the Landsat data obtained ranges from 1984 to 2018. The Normalised Difference Vegetation Index value appears to be very low from 1984 to somewhere around 2011 with -0.4 as the least value on Oct. 3, 1999, this defines that the rate of *Fadama* farming before the Jibia dam was created is very low. Although even after the creation of the dam, there appears a time when the *Fadama* area shows less vegetation cover which in a real sense, the full capacity of the resource was not adequately utilized. However, within recent years, the NDVI values depict that the amount of vegetation cover seems to have improved with a significant amount of the farming process from the year 2012 to the year 2018.

Zobe *Fadama* site NDVI time series **Figure 3-16,** shows that the rate of *Fadama* farming is quite very low from 1984 to 2018 if compared with other *Fadama* site, with the lowest value as -0.7 on January 11th 1987. Hence, as the year progresses, the NDVI value seems to be increasing which shows that the *Fadama* farming around that very location was significantly improving through the years with the highest NDVI value as 0.5 on September, 10th 2017.

At Bakolori *Fadama* area using the GEE NDVI data; **Figure 3-17.** The NDVI time series also range from 1984 to 2017. As observed, in 1986, 2000, 2002, 2003, 2004 and 2012, there appears a time when a portion from the *Fadama* area was left without any vegetation with the least value as -0.3 on September 19th 2003. Though from the general trend, *Fadama* farming is slightly utilized. In essence, the absence of vegetation in some areas as shown in the time series chart might be due to harvesting, pre-planting operations or fallow that may leave the land bare. From the year 2012, it depicts that the *Fadama* farming significantly increased which gave birth to the high amount of green cover as shown in the chart **Figure 3-17** above with a peak at 0.7 on Jul. 7th 2014.

From the Normalized Difference Vegetation Index (NDVI) time series around Goronyo *Fadama* sites; **Figure 3-18**. The general NDVI pattern also shows that the level of *Fadama* farming within this part of the basin is used efficiently. Though due to sensor instrumentation error of Landsat 7, there is a data break between 2003 to 2012. However, the trend is apparent and similar if Goronyo *Fadama* site is compared with the Bakolori *Fadama* area. The least NDVI value is -0.3 on Sept. 29th 2001 while the highest value was 0.5 on Aug. 29th 2016.

From **Figure 3-19** at the Wurno *Fadama* site. The lowest vegetation index value recorded as -0.674 was observed on the 3rd of October 1988 and -0.7 on the 24th September 1988. The general trend shows that the farming pattern using the values of the NDVI through the years is slightly improving as the year is proceeding. The *Fadama* farming seems to have increased from the year 2013 onward if juxtaposed to the trend pattern from 1984 to 2012. The highest value of the NDVI recorded was 0.6 on the 20th of August 2016 and 0.6 on the 5th of September 2016. Hence, it is worthy to note that in spite of the dam being the smallest in size, it appears to have much of the *Fadama* farming going on.

3.3.5 The Pekko NDVI time series data from Global Agricultural Monitoring

MODIS NDVI (Terra) (MOD)(8-day): Jibia and Zobe Dam *Fadama* Sites.

From the dams as observed in Pekko (**Figure A7**), it can be noted that the Jibia and Zobe dams are located in Katsina as part of the Sokoto Rima River Basin. Observing the NDVI pattern in Pekko and to show the validity of the data, a 1.5 km resolution in both Jibia and Zobe *Fadama* site was used to obtain the NDVI values. See (**Figure A7.1 & 2**) for detailed information.

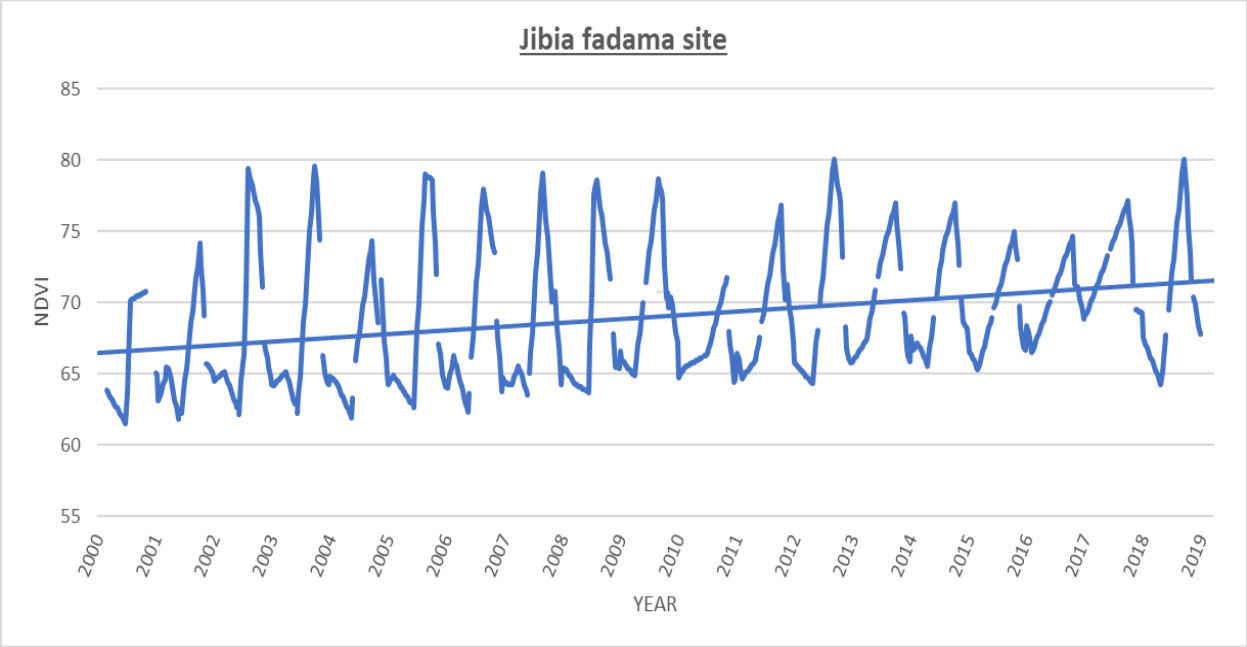

Figure 3-20 (a-b):(a) Pekko NDVI MODIS data of Jibia dam *Fadama* site showing vegetation peaks at 1.5 km spatial resolution. The highest peaks signify the vegetation during the wet season, while other separated peaks inbetween the crest are for the dry season *Fadama* vegetations.

From **Figure 3-20(a)** above, the NDVI data acquired from Pekko depicts that the *Fadama* vegetation pattern is consistent and have green cover vegetation all year round unless for the year 2000 when no data was recorded in some time of the year. The highest peak shows the raining season when vegetation seems to be high all around the *Fadama* area from the year 2000-2019. With the highest value of 80 and 80.06 in the year 2012 and 2018 respectively. However, if observed

carefully, there are other separated peaks as the year progresses which is mostly during the dry season when *Fadama* farming is taking place but with also value decrease which is influenced by post-harvest values before other crops can be planted. As such, this pattern tends to show a significant variation through the years, and obviously showing the data that *Fadama* farming is slightly utilized around Jibia dam using the fitted trend line.

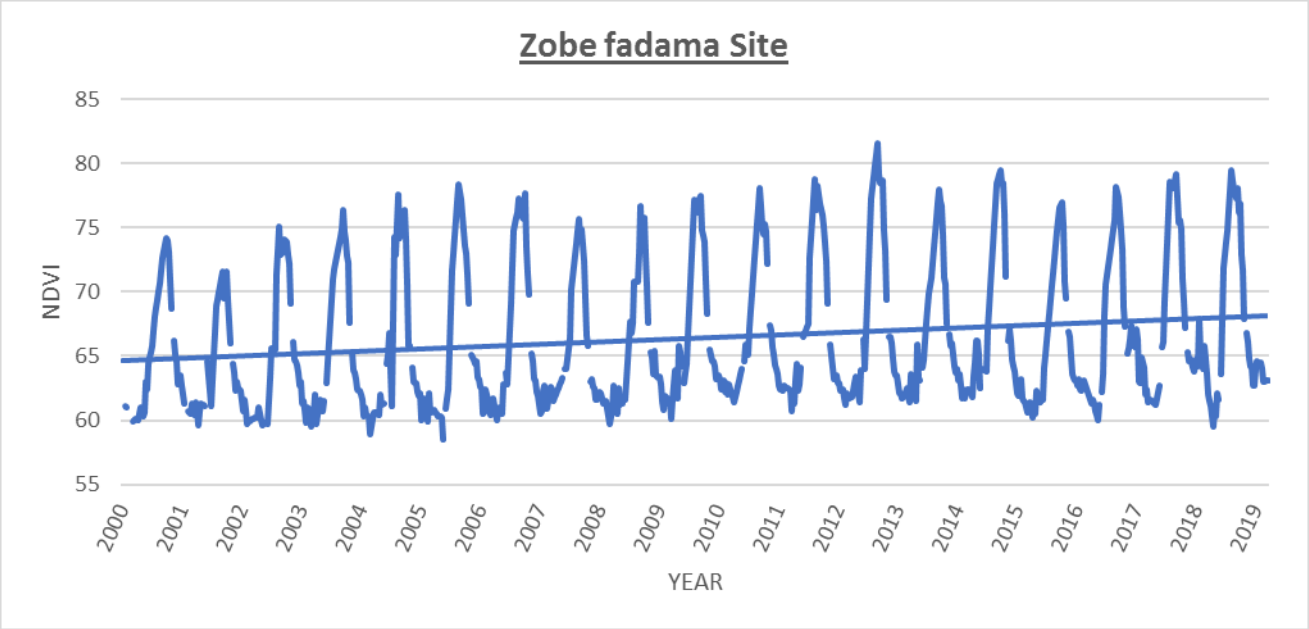

(b): Pekko NDVI MODIS data of Zobe dam *Fadama* site showing vegetation peaks at 1.5 km spatial resolution. The highest peaks signify the vegetation during the wet season, while other separated peaks inbetween the crest are for the dry season *Fadama* vegetations.

At Zobe *Fadama* site, **Figure 3-20(b)**. The vegetation index also shows a significant amount of green cover from 2000 to 2019. Around Zobe *Fadama* sites, there seem to be much drop down on the amount of vegetation because it is showing an undulating pattern with many peaks and nadir as the year progresses. Therefore, the data is showing that the amount of *Fadama* farming seems not to be extensively utilized all year round. Although, in the year 2012, the highest point recorded was 82. In general, the entire *Fadama* farming is increasing using the trend line as shown in the chart.

MODIS NDVI (Terra) (MOD)(8-day): Bakolori, Goronyo and Wurno Dams

The Goronyo and Bakolori dams are quite bigger than Wurno dam, as it is the smallest in size but with a significant amount of *Fadama* farming adjacent to the dam. Bakolori, Goronyo and Wurno dams are located in Sokoto region as shown in **Figure A8**. To ascertain the validity of the data acquired, a 2 km resolution was used in the three *Fadama* sites. See **Figure A8.1-3** for detailed information.

From **Figure 3-21(a)** below, the Pekko NDVI pattern around the Bakolori *Fadama* site appears to be steady even after the raining season. If observed closely, the peak value of most of the years from 2000 to 2019 is maintaining a steady value before slightly attenuating, this depicts that the *Fadama* farming in this ambience is continuous throughout the year. The highest value of the vegetation index recorded was 84.88 in 2016, while the lowest value recorded was 59.34 in the year 2008.

As shown in **Figure 3-21(b)**, the Normalized Difference Vegetation Index around Goronyo *Fadama* area depicts that the general trend from 2000 to 2019 is slightly different if compared with that of the Bakolori *Fadama* site. The highest value recorded was 83 in 2012, while the lowest value through the years is 58 in the year 2003. In general, the vegetation pattern in this part of the basin is observed to be slightly improving from 2008 onward; this indicates that within the recent years more of the *Fadama* farming is taking place unlike from 2000 to somewhere around 2007 where the vegetation index seems to be ebbed.

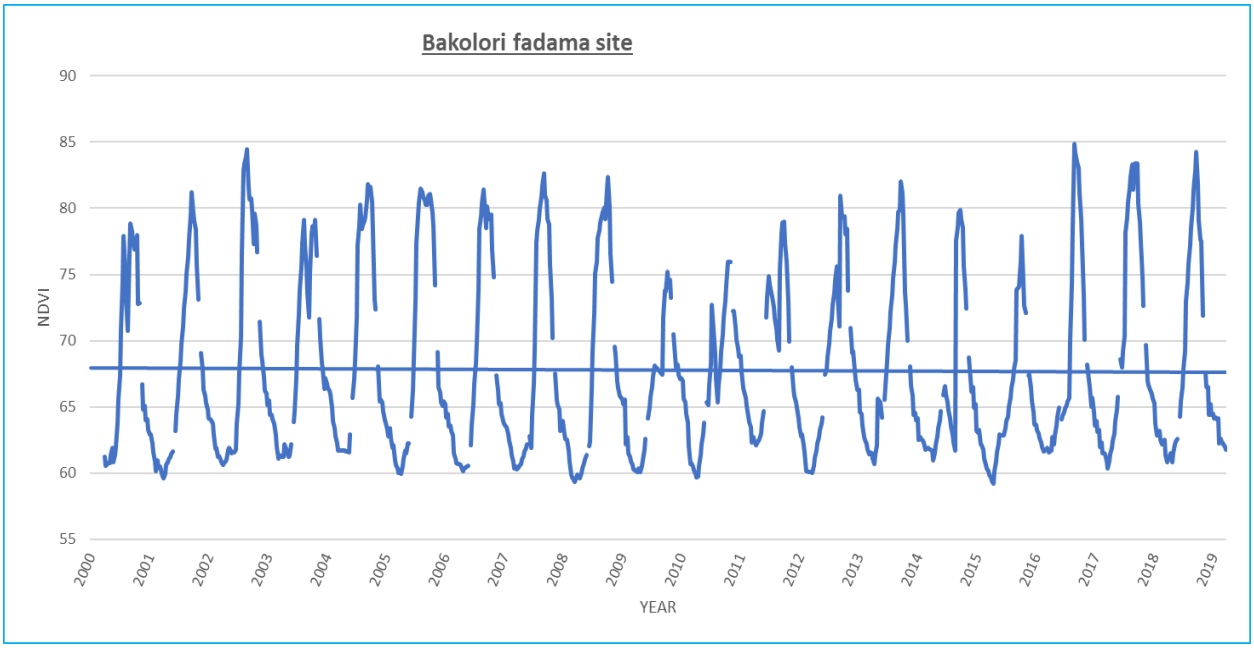

(a) Pekko NDVI data of Bakolori dam *Fadama* site showing vegetation peaks at 2 km spatial resolution. The highest peaks signifies the vegetation during the wet season, while other separated peaks inbetween the crest are for the dry season *Fadama* vegetations.

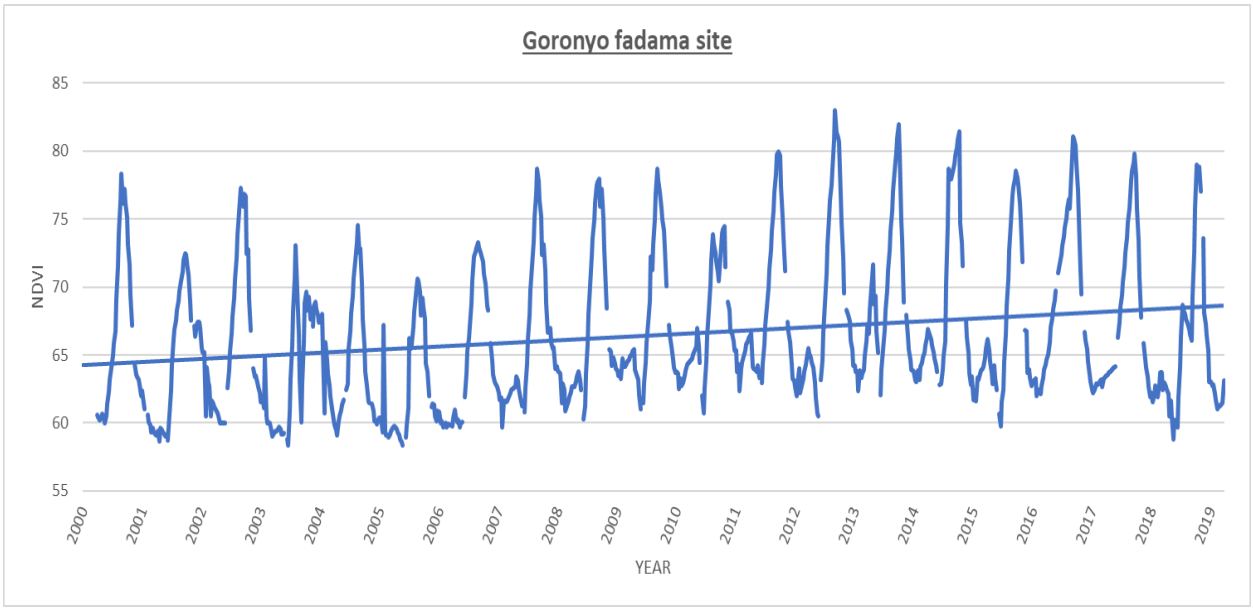

(b): Pekko NDVI MODIS data of Goronyo dam *Fadama* site showing vegetation peaks at 2 km spatial resolution. The highest peaks signify the vegetation during the wet season, while other separated peaks inbetween the crest are for the dry season *Fadama* vegetations.The fall in the NDVI value during the dry season can be affected by post-harvest values which depict that the land is left bare before other crops are replanted. If this is to be compared with the crop yield data, as shown in **Figure 2-5,** it can be deduced that the yield values around Goronyo have a similar pattern with the NDVI values obtained with a rise and fall of the estimated yield from 2000-2005. Between 2001 to 2004, the yield pattern for onion, millet and sorghum shows a perfect correlation with the NDVI values, as such, depicting that remotely sensed data from MODIS can be used to assess the trend.

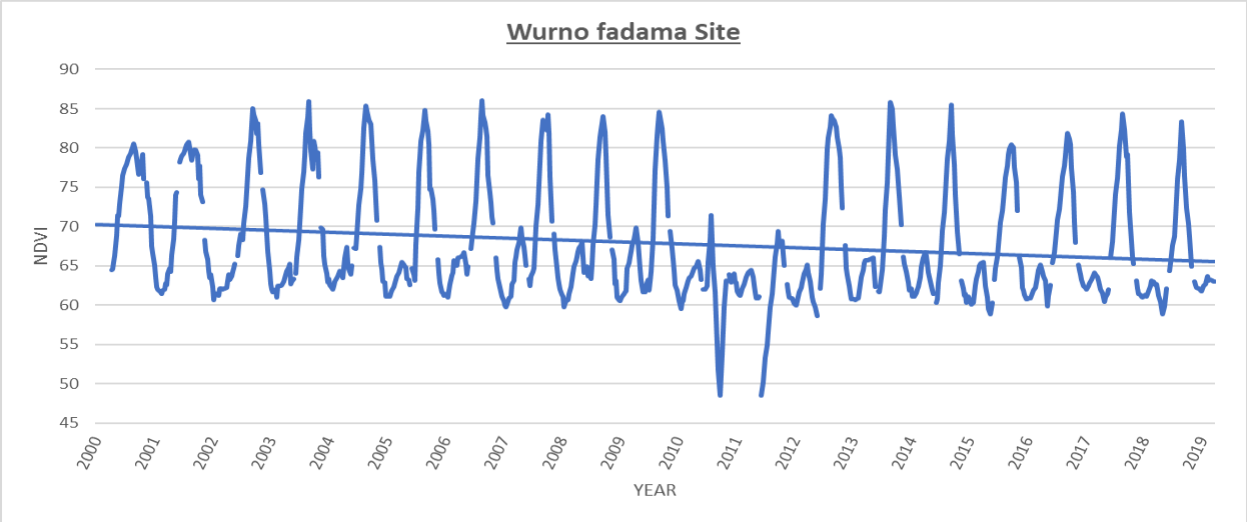

Figure 3-21 (c): Pekko NDVI data of Wurno dam *Fadama* site showing vegetation peaks at 2 km spatial resolution. The highest peaks signify the vegetation during the wet season, while other smaller separated peaks inbetween the crest are for the dry season *Fadama* vegetations. The sharp decline in 2010 and 2011, may have been influenced by long post-harvest value that takes a while before other crops are replanted and rendering the land bare for a long period.

At Wurno *Fadama* site as shown in **Figure 3-21(c)** above. The NDVI values appear to have a sharp decline in 2010-2012 with the lowest value of 49 in the year 2010 and 2011 respectively. This showed that in this time of the year; there was little or no vegetation cover around the *Fadama* area which interprets low *Fadama* farming. This can be related to long post-harvest value that takes a while before other crops are replanted and rendering the land bare for a long period, or high cost of fertilizer or low return in market value of the *Fadama* crops and the cropping pattern as earlier cited may as well be a pulling factor. Hence, as the year progress, the farming seems to have improved because of the vegetation index increases and maintained a slightly regular pattern through the years, with the highest value of 86 in the year 2013 and 2014 respectively

3.4 Discussion

3.4.1 Land use/ cover classification and accuracy assessment

A total of 288 ground truthing (GT) Points **Figure A5.1a** were used for the error matrix assessment within the ArcGIS 10.5 environment. Seventy-five (75) points were allocated to water, while 71 points for each were allotted to *Fadama*, natural vegetation and non-vegetated areas respectively.

Using the Kappa Coefficient, the Overall accuracy (OA) in 1988 classification was 97% accuracy **Figure A5.1**. In the year 1998; the OA was 92% accuracy **Figure A5.2**. While in 2018, it is 90% accuracy **Figure A5.3.** If compared with the normal standard of 85% benchmark for classification accuracy as stipulated by the USGS, (Musa & Odera 2015). This study is is significant to assess the change detection within the basin with OA that is fair enough to draw precisions on the general Land use and Land cover of the floodplain.

The proportion of the correctly classified (PCC) percentage as a measure of the classification accuracy in this study, is significant to affirm that the PCC of 97%, 92% and 90% in the respective epochs is greater than 76% as opined by Diallo & Wen, (2009). However, there is no definite universal standard for thematic mapping in remote sensing (Foody, 2008). Though the PCC percentage of this study will conform to go with that of Munyati, (2000), Chen and Rao, (2008), Gutierrez *et al.,* (2011) and among other related studies. As earlier cited by Musa & Odera, (2015), the classification in this research can tangibly be considered as a good representation of the land use and land cover of the study area of Sokoto Rima River Basin.

3.4.1.1 Land use/ cover change

As shown in **Table 3-1**, between 1988-1998, the landcover types in the study area have measured a decline in *Fadama* areas and the non-vegetated areas respectively, while in 1998 to 2018; the change was observed to be an increase. More so, between 1988 to 1998, water and the vegetated areas was observed to be an increase in their area extent, while on the other hand, between 1998 to 2018 there was a drastic decrease which can be seen as an effect of climate change within the contemporaries.

The overall change analysis shows that the land use and land cover of the floodplain between the three periods, experienced a notable shift in the activities carried out in the basin (Eniolorunda *et al.*, 2017). Among them include a complete loss or conversion of the forested cover, expansion of scrubland and overgrazing, change in crop pattern, a shift in water and the wetlands, and rapid urbanisation.

3.4.1.2 Classification using GEE

One among the advantages of GEE remains the ease-of-use and its robust library of global remotely sensed data. Presently, users from a wide range of disciplines are involved in projects that have been analysed in Google Earth Engine. Nonetheless, the classification accuracy is quite remarkable because there is less spectral confusion of most pixels, unlike other software based classifications.

Cloud computing and the archived Landsat data in the Google Earth Engine has many advantages for broad scale and long time-series mapping, such as the monitoring of woody vegetation clearing and detecting the extent of human settlement (Johansen *et al.*, 2015; Patel *et al.*, 2015; Trianni *et al.*, 2015). More so, it is quite easy to integrate seasonal NDVI time-series and textural features to enhance classification accuracy.

Gorelick *et al.*, (2017) states that as more algorithms within the machine learning and the remote sensing data are incorporated into the GEE API and data catalogue, we expect information extraction from remote sensing data to be simplified even further.

The performance, efficiency, and scaling of the Earth Engine take advantage of the Java Just-In-Time (JIT) compiler to optimise the implementation of chains of per-pixel operations that are attributed in image processing (Gorelick *et al.*, 2017).

Google Earth Engine is now in use across different disciplines, covering topics of discussion such as crop yield estimation (Lobell *et al.*, 2015), urban mapping (Zhang *et al.*, 2015; Patel *et al.*, 2015), global surface water change (Pekel *et al.*, 2016), rice paddy mapping (Dong *et al.*, 2016), fire recovery (Soulard *et al.*, 2016). It has also been used in assessing land use change (Collect Earth, 2016), analysing species habitat ranges (Map of Life, 2016), and monitoring climate (Climate Engine, 2016). The details of these applications will illustrate how Earth Engine's capabilities are being utilized.

Hansen *et al.*, (2013) characterised forest extent, gain, and loss from the year 2000 to 2012 using a decision tree produced from a vast set of training data and a stack of metrics. It was calculated from large Landsat scenes collections and filtering the operations that are supported by the data catalogue by reducing the 1.3 million Landsat scenes available to 654,178 growing-season scenes from the study period. These imageries were then screened for clouds, cloud shadows, and water, then converted from raw Landsat digital numbers to the normalised TOA (top of atmosphere reflectance). All necessary data access, format conversion, cartographic reprojection, and resampling were handled automatically by the system in GEE. Operations in the API were used to compute and input the metrics, such that per-band percentile values and the linear regressions of reflectance value of the image date are produced. The metrics along with training data were used to generate decision trees, which were then applied to the metrics globally to create the final output data. Those results were used for publication and made available as part of the Earth Engine catalogue for further analysis by others.

Hence, both scientific and operational users, have since successfully built on Hansen *et al.*, (2013) results to produce derivative results using the Earth Engine just like this research. Global Forest Watch, (2014) integrate this into an interactive analysis application using Earth Engine to perform on-the-fly computations of summary statistics. Joshi *et al.*, (2016) used it to track the change in tiger habitat by extracting forest loss within the protected areas for each year, finding that the

areas most suitable for doubling the wild tiger population were also the best preserved.

In another example, Lobell *et al.*, (2015) describe this to the output of hundreds of crop model simulations to vegetation index, such as the green chlorophyll vegetation index (GCVI) that are measurable with satellite data. They then associated and simulated yields to measure vegetation index and weather for a set of dates early in the cropping season and late in the farming season. It later resulted in a table of regression coefficients for each pairwise combination of early and late date used. Therefore, they used the GEE to select on a per-pixel basis, the best Landsat scenes for the early and late periods, and first calculating reflectance of the Landsat scenes using LEDAPS (Masek *et al.*, 2006). Automatically removing cloud scenes using (GEE) simple cloud score function, and computing GCVI values, finally selecting the scene with the peak GCVI.

Once the best or a good pair of Landsat scene were observed for a given pixel, weather datasets stored in GEE and the GCVI were obtained to compute the assessed yield. This method was applied to approximately 7 million ha of soy and maize fields in the midwestern United States to calculate annual yields from 2008 to 2012. The total computation completed in approximately 2 min per 10,000 km^2 per annum.

3.4.2 The Normalised Difference Vegetation Index (NDVI)

The NDVI pattern within the basin using the pekko NDVI and the GEE Landsat data shows a varying trend with an increase in vegetation as the year progresses from 1984 to 2018 in GEE, while in Pekko from 2000 to 2019. The *Fadama* farming was observed not to be extensively utilised, rather slightly utilised using the NDVI values obtained. As such, this is showing that the full farming potentials around the basin are yet to be fully harnessed. While the land use distribution shows a fluctuating crop yield due to the underscored utilization but with varying cultivation pattern, and less use of the full resources in the face of the available land, enhanced technical know-how, and the thriving

population growth. Indeed, this has an implication for the workforce and as well as food security (Eniolorunda *et al.*, 2017).

3.4.3 Problems and limitations with the remotely sensed data

Remote sensing data have long been used for earth observation, but it also has its limitations and problems when dealing with large area that requires the mosaicking of several image tiles. Specific to this research, the problems encountered was with the image due to large extent of the river basin. At inception, the whole basin was considered for the change detection analysis, but it was then observed that the area is too large and with different time out error; which was later nested and scaled to ease the computation capacity within the geospatial environments (i.e. ArcGIS and Erdas Imagine).

However, after the image classification, there was spectral confusion of the pixels between the bare soil and the built-up areas. This was because the materials used in the building is usually from the red lateritic soil, as such, this was having the same spectral reflectance on the image. But this was later corrected by combining the classes to come up with only four classes.

Due to sensor error of Landsat 7 from 2003 onward, there appear a continuous scan line corretor failure on the image, though the gaps can be interpolated in some of the images. But specific to this research, it was impossible due to consistent scan line and can not be used to obtain a valid change detection analysis results. However, this was used to obtain the NDVI values but with data gaps in them; see NDVI Landsat data for details **Figure 3-15 to Figure 3-19**. Therefore, using the Pekko NDVI, this data can be used to bridge the gap, and a more refined assessment of the NDVI values in any location can be generated without many hitches.

3.4.3.1 Challenges with GEE

Among the benefits of using Google Earth Engine is that the user is nearly protected from the details of working in a parallel processing environment. The system manages and hides almost every aspect of how the computation is carried out, including parallelism, resource allocation, retries, and data distribution, unlike the manual Landsat analysis. These decisions are strictly administrative, and none of them can affect the result of any query, only the speed at which it is produced is shown. As such, the liberation price from these details is that, the user is not able to influence the process because the system entirely regulates the computation in GEE. This results is somewhat an interesting challenge in both the design and use of the system (Gorelick *et al.*, 2017).

However, in this research, several errors were encountered and were overcome. When using the Earth Engine; the code and the command one is generating needs to be well defined. While dealing with vast area especially when classifying the Landsat data; base on the fact that it is a tile by tile image parallel computation, there is all tendency of running into a time out errors due to several clusters of the training classifier using the point geometry import. However, after the image has been classified, there is a strip that appears at the edge of the Landsat image, but this is more specific to Landsat 4 and 5 and does not appear in Landsat 8.

3.4.4 Fadama utilisation from remote sensing perspective

From the remotely sensed data used to assess the *Fadama* irrigation, and the Land use/cover change within the Sokoto Rima River Basin. The *Fadama* appeared to be utilized by 112% between 1998 to 2018 from the result generated as seen in **Table 3-1,** though not fully utilized because if this is to be compared with **Table 1-2** in terms of the planned irrigation and the operated irrigation, the less utilization can be validated. Although within recent years, the difference between the two

epochs saw a slight improvement of 47% increase within the farming system as shown in the decadal percentage change. But on the other hand, the effect of climate change and recurring moderate drought is drastically affecting the surface water hydrology because the dam size seems to be shrinking in size but not really having much effect to the irrigation since water is still supplied to the field. Though if the full capacity of the river basin is to be utilized, there might be a shortage in the water supply to various *Fadama* fields through the dry season due to the recurring moderate drought as it can be observed in the next chapter.

CHAPTER FOUR

4 Impact of climate on surface water and land use/landcover change

4.1 Introduction

The increase in temperature and the effect of climate change is now an issue of concern within the Sokoto Rima floodable plain due to its vast land resource for agricultural practice, e.g. over the past decades, average monthly temperature around Sokoto has increased to over 40 degree celsius, while average annual rainfall decrease to less than 400 mm, see **Figure 4-1** below. The presage of this natural hazard has long been studied in various fields long before now (Assadollahi, 1975).

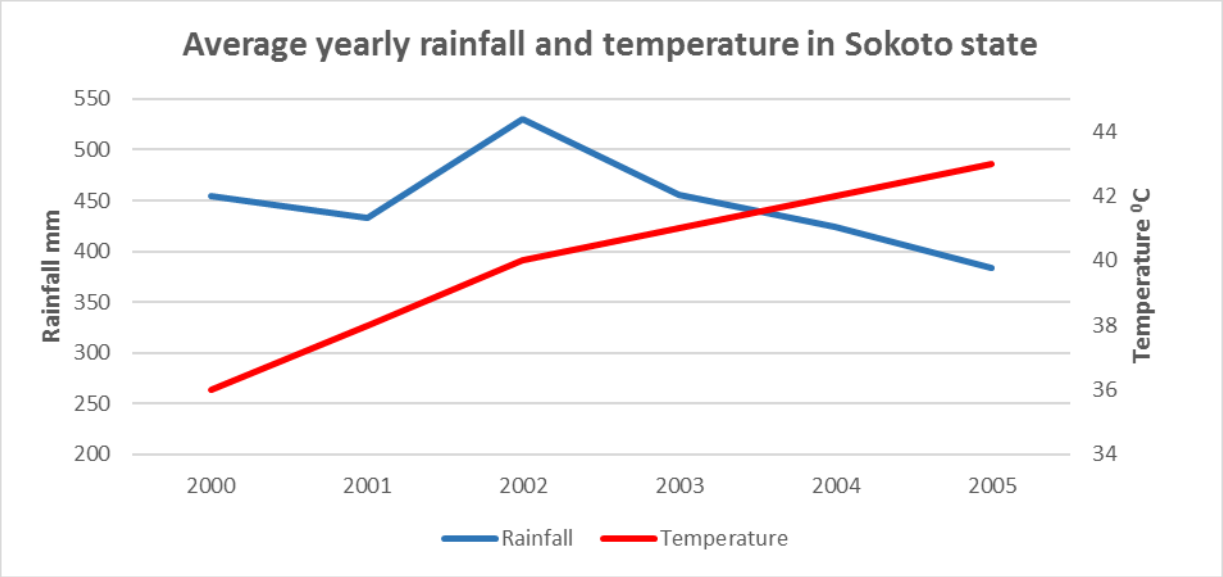

Figure 4-1: Yearly average of temperature and rainfall data in Sokoto from 2000-2005. From the data as shown above, the temperature is increasing over time with 43 degrees recorded in 2005, while the rainfall was observed to be decreasing through the years with 384 mm in 2005. (source: Sokoto statistical year book, 2010)

Drought is a period that is below average in terms of precipitation in a given place which can result in a prolonged shortage in water supply and can be defined in numerous forms. It depends on the amount of water losses, which can be either (hydrological, meteorological, agricultural or socio-economic drought). The impacts of drought are considered to be the costliest (He *et al.*, 2011) and the

second most pervasive condition after flood, those impacts can be anywhere and ranges from short to long term effect (i.e. from months to years), but these depends on their characteristics like severity and frequency (Zahid *et al.*, 2020).

There is no specific way to measure drought, because it is generally calculated based on its impact using different indices (Svoboda & Fuchs, 2017). There are several indices available for this purpose like the PDSI, SPI, SPEI etc, however, the index selection is important because they are area-specific and depends on the input data available.

To understand these phenomena, the SPEI (Standardized Precipitation and Evapotranspiration Index) is considered in this study because it takes into account the effect of temperature on water demands, along with precipitation and potential increase in evapotranspiration (Trenberth et al., 2014). It was also found to work better in areas of the arid and semi arid zones, as it takes the water balance into consideration in evaporation (Zahid et al., 2020). On the other hand, the amount of water change in terms of time and space, was monitored using the global surface water explorer.

4.1.1 The Standardised Precipitation and Evapotranspiration (SPEI) index

The SPEI was initiated by Vicente-Serrano *et al.*, (2010). What led to the development of this index is the fact that other drought indexes like the SPI: standardized precipitation index, SWI: soil moisture index, and MSDI: multi-variable drought index are not efficient in a case of drastic increase in temperature and the associated decrease in precipitation over the years. The research by Vicente-Serrano *et al.*, (2010) observed the influence of climate change and the decline in the amount of precipitation over the duration, and the gravity of drought for a period of about 50 years. Climate change is not limited to a reduction in precipitation only, but also the gradual increase in temperature during the research period. This has been the subject matter that led to the development of this index

which takes into account the precipitation and the temperature data (i.e. evapotranspiration).

Just like the SPI which based on rainfall, the SPEI is computed based on the disparity between rainfall and the potential evapotranspiration. The methodology encompasses the use of methods that estimate the potential evapotranspiration as a function of temperature. The Thornthwaite, (1948) method used in the computation was chosen because it does not require many parameters and is only based on air temperature. Although other evapotranspiration formulas can be used for the index computation like the Penman, (1948) equation, but this may require more climate variables over a stretched period of time resulting in complex and time-consuming mathematical calculations. However, Mavromatis, (2007) state that the use of other PET calculation methodologies leads to much similar drought index results as far as this is concerned.

4.1.1.1 Analysis of the (SPEI) global drought monitor data

The SPEI stands for (Standardised Precipitation-Evapotranspiration Index). The dataset is usually updated during the first days of the coming month based on the most genuine and updated climatic data sources. The mean temperature data are gotten from the gridded dataset of NOAA NCEP CPC GHCN_CAMS. Monthly summation of precipitation data is acquired from the 'first guess' of the Global Precipitation Climatology Centre (GPCC). Hence, the data from the GPC with an original resolution of 0.5 degrees is interpolated to a resolution of 1 degree.

Presently, the SPEI global drought monitor is analysed on the basis of the Thorthwaite equation for the estimation of potential evapotranspiration (PET). The merit of the SPEI global drought monitor is that it is a characteristic best suited for drought monitoring and early warning purposes and a near real-time character. For long-term analysis, other datasets will be preferred to rely on for more robust methods of PET estimation. Use of the SPEIbase dataset which is based on the FAO-56 Penman-Monteith model, is hence, recommended for climatology studies of drought on the other hand.

The SPEI global drought monitor gives a piece of near real-time information about the drought conditions from a global scale perspective using the global SPEI database and SPEIbase. It is characterised with a multi-scale character; It provides SPEI time-scales that ranges between one to forty-eight months i.e. SPEI_1 depicting meteorological drought and SPEI_48 showing hydrological drought. Presently, It covers a period between January 1901 and December 2018.

Table 4-1: SPEI values with description

SPEI values	Categories
≥ 2.0	Extremely wet
1.5 to 1.9	Very wet
1.0 to 1.49	Near normal
-1.0 to 1.49	Moderate drought
-1.5 to -1.49	severe
≤ -2.0	Extreme drought

The drought indices used in the SPEI will show a continuous drough if the values are negative, i.e. -1.0 or less, and stops when the index changes to positive. When the indexes show values between ±1 and ±1.49 the drought status becomes moderately dry for the negative numbers and somewhat wet for the positive numbers. When they show values between ±1.5 and ±2 it depicts a much dry period or a very wet period of the drought pattern respectively, and at the latter, when the value is greater than or equal to 2 and less than or equal to -2 the period is usually an extremely wet or extremely dry state respectively.

4.1.2 The global surface water explorer

Based on the fact that water losses are geographically experienced than gain in most global water bodies that are linked to drought and human activities that may comprise river diversion, damming and unregulated discharge. Have

necessitated the invention of tools that will give us a quick understanding of the earth's surface water holistically.

With the global consistency and a validated dataset, we can easily show the impacts of climate oscillations or rather climate change on surface water existence. It can be quantified, and that evidence can be gathered to display how surface water is altered by human actions, (Pekel *et al.*, 2016). Hence, this freely available data will upgrade the modelling of surface forces, show proofs of the state and the rate of change in most wetland ecotones (i.e. transition points between biomes), and provide information on water-management strategies. This new dataset was developed by the European Commission's Joint Research Center under the framework of the Coperniscus Programme. The global surface water dynamics was acquired from coarse-spatial-resolution satellite observations (Prigent *et al.*, 2012). While the higher resolution of seasonal maps has been generated using the Landsat satellite images from 5 to 10 year intervals (Yamazaki *et al.*, 2015). However, Landsat imageries over multiple decades were observed to be used in mapping the seasonality's change at continental (Mueller, 2016) and sub-continental (Tulbure *et al.*, 2016) scales. The dataset in the global surface water explorer is freely available online, it extends the previous work on water through the use of the entire multi-temporal and orthorectified archives of Landsat 5, 7 and 8, which span through the past 32 years to map out the spatiotemporal variability of global surface water and its long-term change that can be seen (Pekel *et al.*, 2016).

4.1.2.1 The map products

Water occurrence: the water occurrence depicts where surface water exists between March 1984 and October 2015, it shows information that concerns the overall water dynamics. It also captures both intra and inter-annual changes and variability. The water occurrence dataset has the following values and symbology. The values are discrete and range from 1 to 100 (**Figure A6.1**).

Occurrence change intensity: This map product shows the information between 1984-1999 and 2000-2015 on where the surface water occurrence increase, decrease or remained static. In essence, both the direction of change and intensity are recorded. The water cccurrence change intensity dataset has the following values and symbology for the change norm band. The values are discrete and range from 0 to 200 (**Figure A6.2**).

Water seasonality: the map produces the information regarding the intra-annual pattern of water surfaces for a year, i.e. 2014-2015, it shows the permanent water, seasonal water and the number of months that water is present. The seasonality dataset is having the following values and symbology, the digit is discrete and ranges from 1 to 12 (**Figure A6.3**).

Annual water recurrence: the water recurrence provides the user with information concerning the inter-annual pattern of water surface and records the frequency with which the water comes back from one year to another. The symbology and values for the recurrence are discrete and ranges from 1 to 100 (**Figure A6.4**).

Water transition: the transition map shows the information with regards to the change in the seasonality between the first and the last year, while on the other hand, it captures the differences between the three classes without water, the seasonal water and the permanent water. The water transition symbology is as follows, while its value range from 1-10 and are as well discrete (**Figure A6.5**).

Maximum water extent: the maximum water extent gives the information on all the places that were ever detected as water over the past 32 years. It is the union of all other datasets that exist. The dataset value range from 1-10 and the symbology can be seen at (**Figure A6.6**)

4.2 Methods

4.2.1 SPEI data

As as opined by Sureh, (2019), drought is a period of unusual dry state that is quite long and causes an imbalance within the hydrological condition of a place, such as the loss in surface and groundwater resource. In the dry and semi-arid zone like the Sokoto Rima River Basin (SRRB) located in the sahel, precise forecast or the knowledge of droughts plays a vital role in defying the drought challenges and water resource management system. Therefore, for the analysis of drought pattern within the Sokoto Rima River Basin using the SPEI_1 (meteorological drought) and SPEI_48 (hydrological drought), four distinct observation points were used to obtain the SPEI data and to show the extent of drought from 1950 to 2018, see **Figure A9**.

The acquired SPEI data was sampled using a systematic sampling methods by selecting the SPEI_1 as the meteorological drought data and the SPEI_48 as the hydrological drought data. Then 5 months for each year (from 1950 to 2018) when *Fadama* farming is carried out within the SRRB was sampled out and estimated using the Thornwaite method.

4.2.2 Global surface water explorer data

Where and when we can find water on the earth's surface is quite crucial and essential for well-informed earth observation, (Pekel *et al.*, 2016). Hence, in this research, water is the most central to irrigation farming if I may emphasize. Therefore, long-term water history was applied to show the thematic products that store different facets of surface water dynamics.

As such, specific to this research, the dams were assessed with the global surface water explorer to observe the dam's behavior over the years; by clicking a point to acquire the geographical coordinates and to generate the extract from the global products in the surface water explorer around all the dams. However, further analysis could have been done if the raw data is available for download,

but based on the fact that no data is available; we can only have a superficial approach to assess the rate of physical change over the years.

4.3 Results

4.3.1 The SRRB SPEIbase dataset

The SPEI was analysed at different scale to assess the drought condition using two approach. Thus, meteorological drought (SPEI_1) and hydrological drought (SPEI_48), the indices depicts similar patterns at the four observation points, although differed in magnitude and duration. The analysis of the drought at the first month i.e. SPEI_1 series, showed a high frequency of meteorological drought at the observatories. While that of the 48 month i.e. SPEI_48, indicates relatively long term moderate dry spell with few wet seasons, see **Figures 4-2 to 4-7** below.

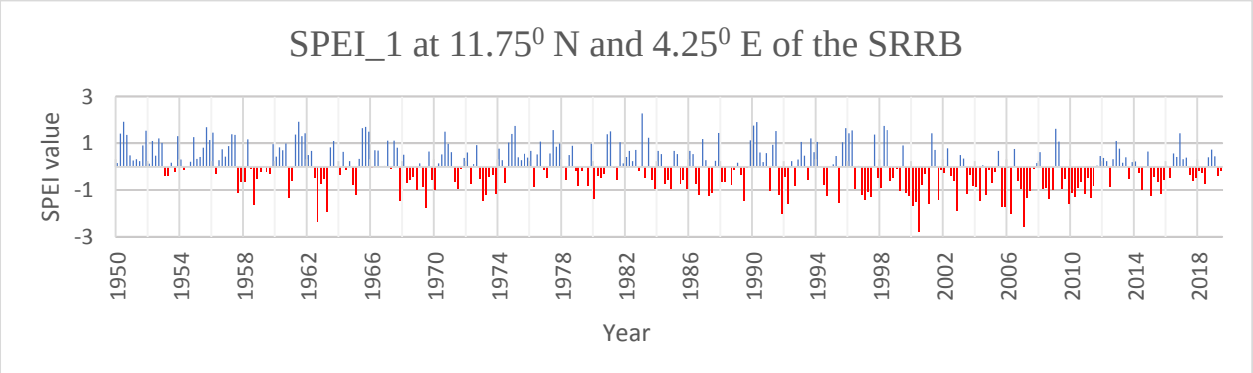

(a)

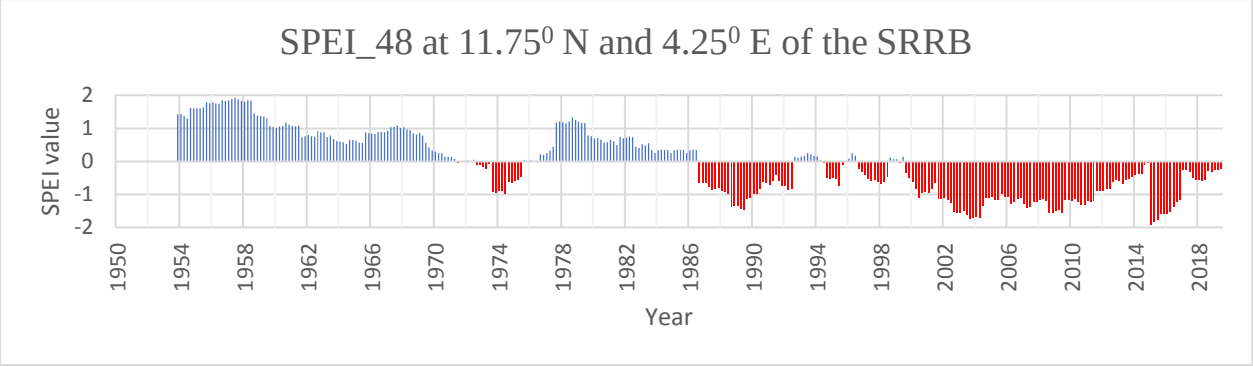

(b)

Figure 4-2 (a, b): SPEI drought pattern from 1950-2017 at 1st and 48th month of the SPEI dataset from Lat. 11.75^0 N and Long. 4.25^0 E in the Sokoto Rima River Basin.

At lat. 11.75^0 N and Long. 4.25^0 E as seen in **Figure 4-2** (a, b), the data is from 1950 to 2018 using the 1st and the 48th month SPEI_1 and SPEI_48 respectively. The SPEI drought pattern at this point shows a recurring moderate hydrological drought within the years. From January 1950 to January 2016, the drought was seen to be intense from the year 2000. While on the other hand, the point with frequent precipitation rate was from 1954 to somewhere around 1969.

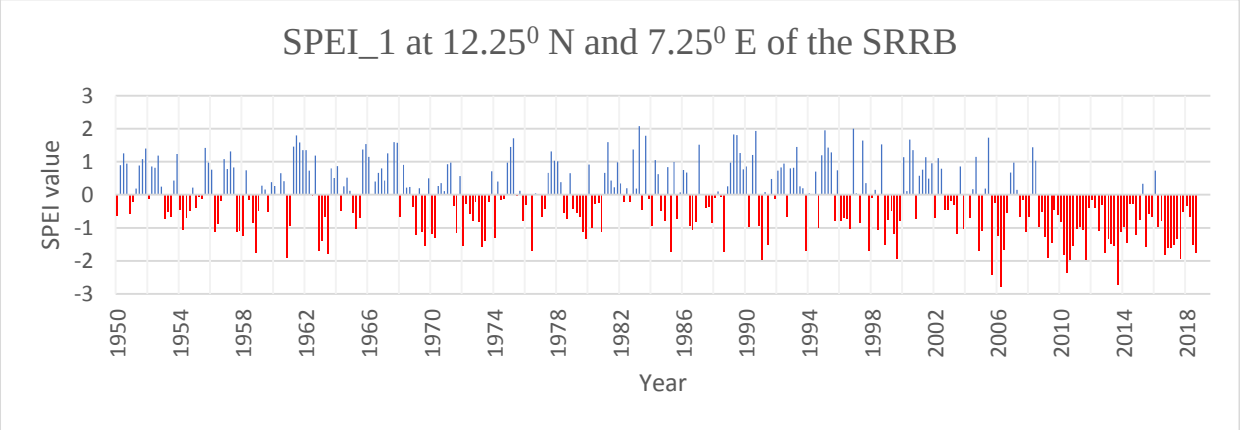

(a)

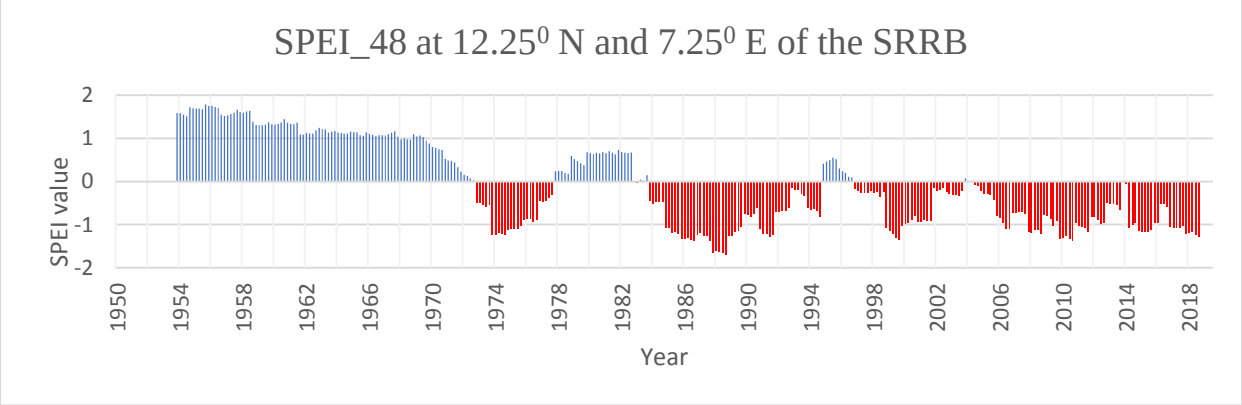

(b)

Figure 4-3 (a, b): SPEI drought pattern from 1950-2017 at 1st and 48th month of the SPEI dataset from Lat. 12.25^0 N and Long. 7.25^0 E in the Sokoto Rima River Basin.

From **Figure 4-3** above, the dataset ranges from 1950 to 2018 at Lat. 12.25^0 N and Long. 7.25^0 E. In this location, the meteorological drought was apparent and fluctuate with few wet season and frequent dry spell over the years, the highest wet moment was 2.1 recorded in 1983, while the driest moment of the time series was recorded to be -2.8 in 2006. Nonetheless, considering the SPEI_48, the

hydrological drought depicts a continuous dry moment from the year 1985 to 2018 with apparent moderate drought.

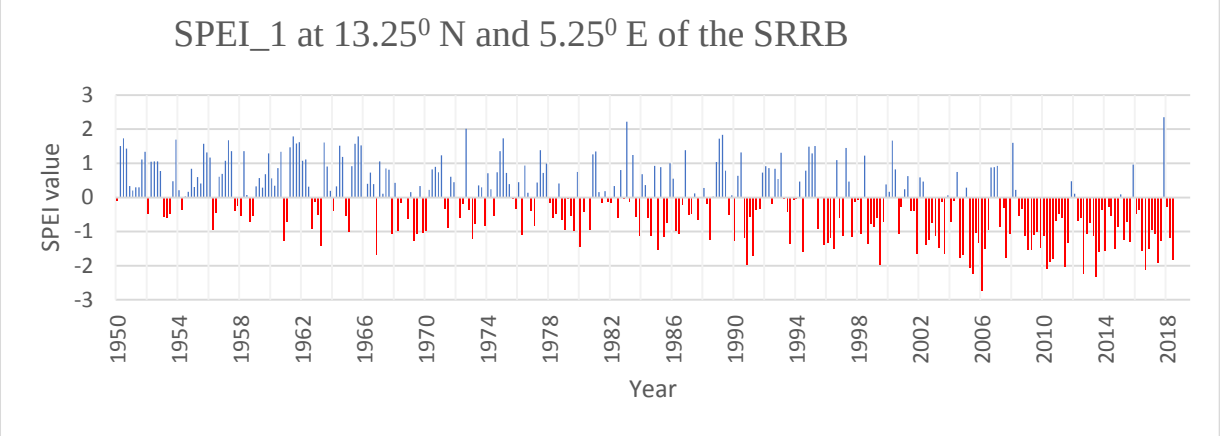

(a)

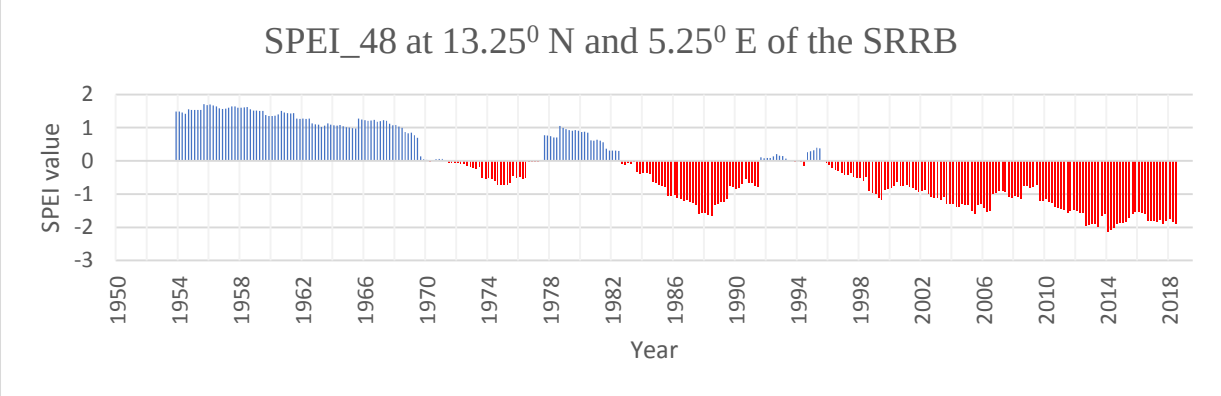

(b)

Figure 4-4 (a, b): SPEI drought pattern from 1950-2017 at 1st and 48th month of the SPEI dataset from Lat. 13.25^0 N and Long. 5.25^0 E in the Sokoto Rima River Basin.

As shown in **Figure 4-4** (a, b), the location at Lat. 13.25^0 N and Long. 5.25^0 E, shows a moderate meteorological drought pattern that depicts the highest precipitation rate in 2018 as 2.3, while the lowest rate was recorded as -2.7 in 2006. From the SPEI_48 data, the hydrological drought pattern fluctuates with few wet season from 1950 with an attenuation point in 1974, from the year 1983 a continuous moderate dry spell is depicted.

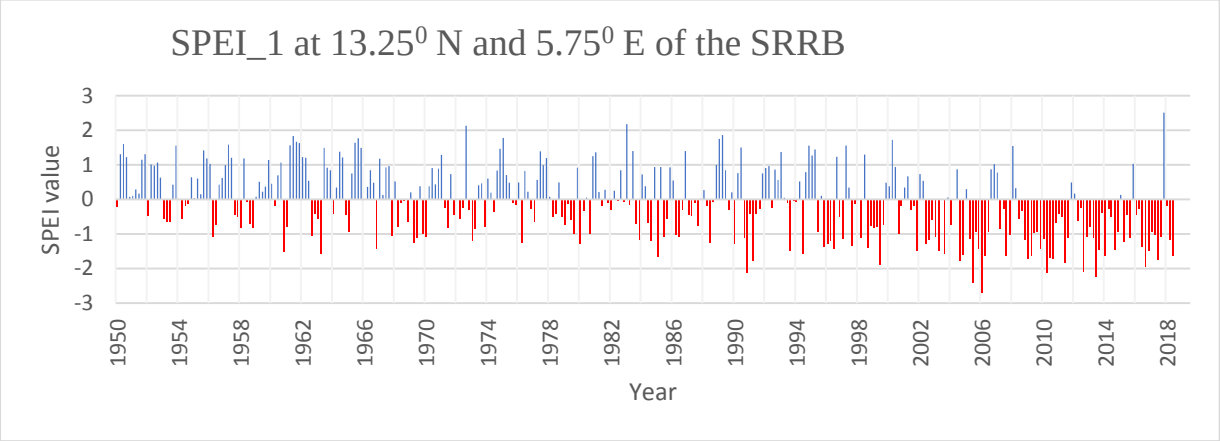

(a)

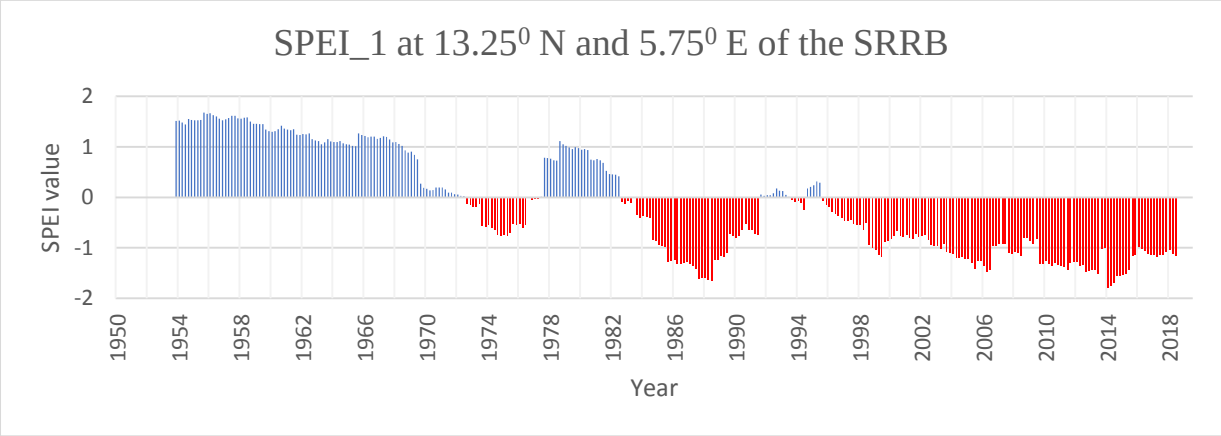

(b)

Figure 4-5 (a, b): SPEI drought pattern from 1950-2017 at 1st and 48th month of the SPEI dataset from Lat. 13.25^0 N and Long. 5.75^0 E in the Sokoto Rima River Basin.

From **Figure 4-5** (a, b), the Standardised Precipitation Evapotranspiration Index shows a peak precipitation rate at Lat. 13.25^0 N and Long. 5.75^0 E to be 2.5 in 2017. Conversely, the lowest point recorded in 2006 was -2.7. The drought pattern in this location is modearate, and depicts a similar trend pattern as in the case of **Figure 4-4** (a, b) with just a slight difference in the values recorded. The SPEI_48 i.e. the hydrological drought pattern in this observatory, maintains a steady moderate drought from 1983 to 2018.

Overall, the SPEI_1 datasets show a variation in meteorological drought conditions with a gentle decline despite few wet season. While the SPEI_48 i.e. the hydrological drought, clearly depict a dryer spell at all four observation points, and suggest that the catchment is getting dryer from 1950-2018.

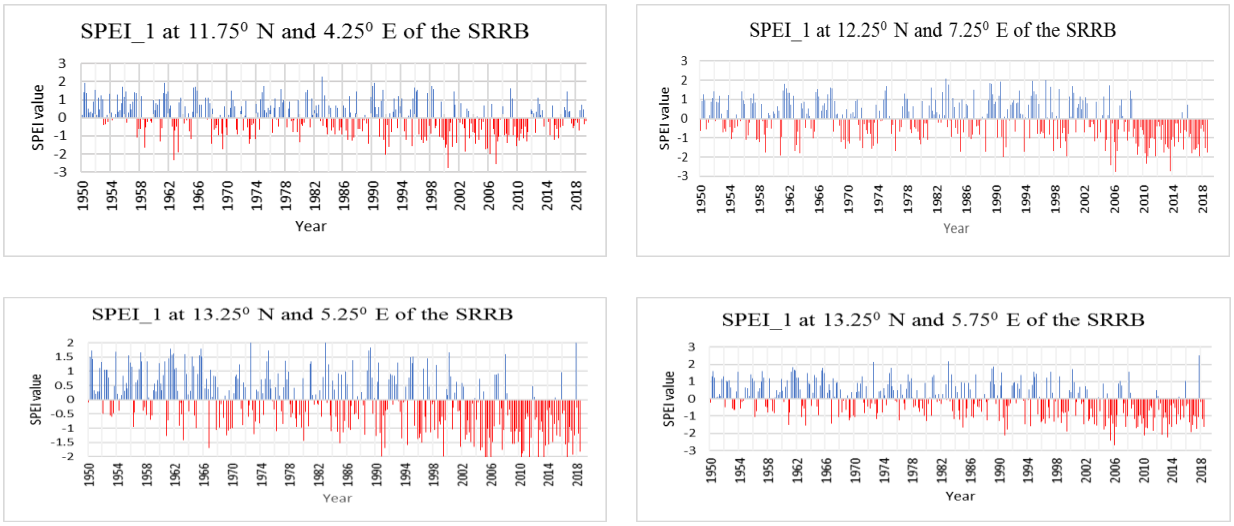

Figure 4-6: showing SPEI_1 meteorological drought data in the four observation points.

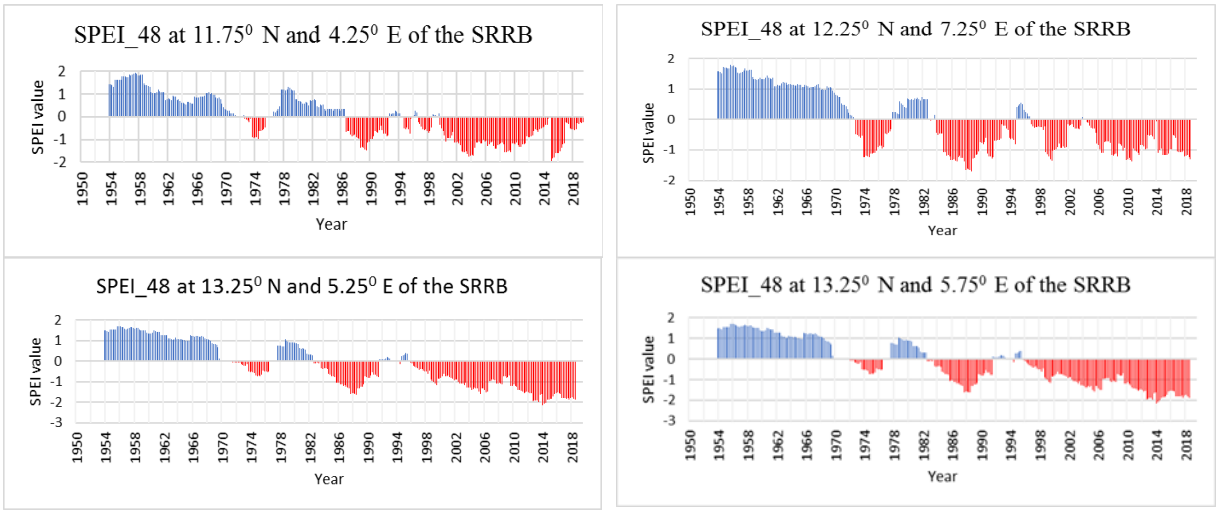

Figure 4-7: showing SPEI_48 hydrological drought in the four observation points

Summarily, the SPEI datasets as shown in the above figure, depicts a dryer spell with fewer wet season from the year 1950 to 2018 at the four locations within the SRRB. As observed from the apparent fluctuation of the datasets, it suggests that the pattern is negative in recent years, and shows that the catchment of the basin is affected by moderate hydrological drought. Hence, this will impose pressure on dams and the irrigation scheme, although with possible water management strategies, the issue can be mollified since the drought is moderate.

4.3.2 Global surface water explorer

Using the global surface water explorer, five of the selected dams were assessed with the water explorer to investigate the parameters over the years.

From the surface water occurrence (SWO) as shown in **Figure 4-8a, Figure 4-9a, Figure 4-10a, Figure 4-11a, & Figure 4-12a**, it can be observed that the pattern is quite similar and at some point, the dams once occupied other areas with water, which then later diminished or reduced. Looking at the symbology, the magnitude of the occurrence can be quantified in percentage. The SWO was calculated using the summation of water detection and the valid observations from 1984, such that the sum of water detection is divided by the sum of valid observations. It is noteworthy that more cloud-free observations are available during the dry season than in wet season. Which if observed in **Figure 4-13 and Figure 4-14** it might seem to be biased by the temporal distribution of valid observation, giving more weight to the dry season than the wet season which is because cloud covers are masked and with no water occurrence.

The water occurrence change intensity between 1984 to 1999 and from 2000-2015, was produced to derive a homologous pair of months that have the same months that contain valid observations. Hence, the occurrence disparity between the two periods is computed for each pair, and the difference between all homologous couple of months were then averaged to create the water occurrence change intensity. At Bakolori, Goronyo, Jibia, Wurno and Zobe dams respectively, **Figure 4-8b, Figure 4-9b, Figure 4-10b, Figure 4-11b, & Figure 4-12b**, it can be assessed on where the area decreases, remain unchanged or increases. This will give us a well-informed understanding that geographical phenomena are temporally dynamic and spatially varying.

The water seasonality was assessed by having that understanding that areas under water coverage are called permanent, while seasonal water is a surface under water for less than twelve months of the year. In some areas, no valid observations are made due to phenological constraint as earlier mentioned.

Hence, in such case, water is taken to be seasonal if the number of months when the water present is less than the number of months where validated observations are shown. As such, within the dam's catchment, it was relatively found on where water is permanent and seasonal using the symbology tab at the topright corner, see **Figure 4-8c, Figure 4-9c, Figure 4-10c, Figure 4-11c, &Figure 4-12c**.

Annual water recurrence is the degree estimation of the inter-annual variability on water presence. It further delineates how frequent water returns from one year to another and is measured in percentage. The water recurrence refers to the temporal pattern of water surfaces which is not like occurrence. Recurrence is not computed systematically over the full span of the Landsat archive; this is because water might not be available from the start to the end of the archive. Hence, water period needs to be defined on the basis of where water is present at least time to time; as such, the recurrence measures this (time to time). Therefore, individual water period is produced for each of the pixels, and the water period runs through the first month of the first year in which water is established and through the last month of the last year with which water is found for the entire span of 32 years.

Additionally, to define the water period, water season is not equivalent to the raining season which needs to be defined as well. The water season is recognized from the monthly water recurrence and then defined as the months of the year when water is seen from time to time. For the water year, is the year observed with at least one water observation, while an observation year is a year with at least one valid observation within the water season. The counts of the number of years begin with the year with which water was first observed and ended with the most recent year with which water was observed. Hence, the years with observation outside the water season are not counted because no observation made and there is no much understanding if water might have occurred in the water season. At the latter, the annual water recurrence for Bakolori, Goronyo, Jibia, Wurno and Zobe dams can be observed from **Figure 4-8d, Figure 4-9d, Figure 4-10d, Figure 4-11d, & Figure 4-12d**

The water transition uses a thematic map and temporal profile to identify a set of water classes that give an attribute to the change between the first and the last year in which representative observations were gotten. Representative years are identified by making a comparison with each year in turn with the annual behaviour of monthly water recurrence from the temporal profile. The profile recognises month with which water was spotted and pointed out the percentage of valid observations classified as water within the given months. Thus, a year is noted as a representative if it has enough valid observations from any union of the months to bring a conviction to the determination of the presence or absence of water. The overall level of assurance is determined by the annual sum of the monthly long-term recurrence of spotted months per year. The logic is that; there is the likelihood for real absence of water in a year if the water is not present for many months and shows a higher long-term water recurrence than from the one that shows small rates of recurrence. At the verge, the absence of water can be described by seasonal drift and does not grant a tangible reason to make conclusions that water was not present much later.

As such, we can put into consideration if the recurrence sum of the examined months is higher than 100, then the non-existence of water observation brings adequate assurance to consider that water was absent. On the other hand, a single presence of water is persuasive to show the presence of water. Therefore, the classes of water in the representative year is then assigned as the first year, while the last year's class remains the class fixed to the last year observation, i.e. October 2014 – October 2015 due to the observation present within that year during this very period.

From the dropdown symbology of the water transition in **Figure 4-8e, Figure 4-9e, Figure 4-10e, Figure 4-11e, & Figure 4-12e** below, a number of the transition were made available to assess the changes over time. With regards to Bakolori, Goronyo, Jibia, Wurno and Zobe dams, we can observe the changes in water behaviour from permanent to seasonal, through the new seasonal and to the ephemeral seasonal.

From the image of the maximum water extent **Figure 4-8f, Figure 4-9f, Figure 4-10f, Figure 4-11f, & Figure 4-12f** this gives us the information on the highest location ever occupied by water within a given water body. Specific to all the dams, we can vividly see the maximum water capacity that the reservoir ever retained, as such, this will provide a well-informed vantage point on how the behavioural pattern is, within a particular surface water.

Bakolori dam

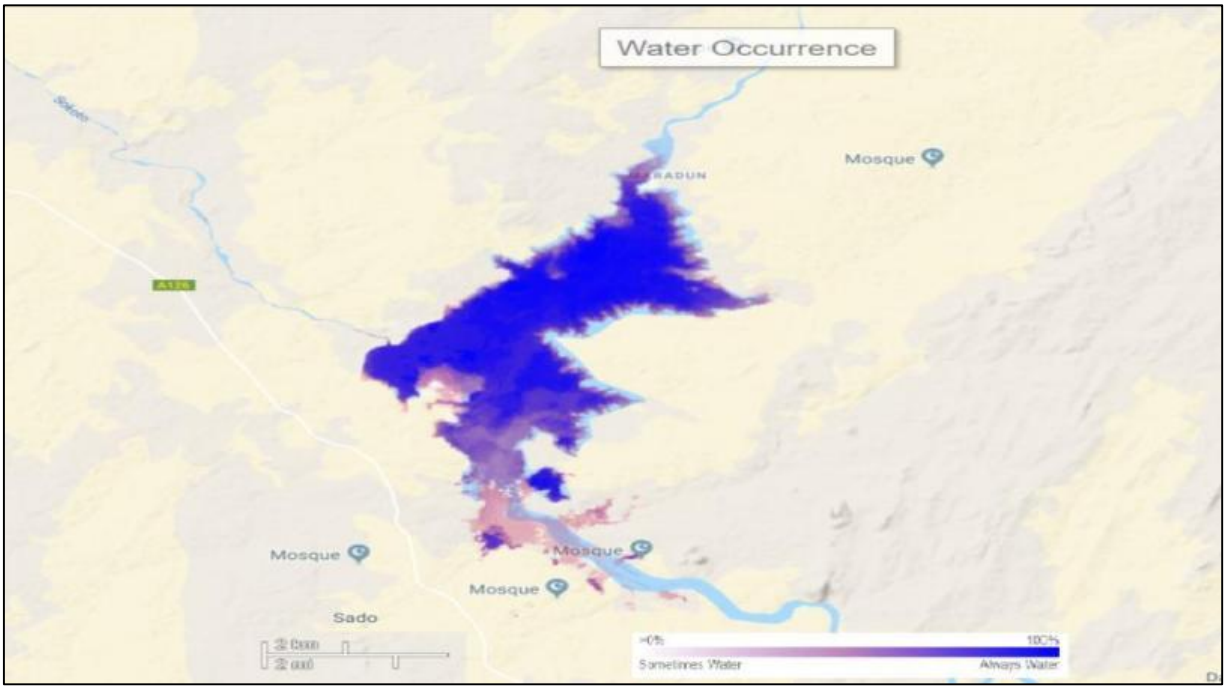

Figure 4-8a: Water occurrence around Bakolori dam. This is showing the portion of the dam where water can be found in the course of the year, and where water is always available through the years. From the symbology, it appears that areas at the periphery tends to be having water at some point in the year, while as you move inwardly, it appears to always have water.

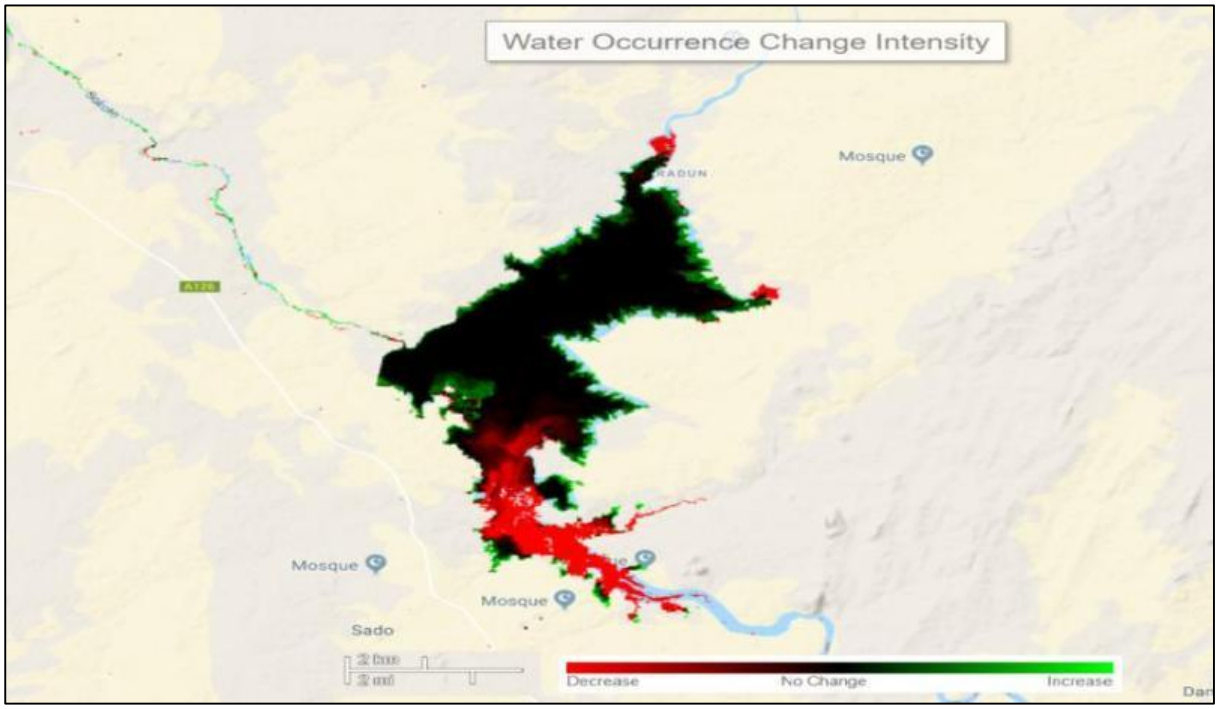

Figure 4-8b: Water occurrence change intensity at Bakolori dam depicts where the dam's water decreases, remained unchanged and increased through the year. Areas around the edge of the dam tends to decrease and increase as shown using the symbology, while areas inside the dam have no changes as observed from the image.

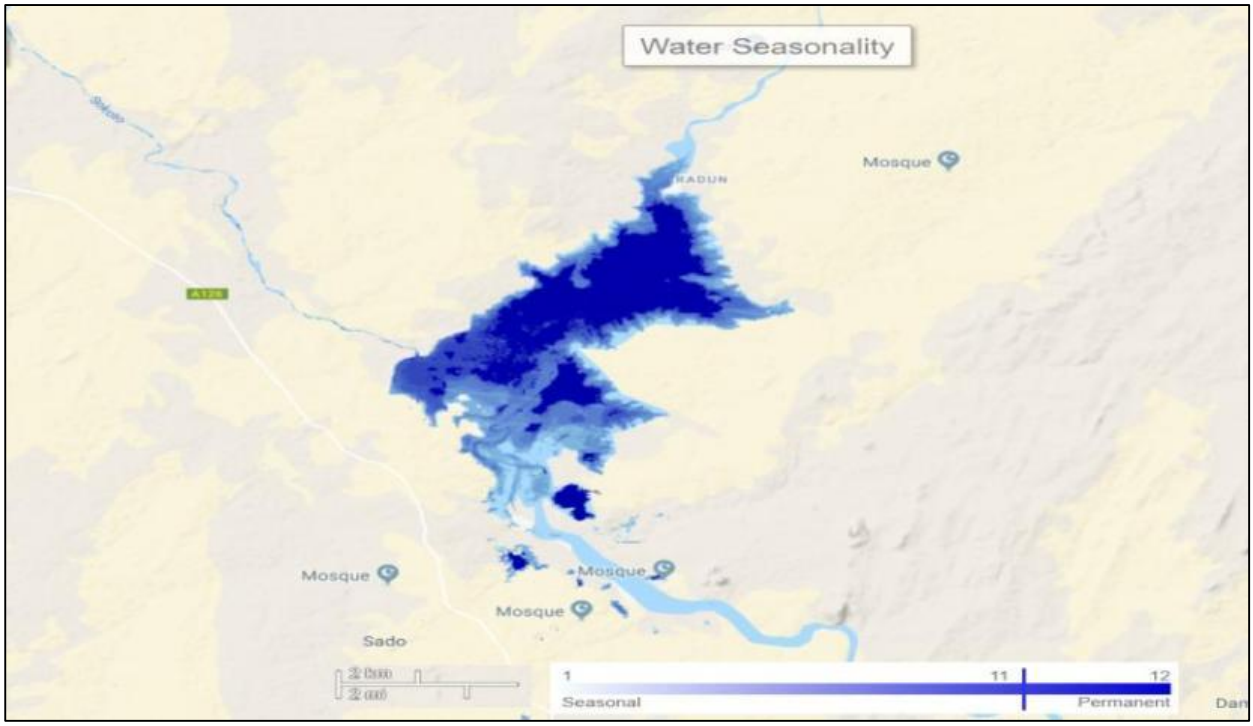

Figure4-8c: Water seasonality at Bakolori dam shows the seasonal water coverage from permanent water to seasonal water where water is not found at some point in the year. At the core of the dam it appears to be mostly permanent water, while at the edge, the water is seasonal and reduces from the inner part of the dam to areas at the periphery.

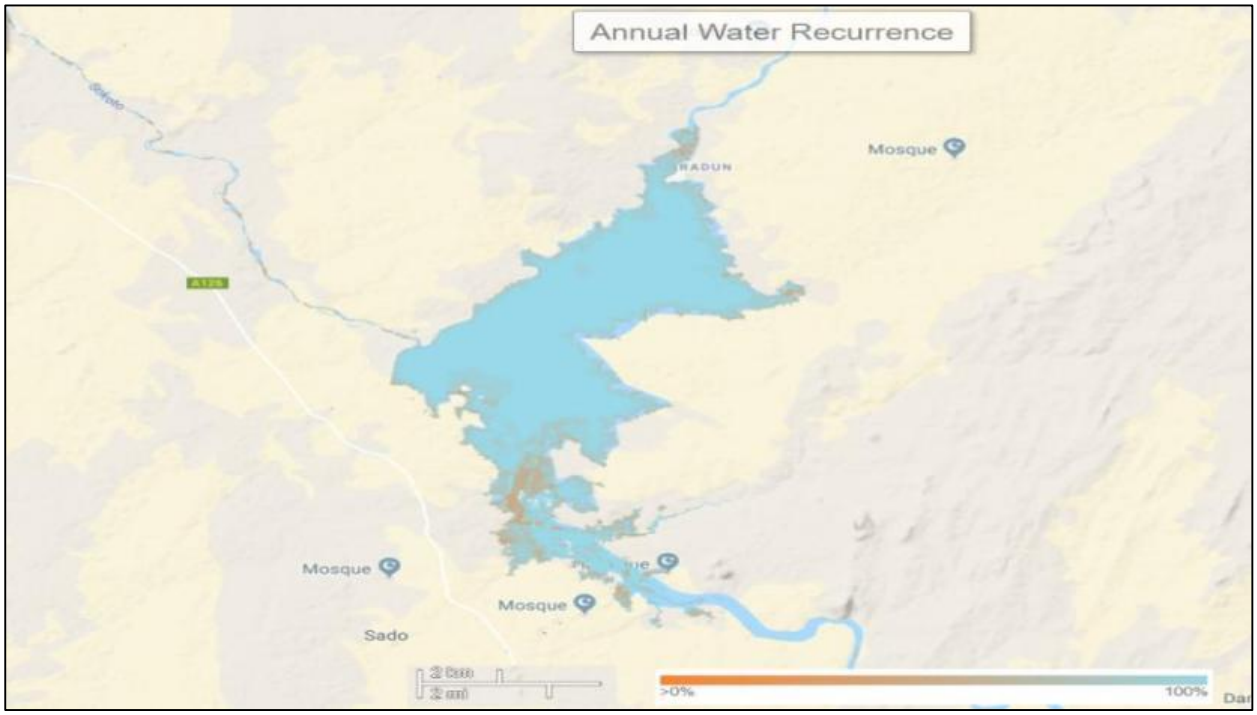

Figure4-8d: Annual water recurrence at Bakolori dam. This shows the degree of estimation in terms of the inter-annual variability on water presence, describing frequent water return from one year to another. From the image, the symbology signifies that only a few portion of the dam at the margin is 0%, while in most part of the dam, the annual water recurrence is 100%.

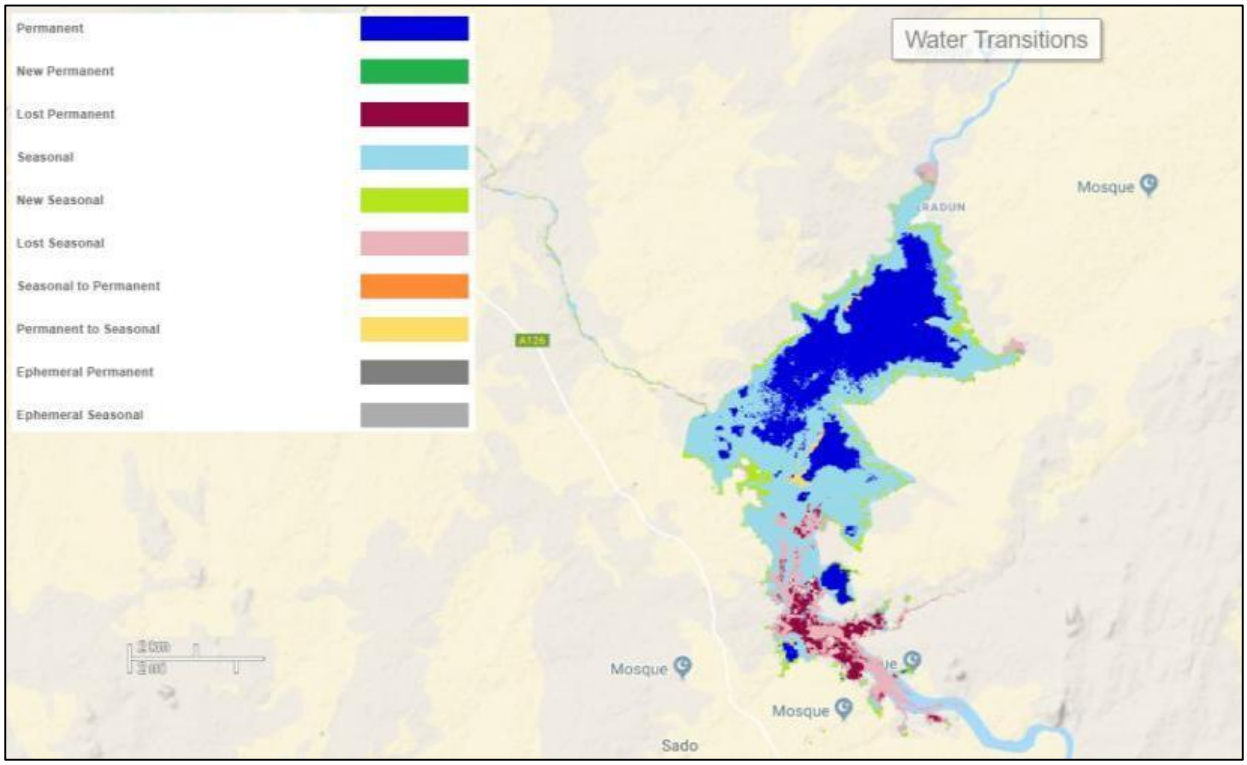

Figure4-8e: Water transition at Bakolori dam shows the spatiotemporal difference with different seasonal pattern from permanent water to ephemeral seasonal within the dam. At the center of the dam, the water is permanent, while eccentrically, the water is seasonal, followed by new seasonal, to lost seasonal, and to lost permanent.

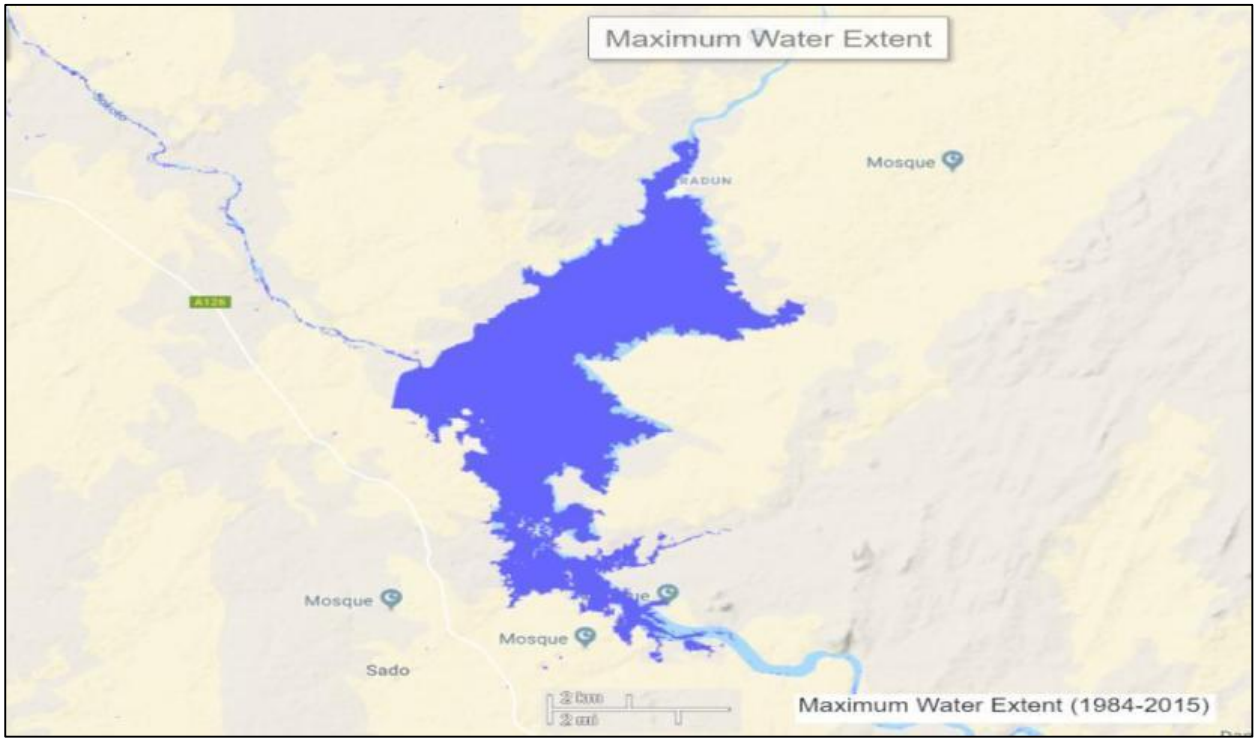

Figure4-8f: Maximum water extent at Bakolori. This shows the highest spatial extent of water ever retained by the dam. From the image, the dam appears to have occupied other areas from 1984 to 2015, while using other parameters above, it can be deduced that water has reduced from this extent in recent years.

Goronyo dam

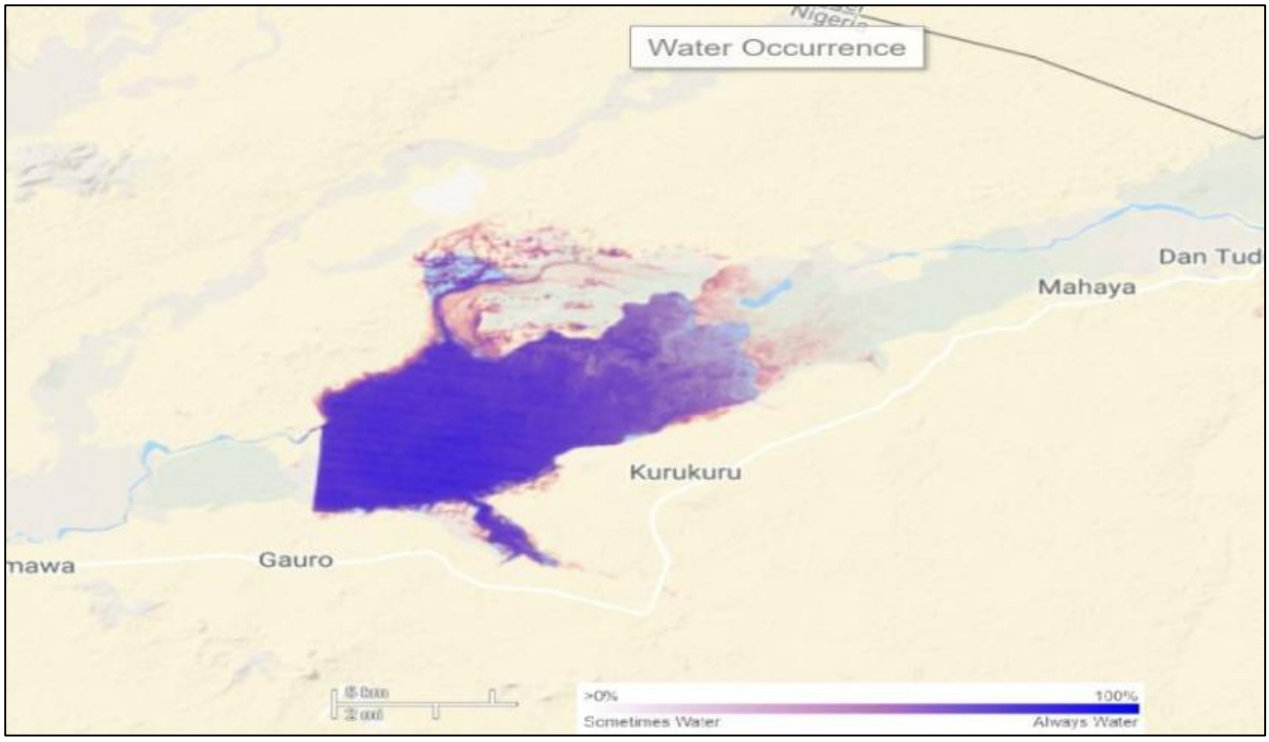

Figure 4-9a: Water occurrence at Goronyo dam. This is showing the portion of the dam where water can be found in the course of the year, and where water is always available through the years. From the symbology, it appears that areas at the periphery tends to be having water at some point in the year, while as you move inwardly, it appears to always have water.

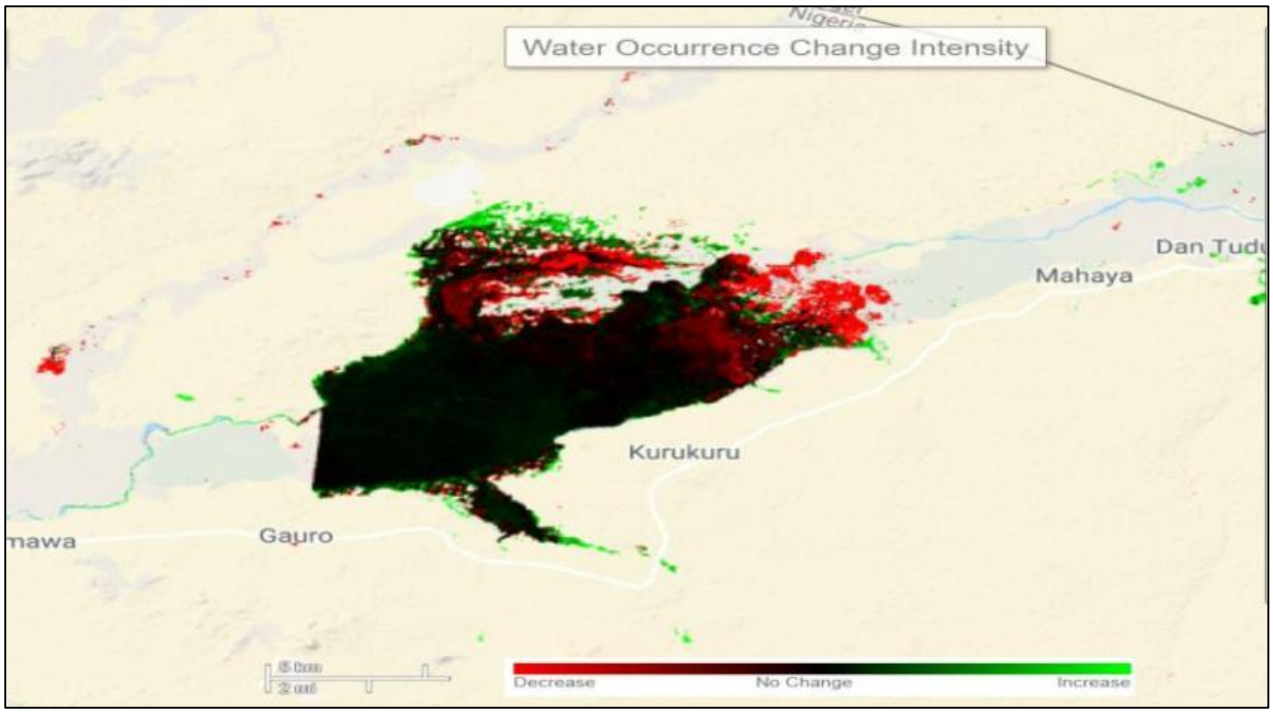

Figure4-9b: Water occurrence change intensity at Goronyo dam depicts where the dam's water decreases, remained unchanged and increased through the year. Areas around the edge of the dam tends to decrease and increase as shown using the symbology, while areas inside the dam have no changes or even increasing as observed from the image.

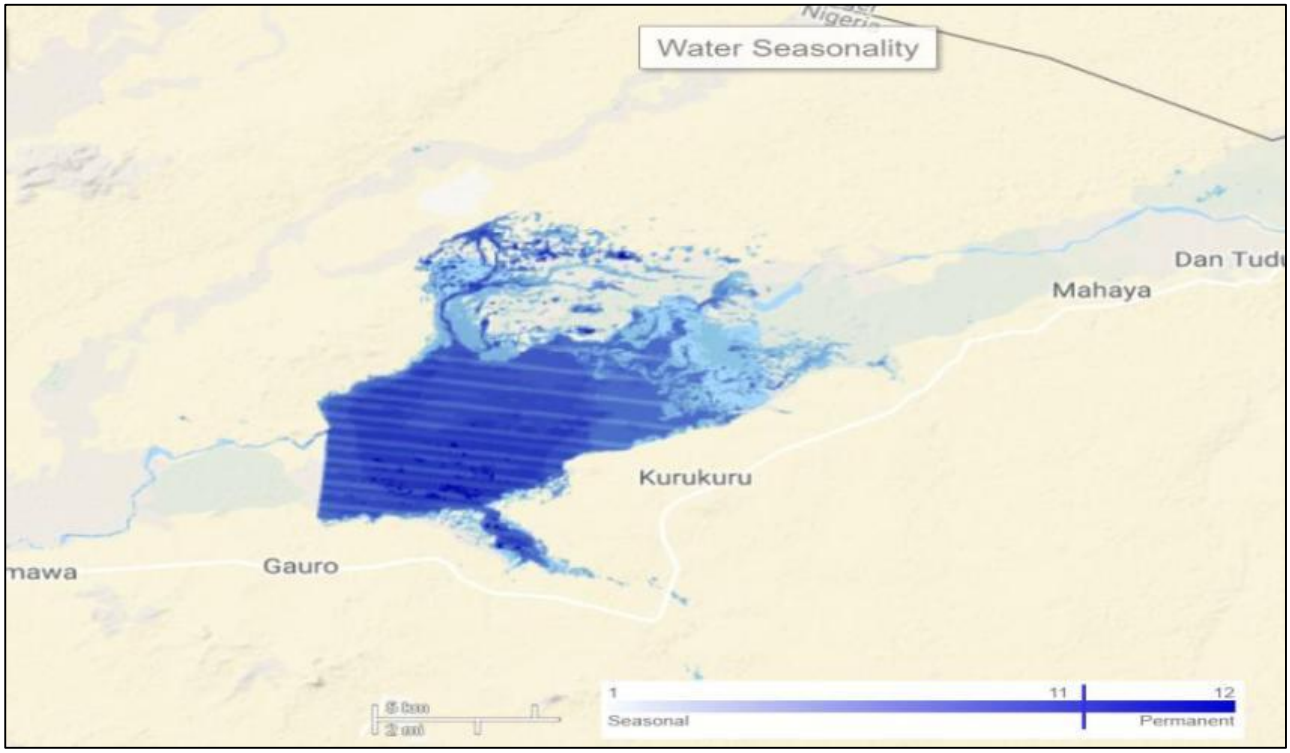

Figure 4-9c: Water seasonality at Goronyo dam shows the seasonal water coverage from permanent water to seasonal water where water is not found at some point in the year. At the core of the dam it appears to be mostly permanent water, while at the edge, the water is seasonal and reduces from the inner part of the dam to areas at the margin.

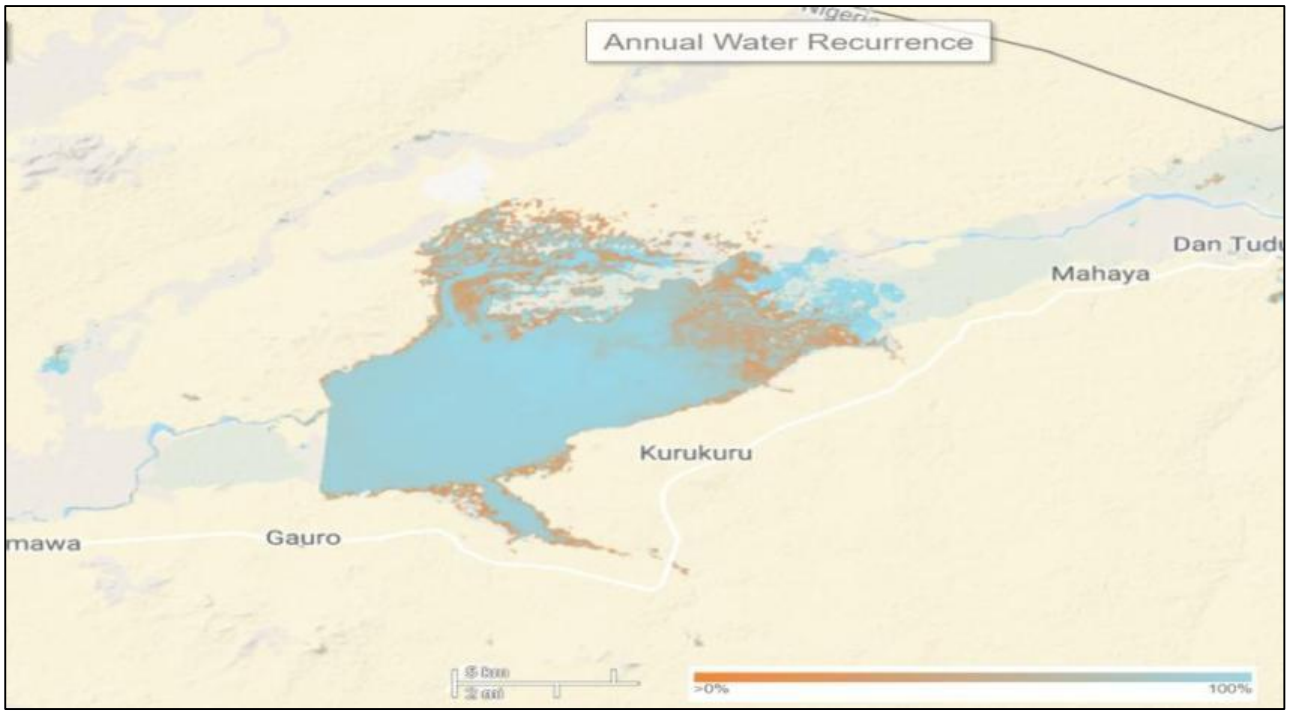

Figure 4-9d: Annual water recurrence at Goronyo dam. This shows the degree of estimation in terms of the inter-annual variability on water presence, describing frequent water return from one year to another. From the image, the symbology signifies that portion around the margin of the dam ranges from 0%, while in most part of the dam at the center, the annual water recurrence is 100%.

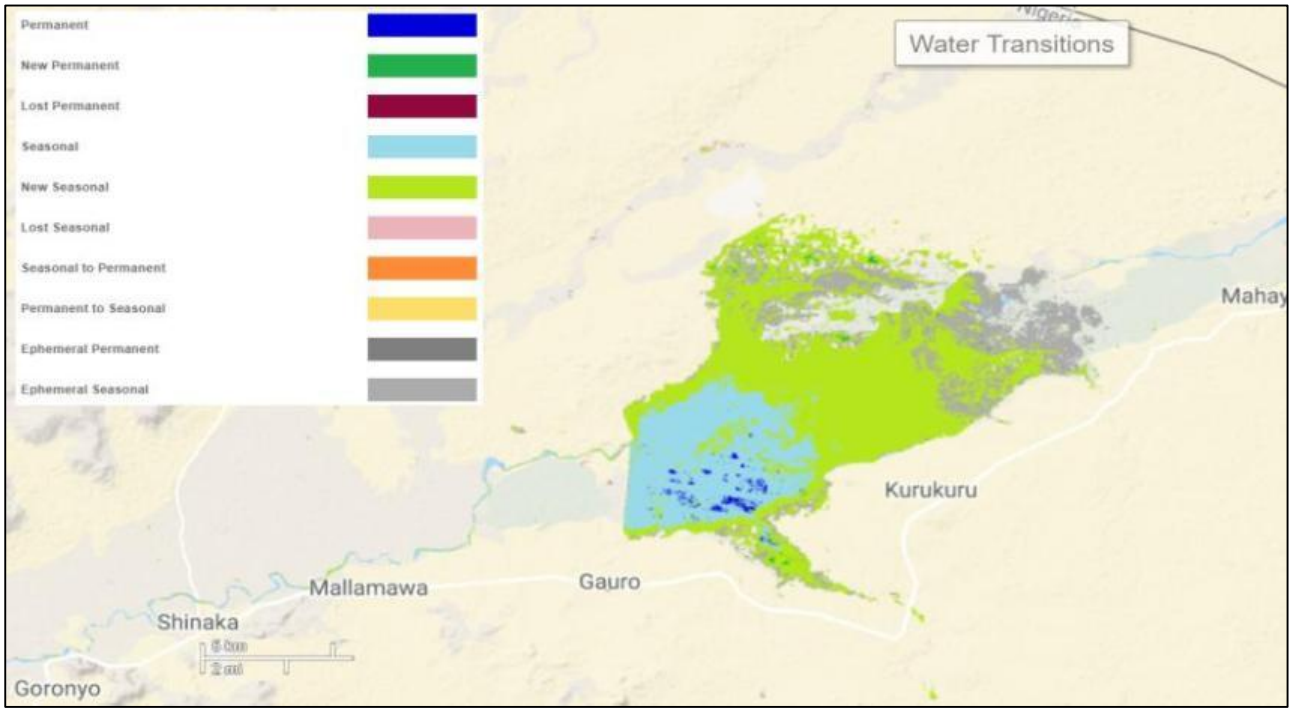

Figure 4-9e: Water transition at Goronyo dam shows the spatiotemporal difference with different seasonal pattern from permanent water to ephemeral seasonal within the dam. At the center of the dam, the water is partially permanent, while eccentrically, the water is seasonal, followed by new seasonal, to lost seasonal, and to ephemeral seasonal.

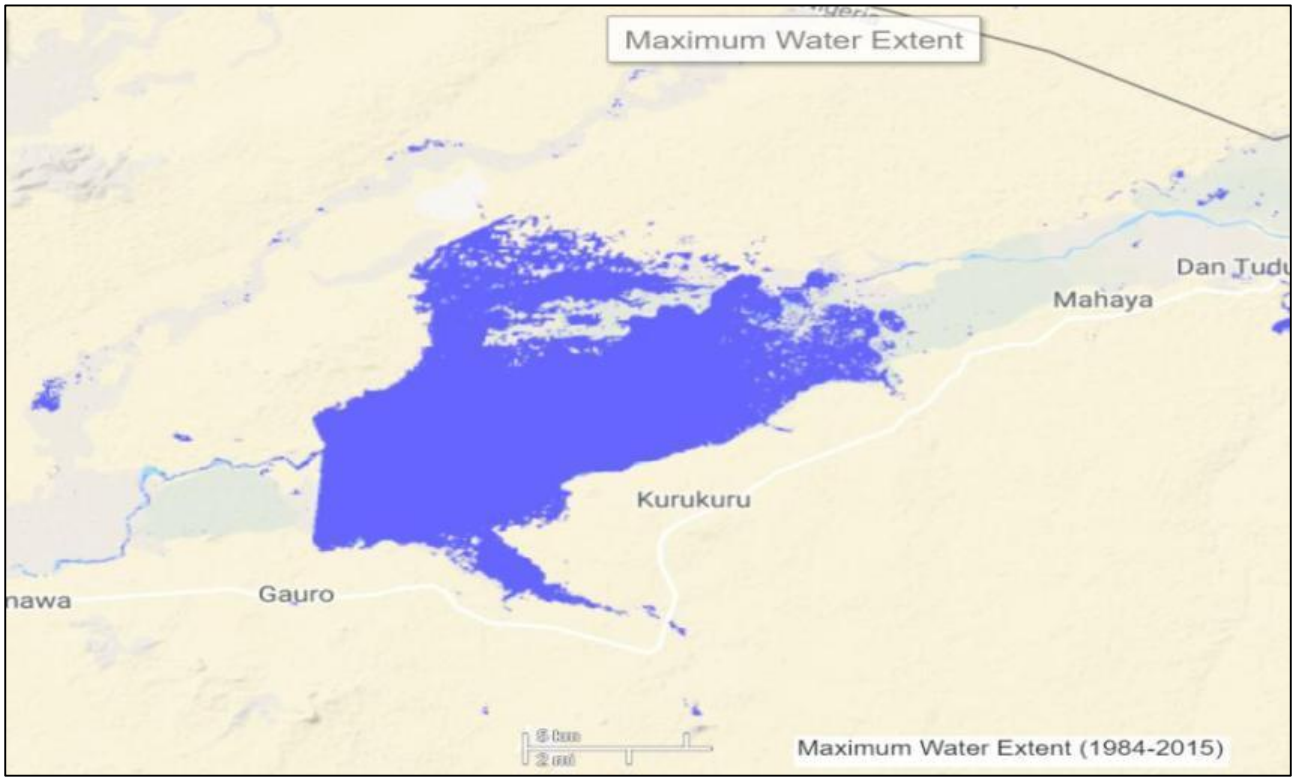

Figure 4-9f: Maximum water extent at Goronyo dam. This shows the highest spatial extent of water ever retained by the dam. From the image, the dam appears to have occupied other areas from 1984 to 2015, while using other parameters above, it can be deduced that water has reduced from this extent in recent years.

Jibia dam

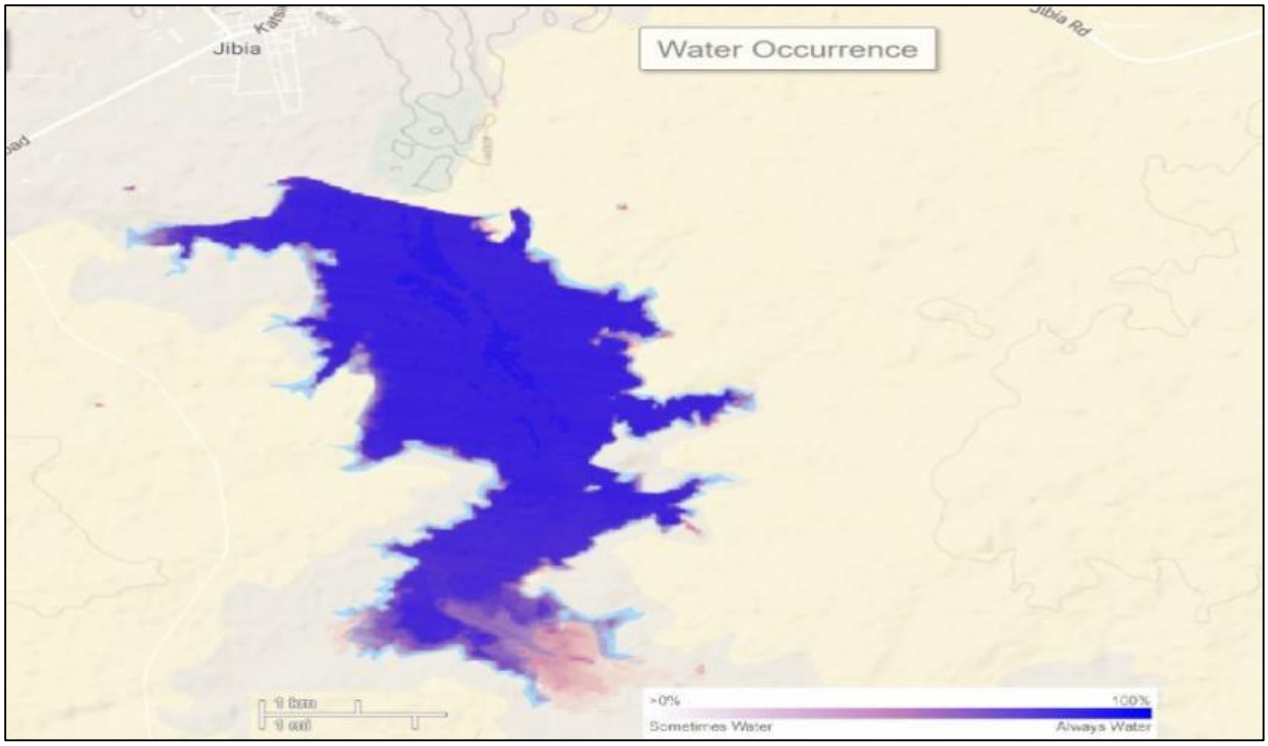

Figure 4-10a: Water occurrence at Jibia dam. This is showing the portion of the dam where water can be found in the course of the year, and where water is always available through the years. From the symbology, it appears that areas at the periphery tends to be having water at some point in the year, while as you move inwardly, it appears to always have water.

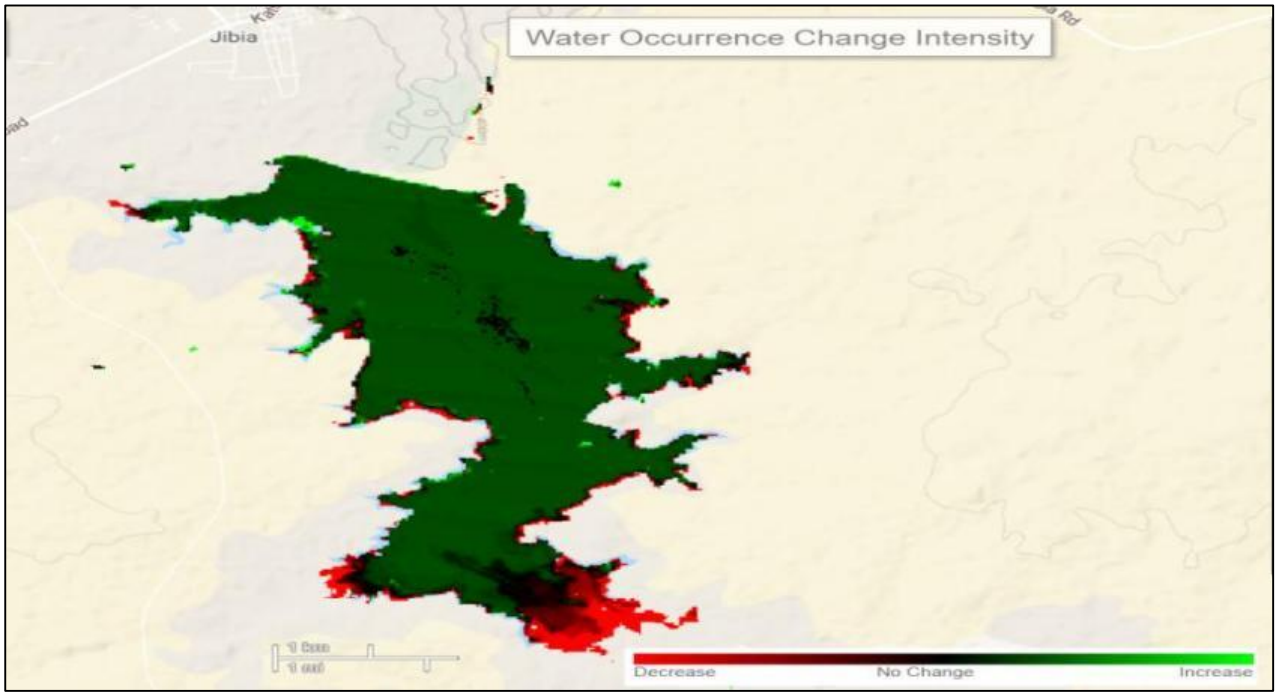

Figure 4-10b: Water occurrence change intensity at Jibia dam depicts where the dam's water decreases, remained unchanged and increased through the year. Areas around the edge of the dam tends to decrease and or with no change as shown using the symbology, while areas inside the dam falls between no change and increase as observed from the image. This depicts that the dam is slightly not changing but also increases as the year goes by.

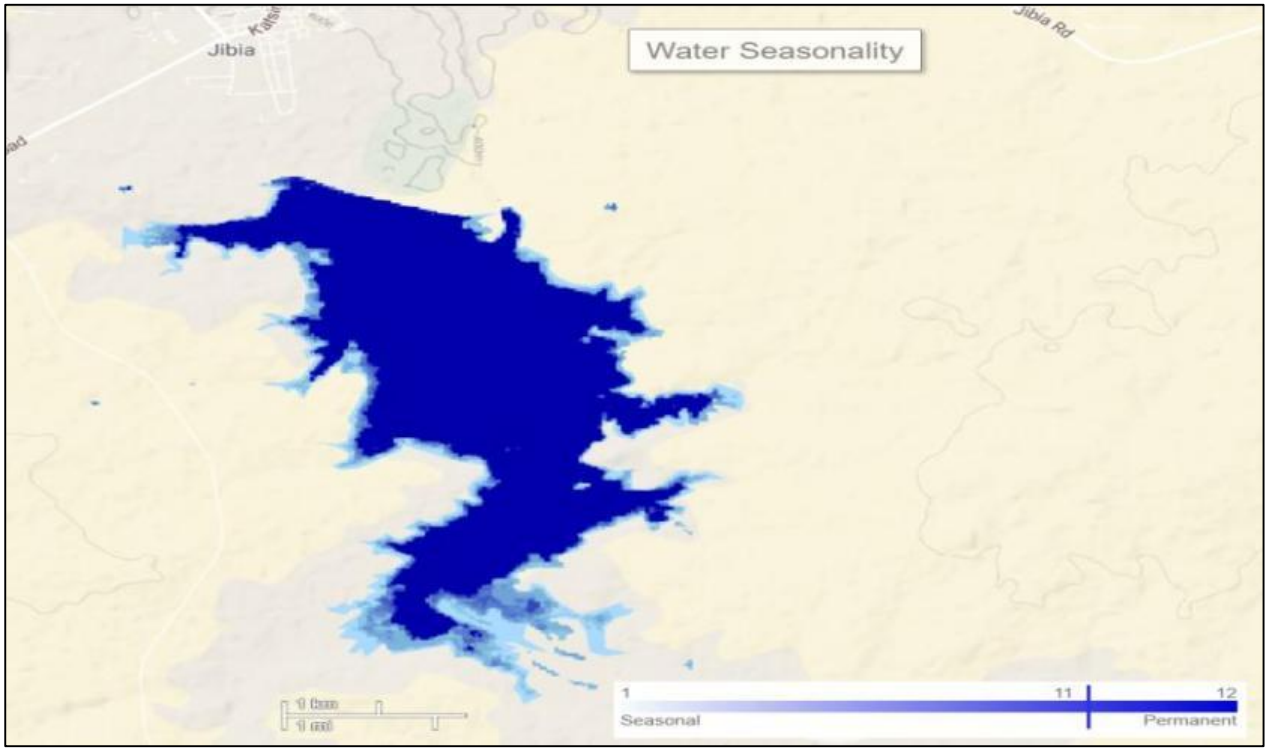

Figure 4-10c: Water seasonality at Jibia dam shows the seasonal water coverage from permanent water to seasonal water where water is not found at some point in the year. At the core of the dam it appears to be mostly permanent water, while at the edge, the water is seasonal with most part of the dam usually permanent.

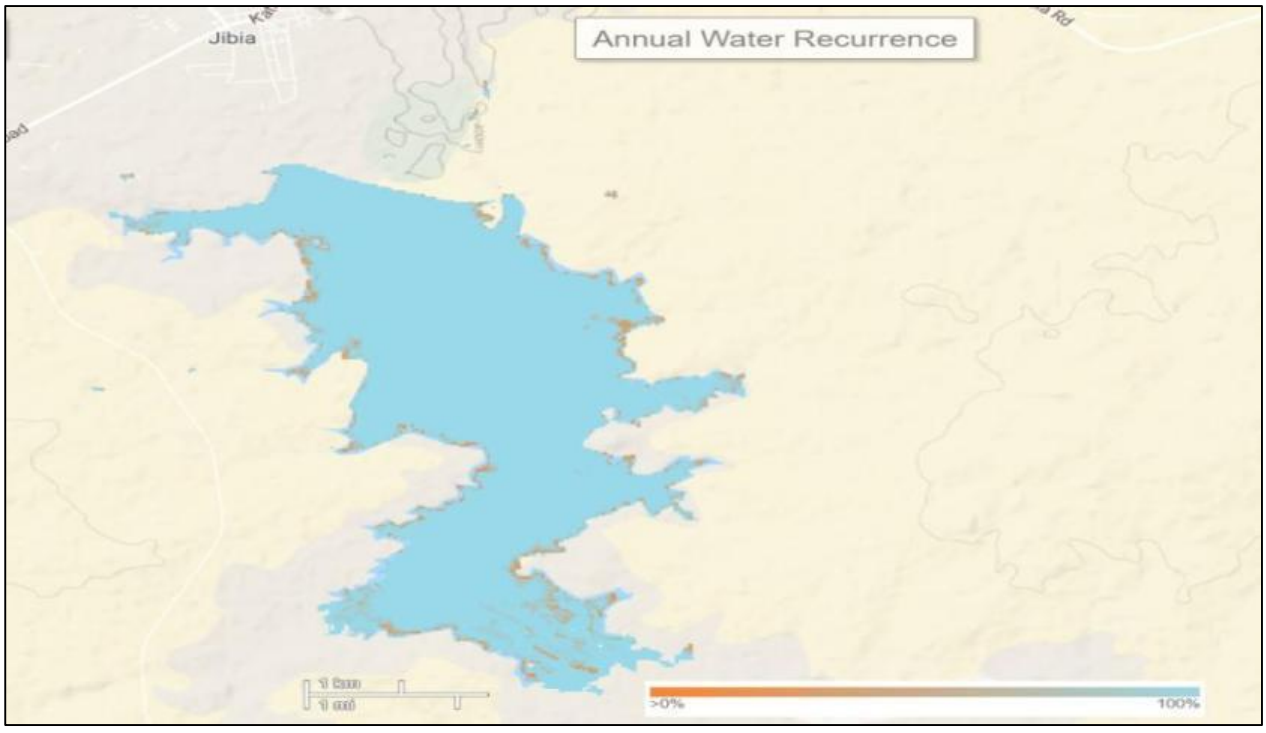

Figure 4-10d: Annual water recurrence at Jibia dam.This shows the degree of estimation in terms of the inter-annual variability on water presence, describing frequent water return from one year to another.From the image, the symbology signifies that only a few portion of the dam at the margin is 0%, while in most part of the dam, the annual water recurrence is 100%.

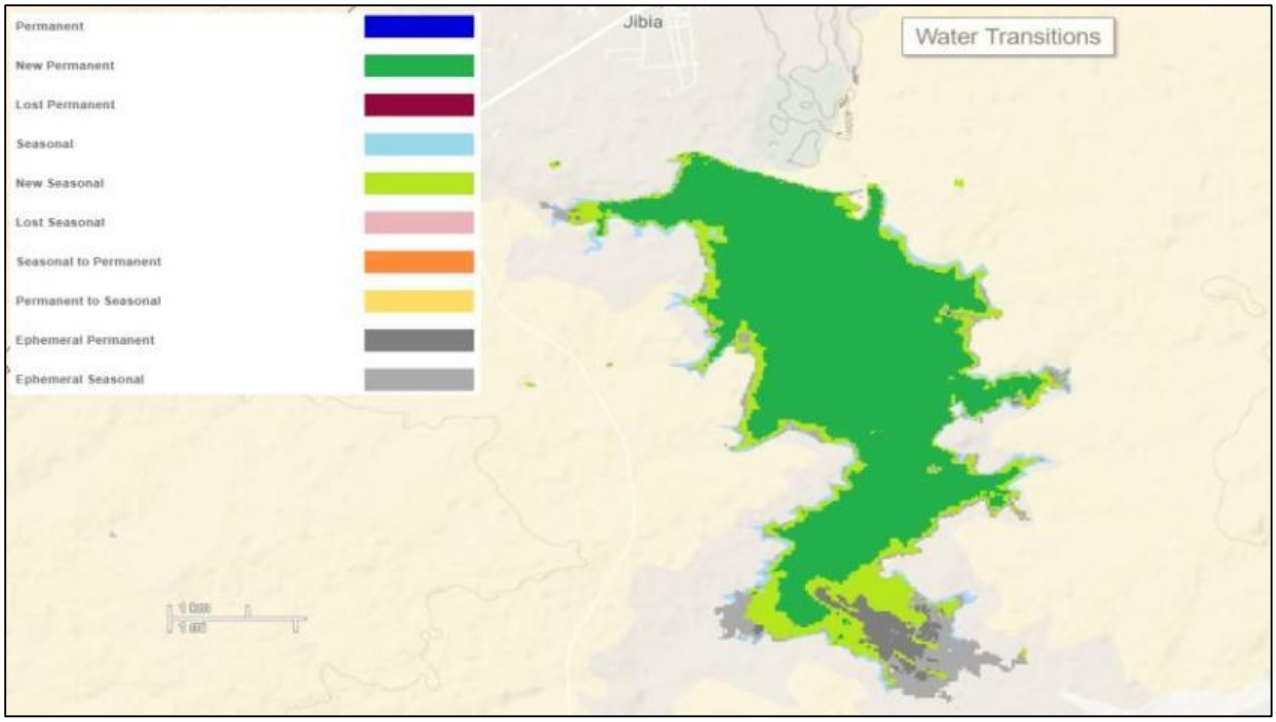

Figure 4-10e: Water transition at Jibia dam shows the spatiotemporal difference with different seasonal pattern from permanent water to ephemeral seasonal within the dam. At the center of the dam, the water is new permanent, while eccentrically, the water is new seasonal, followed by new seasonal, to ephemeral permanent, and to ephemeral seasonal at the edge.

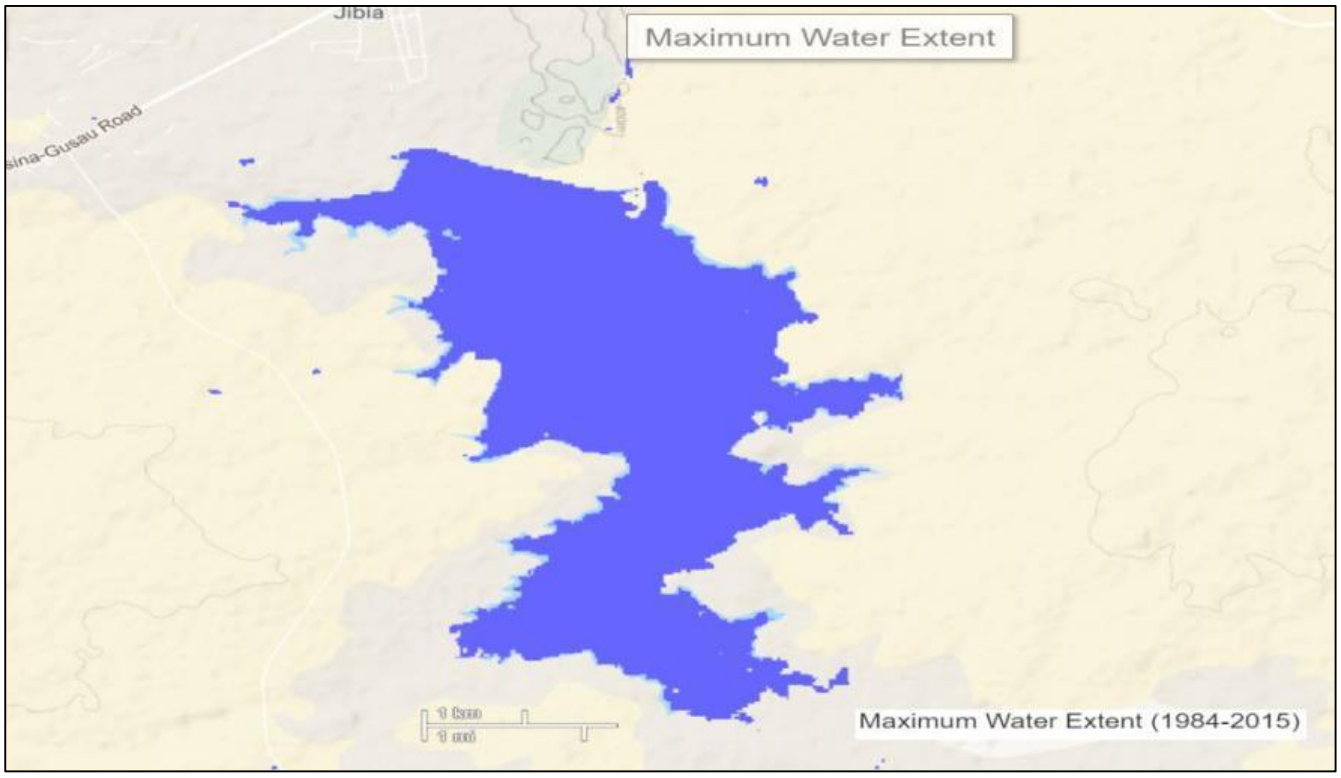

Figure 4-10f: Maximum water extent at Jibia dam. This shows the highest spatial extent of water ever retained by the dam. From the image, the dam appears to have occupied other areas from 1984 to 2015, while using other parameters above, it can be deduced that water has reduced from this extent in recent years.

Wurno dam

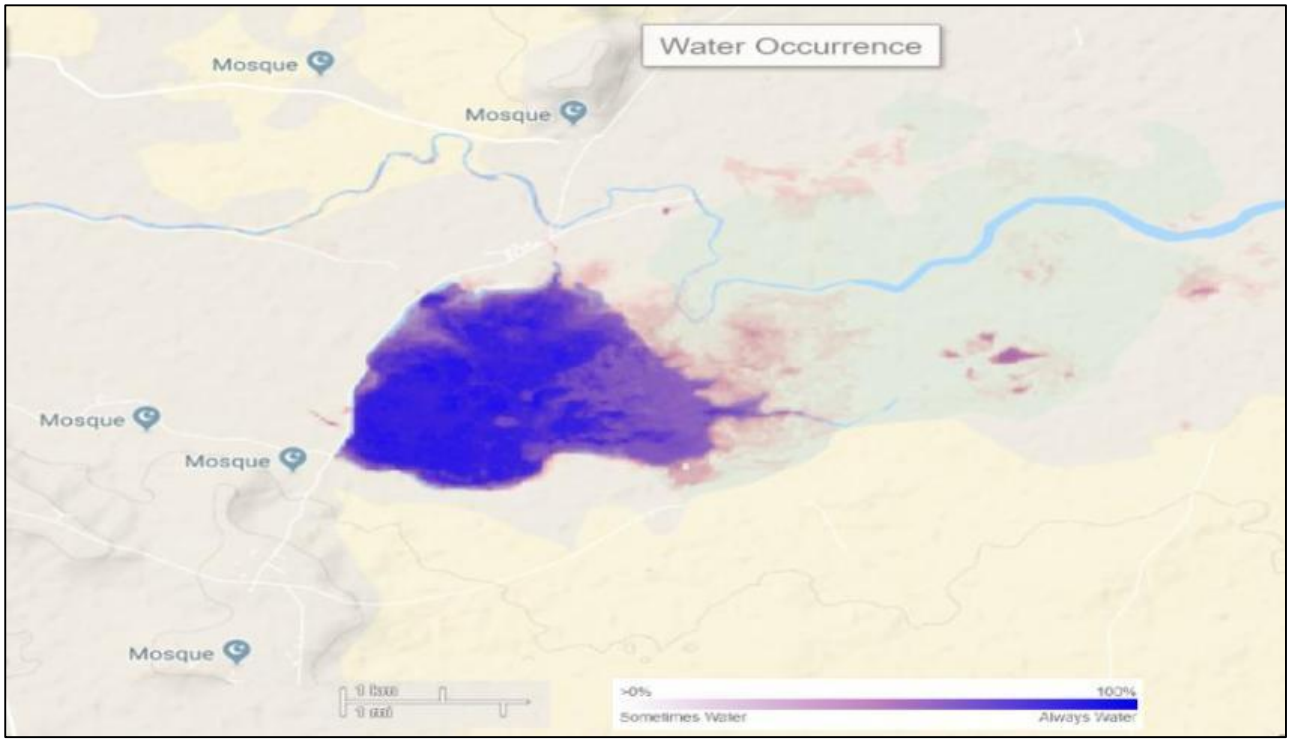

Figure 4-11a: Water occurrence at Wurno dam. This is showing the portion of the dam where water can be found in the course of the year, and where water is always available through the years**.** From the symbology, it appears that areas at the periphery tends to be having water at some point in the year, while as you move inwardly, it appears to always have water.

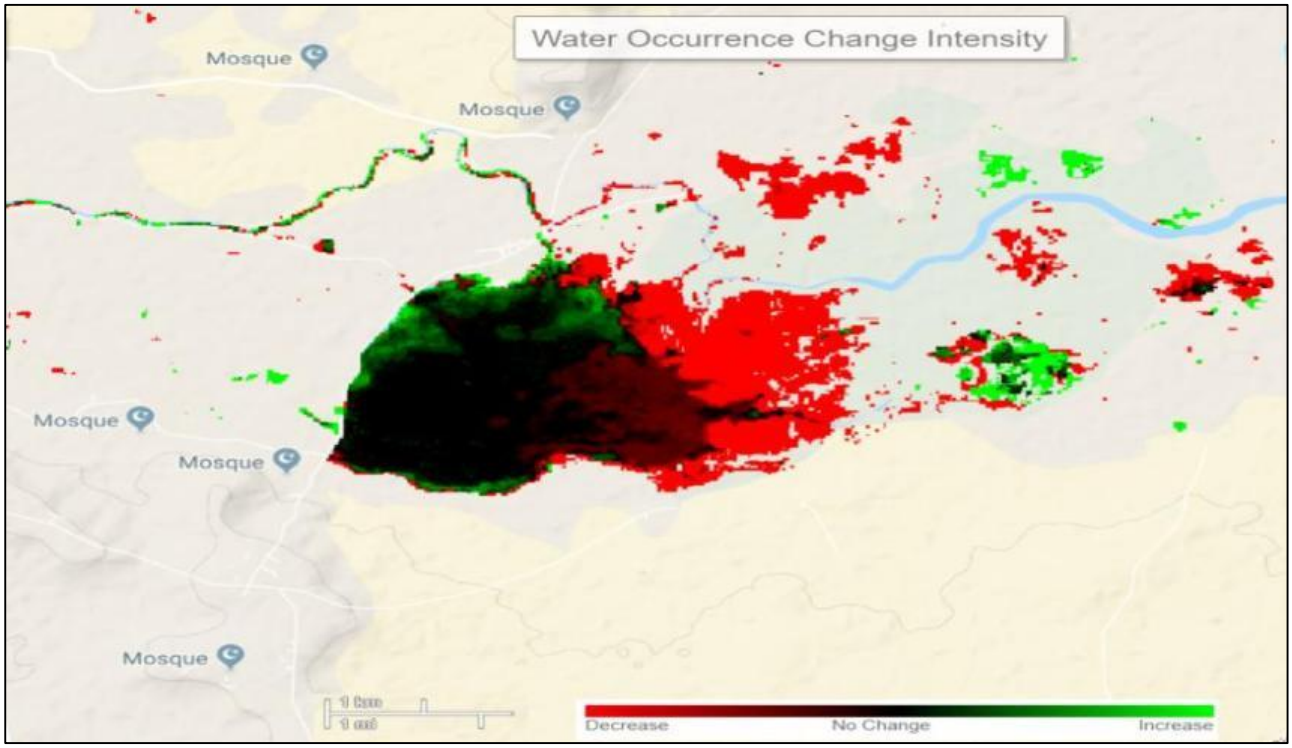

Figure 4-11b: Water occurrence change intensity at Wurno dam depicts where the dam's water decreases, remained unchanged and increased through the years. Areas around the edge of the dam tends to decrease and increase as shown using the symbology, while areas inside the dam have no changes or is increasing as observed from the image.

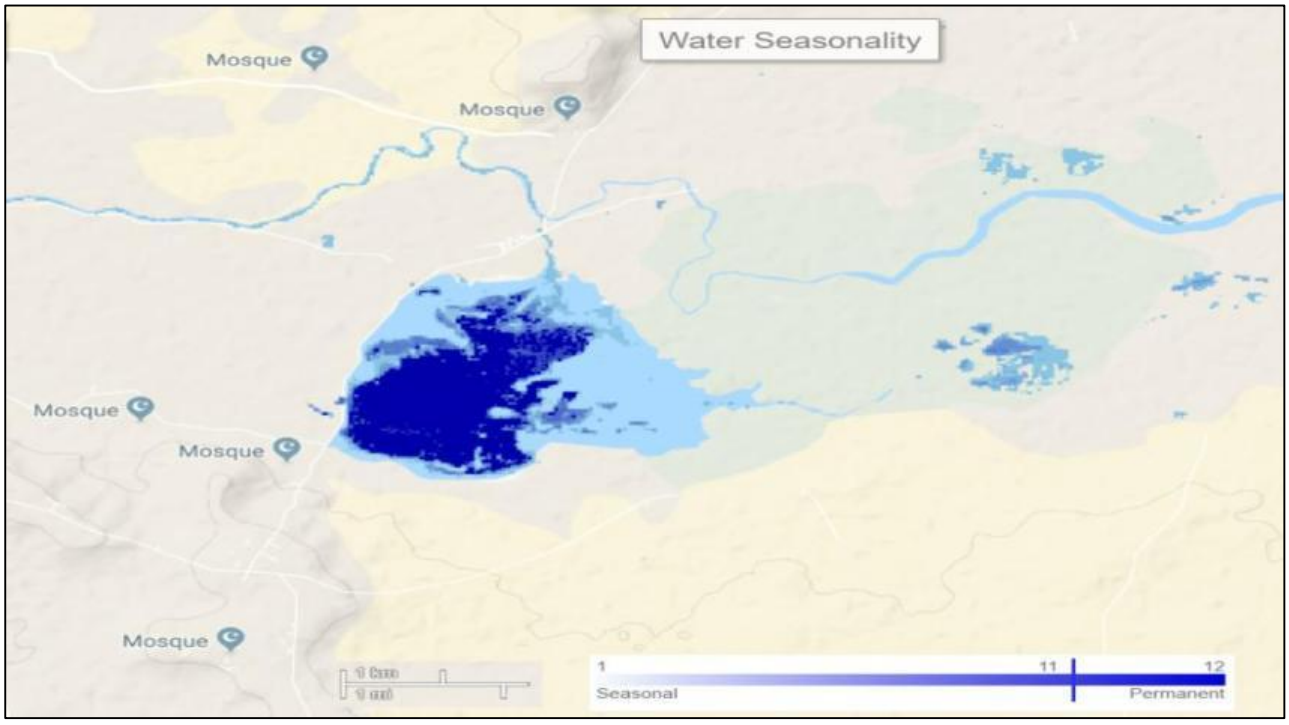

Figure 4-11c: Water seasonality at Wurno dam shows the seasonal water coverage from permanent water to seasonal water where water is not found at some point in the year. At the core of the dam it appears to be mostly permanent water, while at the edge, the water is seasonal and reduces from the inner part of the dam to areas at the periphery.

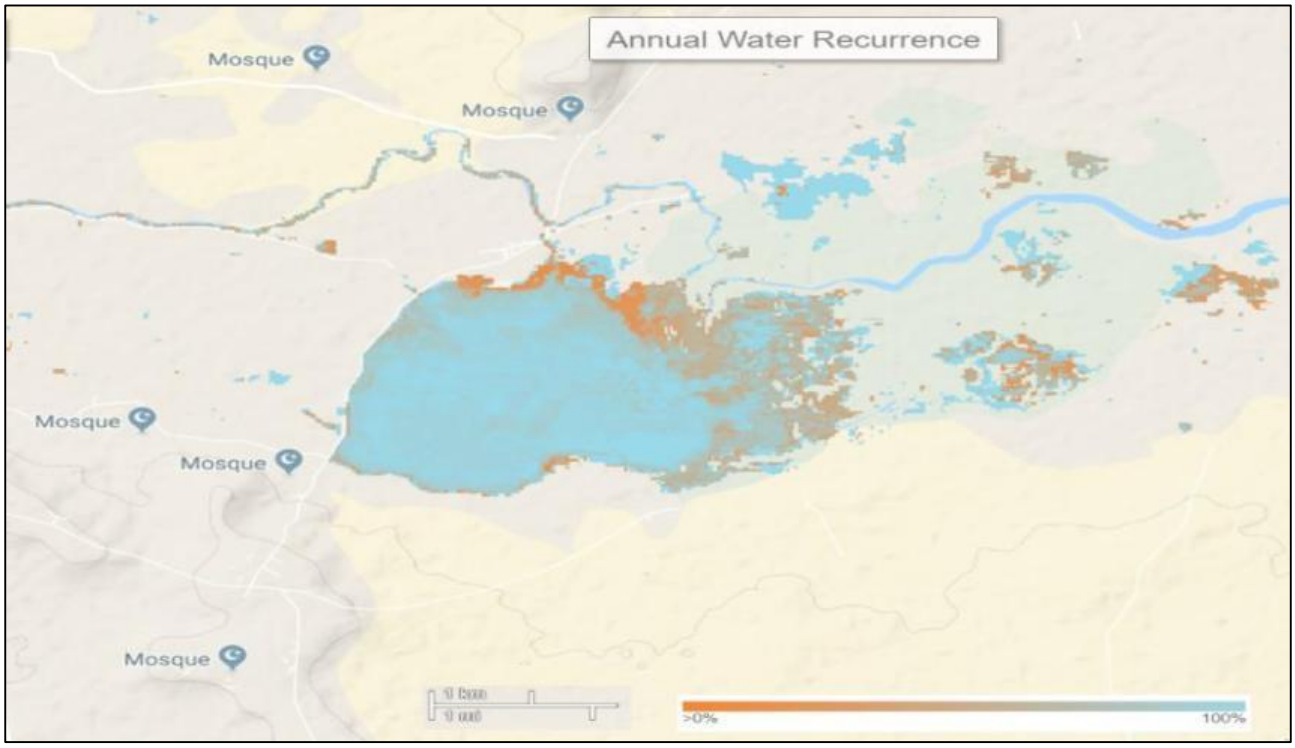

Figure 4-11d: Annual water recurrence at Wurno dam. This shows the degree of estimation in terms of the inter-annual variability on water presence, describing frequent water return from one year to another. From the image, the symbology signifies areas at the verge of the dam to be 0%, while in most part of the dam, the annual water recurrence is 100%.

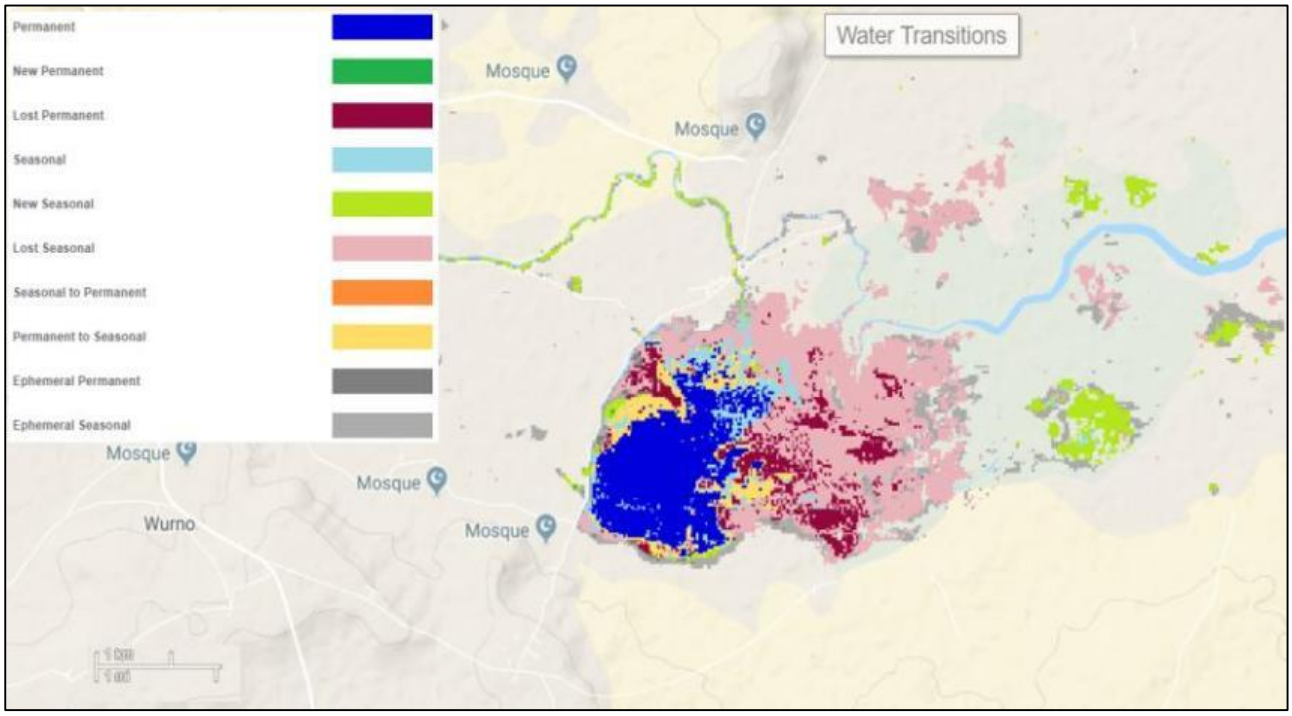

Figure 4-11e: Water transition at Wurno dam shows the spatiotemporal difference with different seasonal pattern from permanent water to ephemeral seasonal within the dam. At the center of the dam, the water is permanent, while eccentrically, the water is permanent to seasonal and lost permanent, followed by lost seasonal, to ephemeral seasonal, and to new season at the fringe of the dam.

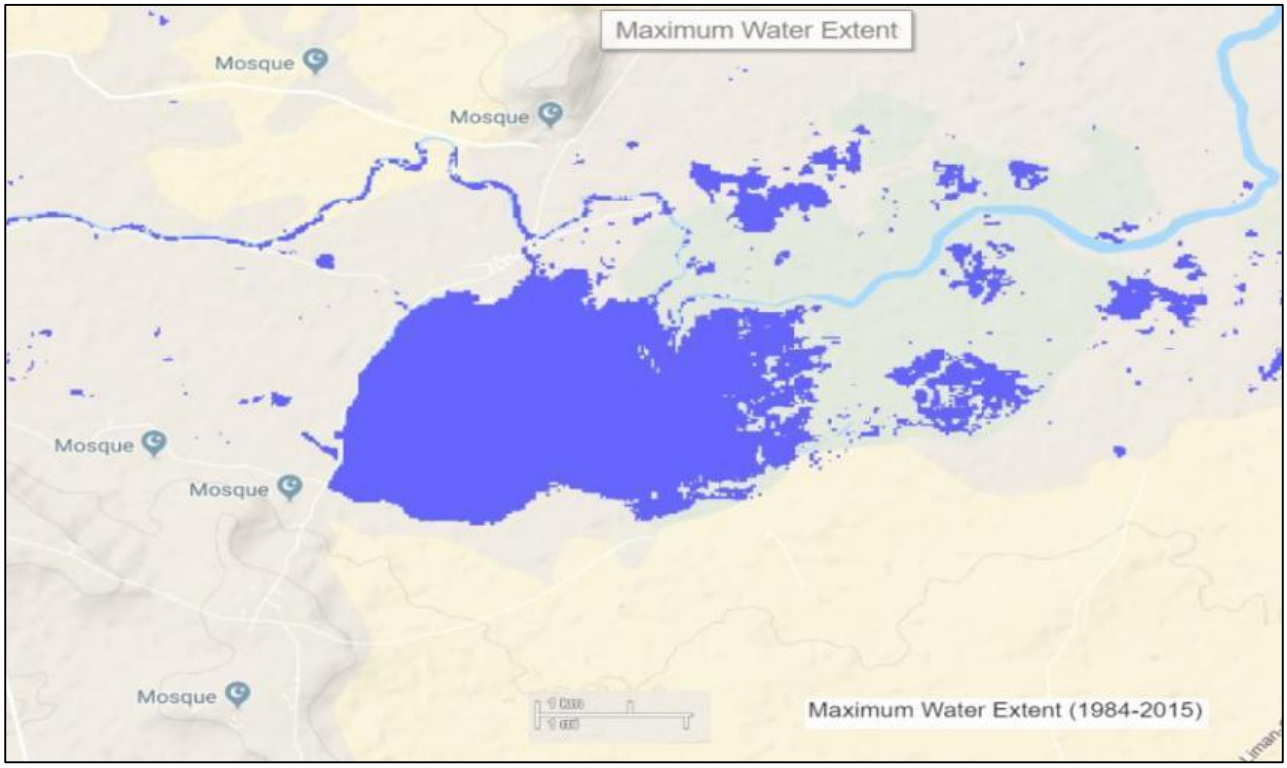

Figure 4-11f: Maximum water extent at Wurno dam. This shows the highest spatial extent of water ever retained by the dam. From the image, the dam appears to have occupied other areas from 1984 to 2015, while using other parameters above, it can be deduced that water has reduced from this extent in recent years.

Zobe dam

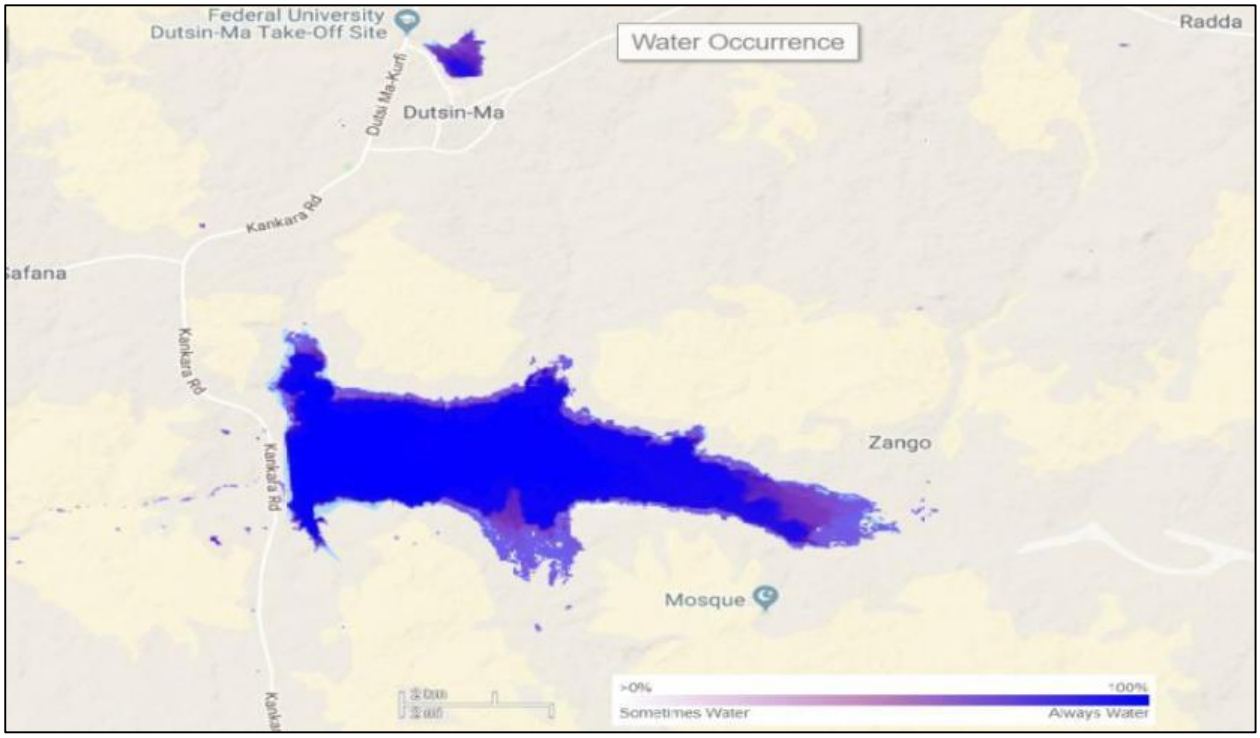

Figure 4-12a: Water occurrence at Zobe dam. This is showing the portion of the dam where water can be found in the course of the year, and where water is always available through the years. From the symbology, it appears that areas at the periphery tends to be having water at some point in the year, while as you move inwardly, it appears to always have water.

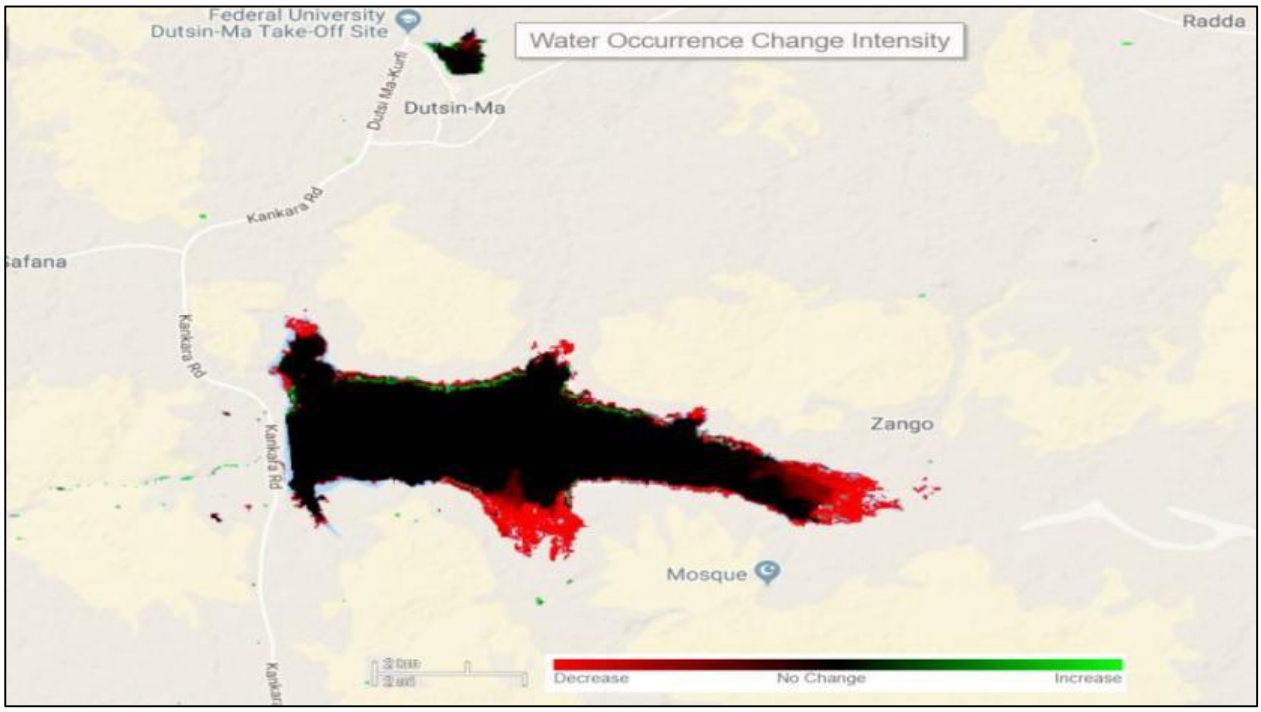

Figure 4-12b: Water occurrence change intensity at Zobe dam depicts where the dam's water decreases, remained unchanged and increased through the year. Areas around the edge of the dam tends to decrease and increase in some part as shown using the symbology, while areas inside the dam have no changes as observed from the image.

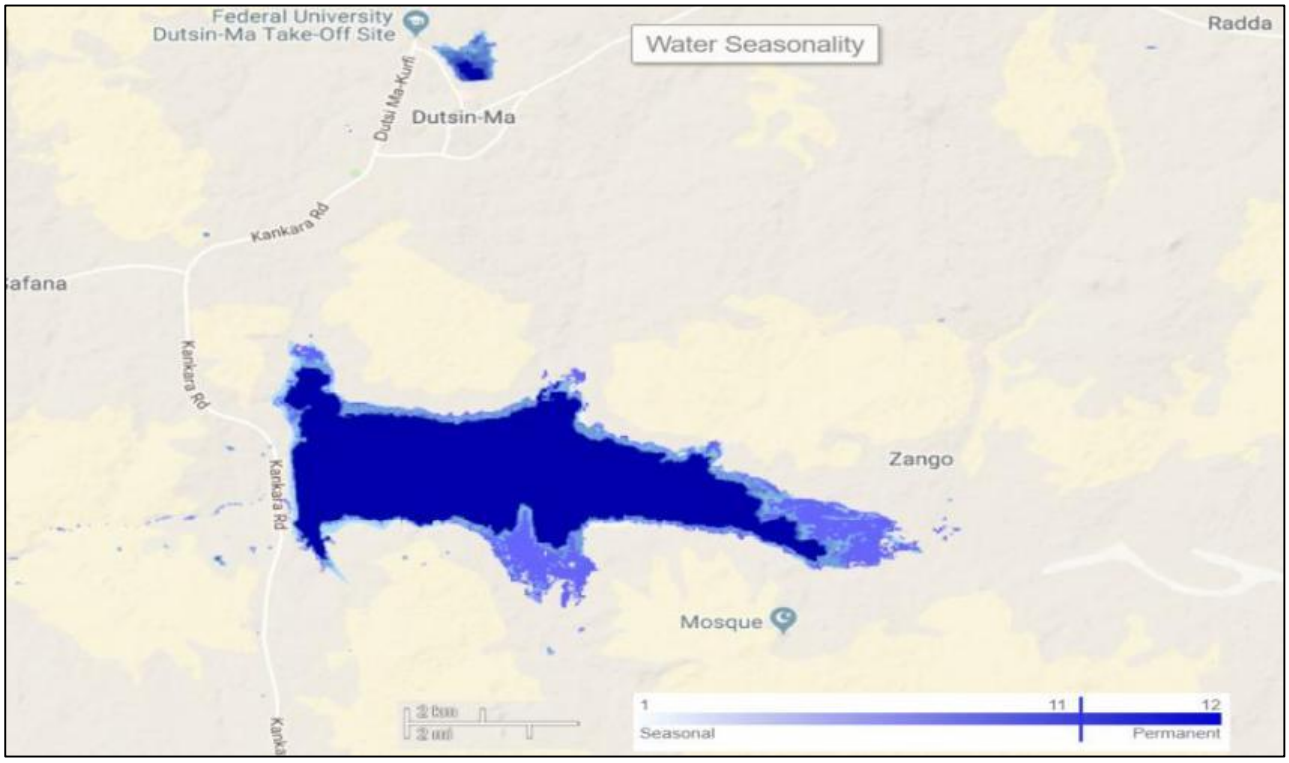

Figure 4-12c: Water seasonality at Zobe dam shows the seasonal water coverage from permanent water to seasonal water where water is not found at some point in the year. At the core of the dam it appears to be mostly permanent water, while at the edge, the water is seasonal and reduces from the inner part of the dam to areas at the fringe.

Figure 4-12d: Annual water recurrence at Zobe dam. This shows the degree of estimation in terms of the inter-annual variability on water presence, describing frequent water return from one year to another. From the image, the symbology signifies that only a few portion of the dam at the margin is 0%, while in most part of the dam, the annual water recurrence is 100%.

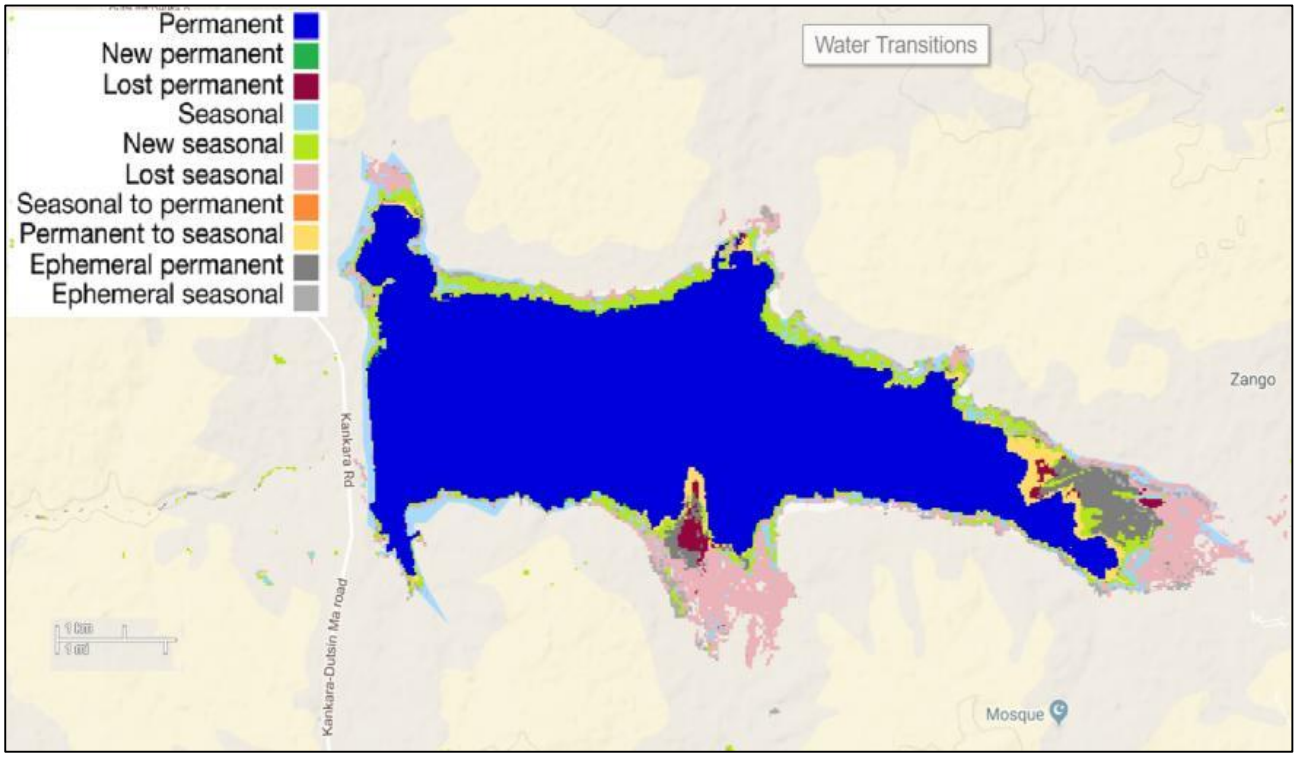

Figure 4-12e: Water transition at Zobe dam shows the spatiotemporal difference with different seasonal pattern from permanent water to ephemeral seasonal within the dam. At the center of the dam, the water is permanent, while eccentrically, the water is new seasonal and permanent to seasonal, followed by lost permanent, to ephemeral permanent, and to lost seasonal and seasonal at the margin of the dam.

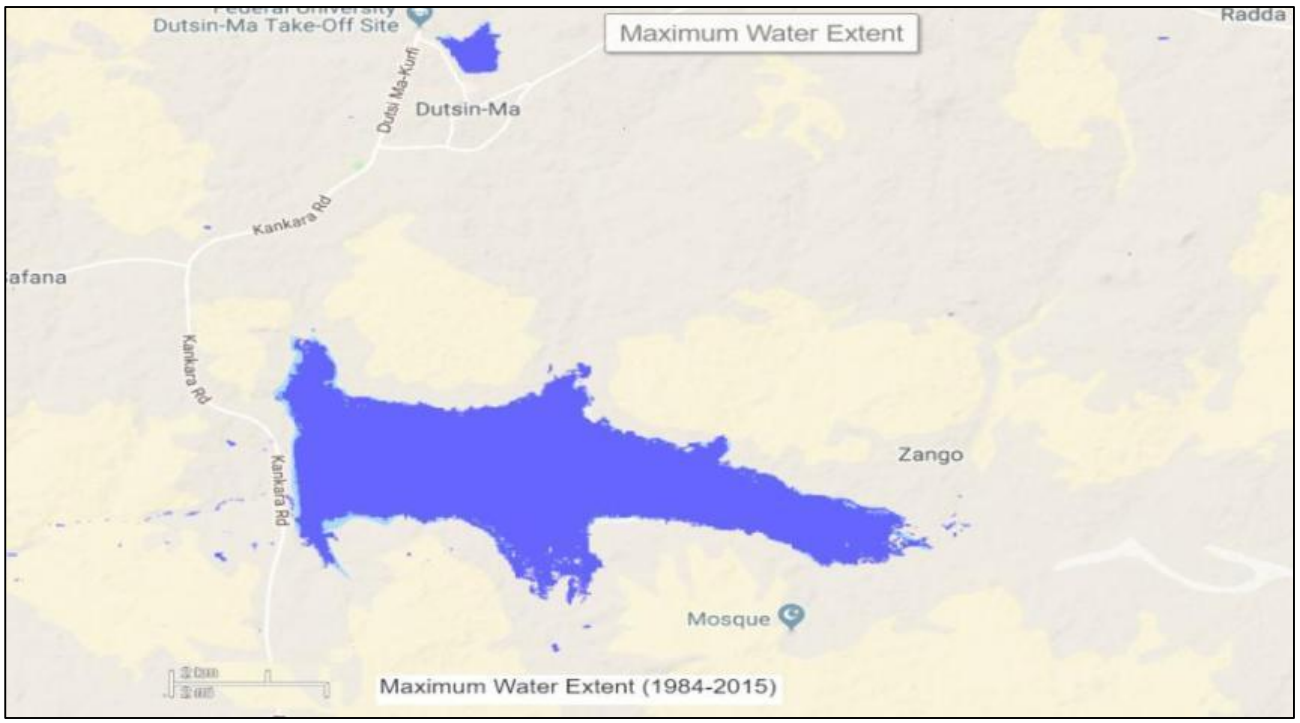

Figure 4-12f: Maximum water extent at Zobe dam. This shows the highest spatial extent of water ever retained by the dam. From the image, the dam appears to have occupied other areas from 1984 to 2015, while using other parameters above, it can be deduced that water has reduced from this extent in recent years.

Monthly water recurrence, water history, and monthly water history

To explicitly understand how water is apportioned temporally through the years, three datasets captures and records the temporal distribution of water in a particular place, thus; the monthly water recurrence which was explained earlier, water history through the years, and monthly water history/presence. These histories are shown in the surface water explorer as depicted in **Figure 4-13**, **Figure 4-14, Figure 4-15, Figure 4-16, & Figure 4-17**, and users can get the appropriate data by clicking anywhere around the water body to get the full history of that place.

The yearly history gives information on the seasonality of water over the 32 years. This contains the same information as the seasonality dataset, though it only covers the years where observations are available from 1984 to 2015.

The monthly water history detects the information on all the water datasets on a monthly basis from March 1984 to October 2015. The main reason is to know when a particular event occurs, e.g. when a dam was constructed can be known using this tool. As such, the dataset can be observed or derived when the user clicks on the yearly history.

Figure 4-13: The monthly water recurrence, water history and monthly water history at Bakolori dam, while where data is not observed or masked due to cloud cover; the space is empty**.**

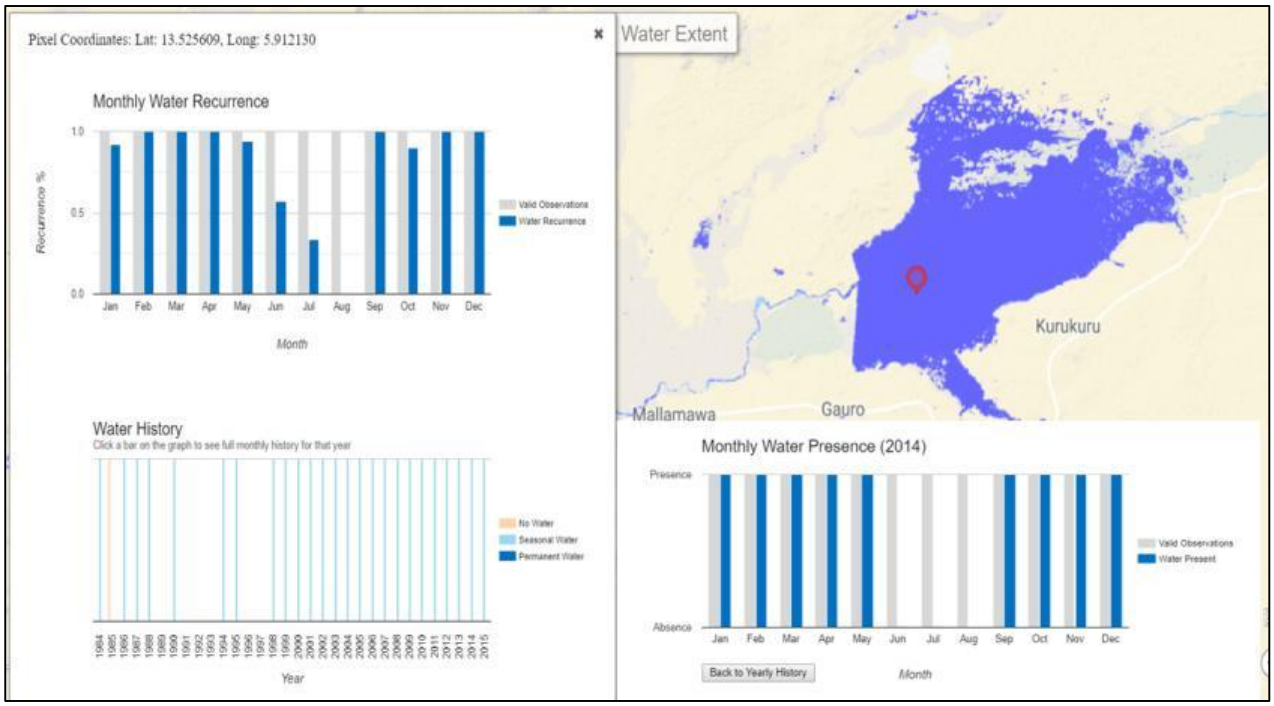

Figure 4-14: The monthly water recurrence, water history and monthly water history at Goronyo dam, while where data is not observed or masked due to cloud cover; the space is empty.

Figure 4-15: The monthly water recurrence, water history and monthly water history at Jibia dam, while where data is not observed or masked due to cloud cover; the space is empty.

Figure 4-16: The monthly water recurrence, water history and monthly water history at Wurno dam, while where data is not observed or masked due to cloud cover; the space is empty.

Figure 4-17: The monthly water recurrence, water history and monthly water history at Zobe dam, while where data is not observed or masked due to cloud cover; the space is empty**.**

4.4 Discussion

The Sokoto Rima River Basin is a vast floodable plain with a huge arable land resource that requires precise confrontation of climatic conditions to know where and when changes have occurred. Climate change impacts have been identified as an essential determinant of land use change in the basin. As opined by Ezemonye & Emeribe, (2015), they have examined the response of precipitation and land temperature in the Sokoto Rima River Basin. Their results showed that the duration of rainfall is reducing with an increase in temperature that is increasing surface temperature and as well evapotranspiration. As such, this research also uncover that the increase in temperature is affecting the dam size due to evaporation.

Using the Standardized Precipitation Evapotranspiration index (SPEI), long-term drought pattern of the basin was monitored which depicts high frequency of moderate drought, with lower frequencies that are apparent (i.e. negative values). The indices showed a moderate meteorological drought with a more consistent

pattern of the hydrological drought. Overall, the SPEI shows a long term drought in the yearly time series, depicting that it is sensitive in detecting severe dry spells (Zahid *et al.*, 2020) that vividly shows the importance of evapotranspiration in the computation of water deficit. Nevertheless, the surface water hydrology, was observed using the Global Surface Water Explorer to know how the drought pattern has affected the water system, because this is indeed crucial to the irrigation *Fadama* farming and quite central to this research.

From the SPEI data as shown in **Figure 4-2** (a, b) to **Figure 4-7,** the drought pattern begins when the indexes show a continuous negative value of -1 or less and end when the index becomes positive (Assadollahi, 1975). Therefore, from the data obtained using the SPEI_1 and SPEI_48 for the entire basin, the meteorological and hydrological drought was seen to be moderate.

Furthermore, the global water explorer was used to describe the water surface area and change that may have occurred within the dams in the basin. As depicted in **Figure 4-8a-f** to **Figure 4-12a-f;** the dams were all assessed based on their water occurrence, the occurrence change intensity, the water seasonality, annual water recurrence, the water transition, and the maximum water extent ever occupied by the dams. All parameters noted in the dam's behaviours was observed to be a continuous physical change, with water volume increasing during the wet season and shrinking in size as the year progresses during the dry season. This is influenced by water demand for *Fadama* irrigation and water loss by evaporation due to rising temperature. Additionally, looking at **Figure 4-13** to **Figure 4-17**, we can have a better understanding on when water is available. The monthly water history, the yearly water history, and the time when water was observed in the dams. Though with regards to this; where no data was observed or areas that are masked due to cloud cover, the time frame appears to be empty.

In general, the dam's behaviour changes over time, and with regards to the physical parameters obtained, rainfall and surface temperature greatly affects the water system in the Sokoto Rima River Basin.

CHAPTER FIVE

5 Conclusion and recommendation

5.1 Conclusion

Several parameters were used in this research to assess the *Fadama* irrigation system within the Sokoto Rima River Basin using ground yield data, remote sensing technique, climate history and surface water dynamics using Global Surface Water Explorer (GSWE). Below is a synopsis generated from the findings.

Table 5-1: showing the resolution of the generated datasets.

Resolution	**Landsat classification**	**Landsat NDVI**	**GEE classification**	**GEE NDVI**	**Pekko NDVI**	**SPEI**	**GSWE**
Spatial	30 m	30 m	30 m	30 m	250 m	¼ degree tile	30 m
Temporal	Decadal	Decadal	Decadal	Decadal	8 days	Monthly	Annual
Pros	User can influence the process	User can influence the process	Completely online and can be masked for NDVI values	Elaborate	Continuous with no data break	Is based on potential evapotranspiration and air temperature	Gives spatio-temporal detail of surfaces water
Cons	Spectral confusion of pixels	Not intensive because values are not plotted	Processing is completely administrative	Have data break due to scan line correction error	Short in duration from the year 2000 onward	Requires large amount of data	No data is available for download

5.1.1 Landsat Classification

High resolution images from the Landsat archives were downloaded from the United State Geological Survey (USGS). The images were obtained between November to March and ranges from 1988, 1998, and 2018 (**Figure A1**). The Geo TIFF images were cloud free and in level 1, tier 1, i.e. the images are georeferenced and does not require further geo tagging. However, a simple radiometric normalization was done using a simple haze adjustment by dark object subtraction in each subset scene.

Spatial resolution of 30 m and 16 days revisit temporal resolution at decadal interval was used. The Landsat 4, 5 TM and Landsat 7 ETM consist of six selected spectral bands (i.e. B1, B2, B3, B4, B5, and B7) respectively. While Landsat 8 OLI data, consist of six selected bands of (B2, B3, B4, B5, B6, and B7)

Among the advantage of remotely sensed data, is that it is good in mapping land use and land cover changes, and very responsive to vegetation and water. However, it provides broader data at global level that is otherwise impossible to collect when using conventional equipment. It is characterized with a tradeoff between the local detail of the measurement and the scale of the area being measured compared other methods like the aerial imagery.

Remote sensing gives the information of geographic spaces i.e. the ecosystem. These allows researchers to predict geographical information and as well detect both naturally occurring and anthropogenic generated changes in a more elaborate and detailed manner than the one provided by traditional field work. We hope to see the state and extend of Fadama coverage, but given that the data is decadal, we are more interested in the longer term trend. The different spectral bands as afore-stated, provides diverse spectral range with differentiated applications, as land cover change detection has become a very common use of Landsat imagery in remote sensing.

In this research, the remotely sensed data was used to assess a decadal land cover change. At inception five classes were identified, but due to spectral confusion of some of the pixels, four classes were then identified, namely; natural vegetation, Fadama areas, water and non-vegetated areas (**Figure 5-1**)

A supervised classification using maximum likelihood was used to identify training sites on the image, with a false colour combination of 5, 4, 3 on Landsat 4, 5, 7 and spectral band of 6, 4, 3 on Landsat 8. Hence, with the band combination as stated earlier, the study was able to set distinction between the identified classes. A total of 288 ground truthing points were used for the accuracy assessment, an overall accuracy of 97% in 1988, 92% in 1998 and 90% in 2018 (**Figure A5**) was

achieved. For an elaborate understanding of the identified classes, the water class comprises of the dams, streams, weir, and turbid water. While the natural vegetation encompasses the dense tree population, scrubs, riparian vegetation, fallow lands, grasslands and montane vegetation. For the *Fadama* class, it covers all the irrigable floodable plain with shallow aquifers, while the non-vegetated areas comprised of the built-up areas, the lateritic rock, sand deposit, bare lands, and other rocky surfaces.

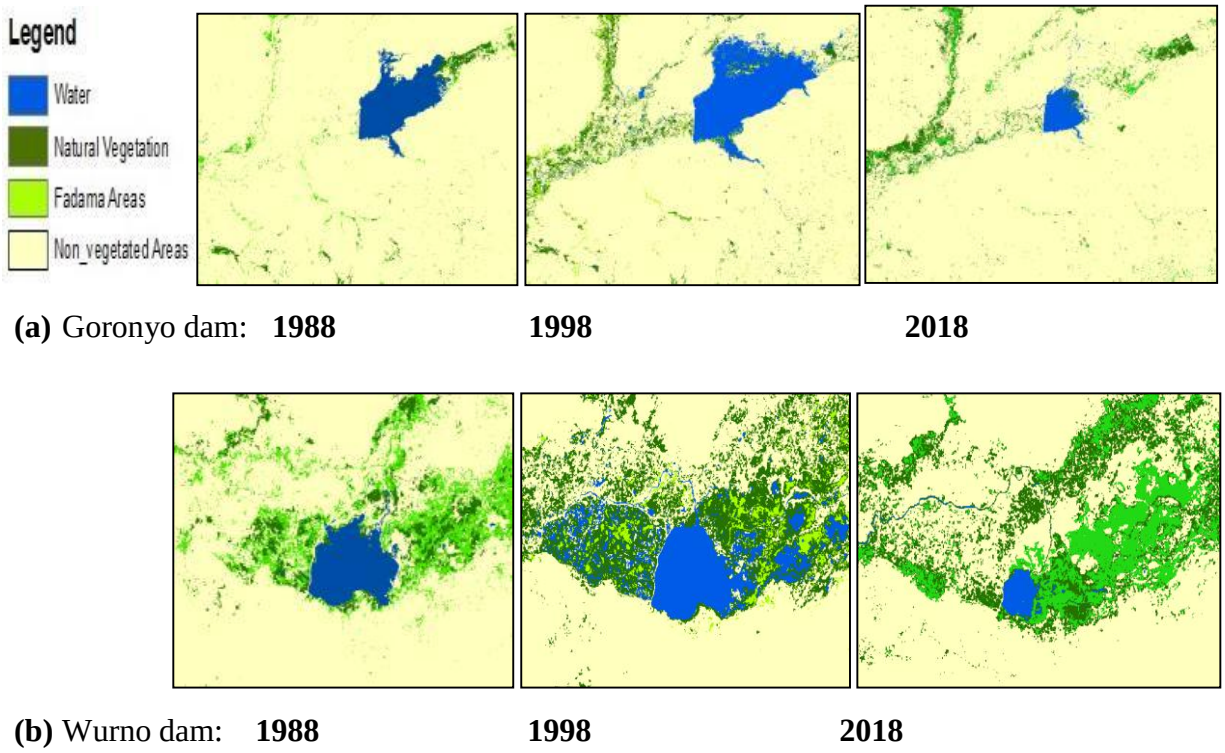

Figure 5-1 (a-b): Decadal trend of Landsat classification at Goronyo/ Wurno dam (**a** & **b**) for three epochs from 1988 through 1998 and to 2018 at dam level between November to March. From the images as depicted above, a more informed picture of how the trend is occurring adjacent to the dams can be explicitly understood. If this is juxtaposed with the result generated in **Table 3-1**, the result can be validated with the physical change, showing the surrounding *Fadama* areas increasing, while the dam extent is reducing through the epochs.

From the overall classification between 1988 to 1998. The percentage change for water was 114% and 166% for the natural vegetation, while that of the Fadama areas decreased by -65% and the non-vegetated areas also decreased by -100%. Between the year 1998 to 2018, reverse of the previous pattern was observed, the percentage change for water was -80% meaning that the water bodies have decreased. The natural vegetation in this epoch also decreased by -23%, while

that of the Fadama areas increased by 112% meaning that a 47% increase was achieved between 1988-1998 and 1998-2018. Lastly, the non-vegetated areas between 1998 to 2018, saw an increase of 3%. Hence, from the calculated percentage, it depicts that the Fadama farming saw an increase of 47% in recent years if compared to the previous decade, clearly stating that the Fadama irrigation is increasing.

The remotely sensed result achieved in this research can be integrated with the yield data in chapter 2. As observed in chapter 2 with a general increase in the yearly tonnage of the Fadama crops, the increase was as well seen in the imagery data as shown above at Goronyo and Wurno Fadama sites (**Figure 5-1**), because the Fadama farming was also increasing, validating that remote sensing is effective in the determination of changes that have or may occur for an informed decision making. However, in recent years as stated in chapter 4, it was observed that the SPEI data showed a recurring moderate drought across the observation stations. Therefore, with the decrease in water by -80%, and -23% with the natural vegetation as cited in **Table 3-1**, there is a perfect correlation that the effect of the moderate drought is eminent but has no much effect on the Fadama farming because it was seen to be increasing. Lastly, the limitation with most remote sensing data when dealing with large areas like the whole catchment of the SRRB is that, a computational timeout error was experienced, and that it is intensive and one can only work with subsets. Therefore, the research only looked at decadal data and a very broad temporal trend was shown. However, the spatial detail is reliable at detecting the changes as described, which is cogent enough to show the classification quantified, and in broad term, Fadama irrigation is taking place despite the moderate drought identified.

5.1.2 Landsat Normalised Difference Vegetation Index (NDVI)

The same in situ remotely sensed data source as stated above was used in the extraction of the Normalised Difference Vegetation Index (NDVI). The temporal and spatial characteristics of the data used in this section was the same as the one gathered in the above description, with 30 m spatial resolution and 16 days temporal resolution at decadal scale.

Spectral vegetation indices are characterized with the red and near-infrared reflectance radiance, they are usually analysed using the active photosynthetic biomass in plant and the chlorophyll presence through the faceted energy absorption capacity in different plants. The NDVI is the most used analysis derived from the remotely sensed imageries gotten through the maximum value composite. It delineates the actual chlorophyll level in plants and can be used to monitor crop growth and the state of the crops in terms of plant stress, yield predictions and among others.

The NDVI values extracted from the satellite imagery was used in this research to assess the range of the value composites of the Fadama areas. This was expected to glean the information required to know if the Fadama cropping system will have a correlation with the ground yield data acquired as cited in chapter 2.

The Landsat NDVI was carried out using the image analysis tab and the nearest neighbor in ArcGIS 10.5. The index value was set to scientific output, with band combination of band 3 as the red band, and band 4 as the near infrared band in Landsat 4, 5, and 7. In Landsat 8, the band combination was different, with band 4 as the red band and band 5 as the near infrared. However, the integer was scaled up by 100, with 15 natural break of classes that set distinction between the natural vegetation and the Fadama vegetation using the value field, see **Figure 3-5** and **Figure** 5-2**.**

From the extracted NDVI values in 1988, the vegetation index range between -21.4 to 38.5 (**Figure 3-5**). Areas with no vegetation show negative values, while areas with vegetation depicts positive values. Hence, values that

range from 14 to 21 with purple colour palette were identified as Fadama, while as the choropleth gets greener, it shows natural vegetation that comprised of dense tree population and other natural vegetation identified. In 1998 (**Figure 3-6),** the NDVI showed the values that range from -100 to 100, all areas that fall between -5 to -100 have no vegetation. While areas between 20.78 to 100 depicts Fadama vegetation. In **Figure 3-7**, i.e. the NDVI map of 2018, the value range is from -99.9 to 99.9. values ranging from 24 to 41 showed Fadama areas. Overall, from the extent indicator as shown in **Figure 3-5** and **Figure** 5-2 (i.e. 1988 and 1998), the area covered by the Fadama irrigation is not as broad if compared with that of 2018. As such, this also indicates that the Fadama farming is improving in recent years.

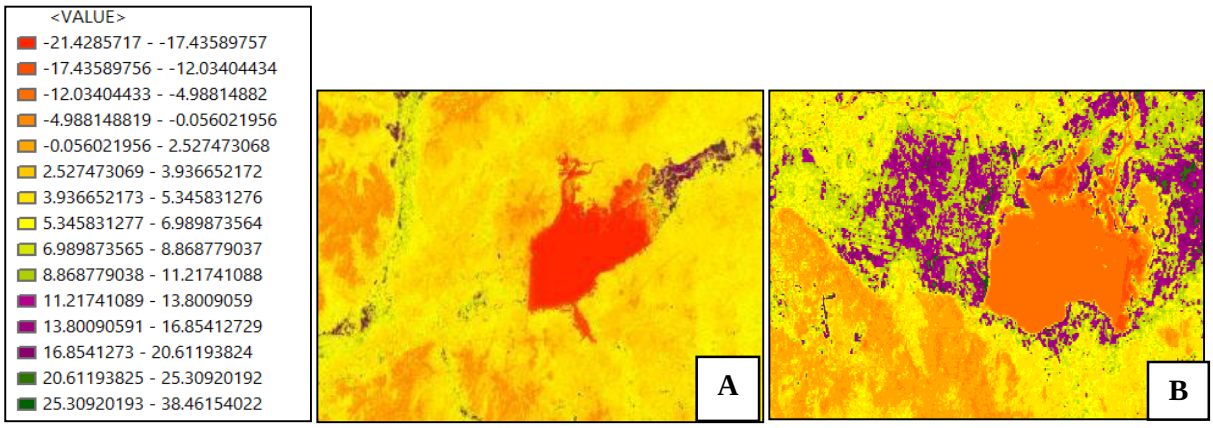

Figure 5-2: Normalized Difference Vegetation Index around (A) Goronyo dam (B) Wurno dam in 1988 from Landsat data with values ranging from -21 to 38. The *Fadama* vegetation ranges from 11 to 21 highlighted in purple, although since it is using a natural break of classes on the vegetation index, some of which are not *Fadama* vegetation are as well included in the range. Values that show negative contains no vegetation at all, while the greener the color palette, the higher the vegetation which is natural vegetation cover that comprises of tree vegetation and scrubs.

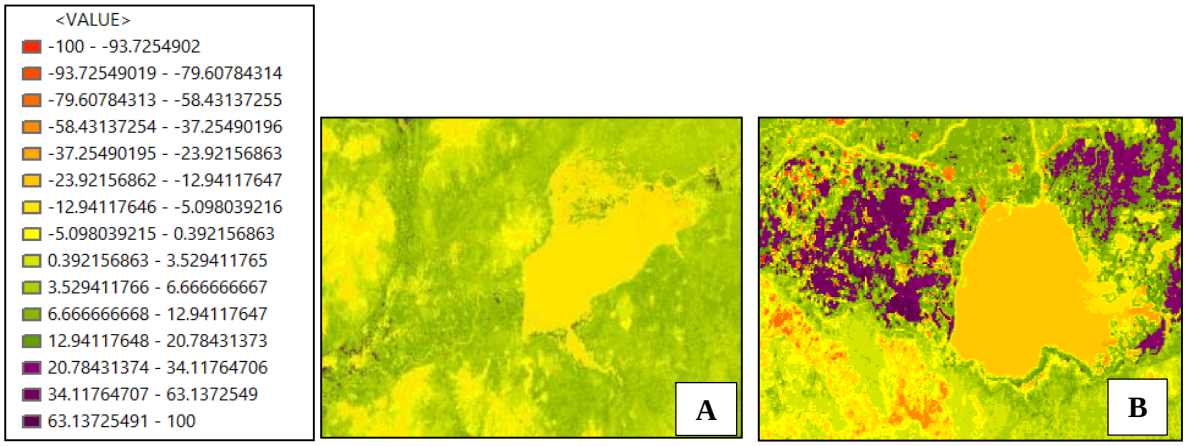

Figure 5-3: Normalized Difference Vegetation Index around (A) Goronyo dam (B) Wurno dam in 1998 from Landsat data with values ranging from -100 to 100. The *Fadama* vegetation ranges from 20.78 to -100 as highlighted in purple, although since it is using a natural break of classes on the vegetation index, some of which are not *Fadama* vegetation are as well included in the range. Values that show negative contains no vegetation at all, while the less green the color palette, the less the vegetation cover is, which comprises of water bodies, bare soil and rocky surface.

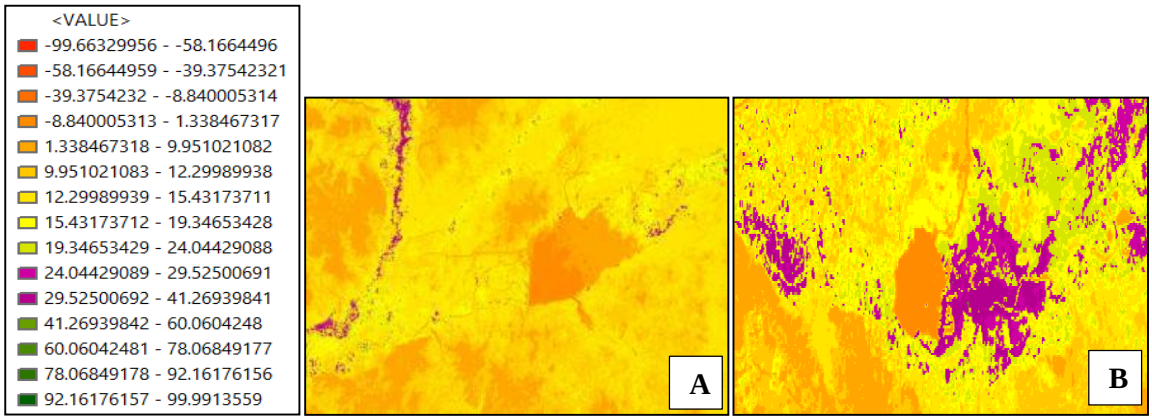

Figure 5-4: Normalized Difference Vegetation Index around (A) Goronyo dam (B) Wurno dam in 2018 from Landsat data with values ranging from -99 to 99. The *Fadama* vegetation ranges from 24 to 41 as highlighted in purple. Values that show negative contains no vegetation at all, while the less green the colour palette, the less the vegetation which is mostly water bodies, bare soil, rocky surfaces and built up areas.

NDVI values clearly indicate vegetation vigour, as such, the range of values here depicts either vegetation or no vegetation. Therefore, the integration of NDVI values to the amount of crop yield in the field can be achieved if the ground data is available as in the case of Goronyo and Wurno. However, where the ground data is not even available, the NDVI values can serve in the prediction of crop yield based on how the values fluctuate.

5.1.3 Landsat Google Earth Engine (GEE)

The imagery data source of the GEE was gotten from the archived Landsat imageries of the Google Earth Engine. The images are automatically imported into the GEE Application Program Interface (API) using the java scripting in the code editor, which is different from the traditional method of image classification because imageries will have to be downloaded before further analysis can be carried out.

The temporal and spatial resolution of the Landsat images remain the same even in the Google Earth Engine. It retains its 30 m spatial resolution, and 16 days temporal resolution and was observed at decadal scale.

Google Earth Engine API is unlike the traditional way of image processing and classification. Here, imagery data is automatically gotten from the archived image repository of the Earth Engine using the image ID and the scripting language in the GEE code editor interface. Hence, image processing time is fast and characterized with parallel computation based on tile by tile computation capability.

The change detection analysis in this study requires image pre-processing and normalization. Therefore, the technique applied on the image was used as a reference layer for training and validating the classification with an aim to get better results if compared with the other traditional way of image classification.

In this study, calibrated top-of-atmosphere (TOA) reflectance data from Landsat 4, 5, 7, and 8 was used (**Figure A2**). The images are orthorectified and calibrated, the change detection technique was applied and evaluated by creating code in the GEE code editor interface, using a supervised classifier algorithm and Landsat time series subsequently for each chosen year (**Figure 5-5**). However, when classifying the image, there is all possibility of running into error due to several cluster of the training points, but this can be avoided if the scripted language

is written well and in line with the command and the variable created in the code editor interface.

For each chosen year, the image classification was carried out within the GEE playground and the code editor interface. The classification was done for 1988, 1998, and 2018 (**Figure 5-5**), and is considerably accurate with no much spectral confusion unlike the traditional method of image classification. The image ID was used to search for the image from the image collections, the ID was then used to filter the Landsat data from the collection repository of the Google Earth engine. A variable was then created to set a command that filter the image by the region of interest (roi) using the point geometry import, filtering the image by the date, sorting it by the least cloud cover and the first in the collection. To know when the image was taken, a command was created that appears in the console with the band combination specified. After the geometry import, four classes were then created and imported as feature collections with a property set as Landcover and numbered 0-3 (i.e. non_vegetated class, water class, *Fadama* class, and natural_vegetation class). To further enhance the classification, the feature collections were merged and printed by creating a command that overlaid the points and inspects the training sites. Finally, to classify the image using the training points on the selected training sites, the classification variable was scripted using the initial band combination and the colour palette.

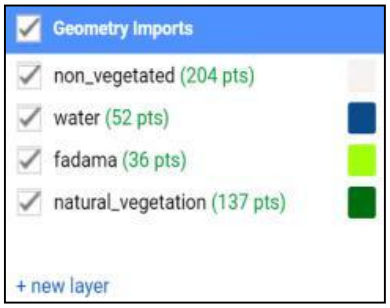

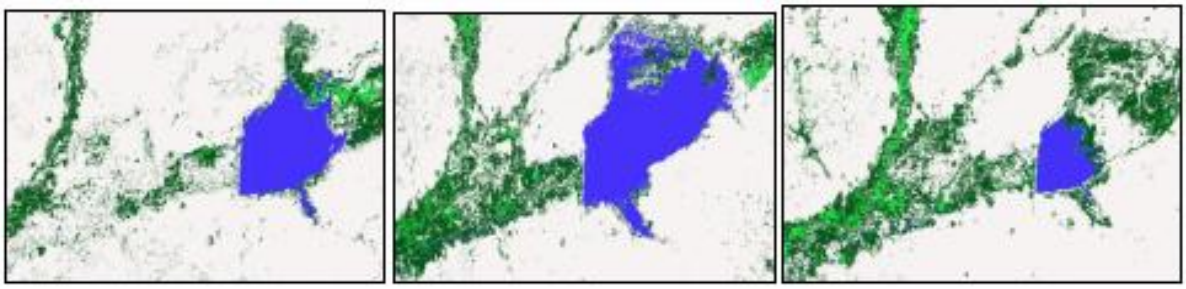

(a) Goronyo dam: **1988** **1998** **2018**

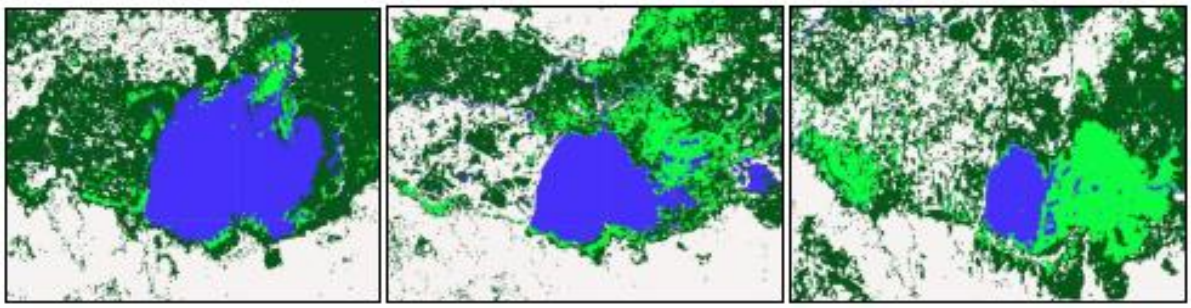

(b) Wurno dam: **1988** **1998** **2018**

Figure 5-5 (a-b): Decadal trend of GEE classification at Goronyo/ Wurno dam for three epochs from 1988 through 1998 and to 2018 at dam level between November to March. From the images as depicted above, a more informed picture of how the trend is occurring adjacent to the dams can be explicitly understood. If this is juxtaposed with the result generated in **Table 3-1**, the result can be validated with the physical change, showing the surrounding *Fadama* areas increasing, while the dam extent is reducing through the epochs.

The GEE classification is similar to the traditional method of image classification but with a disparity in terms of the data source and the accuracy of per pixel spectral classification. In GEE the images are automatically gotten online and do not required download before further analysis can be done on the image, while the classification has no much spectral confusion. The cloud computing in GEE has advantages for broad scale and long time-series mapping, this is because the performance, efficiency and scaling, takes advantage of the Java Just-In-Time

(JIT) compiler to optimise the implementation of chain of per-pixel operations that are characterized in image processing. However, the computation in GEE protects the user from the details working in a parallel processing environment, the system hide and manages almost every aspect of the computation which includes the parallelism, resource allocation, retries and data distribution, which is quite different from the traditional Landsat analysis that is software based. Among other notable limitation is that, the user is not able to influence the process because the decisions are strictly administrative and none will interrupt with any query, and only the speed at which the result is produced is shown. Hence, this is somehow a challenge in the design and use of the system (Gorelick *et al.*, 2017). Overall, the classification with GEE has more accurate result than that of the traditional method of image classification.

5.1.4 Google Earth Engine Normalised Difference Vegetation Index (GEE NDVI)

The Google Earth Engine Normalised Difference Vegetation Index has the same data source with the classified Landsat data of the GEE gotten from the Earth Engine image repository. Since it is the same Landsat data used all through, the temporal resolution still remains 16 days and at decadal scale, while the spatial resolution is 30 m.

The Normalised Difference Vegetation Index used in the GEE does not have much of a difference in terms of the output data generated when compared to the software based method used as stated above. However, the computation used here was generated using the java scripting language in the code editor interface. To compute for NDVI time series in GEE, five (5) Fadama areas adjacent to the dams were masked and calculated using the NDVI formula and the selected bands variables.

The output data expected from the computation depicts a value quantified based the green colour reflectance of the Fadama crops adjacent to the dams. As such, this was used to compare it with the acquired yield data to know how it can be used in the prediction of crop yield from the satellite based values.

The NDVI values computed from the Earth Engine interface was acquired from the buffered areas using the polygon geometry import **(Figure 5-6**). The colour palette variables were created alongside the NDVI function. To show a continuous time series of the NDVI plots, a variable was then created specifying only the region of interest which was then printed in the console. However, the NDVI time series data was having a data break due to scan line correction error on Landsat 7, which allude the research to refer to MODIS data as a substitute to investigate the vegetation index from the year 2000 onward. In general, the NDVI depicts that the Fadama coverage and uses is increasing as the year progresses.

The Normalized Difference Vegetation Index was shown in the GEE playground after the code was scripted in the code editor interface, all buffered areas of the Fadama sites and the generated data were printed in the console to have a view of the times series data through time using Landsat 4, 5, 7, and Landsat 8 (**Figure A4 a-b**). To further show a continuous NDVI values from 1984 to 2018, the CSV format of the data from the Earth Engine was downloaded and plotted, but with an anomaly on Landsat 7 data due to scan line correction error. As such, these values can be assigned to monitor or rather assess yield of crops in the Fadama areas pending on how the values fluctuate through the observation time. From the Figure below, the masked Fadama areas showed values adjacent to the dams that the Fadama farming system is increasing in hectarage, and that the quantified change over the observed period is positive because it shows higher NDVI values.

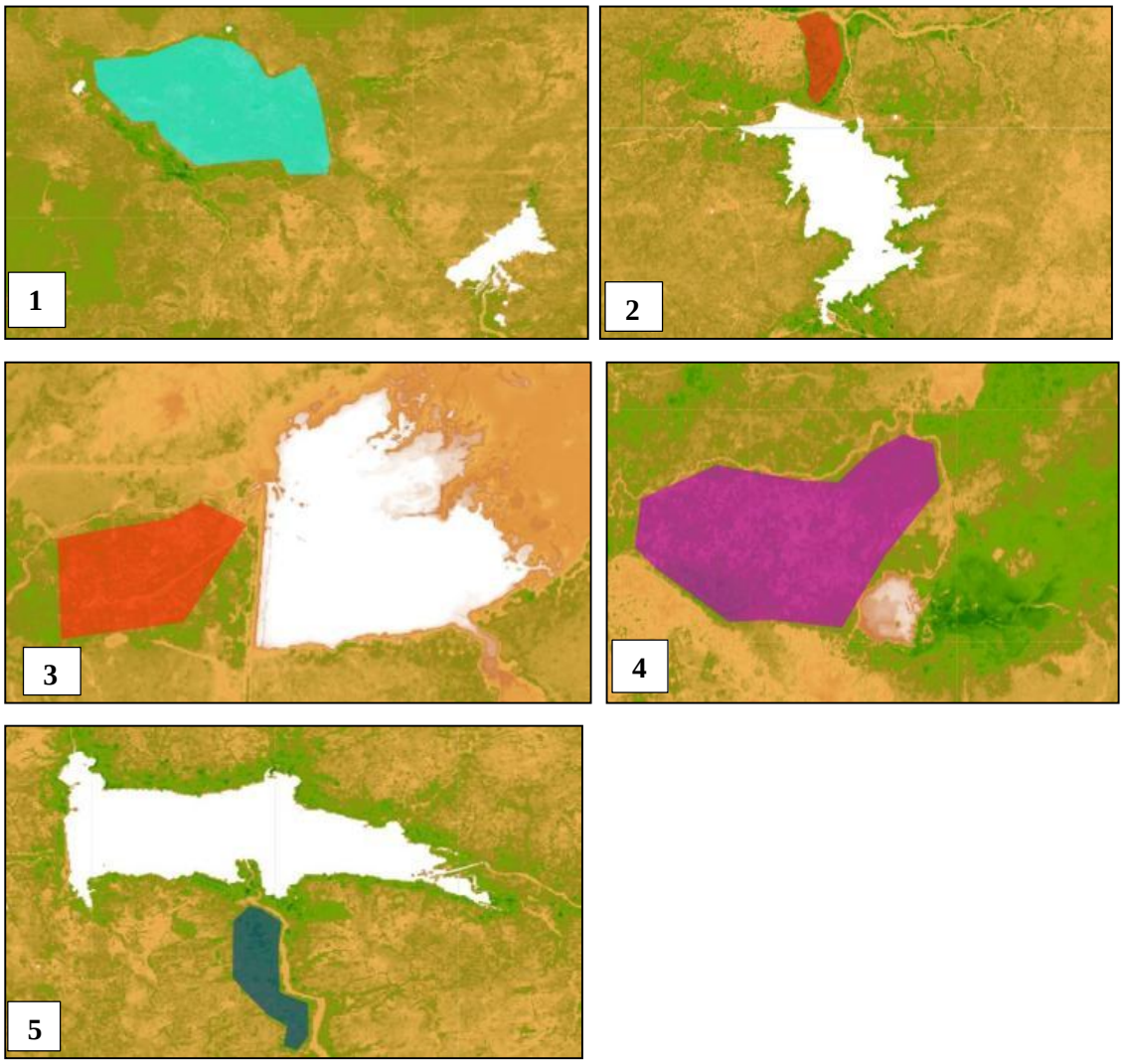

Figure 5-6 (1-5): Images showing the polygon geometry used in the GEE API to mask areas adjacent to the dams, so as to obtain the NDVI values from Landsat data at (1) Bakolori *Fadama* site, 12.64^0 N 5.97^0 E (2) Jibia *Fadama* site, 13.09^0 N 7.24^0 E (3) Goronyo *Fadama* site, 13.51^0 N 5.86^0 E (4) Wurno *Fadama* site, 13.30^0 N 5.45^0 E (5) Zobe *Fadama* site, 12.34^0 N 7.51^0 E.

Vegetation Indices have shown that it can be used effectively to assess yield of crops in the field. This is because, with an increasing index value of the Fadama areas as generated from the polygon geometry import, it depicts that the cultivation in the Fadama areas is progressing from 1984 to 2018. If these is compared with the data produced on the classification and the crop yield data obtained as shown in chapter 2, the data can be integrated to derive meaning that the irrigation Fadama farming saw an increase holistically. However, GEE NDVI is more robust and specific base, because areas can be masked for values unlike the traditional method, but with limitation on Landsat 7 due scan line correction error.

5.1.5 Pekko NDVI MODIS data

The pekko MODIS NDVI time series is a web-based tool from the Global Agriculture Monitoring (GLAM) project. It is used to derive a sketch graph data, it shows the peak and the nadir of greenness within the specified area, and also compare the annual NDVI trend with the long-term average (i.e. NDVI anomalies).

Moderate Resolution Imaging Spectroradiometer (MODIS) data, captures the earth's data in 36 spectral bands that ranges from 0.4 um to 14.4 um at varying spatial resolution of (band 2 at 250 m, band 5 at 500 m, and band 29 at 1 km). Specific to Pekko NDVI MODIS data, the spatial resolution is 250 m and covers from the year 2000 onward. The instrument has a temporal revisit of every 8 days, as such, the instrument is highly efficient in the measurement of large-scale global dynamics when compared to Landsat data.

The Pekko NDVI data has special characteristics that differs from the Landsat data. This is because the data's temporal and spatial resolution is designed to provide prolix global dynamics that is stronger and quicker than that of the Landsat data. However, it is limited and only available from the year 2000 onward, but will serve as an alternative to Landsat 7 data that have a data break in it due to the sensor error.

The data was anticipated to measure the peak and nadir of greenness within the 5 (five) Fadama areas at different resolution for each selected Fadama site. The data obtained was used to measure both the dry season Fadama farming and that of the wet season farming, this was clearly separated and shown for each of the Fadama site (**Figure 3-20).**

For each of the Fadama site, the region of interest was selected by clicking the globe. Under the polygon option, all parameters were selected and the graph was then updated after choosing the date or time of interest. The trend is continuous and with no data break, this gives an overview of the trend that depicts a positive and elaborate NDVI values over the observed period.

A point data was first derived and then expanded to 1.5 km resolution to obtain data for Jibia and Zobe dam Fadama sites. For Goronyo and Bakolori dam Fadama sites, a 2 km resolution was used to acquire the Pekko NDVI data because the irrigation system here is extensive when compared to the former stated Fadama site. Finally, the series of dates were computed to show a continuous time series of the Pekko NDVI data from 2000 to 2019 that separates the Fadama and the wet season farming (**Figure 3-20**).

The Pekko NDVI data serves a good alternative in the investigation of vegetation index since it is available from the year 2000, while Landsat 7 scan line correction error starts from the year 2003. This will give a more defined assessment of the pattern since it is continuous and has short temporal resolution. The data generated from MODIS showed that the Fadama irrigation is increasing over the years, hence, if the data is compared with the yield data in chapter 2, the increase can be validated. Which in essence, showed that remotely sensed images are important and essential in the estimation and prediction of crop yield even before or after they have been harvested for an informed decision making.

5.1.6 Standardised Precipitation Evapotranspiration Index (SPEI)

The SPEI dataset is usually updated during the first days of the coming month based on the most genuine and updated climatic data source. The mean temperature data is acquired from the gridded dataset of NOAA NCEP CPC GHCN_CAMS, while the monthly summation of precipitation data is acquired from the first guess of the Global Precipitation Climatology Centre,

The data from the Global Precipitation Climatology Centre is usually obtained with an original resolution of 0.5 degrees interpolated to 1 degree resolution. It is characterised with a multi-scale charater and a time-scale that ranges between the first month to the fourty-eight month, with the range depicting

different types of drought that can be meteorological, hydrological, agricultural and et cetera.

The SPEI is based on the thornthwaite equation for the estimation of potential evapotranspiration (PET). It is an index best suited for drought monitoring and early warning purposes because it put into consideration the increase in tempearture and the associated decrease in precipitation over the years. This is quite different with other drought index like the SPI, SWI, and MSDI.

Since the methodology encompass the use of procedures that estimate the potential evapotranspiration as a function of temperature. We expect to measure the the relationship between the drastic increase in temperature and the gradual decrease in precipitation using the SPEI, because it does not require many parameters for its computation and only based on air temperature.

The SPEI data were obtained within the SRRB to anlyse the drought pattern at four observation points, i.e. SPEI_1 (meteorological drought) and SPEI_48 (hydrological drought) were sampled out, then 5 month for each year from 1950 to 2018 when Fadama farming is carried out within the SRRB was estimated using the thornwaite method to assess the extend of the drought.

The data obtained from the SPEI were analysed at different scale to assess the drought condtion of the SRRB. The SPEI will show a continuous drought if the values are negative i.e. -1 or less, and stops when the values changes to positive. When the index show values between ±1 and ±1.49 the drought is moderately dry for all negative values and somewhat wet for positive numbers. When the value depicts between ±1.5 and ±2, it shows a much dry period or very wet period for both numbers respectively. When the value is greater than or equal to 2 and less than or equal to -2, the period is usually extremely wet or extremely dry state respectively. Thus, the meteorological drought (SPEI_1) shows high frequency of the meteorological drought at the four observatories. While the SPEI_48 indicates a long term moderate dry spell with few wet season (**Figure 5-7**).

Overall, from the year 1950 to 2018 at the four observation points within the SRRB, it depicts a moderate dryer spell in spite few wet season. As observed from the apparent fluctuation of the dataset, it suggests that the pattern is negative in recent years and depicts that the catchment of the basin if affected by moderate meteorological and hydrolocal drought.

From the SPEI data as shown in chapter 4 of this research, it shows a moderate variation in the drought conditions with a gentle decline despite few wet season from the year 1950 to 2018. As such, integrating this data with the dam's behaviour as shown using the global surface water explorer (**Figure 5-7**), the moderate drought is eminent. But has no much effect on the Fadama farming system if compared with the yield data obatained in chapter 2, and the remotely sensed data in chapter 3 because the Fadama irrigation is improving as the year progresses.

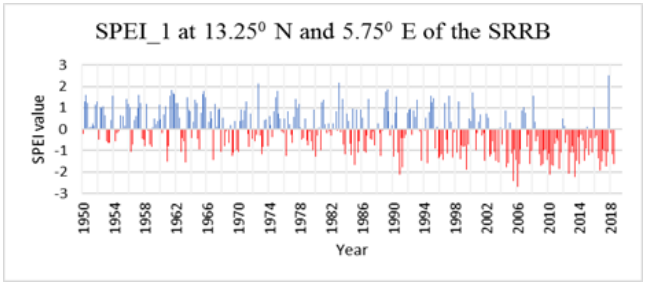

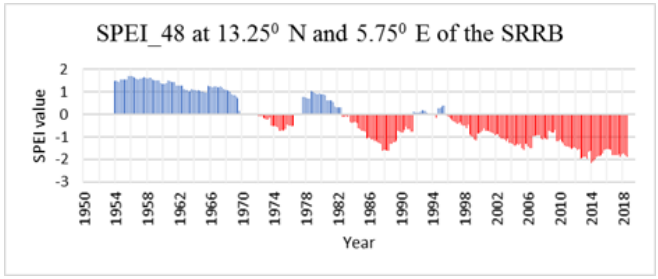

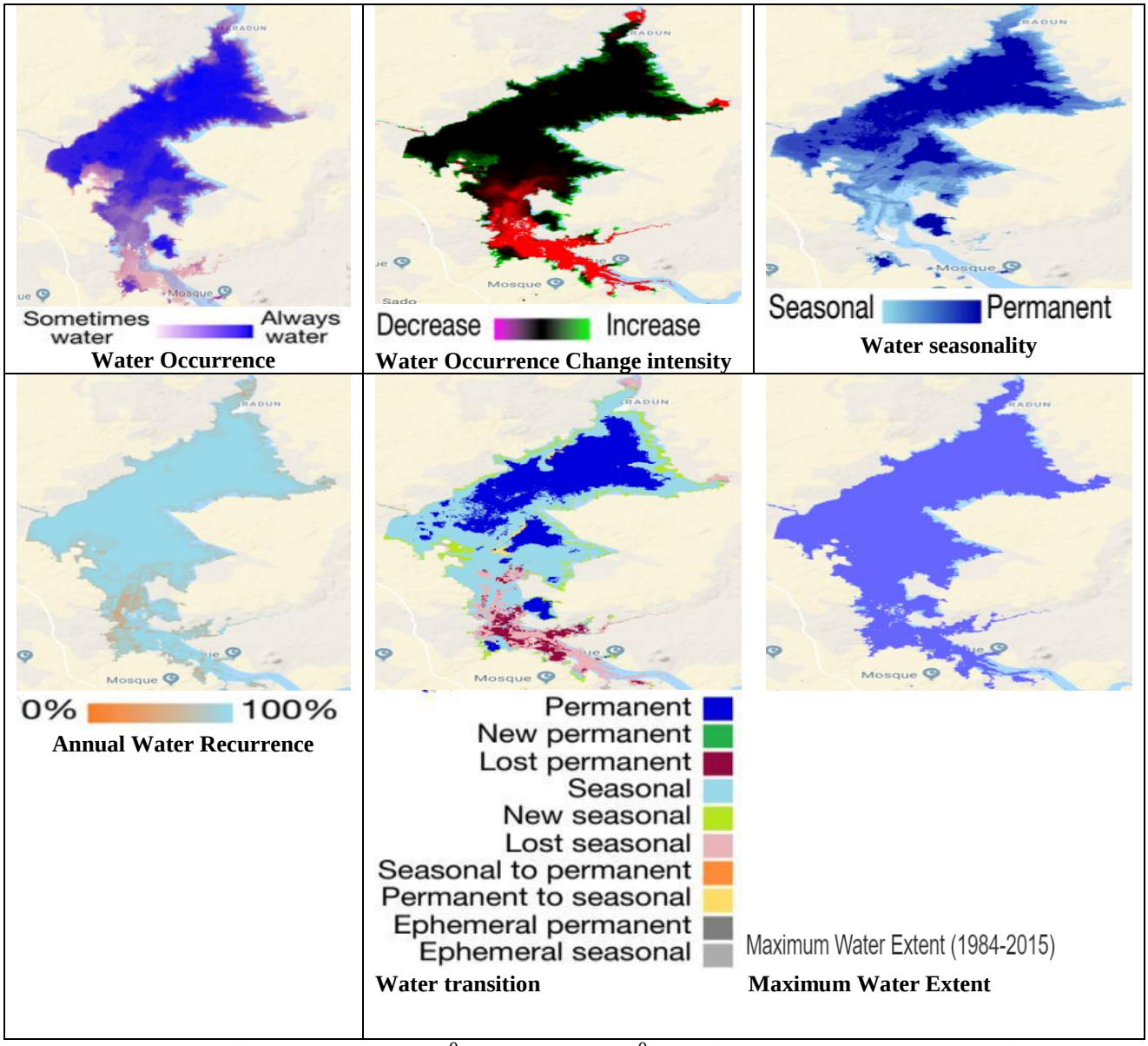

Figure 5-7: SPEI data at Lat. 13.25^0 N Long. 5.75^0 E, showing a consistent moderate meteorological and hydrological drought pattern with few wet season from 1.52 in 1954 to -1.65 in 1988 & to -1.67 in 2018, this in turn affects the Bakolori dam surface water dynamics in terms of the water occurrence, the occurrence change intensity, the seasonality, the recurrence, and how the water is transitioning over 32 years from 1984-2015. While at the latter, the maximum water extent ever occupied by the dam is depicted and this will explain how the changes are occurring using other physical parameters of the dam as afore-stated.

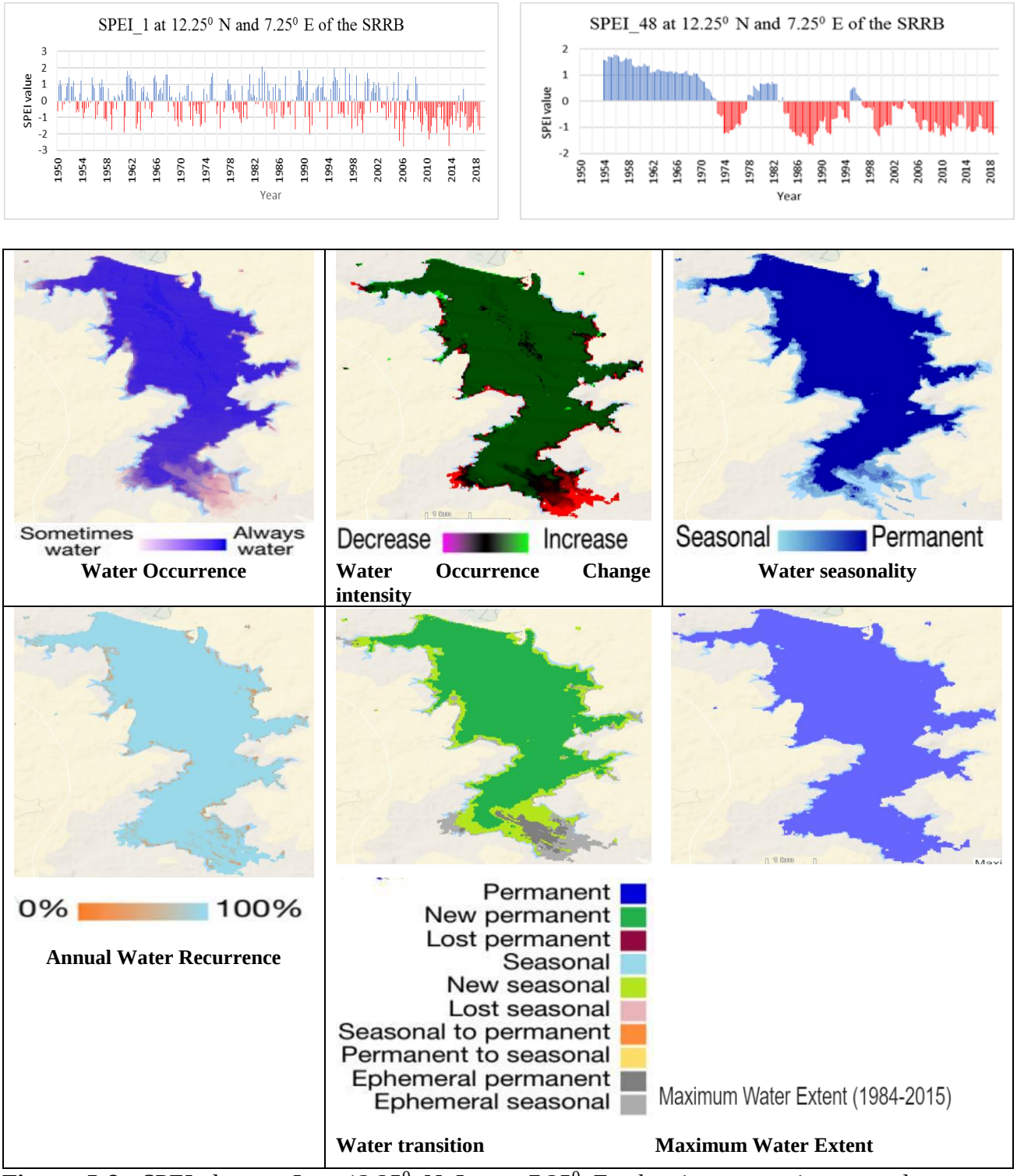

Figure 5-8: SPEI data at Lat. 12.25^0 N Long. 7.25^0 E, showing a consistent moderate meteorological and hydrological drought pattern from 1.59 in 1954 to -1.70 in 1988 & to -1.30 in 2018, this in turn affects the Jibia dam surface water dynamics in terms of the water occurrence, the occurrence change intensity, the seasonality, the recurrence, and how the water is transitioning over 32 years from 1984-2015. While at the latter, the maximum water extent ever occupied by the dam is depicted and this will explain how the changes are occurring using other physical parameters of the dam as afore-stated.

5.1.7 Global Surface Water Explorer (GSWE)

Global Surface Water Explorer was developed by the the Eurpean Commission's Joint Research Centre. It maps precise locations and the temporal distribution of water datasets by providing the statistics, the extent and changes on those water surfaces.

The freely available tool for global water exploration, utilises the Landsat data that upgrades the modelling of surface forces, show proofs of the state and the rate of change on water bodies. As such, the global water dynamics was acquired from the coarse spatial resolution satellite observation from the Landsat data, while the seasonal maps was generated from Landsat satellite images with an annual temporal scale using the entire multi-temporal and orthorectified archives of Landsat 5, 7, and 8, for the past 32 years to map out the spatiotemporal variability of global surface water and its long-term change.

With the global consistency and a validated dataset, the impact of climate oscillation on surface water can be quantified, and the evidence can be gathered to display how water is influenced by human action using the GSWE. Although only the physical parameter of the specified water body can be displayed since the data is not readily available for download.

Water loss is experienced in all global water bodies associated to drought and human activities. Therefore, this research assessed the physical parameter of the major dams within the SRRB, through long-term water history that showed thematic products of surface water dynamics stored in different facet.

Where and when we can find water on the earth's surface is essential for well-informed surface water observations. In this research, water is crucial and central to the irrigation farming system. As such, the dams behaviour over the years were observed in the GSWE by clicking a point to acquire the geographical coordinate and to generate the extract from the global product for each of the selected dam, but only the physical change was assessed.

From the Global Surface Water Explorer dataset, the following were used to assess for each of the selected dam at Bakolori, Goronyo, Jibia, Wurno, and Zobe dams to investigate the parameters over the years. (1): Surface water occurrence, (SWO) was used to observe the pattern where the dam was once occupied with water and later diminished. (2): Water occurrence change intensity from 1984 to 1999 and 2000-2015 was as well used to derive a homologous pair of months that have same months with valid observation. (3): Water seasonality assessed the understanding that areas under water coverage are called permanent, while surfaces with water for less than 12 months are called seasonal. (4): Annual water recurrence measures the degree of inter-annual variability on water presence and further describes how frequent water returns from one year to another in percentage. (5): Water transition uses a thematic map and the temporal profile to identify set of water classes that give an attribute to the change between the first and the last year in which representative observations were gotten. (6): Monthly water history detects the information on all the water datasets on a monthly basis from March 1984 to October 2015. It shows when a particular event occurs, for example when a dam is constructed can be known using this tool. (7): Yearly water history gives the information on the seasonality of water over the 32 years observation. It contains information similar to the seasonality dataset but only covers the years where observations are available from 1984 to 2015.

The dams' physical parameters were quantified to assess the influence of climate oscillation and manmade activities. If the datasets are compared with the climate data as shown in chapter 4 of this research, the moderate drought is apparent (**Figure 5-9**), depicting that the associated rise in temperature despite fewer wet season has influence on the dams' behavior in terms of the water occurrence, occurrence change intensity, the water seasonality, annual water occurrence, water transition, monthly water history, and the yearly water history within SRRB, refer to the figures below.

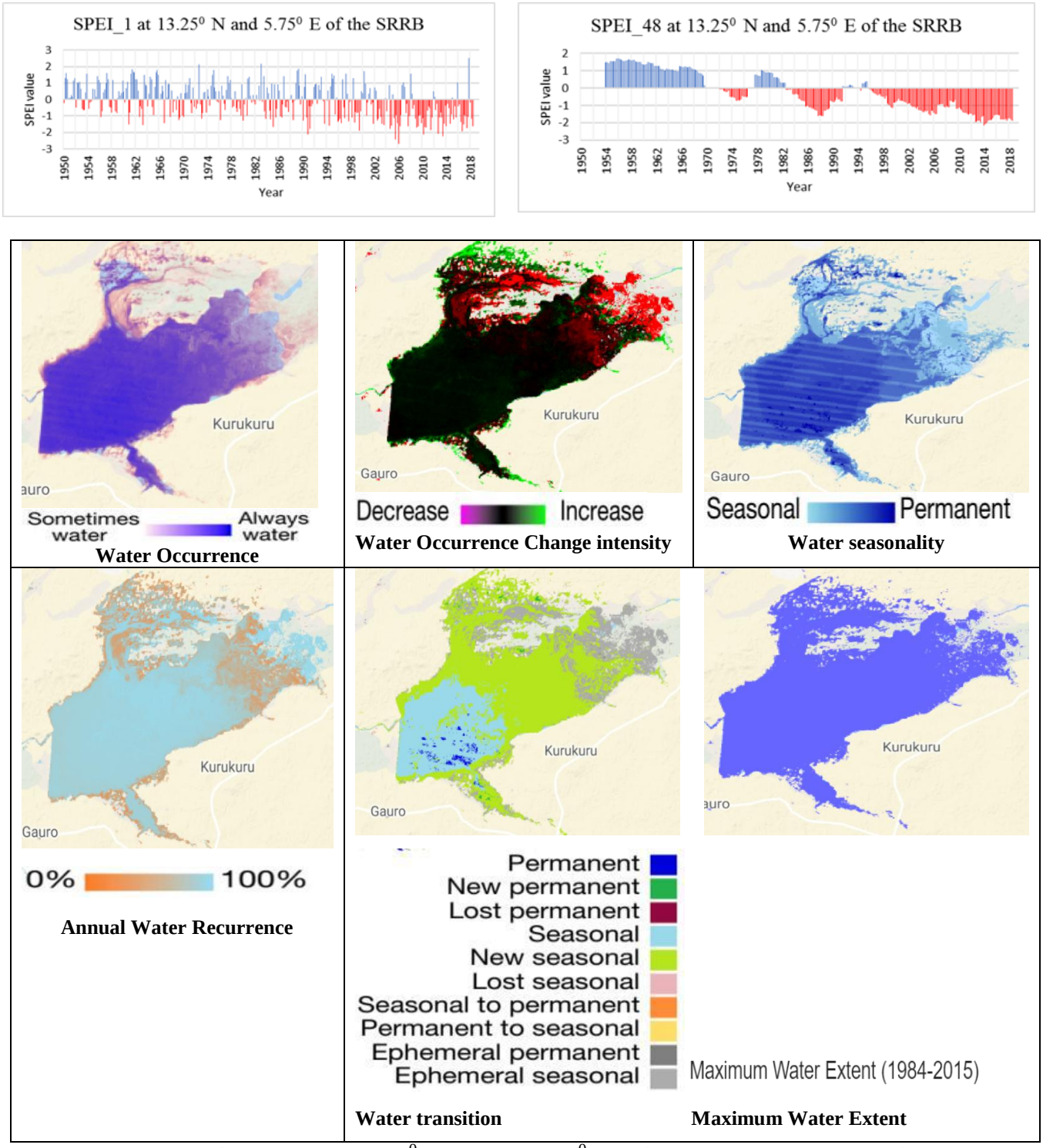

Figure 5-9: SPEI data at Lat. 13.25^0 N Long. 5.75^0 E, showing a recurring moderate meteorological and hydrological drought pattern from 1.52 in 1954 to -1.65 in 1988 & to -1.67 in 2018, this in turn affects the Goronyo dam surface water dynamics in terms of the water occurrence, the occurrence change intensity, the seasonality, the recurrence, and how the water is transitioning over 32 years from 1984-2015. While at the latter, the maximum water extent ever occupied by the dam is depicted and this will explain how the changes are occurring using other physical parameters of the dam as afore-stated.

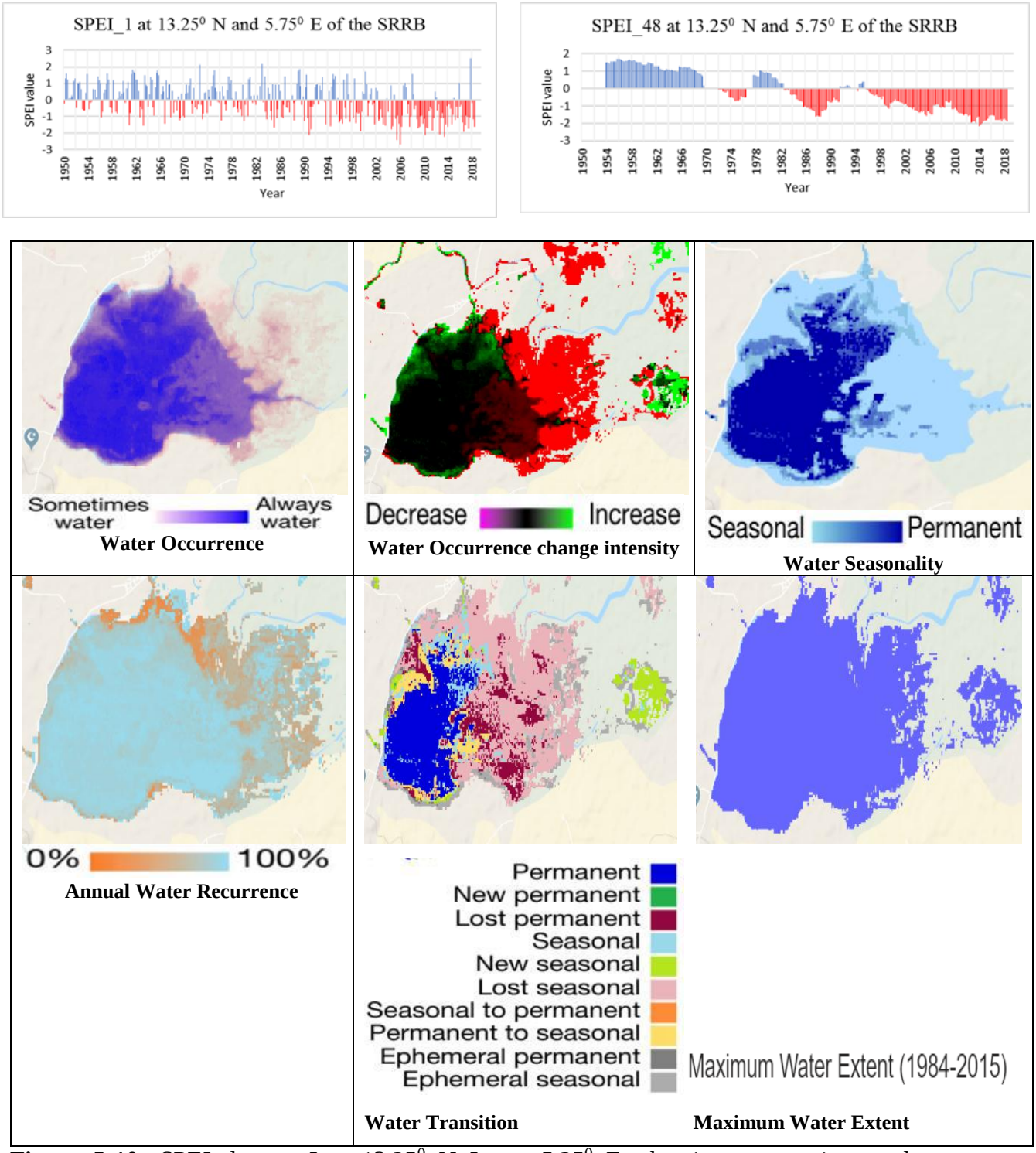

Figure 5-10: SPEI data at Lat. 13.25^0 N Long. 5.25^0 E, showing a recurring moderate hydrological and meteorological drought pattern from 1.49 in 1954 to -1.63 in 1988 & to -1.89 in 2018, this in turn affects the Wurno dam surface water dynamics in terms of the water occurrence, the occurrence change intensity, the seasonality, the recurrence, and how the water is transitioning over 32 years from 1984-2015. While at the latter, the maximum water extent ever occupied by the dam is depicted, and this will explain how the changes are occurring using other physical parameters of the dam as afore-stated.

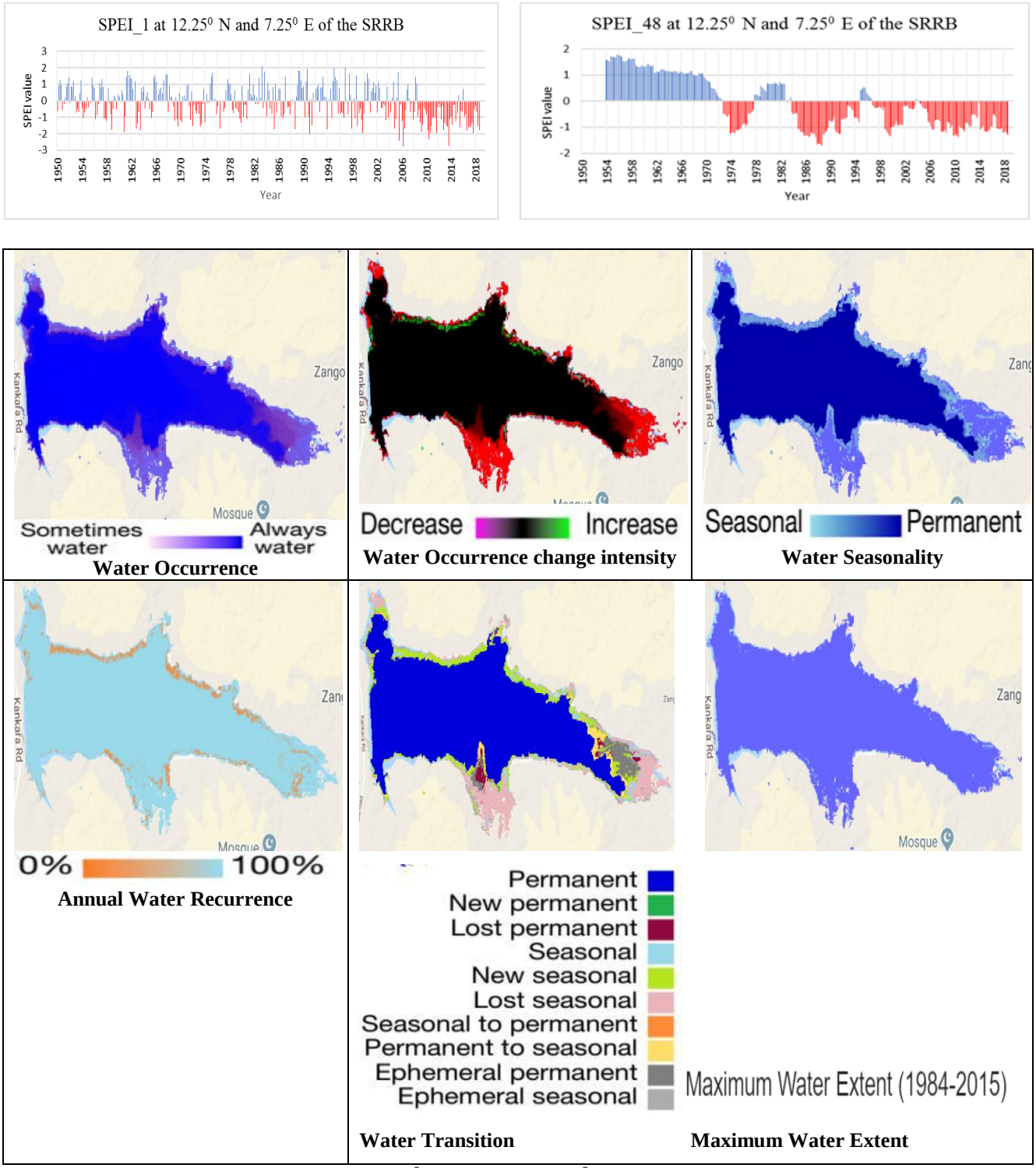

Figure 5-11: SPEI data at Lat. 12.25^0 N Long. 7.25^0 E, showing a recurring moderate meteorological and hydrological drought pattern from 1.59 in 1954 to -1.70 in 1988 & to -1.30 in 2018, this in turn affects the Zobe dam surface water dynamics in terms of the water occurrence, the occurrence change intensity, the seasonality, the recurrence, and how the water is transitioning over 32 years from 1984-2015. While at the latter, the maximum water extent ever occupied by the dam is depicted and this will explain to how the changes are occurring using other physical parameters of the dam as afore-stated.

Overall, if the data is compared with the yield data in chapter 2 and the remote sensing data in chapter 3, the change in surface water dynamics of the river basin has no much effect on the irrigation farming braced by possible adaptation strategies. Although if the full potential of the river basin is to be harnessed in terms of the planned irrigable area, the basin may run short of water in the advent of the drought, while on one hand, with possible water management strategies the issues can still be mollified since the drought is moderate.

5.1.8 Fadama irrigation system within the SRRB.

Table 5-2: Summary of results generated in this research.

Summary of Results	**Bakolori**	**Jibia**	**Goronyo**	**Wurno**	**Zobe**
Ground crop yield data from 2000 to 2005 (**Figure 2-5**).	-	-	increasing	increasing	-
Decadal trends of the Landsat Classification for *Fadama* between 1988/ 1998 and 1998/2018 at 30 m resolution. With -65% to 112% change (i.e. 47% increase), between 88-98 & 98-18 respectively (**Table 3-1/ Figure 5-12**).	*Fadama* areas are increasing	*Fadama* areas are increasing	*Fadama* areas are increasing	*Fadama* areas are increasing	*Fadama* areas are increasing
Decadal trends from Landsat NDVI *Fadama* at 30 m Resolution (**Figure 3-5**).	*Fadama* Farming is increasing	*Fadama* Farming is increasing	*Fadama* Farming is increasing	*Fadama* Farming is increasing	*Fadama* Farming is increasing
Cloud based classification using Google Earth Engine at 30 m Resolution For *Fadama* areas in 2018 (**Figure 3-8**).	*Fadama* Farming is Increasing by 47%	*Fadama* Farming is Increasing by 47%	*Fadama* Farming is Increasing by 47%	*Fadama* Farming is Increasing by 47%	*Fadama* Farming is Increasing by 47%
Google Earth Engine (GEE) NDVI time series data at 30 m resolution by masking on areas within the *Fadama* from 1984 to 2018 **(Figure 3-11**,**Figure** 3-15 **and Figure** 5-6).	Increasing From-0.02 In Oct. 1988 to 0.20 in Feb. 2017	Increasing From 0.06 In Nov 1988 to 0.23 in Mar. 2018	Increasing From 0.05 In Dec. 1988 to 0.18 in Mar. 2017	Increasing From 0.078 In Nov 1988 to 0.33 in Jan. 2017	Increasing From -0.5 In Nov. 1988 to 0.22 in Nov. 2018

The Pekko NDVI time series data from Global Agric. Monitoring with 250 m spatial resolution **(**Figure 3-20) at 1.5 km for Jibia and Zobe *Fadama* areas, and 2 km for Bakolori, Goronyo and Wurno *Fadama* Areas from 2000 to 2019.	Increasing From 61 in (2000) to 62 in (2019)	Increasing From 62 in (2000) to 67 in (2019)	Increasing From 60 in (2000) to 63 in (2019)	Increasing From 62 in (2000) to 64 in (2019)	Increasing From 60 in (2000) to 63 in (2019)
Climate History from SPEI data for drought pattern from 1950-2018 **(Figure 4-2 (a, b)**) at SPEI_1 (Meteorological drought) & SPEI_48 (hydrological drought)	Moderate From 1.52 Jan. 1954 to -1.65 in Mar 1988 and To -1.67 in 2018	Moderate From 1.59 Jan. 1954 to -1.70 in Mar 1988 and to -1.30 in 2018	Moderate From 1.52 Jan. 1954 to -1.65 in Mar 1988 and to -1.67 in 2018	Moderate From 1.49 Jan. 1954 to -1.63 in Mar. 198 and to -1.80 in 2018	Moderate From 1.59 Jan. 1954 to -1.70 in Mar 1988 and to -1.30 in 2018
Water data from Global Surface Water Explorer for 32 years from 1984 to 2015 (**Figure 4-8** and **Figure 5-7**), with dam Size decreasing drastically.	Changes occurred due to moderate drought	Changes occurred due to moderate drought	Changes occurred due moderate drought	Changes occurred due to moderate drought	Changes occurred due to moderate drought
Climate Prediction based on climate Change: Temperature Rainfall Moderate Drought	 Increasing Decreasing Increasing	 Increasing Decreasing Increasing	 Increasing Decreasing Increasing	 Increasing Decreasing Increasing	 Increasing Decreasing Increasing

Fadama farming in the Sokoto Rima River Basin, was observed using various drivers to ascertain its utilization and possible ways to brace the entire process for good policy implementation, and informed decision making within the entire basin and beyond.

From the ground yield data observed in chapter 2, the yield of crops saw an increase in tonnage of the harvested crops through the investigated years from 2000 to 2005. This is depicting that the Fadama irrigation system is improving, because, if this is related to the remotely sensed data of the previous epoch juxtaposed to the

present years. The less utilization of -65% of the Fadama land was obviously observed from 1988 to 1998. As such, from the remote sensing perspective, the Fadama irrigation was observed to be increasing by 112% in recent years from 1998 to 2018 (**Table 3-1**). That is to say, the difference between the previous epoch and the present one saw an increase of 47% see (**Figure 5-12**).

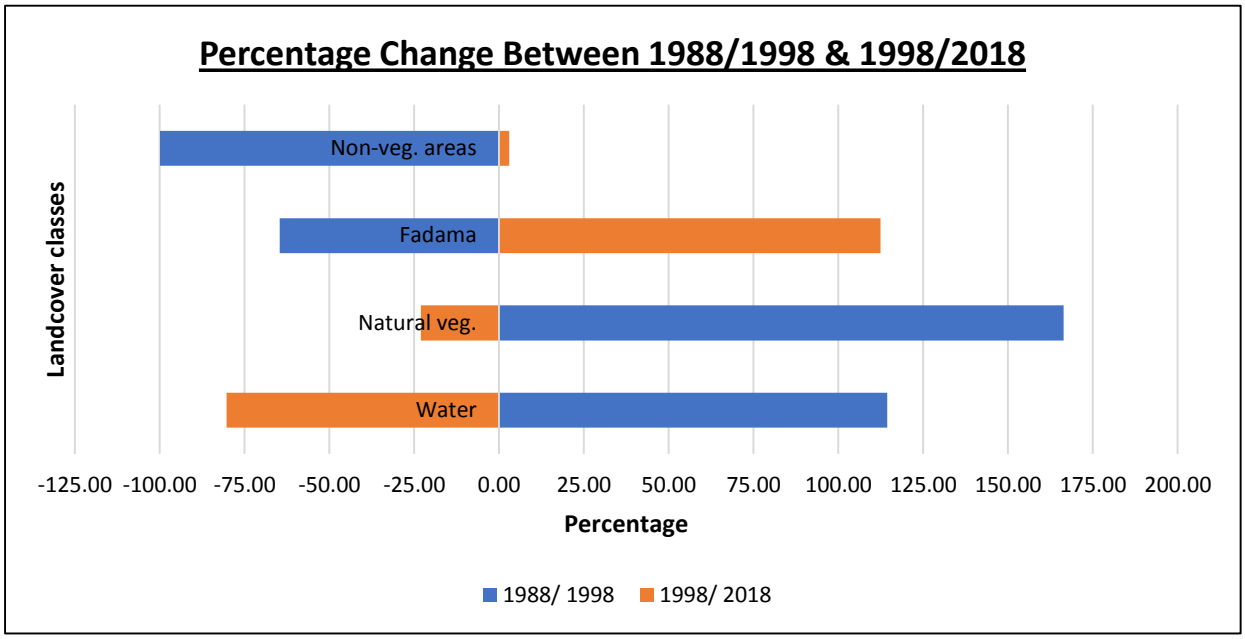

Figure 5-12: **Graph showing the percentage change over a decadal trend of the Land cover classification between 1988/1998 and 1998/2018.** Non-vegetated areas are -100% in the previous epoch, while in recent time, areas that have no vegetation have increased by about 3%. *Fadama* farming declined between 1988 to 1998 with about -65%, while between 1998 to 2018, the *Fadama* farming improved with over 112%, i.e. 47% of the *fadama* areas were put into cultivation in recent years. Natural vegetation appears to be positive with over 166% in the past decade, while in recent time, it has declined with about -23%. lastly, areas covered by water in the dam was having 114% between 1988 to 1998, while between 1998 to 2018, there is a sharp decline with about -80%. Which if this is correlated with the SPEI data and Global Surface Water Explorer data, there is a perfect relationship between the datasets.

However, despite the moderate meteorological and hydrological drought observed using the SPEI data, possible adaptation strategies are supporting the irrigation system since the Fadama farming is increasing. This clearly indicates that the irrigation is not hindered by the phenological constraints and the short duration or early cessation of precipitation as observed using the climate data.

In conclusion, in order to overcome Nigeria's crop yield-gap, series of dams were constructed in the Sokoto Rima River Basin (SRRB) of northern Nigeria.

These dams include (Bakolori, Jibia, Goronyo, Wurno, & Zobe) constructed between 1965-1989 **Table 1-2,** as a means to facilitate *Fadama* irrigation particularly during the dry season between November and March in the basin. With an area covering approximately 13,160,000 ha or 131600 km^2. It was observed that these infrastures are not fully utilized because, the planned irrigation of 105,472 ha and the operated irrigation of 39,907 ha have a clear disparity as shown in **Table 1-2**. This thesis initially aimed to examine this assertion through official yield data as well as field visits during the dry season of 2018 see (**Figure 5-13**). But due to limited ground yield data, only a short period was observed. The yield data for the basin is not only covering a short time span from 2000-2005 but also are directly attributable to smaller specific locations within the large basin. This established the growing of a number of crops such as rice, millet, sorghum, maize, potatoes, onions among other crops. The data also suggests that several hundred thousand tons can be harvested but the data also indicates significant inter-annual variability in yield production.

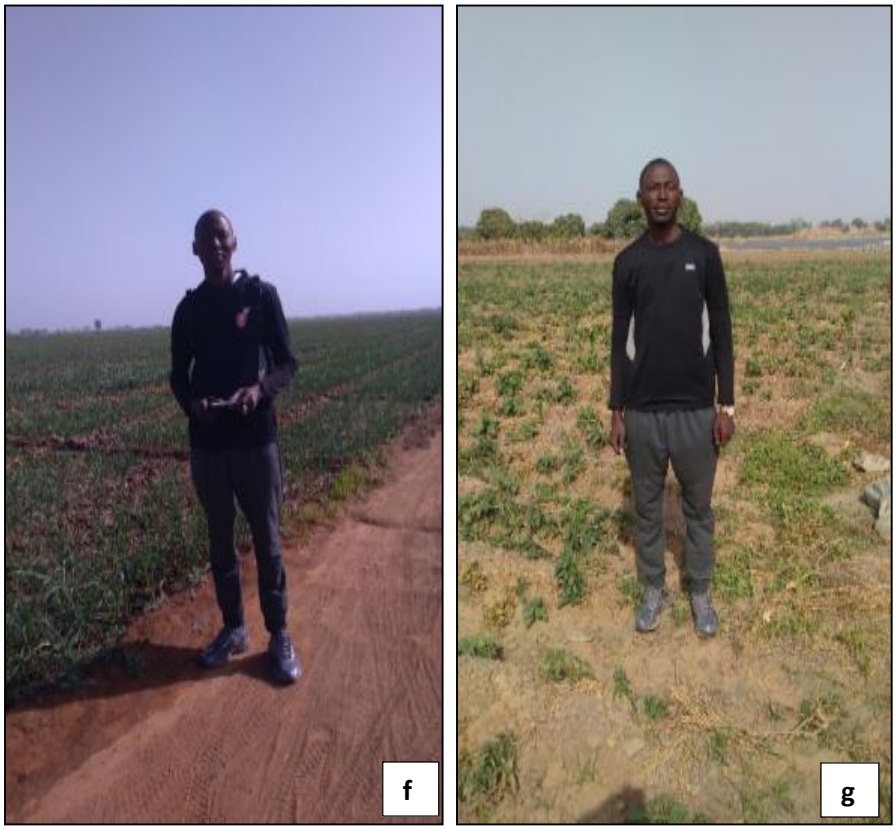

Figure 5-13 (a-g): Pictures taken together with field assistants at different locations within the Sokoto Rima River Basin at Jibia, Goronyo, and Bakolori *Fadama* sites during the January 2018 field visit.

Given the lack of official data it was necessary to resort to remotely sensed time series in line with the yield data period of 2000-2005 and beyond using MODIS data **Figure 3-20,** while from 1984-2018 using GEE Landsat data **Figure 3-15**. Unfortunately, the Landsat 7 data for the early 2000 period was available but with instrumentation problems of the scan line correction error and did not allow for much yield data verification from 2003. Albeit, the examination of the dry season Landsat data classifications at decadal interval including 1988, 1998 and 2018 was done. Two separate image classifications were utilized deploying both computer based image classification techniques and cloud based Google Earth Engine techniques at both the regional catchments scale and also the detailed dam level **Figure 3-2** and **Figure 5-5.** These classifications while different for the following reasons such as: GEE is a cloud based computation that does not require data download and is a tile by tile image analysis with the comparative ease of use. While the computer based image classification require image download and further image radiometric corrections before image classification can be done.

Both classifications demonstrated the longer-term presence and changes in *Fadama* usage such as decrease and increase of cultivated areas in hectares between the decadal trend as shown in **Table 3-1**. The 2018 image classifications were also compared and validated against observation collected during the field visit **Figure 5-13,** from which we learned the following; improved *Fadama* utilization in terms of an increase in the areas cultivated, decrease in natural vegetation, and increase in the non-vegetated areas which is caused by deforestation and urban expansion, while water bodies have decreased drastically Error! Reference source not found.**.** A brief comparison with the local climate r ecord by drawing on the global SPEI index was able to determine the observed recurring moderate meteorological and hydrological drought with the Landsat changes in relation to natural vegetation cover and as well associated dam levels observed with the Global Surface Water Explorer (GSWE), though this has no much effect on *Fadama* areas.

Based on the lack of well-informed ground yield data records as stated earlier, it was deemed necessary to examine *Fadama* usage using a MODIS NDVI product at the 5 dam locations within the (SRRB) to ascertain the yield pattern. The MODIS data, while at a lower spatial resolution (250 m) and 8 days temporal resolution between 2000 to 2018 **Figure 3-20,** compared with the Landsat record was able to detect season long term cycles from 1984-2018 with a temporal resolution of 16 days and spatial resolution of 30 m **Figure 3-15** and **Figure 5-1**. The NDVI extraction was carefully guided by the established extend of *Fadama* as observed in the Landsat record. This established a strong seasonal vegetation cycle but also showed differing but subtle trends in the dry season *Fadama* usage such as a continuous trend of the vegetation index with smaller crest (*Fadama* vegetation) in between the higher crest (i.e. wet season vegetation). As such, this indicates that even within the wet season, some of the *Fadama* areas are still cultivated. The MODIS dry season record was compared with the 2018 Landsat classification which confirmed the presence of dry season crops, also was compared against the SPEI climate record from 1950 to 2018 which shows

recurring moderate meteorological and hydrological drought but has lesser effect on the *Fadama* cultivation in recent years.

The long-term climate record can be interrogated in a number of ways. It broadly suggests that there has been a long-term drying trend in line with the rest of the sahel region as well as significant inter-annual variability. When compared against the coarse but longer decadal dry season record in Landsat, we establish the following: from the year 2012 onward, there is strategic increase in terms of the NDVI values obtained which is an indication that from 1984 to 2011 though with data break from 2003 due to scan line correction error, the *Fadama* farming is not as it is between 2012 to 2018. When comparing this against the shorter but much more temporally detailed MODIS record from 2000-2018. We can see the following: we can observe a continuous trend of the vegetation index without any data gap which can serve as substitute to GEE NDVI Landsat data from 2000 onward, because this will give a more defined and well informed dry season trend that can be used to derive any change between this time frame. Hence, when comparing the SPEI record against the MODIS record and the dam level trends from the global surface water explorer dataset; we are able to see the following: recurring moderate meteorological and hydrological drought between 1950 to 2018, but with improved dry season *Fadama* farming due to certain adaptation methods and as well pushing factors because the government is trying everything possible to enhance the irrigation system. Overall, with these observations, this research will recommend a sustainable management of the basin with regard to *Fadama* usage, water management, and the so-called yield gap specific to *Fadama* farming in northern Nigeria, in line with possible ways to adapt to the dry spells. While to be specific to Jibia, and Zobe *Fadama* site, government's intervention is profoundly needed to enhance the farming system because they are the least utilized in the basin.

5.2 Recommendation

1- From the observed remotely sensed data and the NDVI data, the *Fadama* farming system within the basin is improving. Therefore, more in-depth ground yield data is needed to actually make precisions juxtaposed to the NDVI values obtained. As such, this research will further recommend for the government and the Sokoto Rima River Basin Development Authority to enhance crop yield data collection in the field, so that future research will delve more into synergizing this data with remote sensing for effective management of the entire basin and its resources.

2- Initially, the whole basin was considered for this research, but due to large computational algorithm and time out errors experienced, a nesting and scaling was done and only a part within the basin was examined. Hence, other areas need to be examined within the basin to be precise with the lower part of the basin where the basin makes a confluence with the Niger river in Kebbi state.

3- The Sokoto Rima floodplain has a vast arable land resource that if fully utilized, it can feed not just the region but Nigeria as a whole. Therefore, the government and the agency involved should checkmate the way fertilizer and other incentives are distributed to the farmers. This is because, from the conversation I had with the farmers in the field, they highlighted that even when the government is distributing this fertilizer with a target to reach the farmers at an affordable rate, some individuals intercept everything by hoarding it to sell it to the peasant farmer at an exorbitant rate.

4- Proximity to market and quick access to sell farm produce is one among the challenges farmers face after their harvest. As such, the government should try everything possible to enhance a conduit to which farmers can trade their harvested crops to the market without much hitches or improve storage facilities on one hand. Because this will encourage the farmers to produce more and to meet with up with the thriving population, while self-sufficiency

in food will be redressed rather than depending on imported food into the country since the country has the resource to achieve this target.

5- In areas like the Zobe dam and Jibia dam *Fadama* site respectively, the Sokoto Rima River Basin Development Authority should in conjunction with federal government, do something to make a facelift to the irrigation scheme. This is because, from my field visit and the observed data from remote sensing, a huge amount of money was observed to be invested in infrastructures and yet left without achieving the main aim of their establishment, which am sure farmers will be willing to do more if the process is incentivized.

References

Abd El-Kawy, O.R., (2011): Land Use and Land Cover Change Detection in the Western Nile Delta of Egypt Using Remote Sensing Data, *Applied Geography*. 31(2): 483-494.

Abdullah, F.A., & Lalit K., (2013): Investigating the Use of Remote Sensing and GIS Techniques to Detect Land Use and Land Cover Change. *Advances in Remote Sensing.* 2(2): 193-204.

Abdullahi, S.A., (2011): Assessment on the Impact of Climate Change on Water Resources Availability in the Sokoto Rima River Basin.PhD thesis Ahmadu Bello University Zaria, Nigeria. 4(5): 220-233.

Adams, W.M., (1993): Development's deaf ear: Downstream users and water releases from the Bakolori Dam, Nigeria. *World Development.* 21(9): 1405–1416.

Adams, W.M., (2000): *Downstream Impacts of Dams.* Thematic Review I.1. World Commission on Dams.

Adams, W.M., (2001): *Green development: environment and sustainability in the Third World.* Routledge. New York, ISBN 0-415-14766-2.Pp. 231.

Adams, W.M., (1983): *Downstream impact of river control, Sokoto Valley, Nigeria.* Unpublished PhD Dissertation, University of Cambridge.

Adams, W.M., (1985): *The downstream impacts of dam construction: a case study from the Sokoto valley Nigeria.* Transaction of the Institute of British Geographical. NS (New Series). 10(3): 292.

Adams, W.M. (1986): Traditional Agriculture and Water Use in the Sokoto Valley, Nigeria, *The Royal Geographical Society (with the Institute of British Geographers).* 152(1): 30-40.

Adefolalu, D.O., (1986): Rainfall trends in Nigeria. Theoretical Applied Climatology. *Springer.* 37(4):205–219.

Adejuwon, J.O., (2004): *Crop yield response to climate variability in the Sudano- Sahelian ecological zones of Nigeria in Southwestern Nigeria*. In AIACC Report of Workshop for Africa and Indian Ocean Island. Dakar, Senegal. Pp.15-16.

Adejuwon, J.O., & Odekunle TO., (2006): Variability and the Severity of the "little Dry Season" in southwestern Nigeria. *American Meteorological Society.* 19(3): 483-493.

Adelana, S.M., Olasehinde, P.I., & Vrbka, P., (2003): Isotope and geochemical characterization of surface and subsurface waters in the semi-arid Sokoto Basin, Nigeria. *African Journal of Science and Technology*. 4(2): 80-89.

Adeniyi, P.O., & Ornojola, A. (1999): Landuse and landcover change evaluation in Sokoto- Rima Basin of North - West Nigeria, based on Archival Remote Sensing and G1S Techniques. *Journal of Environment and Earth Science.* 4(5): 119-127.

Akané, H., & Jürgen S., (2005); *Bakolori Dam and Bakolori Irrigation Project – Sokoto River, Nigeria(PDF*). Eawag aquatic research institute. 2010-01-10.

Akumaga U., Tarhule A., Piani C., Traore B., Yusuf A. A. (2018): Utilizing process-based modeling to assess the impact of climate change on crop yields and adaptation options in the Niger River Basin, West Africa. *Agronomy.* Pp 2-19

Aondover, T., & Ming-Ko, W., (1998): Changes in rainfall characteristics of Northern Nigeria. *International Journal Climatology.* 18(11): 23-86.

Anderson, J.R., Hardy, E.T., Roach, J.T., & Witmer, R.E., (1976): *A land use and land cover classification system for use with remote sensor data.* U.S. Geology Survey professional Paper. U.S. Government Printing Office, Washington, DC. 964: 3-28.

Anyadike, R.C.N., (1993): Seasonal and annual rainfall variations over Nigeria. International *Journal of Climatology,* 13: 567-580.

Anyanwole, K.C., (2007): Climate Dynamics of the Tropics (*KAP: Dordrecht*), Pp.488.

Ardo, H.J., (2004): *Natural Resource Management and Conflict Among Fadama Communities*, Paper presented at the Workshopon Environmental Governance and Consensus Building for Sustainable Natural Resource Management in Nigeria. Kaduna Nigeria Pp. 16.

Assadollahi, H., (1975): Characterizing drought in the south of France using the standardized precipitation-evapotranspiration index SPEI.Conference: *The 7th International Conference On Unsaturated Soils*– UNSAT.Hong Kong, (August 2018), China.

Annual Abstract of Statistics (2012, 2017): Yearly annual statistics. National Bureau of Statistics (NBS) Abuja, Nigeria.

Ayuba, H.K., Maryah U.M., & Gwary D.M., (2007): Climate Change Impact onPlant Species Composition in sixsemi-arid rangelands of NorthernNigeria, *Nigerian Geographical Journal*. 5: 35-42.

Baba, M.K., (1993): Irrigation Development Strategies in sub-Saharan Africa: A comparative study of traditional and modern irrigation system in Bauchi State, Nigeria. *Ecosystem and Environment*. 45: 47-58.

Baez-Gonzalez, A.D., Chen, P., Tiscareno-Lopez, M., & Srinivasan, R., (2002): Using satelliteand field data with crop growth modeling to monitor and estimate corn yield inMexico. *Crop Science.* 42(6): 1943-1949.

Becker-Reshef, I., Justice, C., Sullivan, M., Vermote, E., Tucker, C., Anyamba A., Small, J., Pak, E., et al., (2010): Monitoring global croplands with coarse resolution earth observations: The global agriculture monitoring (GLAM) project. *Remote Sensing.* 2(6): 1589-1609.

Butt, A., Shabbir, R., Ahmad, S.S., & Aziz, N., (2015): Land use change mapping and analysisusing Remote Sensing and GIS: A case study of Simly watershed, Islamabad, Pakistan.Egypt. *Journal of Remote Sensing and Space Science.* 18(2): 251-259.

Briffa K.R., Sheffield J., (2014): Global warming and changes in drought. *National climate change.* 4:17-22

Chen, S., & Rao, P., (2008): Land degradation monitoring using multi-temporal Landsat TM/ETM data in a zone between grassland and cropland of northeast China. *International Journal of Remote Sensing.* 29(7): 2055-2073.

Carlson, T., (2003): Applications of remote sensing to urban problems. *Remote Sensing of Environment.* 86(3): 273–274.

Climate Engine, (2016): *Desert Research Institute, University of Idaho*. Available:http://climateengine.org (accessed July 2016).

Cossu, R., Petitdidier, M., Linford, J., Badoux, V., Fusco, L., Gotab, B., Hluchy, L., Lecca, G., et al., (2010): Aroadmap for a dedicated earth science grid platform. *Earth ScienceInformatics.* 3(3): 135-148.

Collect Earth, (2016): United Nations Food and Agriculture Organization.Available: http://www.openforis.org/tools/collect-earth.html.

Cox, A., & Akin, N.,(1979): *Agricultural Ecology: An Analysis of World Food Production*. Freeman Press: San Francisco.

Cracknell, A.P., (1997): The Advanced Very High Resolution Radiometer. London, Bristol; *Taylor & Francis*. 134(6): 877-883.

Cracknell, A.P., (2001): The exciting and totally unanticipated success of the AVHRR in applications for which it was never intended. *Advances in Space Research*. 28(1): 233-240.

Dan-Azumi, J., (2010): *Agricultural sustainability of Smallholder Floodplain Agricultural Systems; A Case Study of Areas in North-Central Nigeria*, PhD Thesis University College London.

Defries, R.S., & Belward, A.S., (2000): Global and regional land cover characterization from satellite data. *International Journal of Remote Sensing*. 21(6-7): 1083-1092.

De Schutter, J., (2003): *Water Resources and Environment Technical Note G.3 Wetlands Management.* Washington, D.C. US: World Bank. Pp. 15.

Diallo, Y., Hu, G., & Wen, X., (2009): Applications of remote sensing in land use/land cover change detection in Puer and Simao countries, Yunnan Province. *Journal of American Science,* 5(4): 157–166.

Dikko, A., Abdullahi, A. & Ousseini, M. (2011): Soil Fertility Assessment of The Lugu Main Canal Of Wurno Irrigation Project, Sokoto State, Nigeria, Five Years After Rehabilitation. *Nigerian Journal of Basic and Applied Sciences,* 18(2): 243–248.

Dronova, I., Gong, P., Wang, L., & Zhong, L., (2015): Mapping dynamic cover types in a largeseasonally flooded wetland using extended principal component analysis and object-based classification. *Remote Sensing of Environment*, 158: 193–206.

D'souza, G., Belward, A.S., Malingreau, J.P., & Jean P., (1996): Advances in the Use of NOAA AVHRR Data for Land Applications. *Earth Science and Geography,* Pp. 21-48.

Dong, J., Xiao, X., Menarguez, M.A., Zhang, G., & Qin, Y., (2016): Mapping paddy rice planting area in northeastern Asia with Landsat 8 images, phenology-based algorithm and Google Earth Engine. *Remote Sensingand Environment,*185: 142-154.

Duflo, E., Kremer M., &Robinson J., (2008): How high are rates of return to fertilizer? Evidence from field experiments in Kenya. *American EconomicReview*, 98:482-488.

Eastman, J.R., (2009): IDRISI Taiga guide to GIS and image processing. Clark Labs for Cartographic Technology and Geographic Analysis, Clark University, Worcester, MA 01610, USA.

Emeribe, C.N.,Uwadia, N.O., Fasipe, O.A., & Isagba, E.S., (2017): Inter-Decadal nature of rainfall character over sudano-sahel, north-west Nigeria, *African Research Review*. 11(4): 55-73.

Eniolorunda, N.B., Mashi, S.A., & Nsofor, G.N., (2017): Toward achieving a sustainable management : characterization of land use/land cover in Sokoto Rima. *Environment, Development and Sustainability, Springer Netherlands*. 19(5): 1855-1878.

En.wikipedia.org/Bakolori_Dam. Available: https://en.wikipedia.org/wiki/Bakolori_Dam

En.wikipedia.org/Goronyo_Dam. Available: https://en.wikipedia.org/wiki/Goronyo_Dam

Enplan Group, (2004): *Review of The Public Sector Irrigation in Nigeria. (Report No: 009/TF/NIR/CPA/27277-2002/TC0T)* Federal Ministry of Water Resources / UN Food & Agricultural Organization, Nigeria.

Ewuim, S.C., Zegwu, N.Y., & Anasos, H.U., (1998): *Sustainability in traditional agriculture in the tropics.* IN BADEJO, A. M. & TOGUN, A. O. (Eds.) *Strategies and Tactics of Sustainable Agriculture in the Tropics.* Oyo State, Nigeria, College Press Ltd.

Ekpoh, I.J., & Ekpenyong N. (2011): The Effects of Recent Climatic Variations on Water Yield in the Sokoto Region of Northern Nigeria. *International Journal of Business and Social Science.* 2(7): 251-256.

Ekpoh, I.J., (1999): Estimating the sensitivity of crop yields to potential climate change in north-western Nigeria.*Global Journal of Pure & Applied Science.* 5(3): 303-308.

Ekpoh, I.J., (2010): Adaptation to the Impact of Climatic Variations on Agriculture by Rural Farmers in North-Western Nigeria. *Journal of Sustainable Development*, 3(4): 194-202.

Erhabho, R.P.O., & Nwagbo, E.C., (1985): List-cost analysis of small-scale lift irrigation technology: Shadoof and pump in savannah ecological zone of Nigeria. *The NigeriaJournal of Agriculture,* 3(1-2): 18.

Ezemonye, M. N., & Emeribe, C. N. (2015). Spatial and temporal patterns of climatic change in the Sokoto-Rima River Basin, Sudano-Sahel region, Nigeria. *European Scientific Journal, 11*(26), 392–403.

FAO, (2010): *Fishery resources of Nigerian inland waters - the niger/sokoto river basin.* Food and Agriculture Organization.Rome.

FAO & IITA, (1999): *Agricultural policies for sustainable management and use of natural resources in Mrica,* FAO and IITA.

Faulkingham, R.H.,(1977): Ecological constraints and subsistence strategies: the impact of drought in a Hausa village. InDalbyD. R., Harrison-ChurchR. J., and Bezzaz F., (eds); Drought Africa. International African Institute, George.

Foody, G.M., (2008): Harshness in image classification accuracy assessment. *International Journal of Remote Sensing*, 29(11): 3137-3158.

Fox, J., Rindfuss R.R., Walsh, S.J., & Mishra, V., (2003): People and the Environment: Approaches for Linking Household and Community Surveys to Remote Sensing and GIS. Kluwer Academic Publishers. Pp. 224.

Funk, C., & Budde, M., (2009): Phenologically-tuned MODIS NDVI-based production anomaly estimates for Zimbabwe. *Remote Sensing of Environment*. 113(1): 115-125.

Gerten, D., Heinke J., Hoff H., Biemans H., Fader M., & Waha, K., (2011): Global water availability and requirements for future food production. *Journal of Hydrometeorology*, 12: 885-899

Global Forest Watch, (2014): World Resources Institute, Washington, DC. Available:http://www.globalforestwatch.org (accessed June 30, 2016).

Gong, P., (2012): Remote sensing of environmental change over China: a review. *China Science Bulletin* 57: 2793–2801.

Gonzalez, H., Halevy, A., Jensen, C.S., Langen, A., Madhavan, J., Shapeley R., & Shen, W., (2010): Google fusion tables: web-centred data management and collaboration in the cloud. ACMSIGMOD,Pp.1061–1066.

Google Earth 9.3 (2018, 2019), Sokoto rima river basin, https://www.google.com/earth/index.html

Google Earth Engine Team (2015): *Google Earth Engine: A planetary-scale geo-spatial analysis platform*, Available:http://earthengine.google.com.

Gopala, P.S., & Tian, L., (1999): In-field variability detection and yield prediction in corn using digital aerial imaging. *Transport ASAE*. 42: 1911-1920.

Gorelick, N., Hancher, M., Dixon, M., Ilyushchenko, S., Thau, David., & Moore, R., (2017): Remote Sensing of Environment Google Earth Engine : Planetary-scale geospatial analysis for everyone. *Remote Sensing of Environment*, 202: 18-27.

Griffiths, P., Kuemmerle, T., Baumann, M., Radeloff, V.C., Abrudan, I.V., Lieskovsky, C.M., Ostapowicz K., & Hostert, P., (2014): Forest disturbances, forest recovery,and changes in forest types across the Carpathian ecoregion from 1985 to 2010based on Landsat image composites. *Remote Sensing of Environment*, 151: 72–88.

Gutierrez, J.A., Seijmonsbergen, A., & Duivenvoorden, J., (2011): Optimizing land cover change detection using combined pixel-based and object-based image classification in a mountainous area in Mexico. Anais XV Simpo´sio Brasileiro de Sensoriamento Remoto - SBSR, Curitiba, PR, Brasil, 30 de abril a 05 de maio de 2011, INPE Pp. 6556.

Hansen, M.C., Potapov, P.V., Moore, R., Hancher, M., Turubanova, S.A., Turubanova, A., Thau, D., Stehman S.V., et al., (2013): High-resolution global maps of 21st-century forest cover change. *Science,* 342(6160): 850-853.

He B., Lu A., Wu J., Zhao L., Liu M., (2011): Drought hazard and spatial characteristic analysis in China. *Journal of Geographical Science*, 21:235-249.

Holben, B.N., (1986): Characteristics of maximum-value composite images from temporal AVHRR data. *International Journal of Remote Sensing,* 7(11): 1417-1434.

Housman, I., Tanpipat, V., Biswas, T., Clark, A., & Stephen, P., (2015): Monitoring Forest Change in Southeast Asia: Case Studies for USAID Lowering Emissions in Asia's Forests. RSAC-10108-RPT1. U.S. Department of Agriculture, Forest Service, Remote Sensing Applications Center, Salt Lake City.

Huang, H.,Chen, Y., Clinton, N., Wang, J., Wang, X., Liu, C., Gong, P., Yang, J., et al., (2017): Remote Sensing of Environment Mapping major land cover dynamics in Beijing using all Landsat images in Google Earth Engine, *Remote Sensing of Environment, Elsevier*. 202: 1-11.

Ijir, T. A. (1994): *The Performance of Medium Scale Jointly Managed Irrigation Schemes in Sub-Saharan Africa: A Study of the Wurno Irrigation Scheme, Nigeria*. Unpublished Doctoral Dissertation, Pp. 272.

Ikusemoran, M., (2001)*: Landuse and Landcover change detection on Kainji Lake, Nigeria: Remote Sensing and GIS Approach*. An Unpublished GISMasters Dissertation, University of Ibadan.

Ikpe, B.M., & Sawa A.D.B., (2016): Adaptation Strategies To Climate Change Among Grain Farmers in Goronyo Local Government Area of Sokoto State, (21-24 March 2016), Pp.1-13. FUTA, Nigeria.

Imager, L., (2014): The Spectral Response of the Landsat-8 Operational Land Imager,Pp. 10232–10251.

Independent, O., (2007): *Presidential candidate is not accessible.* Retrieved 2010-05-21.

International database and gallery structures available: https://structurae.net/structures/zobe-dam

International Food Policy Research Institute (IFPRI) 2009. *Climate Change: Impact on Agriculture and Costs of Adaptation*; International Food Policy Research Institute: Washington, DC, USA, pp. 1–16.

Ishaya, S., Mashi, S.A., & Ifatimehin, O.O., (2008): Application of Remote Sensing and GIS Techniques in Mapping Areas Favourable for Fadama Farming in Gwagwalada, Abuja, Nigeria. *Eurasian Journal of Sustainable Agriculture*, 2(3): 196-204.

IPCC, (2001): IPCC Special Report. The Regional Impacts of Climate Change: An Assessment of Vulnerability. Cambridge University Press, UK. Pp. 976.

IPCC (2007a): Climate Change 2007: Impacts, Adaptation, and Vulnerability. Contribution of Working Group II to the Fourth Assessment Report of the Intergovernmental Panel on Climate Change. Cambridge University Press, UK, Pp. 976.

IPCC. (2007b): Regional Climate Projections II: Climate Change 2007: The Physical Science Basis. Contribution of Working Group I to the Fourth Assessment Report of the Intergovernmental Panel on Climate Change. Cambridge University Press, Cambridge, United Kingdom.

Irin, W.A. (1999): The new humanitarian, Integrated Regional Information Network, Available: https://en.wikipedia.org/wiki/IRIN

Ita, E.O., (1993): Inland Fishery Resources of Nigeria CIFA Occasional PaperNo 20. Rome, FAO. 1993. Pp. 120.

Jamusz, R.R., (1990): Irrigation in Africa: Irrigation a viable Development Strategy. *The Geographical Journal*,156(2): 175-179.

Johansen, K., Phinn, S., & Taylor, M., (2015): Mapping woody vegetation clearing inQueensland, Australia from Landsat imagery using the Google Earth Engine. *Remote Sensing applications: Society and Environment*, 1:36-49

Joshi, A.R., Dinerstein, E., Wikramanayake, E., Anderson, M.L.,Olson, D., Jones B.S., Seidensticker J., Lumpkin S., et al.,(2016): Tracking changes and preventing loss in critical tiger habitat. *Science Advances*. 2(4): e1501675.

Kebbeh, M., HaefeleS.,& Fagade1S. O., (2003): Challenges and Opportunities for Improving Irrigated Rice Productivity in Nigeria.West Africa Rice Development Association (WARDA). Abidjan, Cote'Ivoire.

Ken, S. (1985): African Farm Labour. Cambridge: Cambridge University Press.

Keys, E., & McConnell W.J., (2005): Global change and the intensification ofagriculture in the tropics. *Global Environmental Change*. 15(4): 320-337.

Kim, D.H., Sexton, J.O., Noojipady, P., Huang, C.,& Anand, A., (2014): Global, Landsat-based forest-cover change from 1990 to 2000. *Remote Sensing of Environment*, 155: 178-193

Lam, N.S.N., (2008): Methodologies for mapping land cover/land use and its change. In: Liang, S., (Ed.), *Advances in Land Remote Sensing*. *Springer,* Netherlands.

Lambin, E.F., & Geist H.J. (2006): Land-Use and Land-Cover Change, Local Processes and Global Impacts. *Global Change the IGBP Series*. Springer-Verlag.

Lawal, I., (2003): *Rep faults delay in completion of Zobe dam*. Available: https://allafrica.com/stories/200308260171.html

Li, X., & Yeh, A., (1998): Principal Component Analysis of Stacked Multi-Temporal Images for the Monitoring of Rapid Urban Expansion in the Pearl River Delta. *International Journal of Remote Sensing.*19(8): 1501-1518.

Lobell, D.B., Ortiz-Monasterio, J.I., Asner, G.P., Naylor, R.L., & Falcon, W.P., (2005):Combining field surveys, remote sensing, and regression trees to understand yield variations in an irrigated wheat landscape. *Agronomy Journal*, 97: 241-249.

Lobell, D.B., Cassman K.G., & Field C.B., (2009): Crop yield gaps: their importance, magnitudes, and causes. *Annual Review of Environmental Resource*. 34: 179-204.

Lobell, D.B., (2013): The use of satellite data for crop yield gap analysis. *Field Crops Research.* 143: 56–64.

Lobell, D., Thau, D., Seifert, C., Engle, E., & Little, B., (2015): A scalable satellite-based crop yieldmapper. *Remote Sensing of Environment*, 164: 324–333.

Loveland, T.R., & Dwyer, J.L., (2012): Landsat: building a strong future. *Remote Sensingof Environment*. 122: 22-29.

Macdonald, R.B., & Hall, F.G., (1980): Global crop forecasting. *Science*, 208(80): 670–679.

Macleod, C., & Congalton, R.G., (1998): A Quantitative Comparison of Change Detection Algorithms for Monitoring Eelgrass from Remotely Sensed Data. *Photogrammetric Engineering & Remote Sensing*, 64(3): 207-216.

Map of Life, (2016): Available:http://www.mol.org (accessed June 30, 2016).

Masek, J.G., Huang, C., Wolfe, R., Cohen, W., Hall, F., Kutler, J., & Nelson, P., (2008): NorthAmerican forest disturbance mapped from a decadal Landsat record.*Remote Sensingof Environment.* 112(6): 2914-2926.

Masek, J.G., Vermote, E.F., Saleous, N.E., Wolfe, R., Hall, F.G., Huemmrich, K.F., Gao, F., Kutler J., et al., (2006): A Landsat surface reflectance dataset for North America, 1990–2000. *Geoscience Remote Sensing*, 3(3): 68-72.

Mattikalli, N.M., (1995): Integration of remotely sensed raster data with a vector-based geographical information system for land-use change detection. *International Journalof Remote Sensing*, 16(15): 2813-2828.

Mavromatis, T., (2007): Drought index evaluation for assessing future wheat production in Greece. *International Journal of Climatology*, 27(7): 911-924.

McCarl, B.A., Adams, R.M., & Hurd, B.H., (2001): Global climate change and its impact on agriculture. Texas A&M University.Texas, USA.

Mendelsohn, R., (2008): The Impact of Climate Change on Agriculture in Developing Countries. *Journal of Natural Resources Policy Research*, 1:(1) 5-19

Mohammed, K.Y., (2002): Development and Challenges of Bakolori Irrigation Project in Sokoto State, Nigeria. *Nordic Journal of African Studies*,11(3): 411-430

Mortimore, M., (1989*):* Adaptating to Drought: Farmers, Famines and Desertification in West Africa. Cambridge University Press, Cambridge.UK.

Mortimore, M., & Adams, W.M., (2001*):* Farmer adaptation change and 'crises' in the Sahel. *Global Environmental Change*,11(1): 49-57.

Mueller, N.D., Gerber, J.S., Johnston, M., Ray, D.K., Ramankutty, N.,&Foley, J.A.,(2012): Closing yield gaps through nutrient and water management. *Nature*, 4904(19): 254-257.

Mueller, N., (2016): Water observations from space: mapping surface water from 25 years of Landsat imagery across Australia. *Remote Sensing of Environment*. 174(1): 341-352.

Musa, M.K., & Odera P.A., (2015): Land Use Land Cover Changes and their Effects on Agricultural Land: A Case Study of Kiambu County – Kenya. *Kabarak Journal of Research & Innovation*.3(1): 74-86.

Munyati, C., (2000): Wetland change detection on the Kafue Flats, Zambia, by classification of a multi-temporal remote sensing image dataset. *International Journal of Remote Sensing,* 21(9): 1787-1806.

Myneni, R.B., Hall, F.G., Sellers, P.J., & Marshak, A.L., (1995): The interpretation of spectral vegetation indexes. *IEEE Transactions on Geoscience and Remote Sensing*, 3(2): 481-486.

NASA, National Aeronautics and Space Administration, Goddard Institute for Space Studies Available: http://www.giss.nasa.gov/

Nemani, R., Votava, P., Michaelis, A., Melton, F., &Milesi, C., (2011):Collaborativesupercomputing for global change science. *EOS Transaction American Geophysical*. *Union*. 92(13): 109-116

Neumann, K., Verburg, P.H., Stehfest, E., &Muller, C., (2010): The yield gap of global grain production: a spatial analysis. *Agricultural Systems*. 103(5): 316-326.

Neumann, K., Stehfest E., Verburg P.H., Siebert, S., Mu¨ller, C.,&Veldkamp, T.,(2011): Exploring global irrigation patterns: a multi level modelling approach. *Agricultural Systems*. 104(9): 703-713.

NEST, Nigerian Environmental Study/Action Team (2003): *Climate change in Nigeria*: A *communication guide for reporters and educators*, NEST, Ibadan, Nigeria.

Norman, W.R. (1996): Indigenous community managed irrigation in Sahelian WestAfrica. *Agriculture Ecosystems & Environment*. 61: 83-95.

Orode, M.O.E., (1984): Tropical grain legume bulletin. *International Grain Legume Information Centre,* Pp. 88.

Odjugo, P.A., & Ikhuoria, A.I., (2003):The impacts of climate change and anthropogenic factors on desertification in the semi-arid region of Nigeria, *Global Journal of Environmental Science*. 2(2): 118-127.

Odjugo, P.A., (2005): An analysis of Rainfall Pattern in Nigeria. *Global Journal of Environmental Science*. 4(2): 139-145.

Odjugo, P.A.O., (2009): Global and regional analysis of the causes and rate ofclimate change. *Proceeding of theNational Conference on ClimateChange and Nigerian Environmentheld at the Department ofGeography*, University of Nsukka, Nsukka, Nigeria.

Odjugo, P.A. (2010): Regional evidence of climate change in Nigeria. *Journal of Geography and Regional Planning,* 3(6): 142-150.

Okhimanhe, A.O., (1993): *Assessment of environmental impact of dam construction in Nigeria, A case study of Tiga Dam. Kano state*. An Unpublished M.Tech Dissertation in Remote Sensing. Federal University of Technology Minna, Nigeria.

Onafeso, O.D., Akanni, C.O., Badejo, B.A., (2015): Climate change dynamics and imperatives for food security in Nigeria. *Indonesian journal of Geography*, 47(2): 151-159.

Patel, N., Angiuli, E., Gamba, P., Gaughan, A., Lisini, G., Steven, F.R., Tatem, A.J., & Trianni G., (2015): Multitemporal settlement and population mapping from Landsat using GoogleEarth Engine. *International Journal of Applied Earth Observation Geoinformatics.* 35:199-208.

Pekel, J.F., Cottam, A., Gorelick, N., & Belward, A.S., (2016): High-resolution mapping of global surface water and its long-term changes. *Nature*, 540(7633): 418-422.

Penman, H.L.,(1948): Natural evapotranspiration from open-water, bare soil and grass. *Procedings of the Royal SocietyAcademy*. Harpenden, Hert. Pp. 120-145.

Place, F., (2009): Land tenure and agricultural productivity in Africa: acomparative analysis of the economics literature and recent policy strategies and reforms. *World Development.* 37(8): 1326-1336.

Pramanik M., Murai, M.S., Honda Y., Herathand A.H., & Kakiuchi, (1992): *Flood Studies in Asia by Remote Sensing. GIS-Development/AARS/ACRS/1992* Water Resources.

Pretty, J.N., Noble, A.D., Bossio, D., Dixon, J., Hine, R.E., Penning de Vries, F.W.T., & Morison, J.I.L., (2005): Resource-conserving agriculture increases yields in developing countries. *Environment Scienceand Technology*, 40(4): 1114-1119.

Pretty J., Toulmin C., & Williams S., (2011): Sustainable intensification in African agriculture. *International Journal of Agricultural Sustainability*, 9(1): 5-24.

Prigent, C., Papa, F., Aires, F., Jimenez, C., Rossow, W.B., &Mattews E., (2012): Changes in land surface water dynamics since the 1990s and relation to population pressure. *Geophysical Research Letter*. 39(8): 1-5.

Rindfuss, R.R., Walsh, S.J., Turner II, B.L., Fox, J., & Mishra, V., (2004): Developing a science of land change: challenges and methodological issues. *Proceeding National Academyof ScienceU.S.A.* 101(39): 13976-13981.

Rudel, T.K., Schneider, L., Uriart, M., Turner, B.L., Defries R., Lawrence, D., Geoghegan J., Hecht S., et al., (2009): Agricultural intensification and changes in cultivated areas, 1970-2005. *Proceeding of National Academy of Science U.S.A.* 106(49): 20675-20680.

Salisu, N. D., (2003). Obasanjo revisits Zobe dam. *daily trust* 20 May 2010.

Schmidt, A., Leadbetter, S., Theys, N., Caboni, E., Witham, C.S., Stevenson, J.A., Birch, C.E., Thordarson, T., et al., (2015): Satellite detection, long-range transport, and air quality impacts of volcanic sulfur dioxide from the 2014–2015 flood lava eruption at Bárðarbunga (Iceland). *Journal of Geophysical resource: Atmosphere*, 120: 9739-9757.

Sembenelli Consulting (2011): *Jibiya Dam.*Available: https://en.wikipedia.org/wiki/Jibiya_Dam.

Shao, J., Ni, J., Wei, C., & Xie, D. (2005). Landuse change and its corresponding ecological responses: A review. *Journal of Geographical Sciences*, 15(3): 305–328.

Sidhu, N., Pebesma, E., & Camara, G., (2018): Using Google Earth Engine to detect land cover change: Singapore as a use case.*European Journal of Remote Sensing*, 51(1): 486-500.

Sivakumar, M.V.K., (1988): Predicting rainy season potential from the onset of rains in southern Sahelian and Sudanian climatic zones of West Africa. *Agriculture and Forest Meteorology*, 42(4): 295-305.

Singh, A. (1989): Digital Change DetectionTechniques Using Remotely-Sensed Data. *International Journal of Remote Sensing*, 10: 989-1003.

Sokoto statistical year book, (2010): Statistics department, ministry of budget and economic planning, Sokoto state Nigeria.

Soulard, C.E., Albano, C.M., Villarreal, M.L., & Walker, J.J., (2016):Continuous 1985–2012Landsat monitoring to assess fire effects on meadows in Yosemite National Park.California. *Remote Sensing*.8(5): 371.

SRRBDA, Sokoto Rima River Basin Development Authority, (1992). Annual Report. Available: http://worldcat.org/identities/lccn-n83329283/

Sulla-Menashe, D., Tan B., Schneider, A., Ramankutty, N., Sibley, A., & Huang, X., (2010): MODIS collection 5 global land cover: Algorithm refinements and characterization of new datasets.*Remote Sensing of Environment*,114: 168–182.

Sultan, B., Baron, C., Dingkuhn, M., Sarr, B., &Janicot, S., (2005). Agricultural impacts of large-scale variability of the West African monsoon. *Agricultural and Forest Meteorology*, 128(1-2): 93-110.

Sureh, F.S., (2019): Drought Prediction based on Standardized Precipitation-Evapotranspiration Index by using m5 tree model drought prediction based on standardized precipitation, *conference paper (April 2019). Trabzon, Turkey*.

Svoboda M, Fuchs B (2017): Handbook of Drought Indicators and Indices

Teferi, E., Bewket, W., Uhlenbrook, S., & Wenninger, J., (2013): Understanding recent land useand land cover dynamics in the source region of the Upper Blue Nile, Ethiopia: spatially explicit statistical modelling of systematic transitions. *Agriculture Ecosystem and Environment*, 165: 98-117.

Thornton, P.K.; Jones, P.G.; Ericksen, P.J.; Challinor, A.J.: Agriculture and food systems in sub-Saharan Africa in a 4 ◦C+ world (2011). *Philos. Trans. R. Soc. A. 369*, 117–136.

Thornthwaite, C.W., (1948). An approach toward a rational classification of climate. *Geographical Review*, 38(1): 55-94.

Tim, H., (2000): *The impact of climatic variability over the period 1961 1990 on the soil water balance of upland soils in the North East Arid Zone of Nigeria.* Cranfield CERES, Cranfield University. UK.

Tingem, M.; Rivington, M. (2009): Adaptation for crop agriculture to climate change in Cameroon: Turning on the heat. Mitigation Adaptation Strategies. *Global Change* 2009, 14, 153–168.

Tilman, D., Balzer, C., Hill, J. & Befort, B.L. (2011): Global food demand and the sustainable intensification of agriculture. *Proceedings of the National Academy of Sciences of the United States of America*, 108: 20260-20264.

Thiam, S., & Eastmen, R.J., (1999): In Guide to GIS and Image Processing, Volume 2; Idrisi Production: Clarke University, Worcester, MA, USA. Pp. 89-100.

Trenberth, K.E., P.D. Jones, P. Ambenje, R. Bojariu, D. Easterling, A. Klein Tank, D. Parker, F. Rahimzadeh, J.A. Renwick, M. Rusticucci,B. Soden and P. Zhai, (2007). Observations: Surface and Atmospheric Climate Change. In: Climate Change 2007: The Physical Science Basis. Contribution of Working Group I to the Fourth Assessment Report of the Intergovernmental Panel on Climate Change [Solomon, S.,D. Qin, M. Manning, Z. Chen, M. Marquis, K.B. Averyt, M. Tignor and H.L. Miller (eds.)]. Cambridge University Press, Cambridge, UnitedKingdom and New York, NY, USA

Trenberth K.E., Dai A., Van der Schrier G., Jones P. D., Barichivich J., Briffa K.R., Sheffield J., (2014): Global warming and changes in drought. National climate change, 4:17-22

Trianni, G., Lisini, G., Angiuli, E., Moreno, E.A., Dondi, P., Gaggia, A., & Gamba, P., (2015): Scalingup to national/regional urban extent mapping using Landsat data. *IEEE Journal of Selected Topics in Applied Earth Observations and Remote Sensing*. 8(7): 3710-3719.

Townshend, J.R.G., (1994): Global data sets for land applications from the advanced very high-resolution radiometer: an introduction. *International Journal of Remote Sensing*. 15(17): 3319-3332.

Tucker, C.J., (1979): Red and photographic infraredlinear combinationsfor monitoringvegetation. *Remote Sensing of Environment*. 8(2): 127-150.

Turner, B.L., Skole, D., Sanderson, S., Fischer, G., & Fresco, L., (1995): *Land-Use and Land-cover change science/research plan. IGBP Report No. 35; HDP Report No. 7.* International Social Science Council, Stockholm and Geneva.

Tulbure, M.G., Broich, M., Stehman, S.V., & Kommareddy, A., (2016): Surface water extent dynamics from three decades of seasonally continuous Landsat time series at subcontinental scale in a semi-arid region. *Remote Sensing of Environment*. 178: 142-157.

Umar, F.B., (1994): *Factors affecting the adoption of small-holder irrigation technology by Farmers in Jega LGA of Kebbi State, Nigeria*. Unpublished M. Sc thesis, University of Ibadan, Nigeria.

UN, (2010): *Background on issues relating to Water*. United Nations. Available: https://www.un.org/waterforlifedecade/pdf/unwdpac_biennial_report_2010_2011.pdf

UNEP, United Nations Environment Programme, (2005): *Division of Technology, Industry, and Economics. Economics and Trade Unit. Integrated assessment of the impact of trade liberalization: a country study on the Nigerian rice sector.* UNEP/Earth*ISBN 92-807-2450-9*. Pp. 81.

U.S. Geological Survey, (2010): Thousands of Landsat Scenes in Google's Earth Engine.Available: https://landsat.usgs.gov/google-earth-engine .

Verburg, P.H., Chen, Y.Q., & Veldkamp A., (2000): Spatial explorations of land-use change and grain production in China. Agriculture. *Ecosystem and Environment*, 82: 333-354.

Verburg, P.H., Soepboer, W., Valdkamp, A., Limpiada, R., Espaldon V., & Mastura, S.S., (2002): Modeling the spatial dynamics of regional landuse: the CLUE-S model. *Environmental Management*, 30(3): 391-405.

Vicente-Serrano, S.M., Beguería, S. & López-Moreno, J.I. (2010): A multi-scalardrought index sensitive to global warming: The Standardized Precipitation Evapotranspiration Index – SPEI.*Journal of Climate*. 23(7) :1696–1718.

Wharton, C.R., (1971): Risk, uncertainty and the subsistence farmer. In Dalton, G., (ed.) Economic development and social change. The Natural History Press, New York.

Wingate, V.R., Phinn, S.R., Kuhn, N., Bloemertz, L.,& Dhanjal-Adams, K.L., (2016): Mapping decadal land cover changes in the woodlands of northeastern Namibia from 1975 to 2014 using the Landsat satellite archived data. *Remote Sensing*, 8(8): 681.

World Bank, (1989): *Option and Investment Priorities in Irrigation development*. Nigeria sector review 1987.1995.

World Bank (1995): *Nigeria Impact Evaluation Report: Kano and Sokoto States Agricultural Development Project*. *Report No. 14767 – UNI*. Nigeria.

World Bank,(2010): Fadama III Agricultural Project Fast Becoming a Household Name in Nigeria, July 28, Available: *www.worldbank.org/en/news/feature/2010/07/28/fadama-iii-rural-agriculture-project-fast-becoming-a-household-name-in-nigeria*

Yamazaki, D., Trigg, M.A., & Ikeshima, D., (2015): Development of a global ~90m water body map using multi-temporal Landsat images. *Remote Sensing of Environment*. 171: 337-351.

Yaqub, C.N., (2007): Desert encroachment in Africa: Extent, causes and impacts. *Journal of Arid Environment.* 4(1): 14-20.

Zahid N.Q., Narissara N., Kuaanan T., Asadullah (2020): Drought monitoring based on Standardized Precipitation Index and Standardized Precipitation Evaporation Index in the arid zone of Balochistan province, Pakistan. *Arabian Journal of Geoscience* 2021:14:11

Zhang, Q., Li, B., Thau, D., & Moore, R., (2015): Building a better urban picture: combining dayand night remote sensing imagery. *Remote Sensing*, 7(9): 11887-11913.

Zurqani, H.A., (2018): Geoinformation Geospatial analysis of land use change in the Savannah River Basin using Google Earth Engine. *International Journal of Applied Earth Observation Geoinformation*, 69: 175-185.

APPENDICES

LANDSAT TYPE	YEAR	ACQUISITION DATE	PATH	ROW
Landsat Collection 1 Level-1	Landsat 5/1988	11-Jan-87	189	51
Landsat 4-5 TM C1 Level-1		11-Jan-87		52
		18-Jan-87	190	50
		18-Jan-87		51
		18-Jan-87		52
		09-Jan-87	191	50
		09-Jan-87		51
		09-Jan-87		52
Landsat Collection 1 Level-1	Landsat 5/1998	28-Jan-99	189	51
Landsat 4-5 TM C1 Level-1		01-Jan-99		52
		16-Nov-98	190	50
		16-Nov-98		51
		16-Nov-98		52
		23-Nov-98	191	50
		23-Nov-98		51
		23-Nov-98		52
Landsat Collection 1 Level-1	Landsat8/2018	01-Feb-18	189	51
Landsat 8 OLI/TIRS C1 Level-1		01-Feb-18		52
		08-Feb-18	190	50
		08-Feb-18		51
		08-Feb-18		52
		30-Jan-18	191	50
		30-Jan-18		51
		30-Jan-18		52

Fig. A1: Landsat data.

Google Earth Engine Data

LANDSAT TYPE	IMAGE ID	ACQUISITION	DATE
Landsat 4 TOA	LANDSAT/LT04/C01/T1_TOA	29/01/1988	&21/12/1987
Landsat 5 TOA	LANDSAT/LT05/C01/T1_TOA	16/11/1998	&28/01/1999
Landsat 7 TOA	LANDSAT/LE07/C01/T1_TOA	06/12/1999	&15/02/2000
Landsat 8 TOA	LANDSAT/LC08/C01/T1_TOA	23/01/2018	&17/02/2018

Figure. A2: GEE Landsat data.

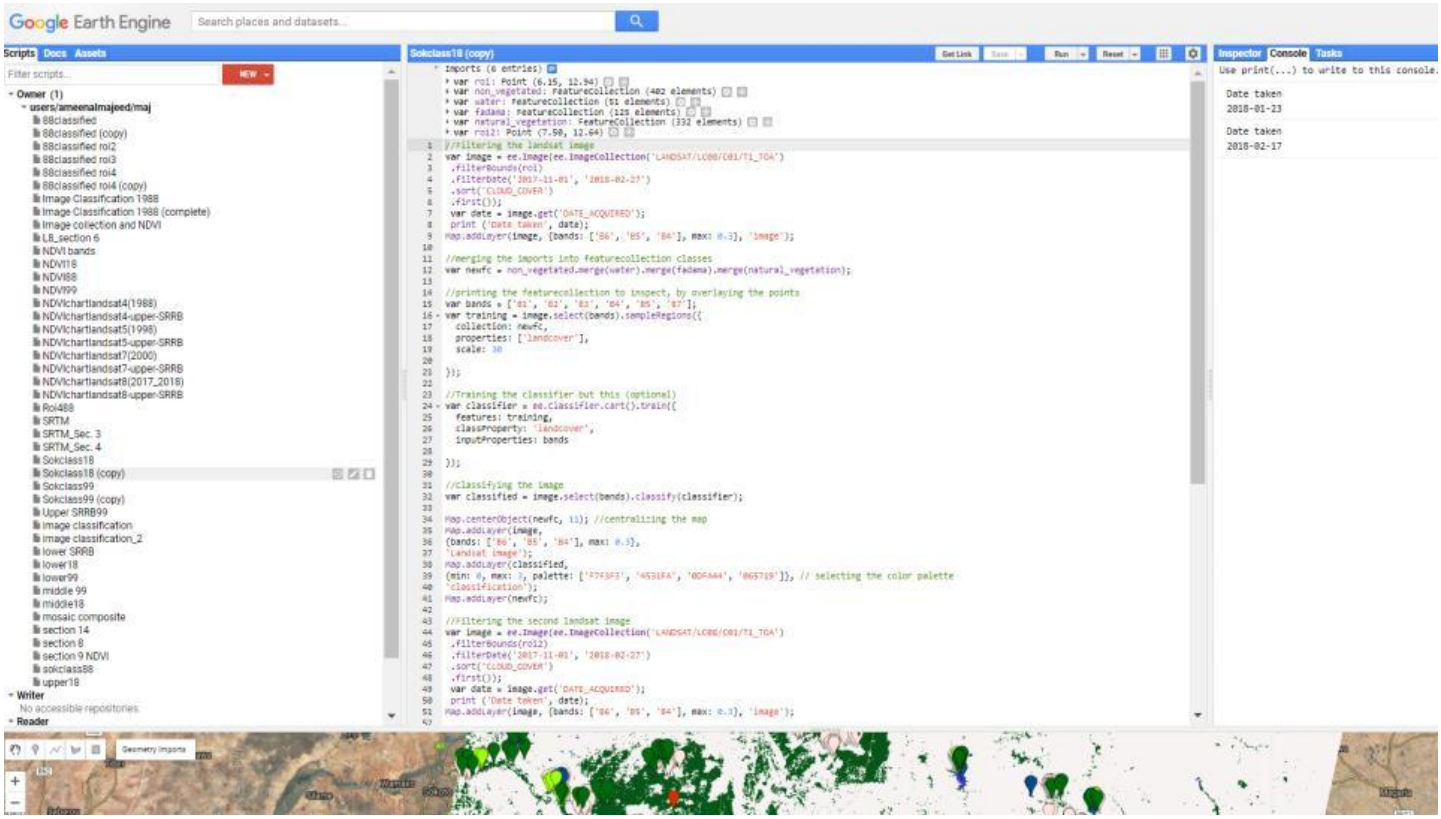

Figure A3: GEE classification code.

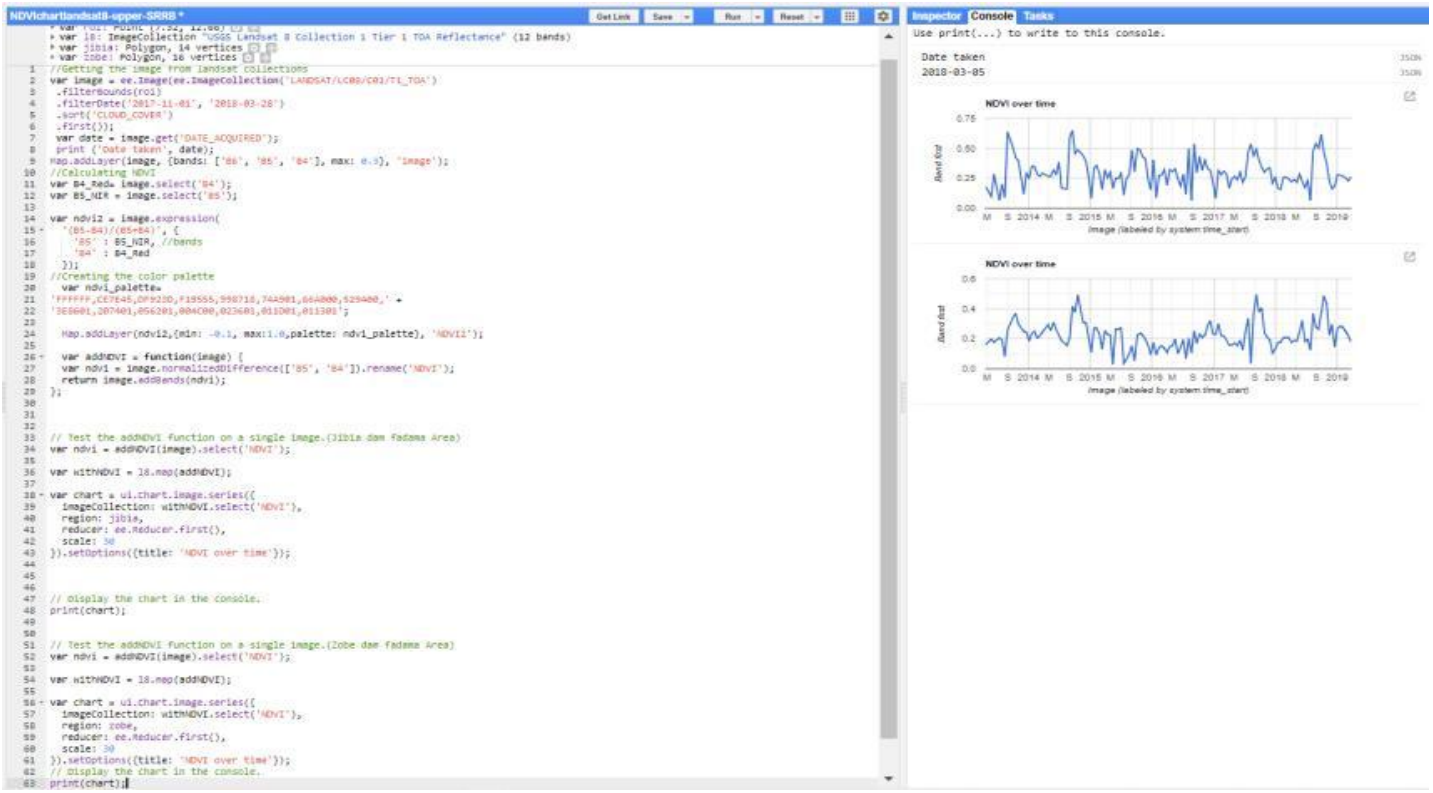

Figure A4 (a): GEE NDVI time series code upper SRRB.

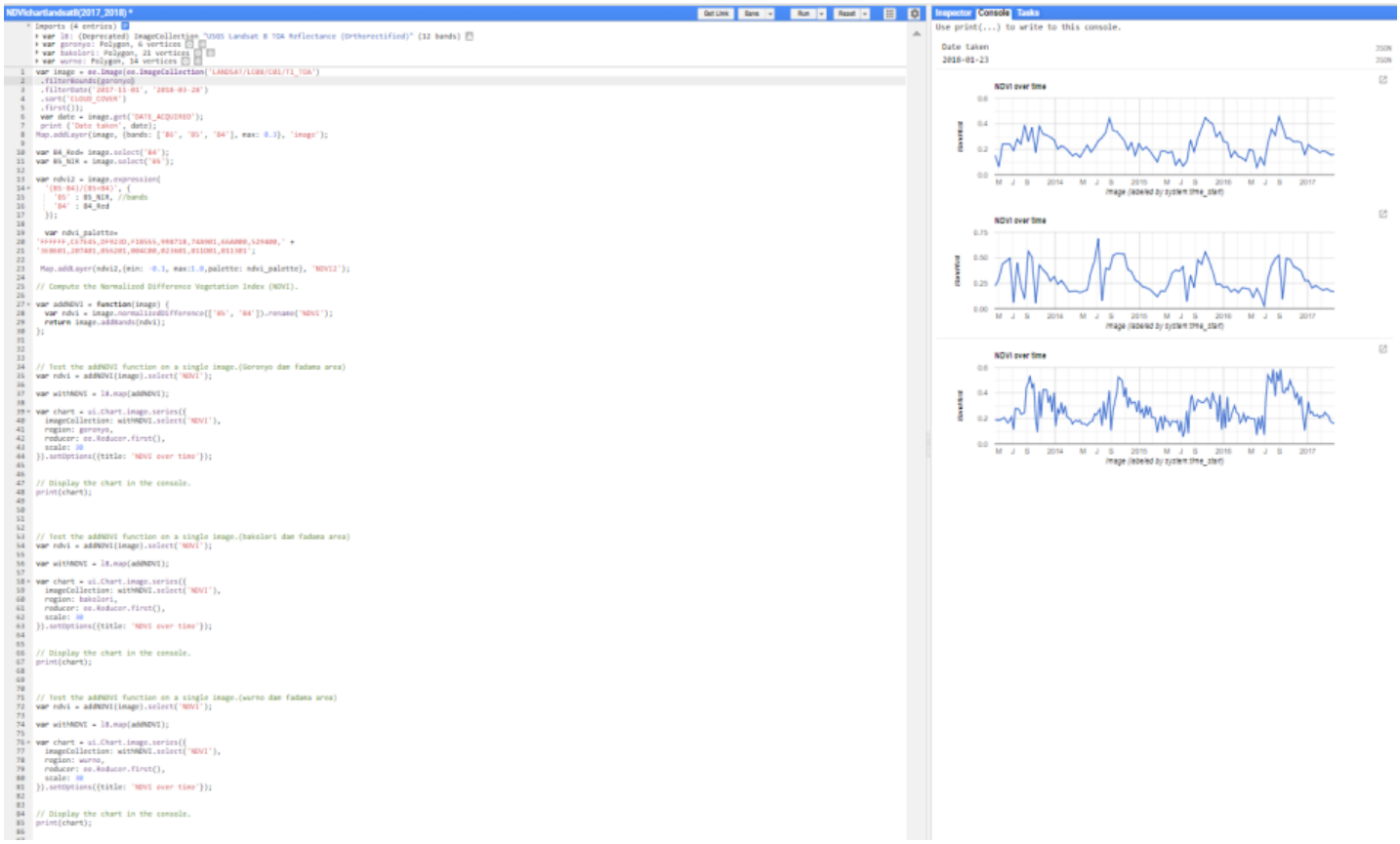

Figure A4 (b): GEE NDVI time series code mid SRRB.

Epoch 1: 1988 Classification Error Matrix

ID	Landcover	POINT1	POINT2	POINT3	POINT4	GTpoint
1	Water	**71**	0	0	0	71
2	Natural Veg.	2	**71**	2	1	76
3	Fadama	0	0	**69**	0	69
4	Non_Vegetated	2	0	0	**70**	72
	Total	75	71	71	71	**288**

GTpoint percentage

Landcover	POINT1	POINT2	POINT3	POINT4
Water	**94.67**	0	0	0
Natural Veg.	2.67	**100**	2.82	1.41
Fadama	0	0	**97.18**	0
Non-Vegetated	2.67	0	0	**98.60**

Comission Error

Landcover	Wrongly classified	Row total	Percentage
Water	0	71	0
Natural Veg.	5	76	6.58

Fadama	0	69	0
Non_Vegetated	2	72	2.78

Omission Error

Landcover	Wrongly classified	Column total	Percentage
Water	4	75	5.33
Natural Veg.	0	71	0
Fadama	2	71	2.82
Non_Vegetated	1	71	1.41

Producer's accuracy

Landcover	correctly classified	Column total	Percentage
Water	71	75	94.67
Natural Veg.	71	71	100
Fadama	69	71	97.19
Non_Vegetated	70	71	98.60

User's accuracy

Landcover	correctly classified	Row total	Percentage
Water	71	71	100
Natural Veg.	71	76	93.42
Fadama	69	69	100
Non-Vegetated	70	72	97.22

Therefore; the Overall Accuracy **OA** using Kappa Coefficient = **0.96 or 96%**

Figure A5.1: 1988 classification accuracy assessment.

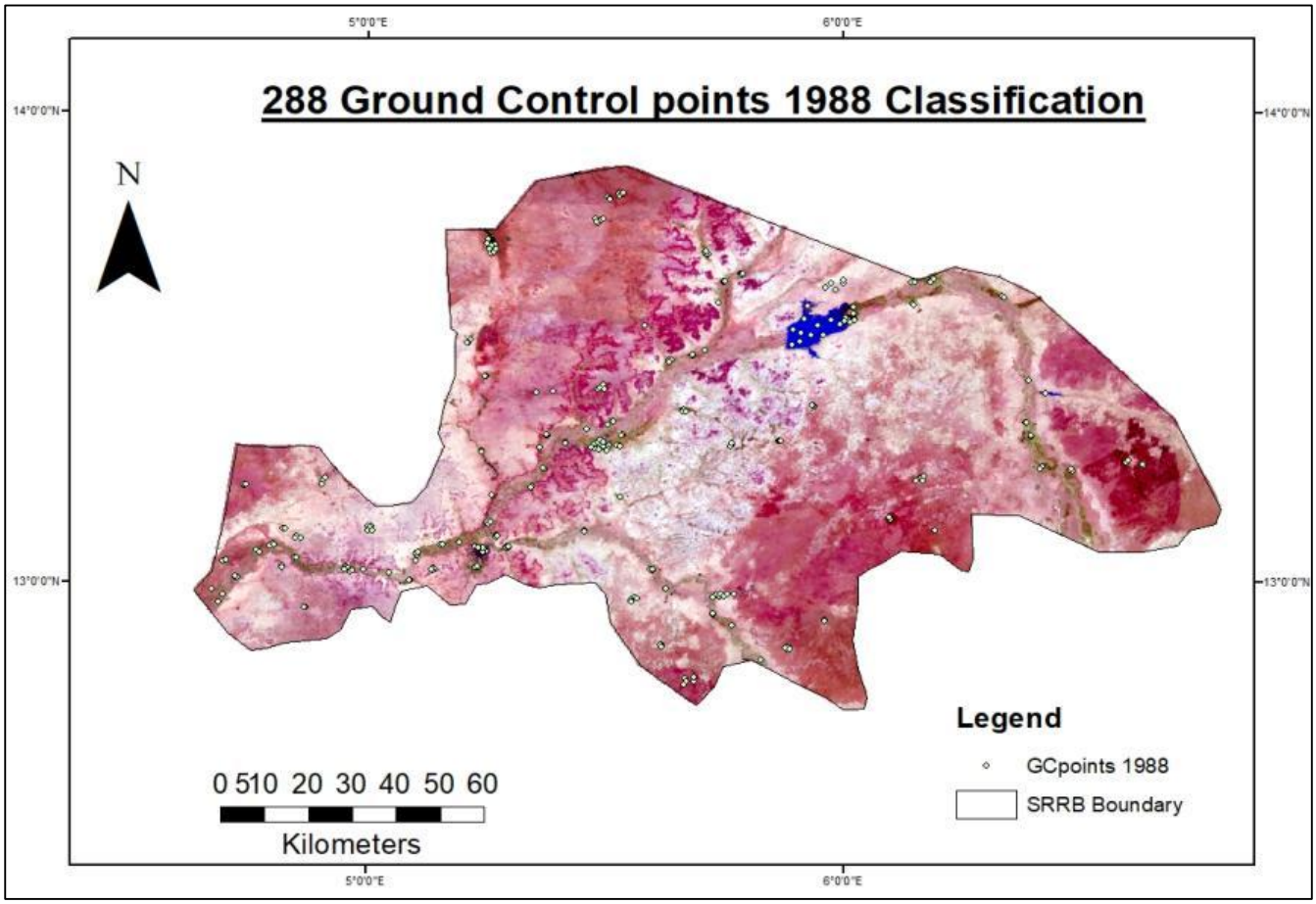

Figure A5.1a: Map showing the 288 ground control point used in the error matrix in 1988 classification.

Epoch 2: 1998 Classification Error Matrix

ID	Landcover	POINT1	POINT2	POINT3	POINT4	GTpoint
1	Water	**60**	1	0	0	61
2	Natural veg.	0	**68**	0	0	68
3	Fadama	0	1	**71**	0	72
4	Non_vegetated	15	1	0	**71**	87
	Total	75	71	71	71	288

GTpoint percentage

Landcover	POINT1	POINT2	POINT3	POINT4
Water	**80**	1.41	0	0
Natural veg.	0	**95.77**	0	0
Fadama	0	1.41	**100**	0
Non_vegetated	20	1.41	0	**100**

Comission Error

Landcover	Wrongly classified	Row tota	Percentage
Water	1	61	1.64
Natural Veg.	0	68	0
Fadama	1	72	1.39

Non_Vegetated	16	82	18.39

Omission Error

Landcover	Wrongly classified	Column total	Percentage
Water	15	75	20
Natural Veg.	3	71	4.23
Fadama	0	71	0
Non_Vegetated	0	71	0

Producer's accuracy

Landcover	correctly classified	Column total	percentage
Water	60	75	80
Natural Veg.	68	71	95.77
Fadama	71	71	100
Non_Vegetated	71	71	100

User's accuracy

Landcover	correctly classified	Row total	percentage
Water	60	61	98.36
Natural Veg.	68	68	100
Fadama	71	72	98.61
Non-Vegetated	71	87	81.61

Therefore; the Overall Accuracy **OA** using Kappa Coefficient = **0.92 or 92%**

Figure A5.2: 1998 Classification accuracy assessment.

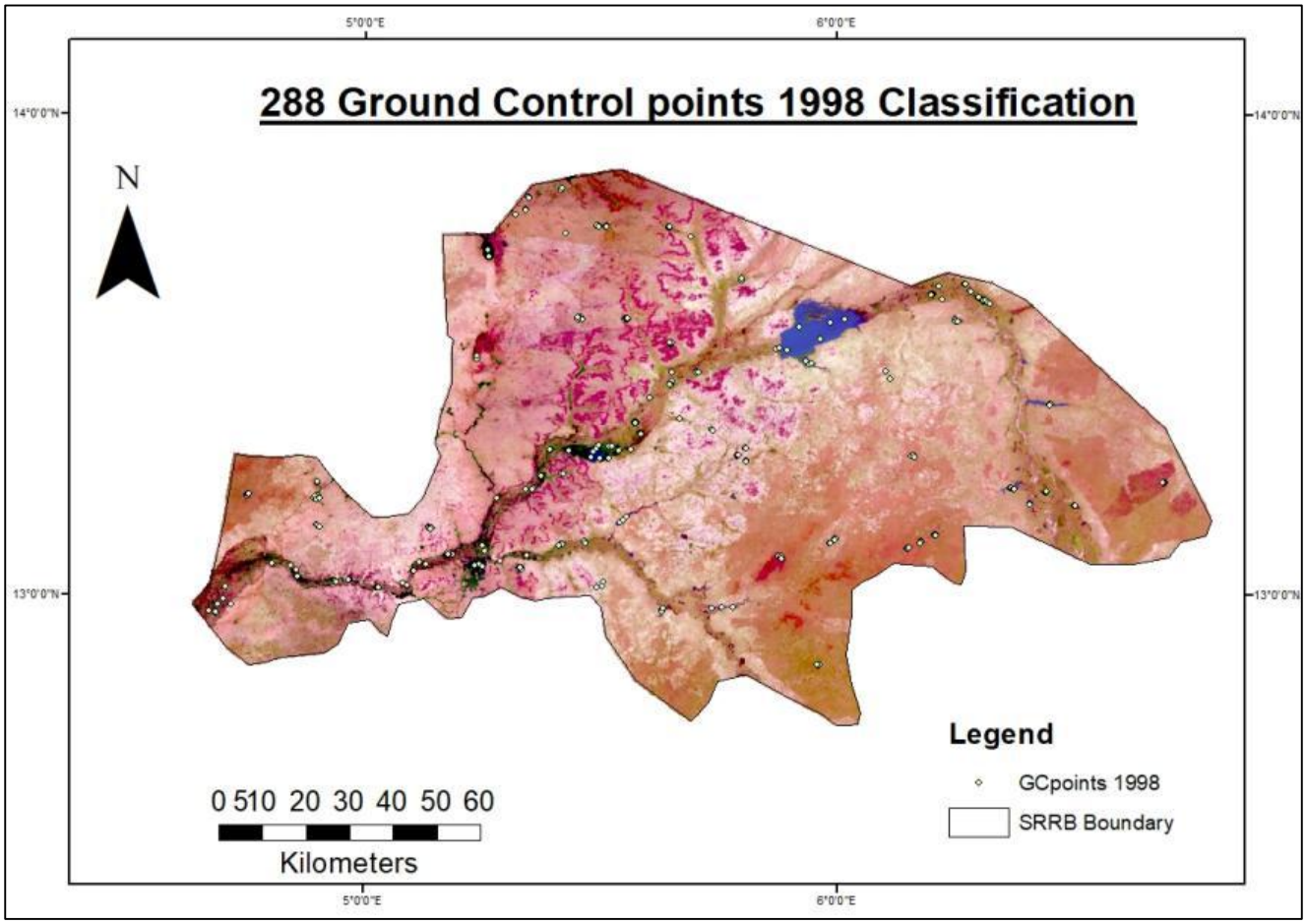

Figure A5.2a: Map showing the 288 ground control point used in the error matrix in 1998 classification.

Epoch 3: 2018 Classification Error Matrix

ID	Landcover	POINT1	POINT2	POINT3	POINT4	GTpoint
1	Water	**51**	0	0	0	51
2	Non_Vegetated	8	**69**	1	1	79
3	Natural Veg.	16	2	**70**	0	88
4	Fadama	0	0	0	**70**	70
	Total	75	71	71	71	**288**

GTpoint percentage

Landcover	POINT1	POINT2	POINT3	POINT4
Water	**68**	0	0	0
Non_vegetated	10.67	**97.18**	1.41	1.41
Natural Veg.	21.33	2.82	**98.59**	0
Fadama	0	0	0	**98.59**

Comission Error

Landcover	Wrongly classified	Row total	Percentage
Water	0	51	0
Non_Vegetated	10	79	12.66
Natural Veg.	18	88	20.45
Fadama	0	70	0

Omission Error

Landcover	Wrongly classified	Column total	Percentage
Water	0	75	0
Non_Vegetated	10	71	14.08
Natural Veg.	18	71	25.35
Fadama	0	71	0

Producer's accuracy

Landcover	correctly classified	Column total	percentage
Water	51	75	68
Non_Vegetated	69	71	97.18
Natural Veg.	70	71	98.59
Fadama	70	71	98.59

User's accuracy

Landcover	correctly classified	Row total	percentage
Water	51	51	100
Non-Vegetated	69	79	87.34
Natural Veg.	70	88	79.55
Fadama	70	70	100

Therefore; the Overall Accuracy **OA** using Kappa Coefficient = **0.90 or 90%**

Figure A5.3: 2018 classification accuracy assessment.

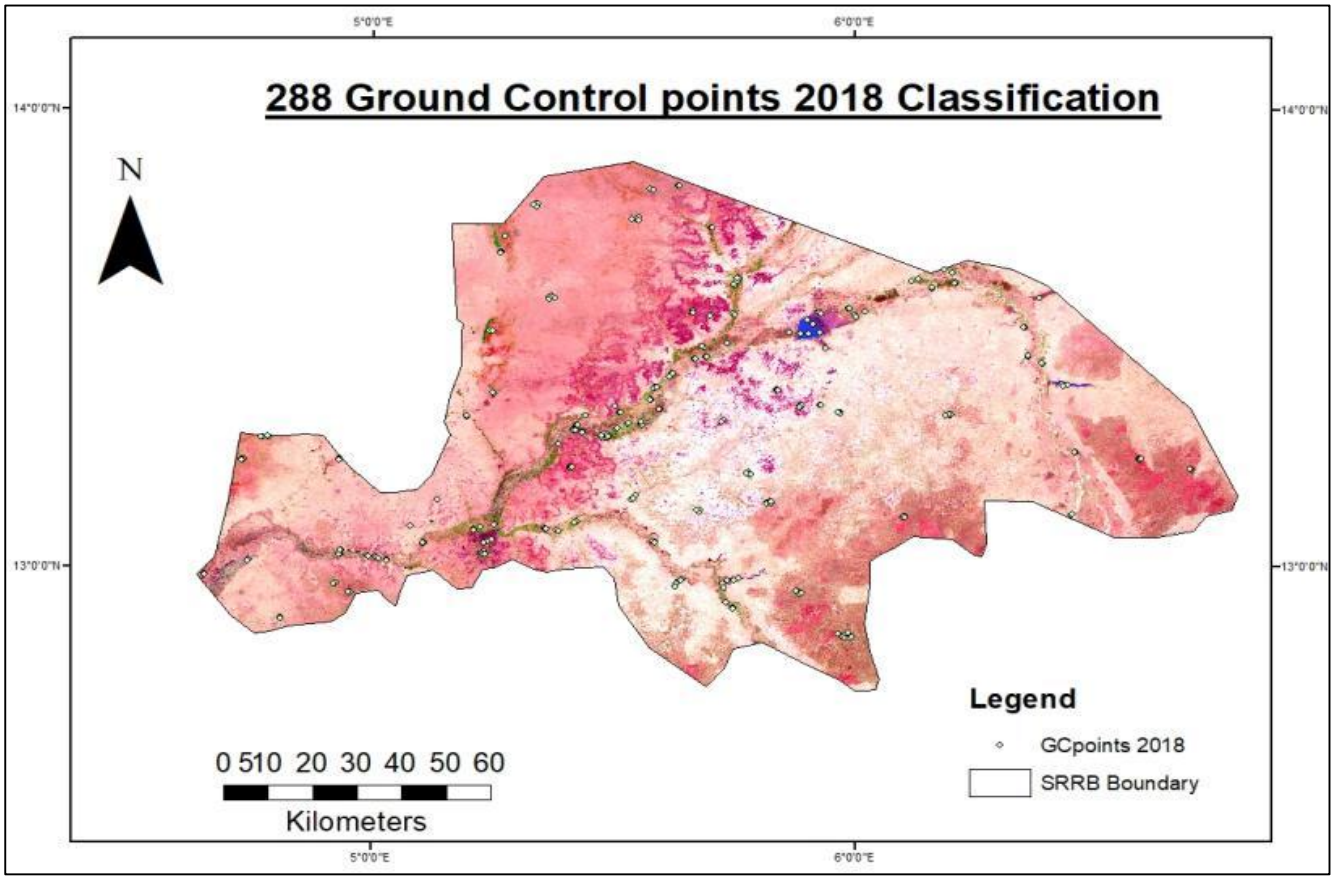

Figure A5.3a: Map showing the 288 ground control point used in the error matrix in 2018 classification.

Value	Symbol	Colour	Label
0		#FFFFFF	Not water
1		#FF0000 (1% opacity)	1% occurrence
100		#0000FF (100% opacity)	100% occurrence
255		#CCCCCC	No data

Figure A6.1: Water occurrence symbology

Value (TIFF)	Value (GEE)	Symbol	Colour	Label
0	-100		#FF0000	-100% loss of occurrence
100	0		#000000	No change
200	100		#00FF00	100% increase in occurrence
253	masked		#FFFFFF	Not water
254	-128		#888888	Unable to calculate a value due to no homologous months
255	127		#CCCCCC	No data

Figure A6.2: Water occurrence intensity symbology.

Value	Symbol	Colour	Label
0		#FFFFFF	Not water
1		#99D9EA	1 month of water
12		#0000AA	12 months of water (permanent water)
255		#CCCCCC	No data

Figure A6.3: Water seasonality symbology.

Value	Symbol	Colour	Label
0		#FFFFFF	Not water
1		#FF7F27	1% recurrence
100		#99D9EA	100% recurrence
255		#CCCCCC	No data

Figure A6.4: Annual water recurrence symbology.

Value	Symbol	Colour	Label
0		#FFFFFF	Not water
1		#0000FF	Permanent
2		#22B14C	New permanent
3		#D1102D	Lost permanent
4		#99D9EA	Seasonal
5		#B5E61D	New seasonal
6		#E6A1AA	Lost seasonal
7		#FF7F27	Seasonal to permanent
8		#FFC90E	Permanent to seasonal
9		#7F7F7F	Ephemeral permanent
10		#C3C3C3	Ephemeral seasonal
255		#CCCCCC	No data

Figure A6.5: Water transition symbology.

Value	Symbol	Colour	Label
0		#FFFFFF	Not water
1		# 6666FF	Water detected
255		#CCCCCC	No data

Figure A6.6: Maximum water extent symbology.

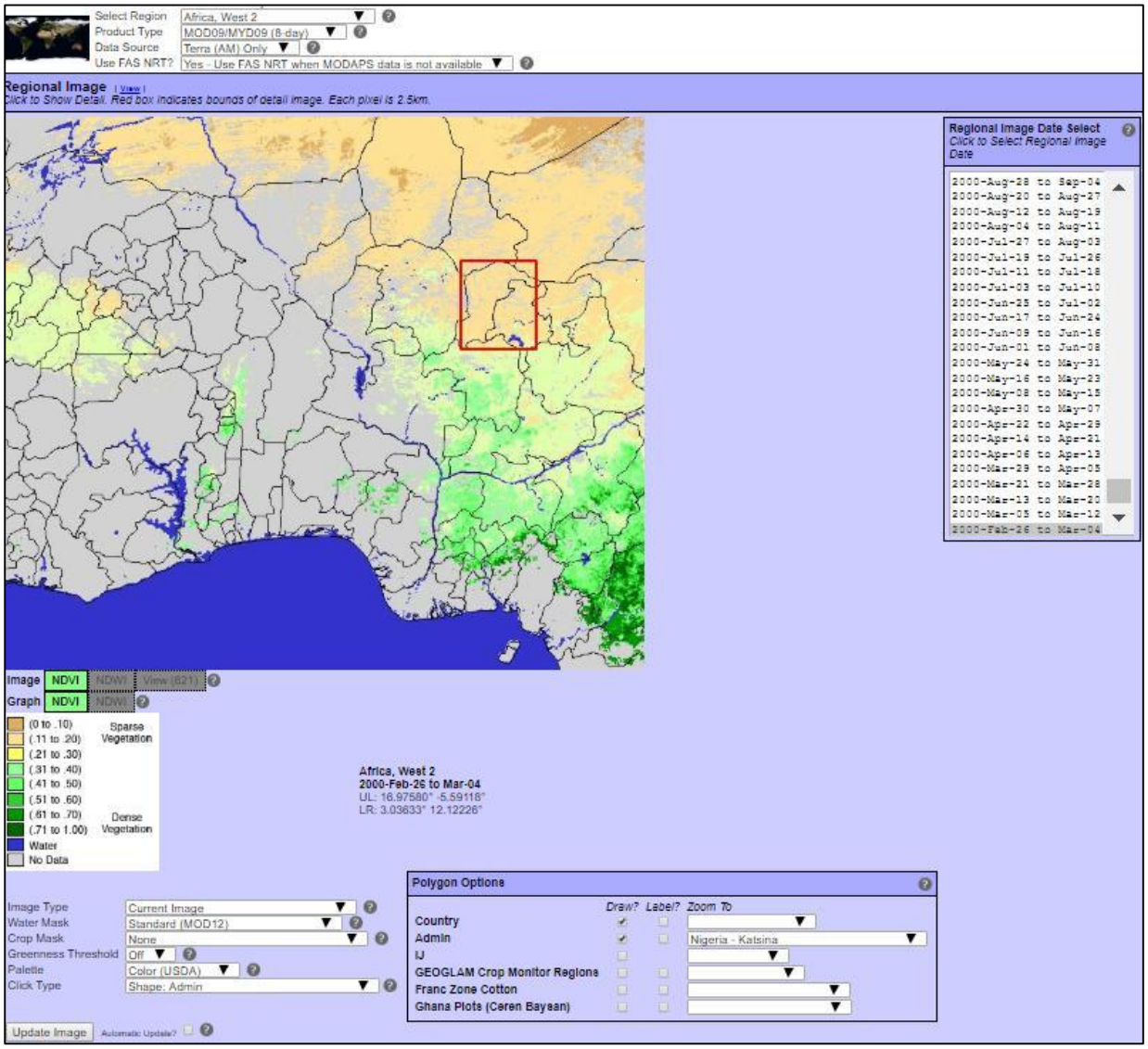

Figure A7: Katsina regional image showing the katsina boundary in the red box

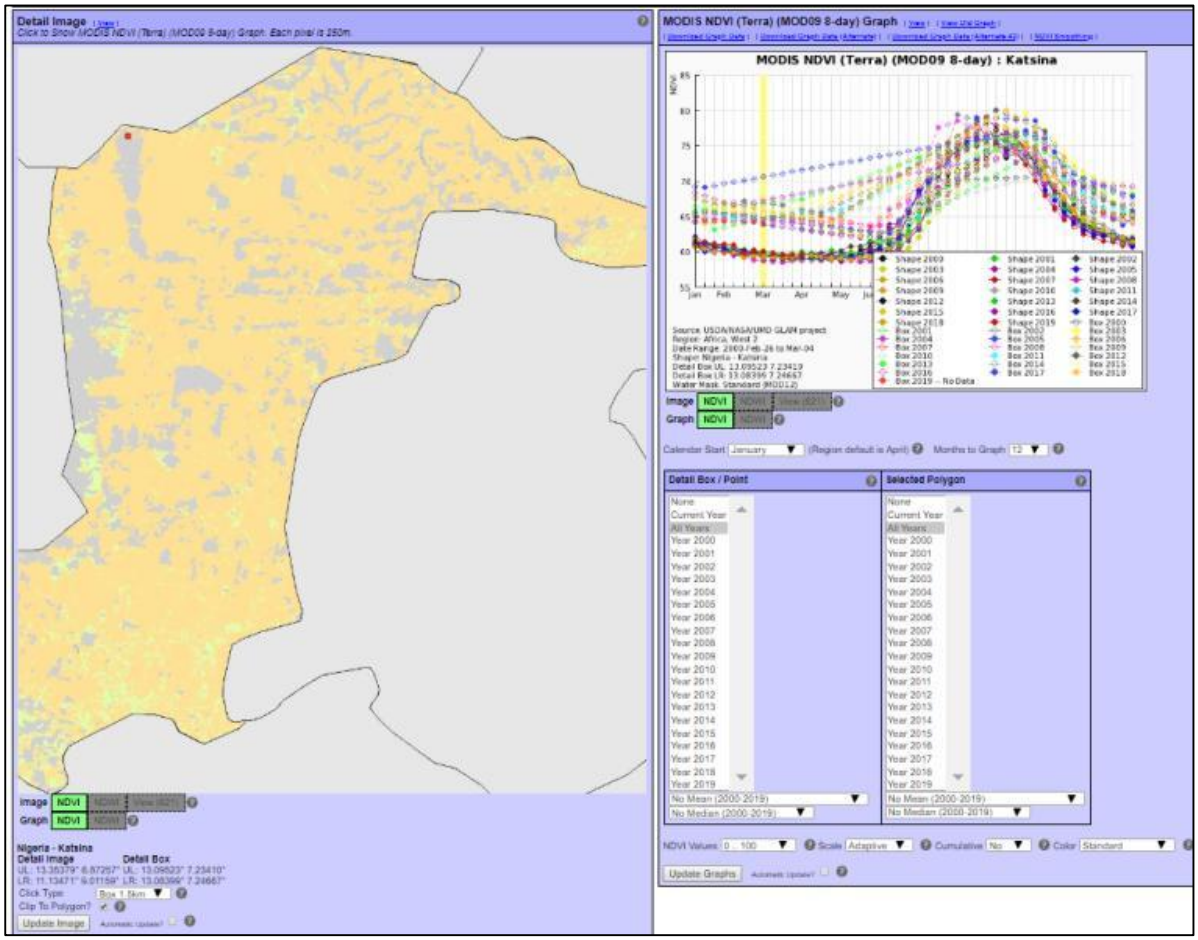

Figure A7.1: Jibia dam Fadama site using 1.5 km box at UL: 13.095^0, 7.234^0 and LR: 13.083^0, 7.247^0

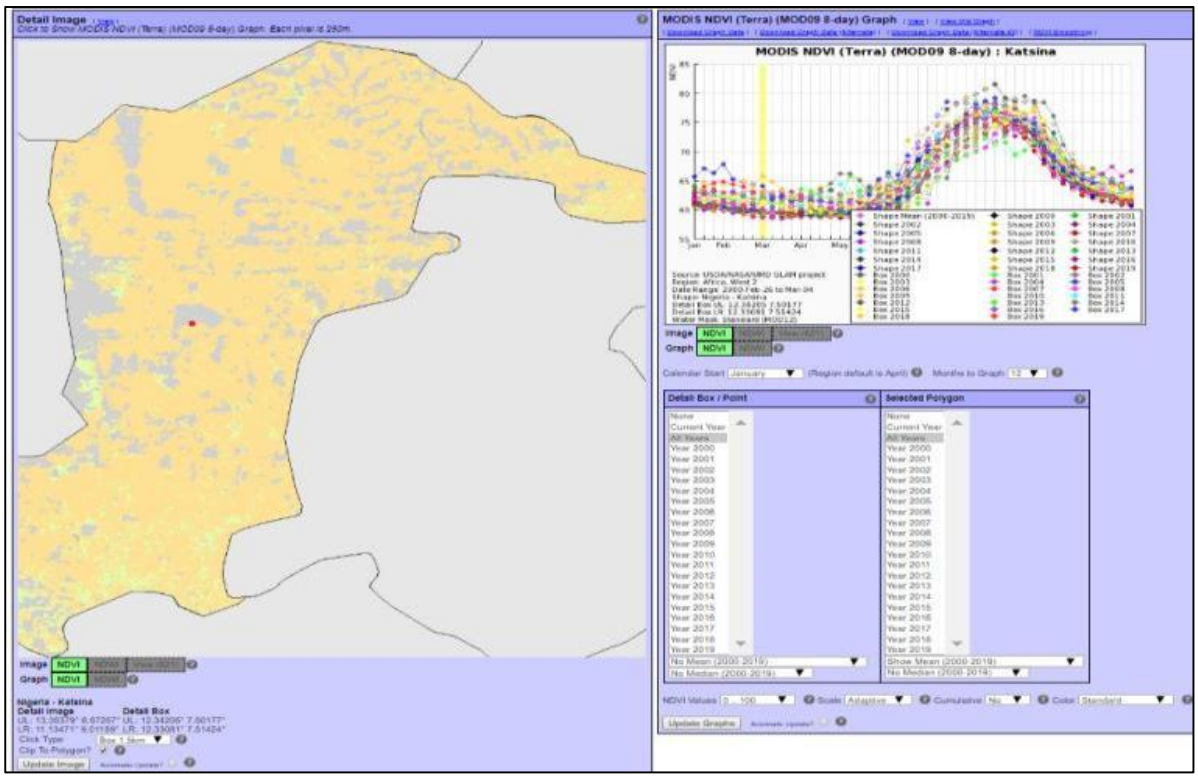

Figure A7.2: Zobe dam Fadama site using 1.5 km box at UL: 12.342^0, 7.502^0 and LR: 12.331^0, 7.514^0

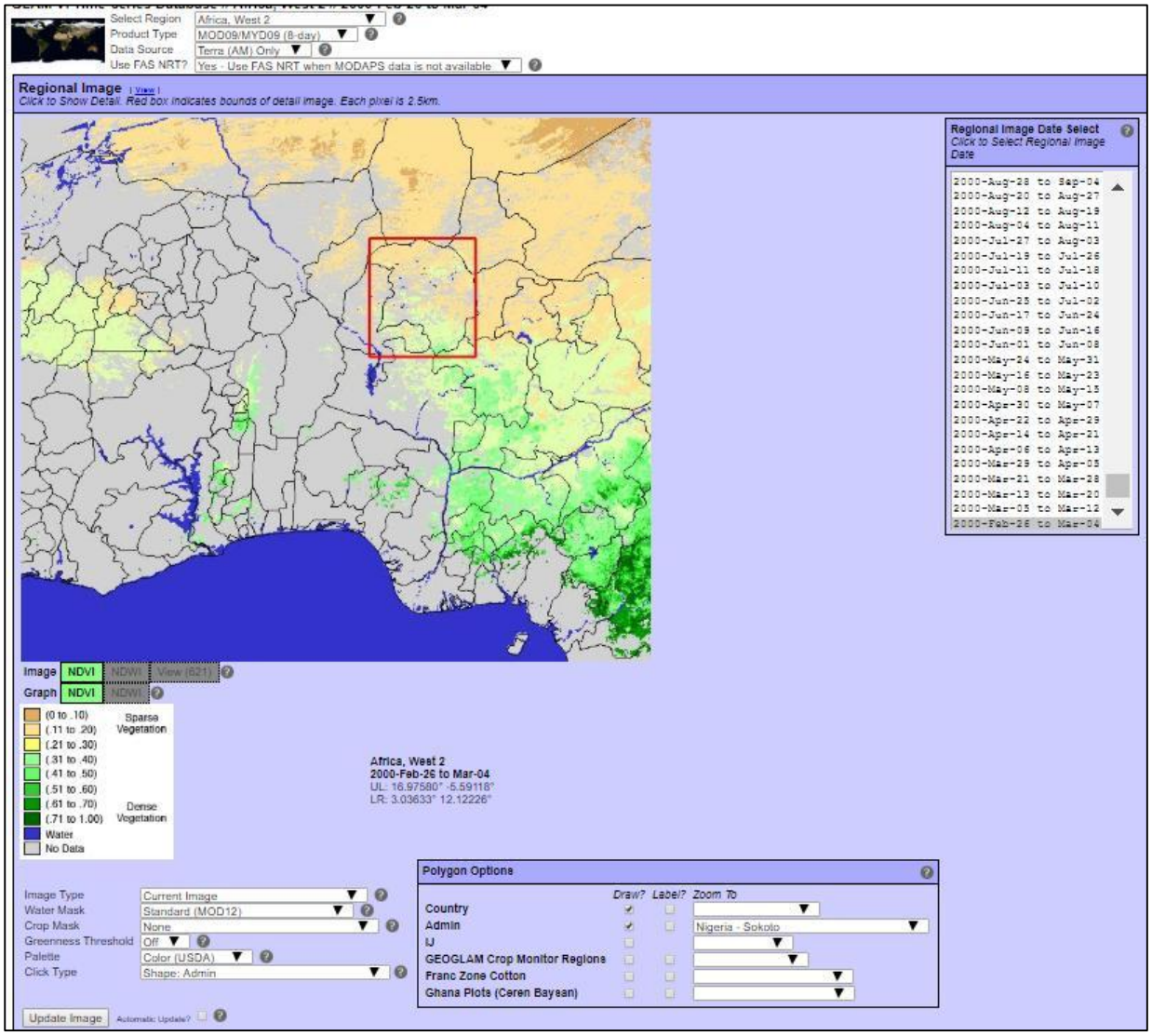

Figure A8: Sokoto regional image showing Sokoto boundary in the red box.

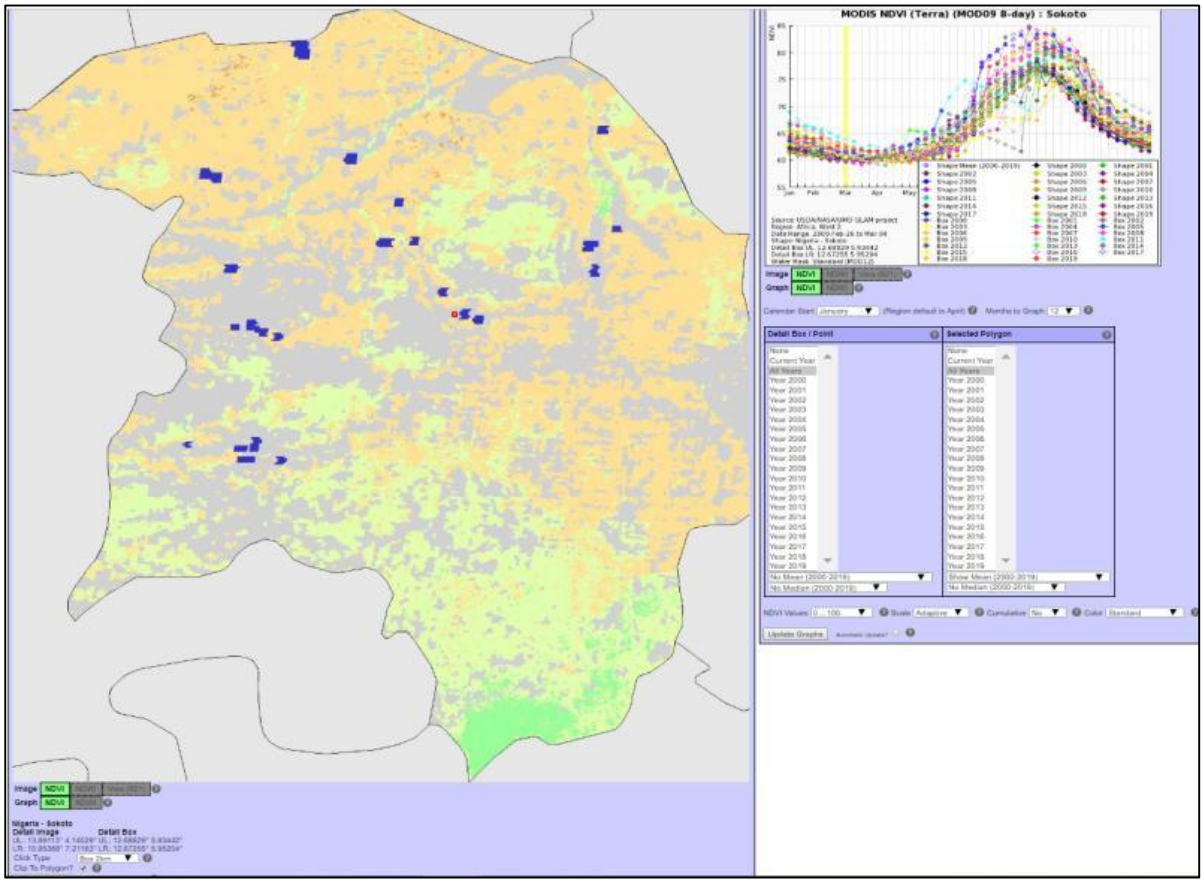

Figure A8.1: Bakolori dam Fadama site using 2 km box at UL: 12.688^0, 5.934^0 LR: 12.673^0

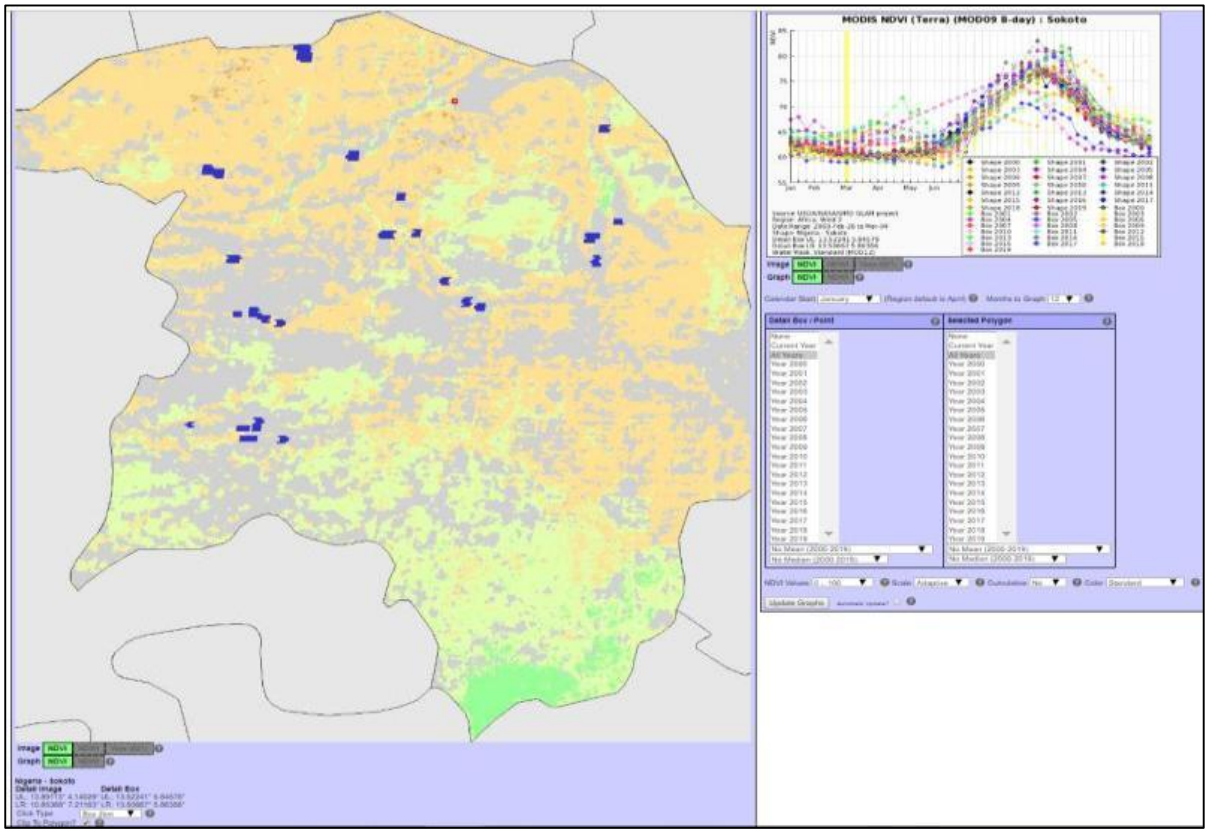

Figure A8.2: Goronyo dam Fadama site using 2 km box at UL: 13.522^0, 5.846^0 LR: 13.507^0, 5.864^0

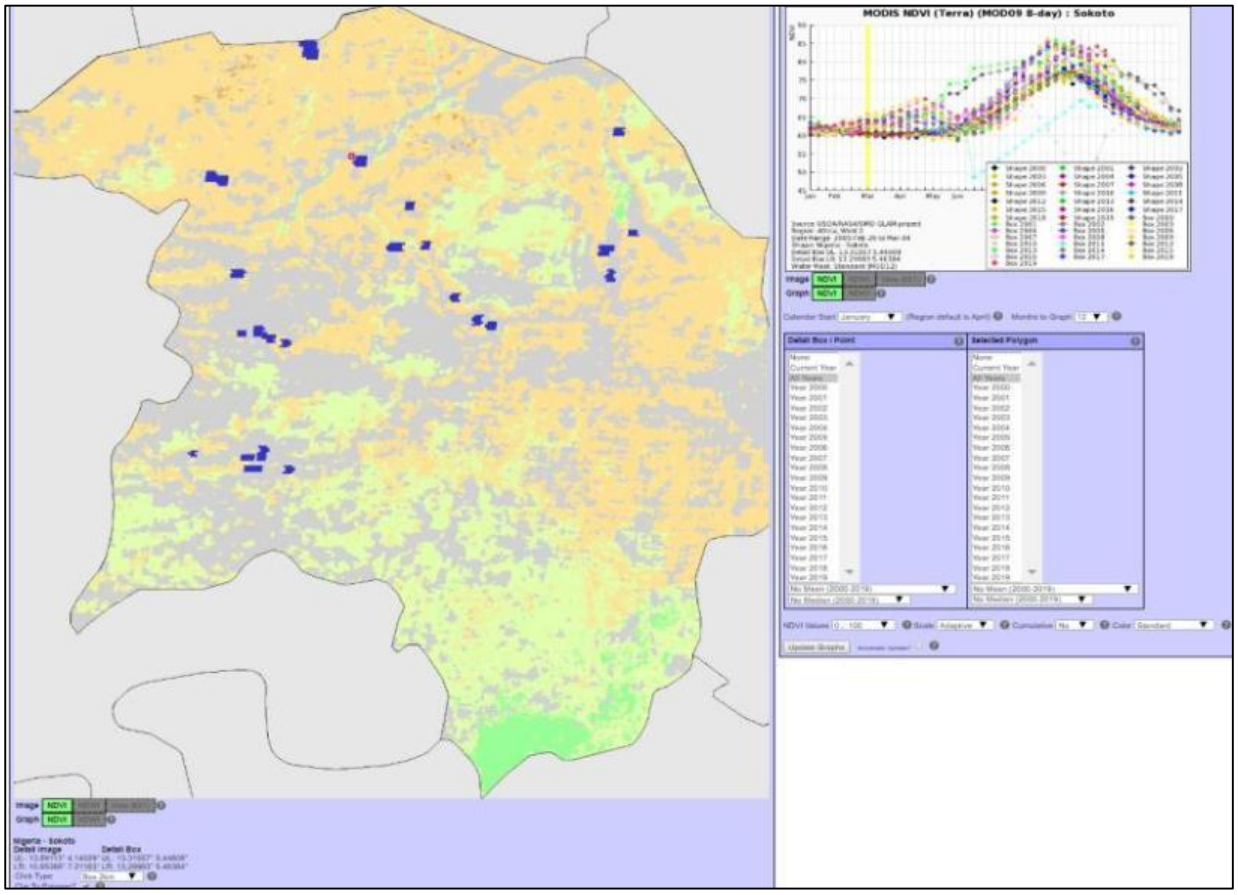

Figure A8.3: Wurno dam Fadama site using 2 km box at UL: 13.316^0, 5.446^0 LR: 13.299^0

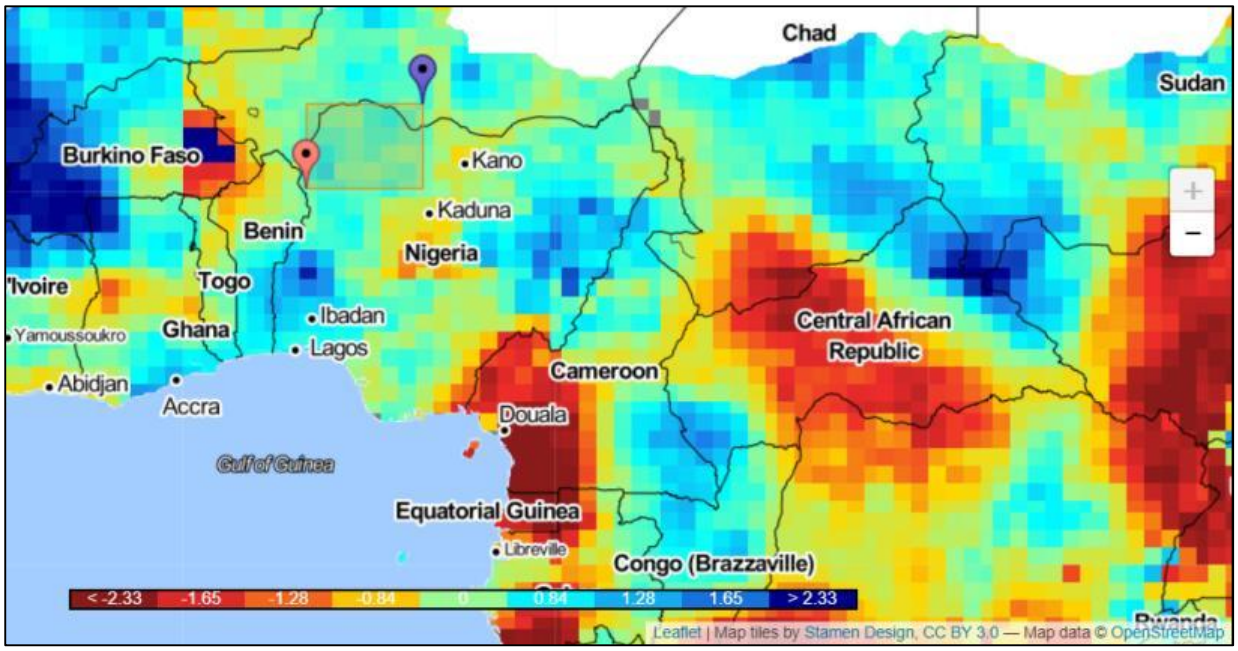

Figure A9: Map showing the location where the SPEI data was obtained from the Standardized Precipitation and Evapotranspiration Index around the Sokoto Rima River Basin in Nigeria.